Blank Page

Determining Important Pulmonary Regulators of Immunity to the Bacterium *Francisella tularensis*

A thesis submitted to The University of Manchester
for the degree of Doctor of Philosophy in the
Faculty of Biology, Medicine and Health

2018

Joshua Casulli

School of Biological Sciences
Division of Infection, Immunity and Respiratory Medicine

Contents

Word count: 46,655

List of Figures

Chapter 1

Chapter 3

Chapter 4

Chapter 5

Chapter 6

List of Tables

Chapter 1

Chapter 2

List of Abbreviations

3-MA	3-Methyladenine
AIM2	Absent In Melanoma 2
ASC	Apoptosis-associated Speck-like protein containing a CARD
ATII	Type II Alveolar Epithelial
BAL	Bronchoalveolar Lavage
BCGA	Blood Cysteine Glucose Agar
BCR	B Cell Receptor
BMDM	Bone Marrow-Derived Macrophage
CARD	Caspase Activation and Recruitment Domain
CD	Cluster of Differentiation
CGD	Chronic Granuloma Disease
CFU	Colony Forming Units
CL	Containment Level
CR	Complement Receptor
Crk	CT10 sarcoma oncogene cellular homologue
CrkL	Crk-Like
DC	Dendritic Cell
DT	Diptheria Toxin
DNA	Deoxyribonucleic Acid
Dok	Docking protein
EDTA	Ethylenediaminetetraacetic Acid
ERK	Extracellular signal–Regulated Kinase
FACS	Fluoresence-Activated Cell Sorting
FCS	Fetal Calf Serum
FCV	*Francisella*-Containing Vacuole
FDA	Food and Drug Administration
GBP	Guanylate-Binding Protein
HMGB1	High-Mobility Group Protein B1
HSV	Herpes Simplex Virus
ID	Intradermal
IFN	Interferon
IL	Interleukin
IN	Intranasal
iNOS	inducible Nitric Oxide Synthase
IRF	Interferon Regulatory Factor

ITIM	Immunotyrosine-based Inhibitory Motif
JNK	c-Jun N-terminal Kinase
KC	Keratinocyte Chemoattractant
KSHV	Kaposi's Sarcoma-associated Herpesvirus
LPS	Lipopolysaccharide
LVS	Live Vaccine Strain
mAb	monoclonal Antibody
MAC	Membrane Attack Complex
MACS	Magnetic-Activated Cell Sorting
MAPK	Mitogen-Activated Protein Kinase
MCP	Monocyte Chemoattractant Protein
M-CSF	Macrophage Colony-Stimulating Factor
MDM	Monocyte-Derived Macrophages
MFI	Mean Fluorescence Intensity
MHC	Major Histocompatibility Complex
MIG	Monokine Induced by IFNγ
MMP	Matrix Metalloprotease
MOI	Multiplicity Of Infection
MPO	Myeloperoxidase
NADPH	Nicotinamide Adenine Dinucleotide Phosphate
NE	Neutrophil Elastase
NET	Neutrophil Extracellular Trap
NF-κB	Nuclear Factor kappa-light-chain-enhancer of activated B cells
NK	Natural Killer
NLR	NOD-Like Receptor
NRAMP	Natural Resistance-Associated Macrophage Protein
OD	Optical Density
PBS	Phosphate-Buffered Saline
PGE_2	Prostaglandin E_2
PRR	Pattern Recognition Receptor
RNA	Ribonucleic Acid
ROS	Reactive Oxygen Species
RPMI	Roswell Park Memorial Institute
SRA	Scavenger Receptor A
SCID	Severe Combined Immunodeficiency
SHIP	Src Homology 2-containing Inositol Phosphatase
SHP	Small Heterodimer Partner

SIRPα	Signal Inhibitory Regulatory Protein α
SOCS	Suppressor of Cytokine Signalling
SOD	Superoxide Dismutase
SP	Surfactant Protein
SV40	Simian Virus 40
STAT	Signal Transducer and Activator of Transcription
TAM	Tyro3, Axl and Mertk
TCR	T Cell Receptor
TGF	Transforming Growth Factor
Th	T helper
TLR	Toll-Like Receptor
TNF	Tumour Necrosis Factor
TREM	Triggering Receptor Expressed on Myeloid cells
WT	Wild Type

Abstract

Joshua Casulli
The University of Manchester
PhD Immunology

2018

Determining Important Pulmonary Regulators of Immunity to the Bacterium *Francisella tularensis*

The regulation of pulmonary immune homeostasis is important in maintaining immune ignorance to harmless stimuli, to avoid a continuous inflammatory environment. Yet, it must also allow for the production of appropriate protective immune responses against potentially harmful pathogens. However, some pathogens can subvert the immune response to increase survival. An important example is *Francisella tularensis*, a highly infectious Gram-negative intracellular bacterium that dampens the immune response early in infection to aid bacterial replication. Understanding the function of host pulmonary regulatory pathways during *F. tularensis* infection may allow novel therapeutic targets to be identified.

This PhD thesis identifies an unexpected pathway that promotes host responses during bacterial infection of the lung. Thus, expression of the CD200 receptor (CD200R), a molecule previously associated with dampening immune responses in the lung, is required to limit infection by the lethal intracellular bacterium *F. tularensis*. Lack of CD200R expression enhanced infectious burden *in vitro* and *in vivo*. Exacerbated pulmonary *F. tularensis* burden was determined to be neutrophil-dependent, with depletion of neutrophils *in vivo* during *F. tularensis* infection abrogating the increased bacterial burden in lungs of $CD200R^{-/-}$ mice. Mechanistically, it was determined that $CD200R^{-/-}$ neutrophils having a significantly decreased ability to produce ROS compared to WT, thus contributing to a reduced capability to deal with *F. tularensis* infection.

Data in this thesis suggests that the absence of CD200R on neutrophils aids the colonisation and proliferation of *F. tularensis* in the lung via reduction of neutrophil ROS production; highlighting the important role this pathway plays in promoting immunity to infection. Maintaining the antimicrobial properties of neutrophils via the CD200R pathway may represent a novel therapeutic approach for treating intracellular pathogens.

Declaration

I declare that no portion of the work referred to in the thesis has been submitted in support of an application for another degree or qualification of this or any other university or other institute of learning.

Copyright Statement

i. The author of this thesis (including any appendices and/or schedules to this thesis) owns certain copyright or related rights in it (the “Copyright”) and he has given The University of Manchester certain rights to use such Copyright, including for administrative purposes.

ii. Copies of this thesis, either in full or in extracts and whether in hard or electronic copy, may be made only in accordance with the Copyright, Designs and Patents Act 1988 (as amended) and regulations issued under it or, where appropriate, in accordance with licensing agreements which the University has from time to time. This page must form part of any such copies made.

iii. The ownership of certain Copyright, patents, designs, trademarks and other intellectual property (the “Intellectual Property”) and any reproductions of copyright works in the thesis, for example graphs and tables (“Reproductions”), which may be described in this thesis, may not be owned by the author and may be owned by third parties. Such Intellectual Property and Reproductions cannot and must not be made available for use without the prior written permission of the owner(s) of the relevant Intellectual Property and/or Reproductions. iv. Further information on the conditions under which disclosure, publication and commercialisation of this thesis, the Copyright and any Intellectual Property and/or Reproductions described in it may take place is available in the University IP Policy (see http://documents.manchester.ac.uk/DocuInfo.aspx?DocID=24420), in any relevant Thesis restriction declarations deposited in the University Library, The University Library’s regulations (see http://www.library.manchester.ac.uk/about/regulations/) and in The University’s policy on Presentation of Theses.

Acknowledgments

Firstly, I would like to thank my supervisor Dr. Mark Travis. His door was always open and he was never too busy for a chat. He has provided me with constant support and guidance throughout the whole of my PhD. I would also like to thank my co-supervisor Professor Tracy Hussell and my advisor Professor Richard Grencis for their help and advice.

I must also thank the Dstl for funding this PhD and providing me with the foundations I needed to study *Francisella tularensis*. Thanks go to Graeme Clark, Di Williamson, Caroline Rowland and Charlotte Hall. Special thanks to Riccardo D'Elia who was always on hand to give advice and help solve bacteriology problems.

As well as having a fantastic supervisor, I have been lucky to work with amazing people in the Travis lab, both past and present. Kat made the lab tick. Flow cytometry would have been infinitely harder without Steph's assistance. Josh will carry the *Francisella* torch with pride. Aoife, Elinor, Eleanor, Tom, Felipe, Kevin, Sezin, Craig, Abdulelah and Stefano: lab social events have always been a highlight and I have thoroughly enjoyed working with everyone.

Beyond the Travis lab, it has been a pleasure working in the MCCIR and I have made some amazing friends along the way. Mark Fife was crucial in helping me with animal work. Thanks to Mark, Emma, Dave, Jonathan, Steph, James, Holly, Pablo, Tamsin, Michelle, Ben, Olly, Pio and Björn for their xpert advice and lengthy Grafton discussions. I also want to thank other MCCIR members for support throughout my PhD: Gareth Howell, Anu in bacteria club, Jagger, Karishma, Emma, Rajia, Ash, Eric, Katie, Sheila, Fiona Foster, Mel Ward and everyone else who has helped me. Thanks also to the BSF staff, in particular Ray Hodgkiss.

Those in my personal life cannot be forgotten. Thanks to Jake Mills and Jaimie Roden who have always provided an ear for any PhD rants. Huge thanks to all of my family. In particular, my mum and dad, Debbie and Marco, who have always provided me with unwavering support and taught me to always challenge myself. I would undoubtedly not be where I am today without them. To my brother and sister, James and Vally, who have supported me in the way only siblings can.

Finally, to my fiancée, Sophie Quinn. She has been there for me through high and low, inspiring me throughout my PhD to work to the best of my ability. No doubt she will continue to do so for the rest of our lives together. Special thanks to Millie, the best companion to have during the writing of this thesis.

I am extremely grateful to all my colleagues and friends who have made this PhD a thoroughly enjoyable and memorable experience.

Sempre Forza Roma.

Chapter 1

Introduction

1.1 Introduction

The lungs have evolved to maintain their vital function of gaseous exchange, while interacting with a myriad of airborne microorganisms. As the mucosal surfaces of the airways are essentially in direct contact with the external environment, they constantly encounter harmless innocuous antigens and often harmful pathogens. The regulation of pulmonary immune homeostasis is therefore extremely important in developing immune tolerance or ignorance to harmless stimuli to avoid a continuous inflammatory environment, while producing appropriate protective immune responses against potentially harmful pathogens. A highly infectious Gram-negative intracellular bacterium that is characterised by its ability to evade the immune system early during respiratory infection is *Francisella tularensis* (Bosio, 2011).

F. tularensis targets and infects multiple cell types that are involved in the early host innate response, such as alveolar macrophages and neutrophils (Hall et al., 2008). A large area of interest lies in understanding how the early interactions during respiratory infection with *F. tularensis* shape the immune response to the bacterium. Therefore, investigating the negative regulatory signals that modulate innate cell functions during disease may shed some light on the mechanisms of early immune evasion characteristic of *F. tularensis* infection. One such signal is achieved through the binding of CD200 receptor (highly expressed on alveolar macrophages) with its ligand CD200, leading to a unidirectional negative signal where only cells expressing CD200R are negatively affected (Wissinger et al., 2009). There are many other mechanisms in place to both inhibit and elicit an immune response, and it is possibly through the modulation of these signals that certain bacteria are able to grow and replicate undetected causing harm to the host.

This PhD thesis researches the role of the negative immune regulator CD200R during pulmonary *F. tularensis* infection. This thesis aims to understand whether modulating this regulatory pathway in multiple cell types targeted by *F. tularensis* can influence immune evasion characteristic of this bacterium. Different aspects of *F. tularensis* infection will be introduced below, including cell entry and escape, as well the host immune response. Similarly the importance of pulmonary negative immune regulators with a focus on CD200R will be discussed. Understanding the regulatory pathways involved in such respiratory infections is extremely important to be able to identify targets within the pathways and improve potential therapeutic treatments.

1.2 *Francisella tularensis*

1.2.1 Taxonomy, epidemiology, clinical manifestations and treatment

F. tularensis is the causative agent of the disease tularemia, which was first described in 1912 as a plague-like illness (McCoy and Chapin, 1912). *F. tularensis* has a large number of host species that act as reservoirs for the bacterium in the environment, ranging from small mammals such as rabbits, voles and squirrels to aquatic amoeba (Boyce, 1975, Berdal et al., 1996). Transmission between mammalian hosts, as well as transmission of the disease to humans, is commonly attributed to arthropod vectors such as ticks, mosquitos and biting flies (Morner, 1992, Hubalek et al., 1998).

There are three subspecies of *F. tularensis*, but only two are the main cause of disease in humans, each with varying virulence, geographical location and disease outcome (Conlan and Oyston, 2007). There is also a closely related species called *Francisella novicida*, which many consider to be a subspecies of *F. tularensis* (Keim et al., 2007). However, human infection from *F. novicida* is very rare and never lethal (Cowley and Elkins, 2011). *F. tularensis* subspecies *tularensis* (type A) is the most virulent and is predominantly found in North America (Farlow et al., 2005). *F. tularensis* subspecies *holarctica* (type B) is less virulent, but is also able to cause disease in humans and is spread more globally in the Northern hemisphere. Varying virulence between subspecies can be in part attributed to variation in the lipopolysaccharide O-antigen. For example, *F. tularensis* subspecies *tularensis* and *F. novicida* share O-antigen biosynthetic gene clusters, while leading to differing functions. *F. tularensis* subspecies *tularensis* O-antigen is important for intracellular survival and replication, while the O-antigen of *F. novicida* is more important for the extracellular viability of the bacterium {Thomas, 2007 #1366}.

In the USA, the number of reported human tularemia cases has reduced dramatically from 2291 in 1939, to an average of 124 annual cases between 1990 and 2000 (Feldman, 2003). Similarly low numbers of have been reported across Europe, with an average incidence rate of 0.04 cases per 100 000 inhabitants between 2005-2012. There have however been a number of high case numbers in specific countries that could be considered outbreaks: Finland and Sweden in 2000 (917 and 464 cases, respectively) and 2003 (823 and 798 cases, respectively), by Sweden in 2010 (484 cases), Norway in 2011 (178 cases), Spain in 1997 and 2007

(585 and 493, cases respectively), and Turkey in 2010 (1531 cases) (Hestvik et al., 2015).

Beyond the confirmed infectious cases, seroprevalence remains quite low in the general population. Seropositivity for anti-*F. tularensis* antibodies is estimated to be <1% in the USA, with this rising to as high as 17.5% in high-risk groups such as Native Americans, landscapers and hunters (Feldman et al., 2003). Cases of tularemia have been on the decline in recent decades, however there is evidence of increased cases over the past years that may suggest a re-emergence of tularemia particularly across Europe (Larssen et al., 2014, D'Alessandro et al., 2015, Dupont et al., 2015). Serological investigation of animals has also taken place across Europe, with 6.6% seropositivity in hares tested across Hungary between 1992-2010 (Gyuranecz et al., 2012). Similarly, studies looking at European brown hare, red fox and wild boars across Austria, the Czech Republic and Germany suggested seroprevalence between 1·4% and 10·8% (Hestvik et al., 2015).

The type of disease is dependent on the route of transmission. One of the most common manifestations, particularly in Europe, is oropharyngeal tularemia that is contracted by ingesting contaminated meat or water (Gurcan, 2014). Similarly, another common case of the disease is ulceroglandular tularemia and is usually contracted by subcutaneous vector-borne transmission (Oyston et al., 2004). These forms of tularemia are rarely lethal with a mortality rate of less than 3% and clinical manifestations of the disease usually present after an incubation period of 3-6 days (but can range from 1-14 days). These include flu-like symptoms such as fever and headache, as well as lymphoadenopathy as the bacteria disseminates through the lymphatic system and peripheral organs such as liver and spleen (Evans et al., 1985, Ohara et al., 1991).

On the other hand, pneumonic tularemia is a much more severe form of the disease. Pneumonia can occur through inhalational transmission of as little as 25 colony forming units (CFU) of *F. tularensis* (Gurycova, 1998), but also as a secondary complication of ulceroglandular and oropharyngeal tularemia (Gill and Cunha, 1997). Pneumonic tularemia in humans has strong associations with hunters who skin infected small mammals and farmers that handle hay previously inhabited by infected rodents (Stewart, 1996). Unlike other forms of tularemia, pneumonic tularemia can have a mortality rate of 30-60% if left untreated (McLendon et al., 2006). Interestingly, the clinical manifestations of pneumonic tularemia are highly variable and are similar to other disorders such as other

bacterial pneumonias, tuberculosis or even lung cancer, sometimes leading to misdiagnosis (Gill and Cunha, 1997, Fachinger et al., 2015, Odegaard et al., 2017).

Animal models have helped determine the natural history of aerosolised *F. tularensis* infection that replicates and gives a good understanding of disease in humans. Inhalation of the virulent *F. tularensis* in Fischer 344 rats led to dissemination of the bacteria to peripheral organs by 2 p.i. Shortly after, clinical manifestations of the disease developed and persisted for 24-36 hours, before rapidly decreasing before death at 5-8 days after exposure. A decrease in core body temperature and blood pressure preceded death, which was attributed to very high bacterial burdens, sepsis and disseminated intravascular coagulation (Hutt et al., 2017).

Streptomycin and gentamicin (aminoglycosides) given intramuscularly or intravenously are the preferred choices for antibiotic treatment of tularemia when a single patient can be treated and contained (Enderlin et al., 1994). A retrospective study of 87 patients treated with streptomycin demonstrated a reduction in fever within 48 hours in 77% of patients, with only 7% showing signs of relapse. Relapse following gentamicin treatment was higher at 33% (Evans et al., 1985). In the case of mass infection, perhaps from a large outbreak or bioterrorism scenario, oral administration of ciprofloxacin and doxycycline is preferred (Dennis et al., 2001). Although these antibiotics have been shown to have a higher rate of treatment failure when compared to streptomycin, benefits of faster oral administration and shorter courses of treatment outweigh the risks (Evans et al., 1985, Dennis et al., 2001). Tetracyclines are usually avoided as treatments in children less than 8 years old because of the risk of teeth discoloration, and in pregnant women because of foetal bone toxicity. Thus it is important to continue the search for therapeutic alternatives. Recent experimental data suggests that a combination of aminoglycosides and ciprofloxacin may give the most efficient bactericidal activity in patients with severe tularemia (Caspar and Maurin, 2017).

1.2.2 Use as a biological weapon

Due to the high virulence of *F. tularensis,* with as few as 25 CFU causing severe pneumonic tularemia (Gurycova, 1998), it has long been considered to be a potential biological weapon. It was studied as a potential biological agent in Japanese germ warfare units between 1932 and 1945 (Harris, 1992). Similarly, it is thought to have been stockpiled by the US and Soviet Union militaries, and it has been suggested that tularemia outbreaks affecting thousands of Soviet and German

soldiers during World War II was from intentional use (Christopher et al., 1997, Dennis et al., 2001). Despite the available treatments against tularemia highlighted above, it must be considered that these would only be reactive in response to a potential biological attack. Similarly, the threat of antimicrobial resistance in *F. tularensis* species highlights the importance of investigating novel therapeutic alternatives (Sutera et al., 2014).

1.2.3 *F. tularensis* live vaccine strain (LVS)

Despite its highly infectious nature, there is yet to be a widely effective vaccine against *F. tularensis*, with the most promising attempt being the live vaccinated strain (LVS) derived from the *holarctica* subspecies by passaging it five times through mice (Eigelsbach and Downs, 1961). Oral and aerosol administration of *F. tularensis* LVS has been shown to confer protection against the more virulent type A *F. tularensis* subspecies *tularensis* in a number of organisms such as guinea pigs, rabbits and non-human primates (Eigelsbach and Downs, 1961, Tulis et al., 1970, Stinson et al., 2016). Due to the success of *F. tularensis* LVS in animal models, vaccination studies in humans were undertaken and showed strong protection against low doses of respiratory challenge with a virulent type A strain, with less protection and modified disease symptoms following infection with higher doses (Eigelsbach et al., 1962, Eigelsbach et al., 1967).

In the early 1960s, the Food and Drug Administration (FDA) licensed *F. tularensis* LVS for use in clinical trials and it was used in the USA to prevent laboratory-acquired tularemia. Interestingly, it was shown that incidences of pneumonic, but not ulceroglandular, tularemia were reduced during the period *F. tularensis* LVS was used to protect laboratory workers (Burke, 1977). Despite its relative success at protecting against respiratory tularemia, the FDA has never approved *F. tularensis* LVS as a fully licenced vaccine. This is mainly due to the unknown attenuation source of *F. tularensis* LVS and fears of a potential reversion to virulence (Rohmer et al., 2006). Nevertheless, attempts are still being made to improve the safety and immunogenicity of *F. tularensis* LVS in order to fully licence the vaccine (Pasetti et al., 2008, Mulligan et al., 2017).

Despite not being a fully licensed vaccine, as *F. tularensis* LVS is attenuated in humans while maintaining virulence in mice it has been a crucial research model for better understanding virulent *F. tularensis* infection (Elkins et al., 2003). The median lethal dose (LD_{50}) in mice for LVS is much lower if infected intranasally compared to intradermally (1×10^3 - 10^4 CFU and 1×10^6 - 10^7 CFU respectively) (Cowley and

Elkins, 2011), reflecting difference seen in humans from pneumonic and ulceroglandular tularemia. The Schu S4 strain of *F. tularensis* subspecies *tularensis* has been extensively used as the prototypic model for virulent type A strains since it was isolated (Eigelsbach et al., 1951, Larsson et al., 2005). However, as *F. tularensis* LVS is less virulent than Type A strains such as Schu S4, it is much easier to handle safely and can be used at containment level (CL) 2 instead of CL3. This not only makes it safer to use, but also less expensive. The use of *F. tularensis* LVS has been instrumental in better understanding the course of infection and the host immune response, in the hope of developing successful treatments and vaccines for human tularemia (Golovliov et al., 1995, Conlan et al., 2002, Malik et al., 2006, Roberts et al., 2014).

1.2.4 Cell types involved in *F. tularensis* infection

The high virulence of *F. tularensis* and its potential for use as an aerosolised biological weapon has led to research to understand the host response to the bacterium. The key cell types involved in the early innate immune defence against *F. tularensis* infection are introduced here. The role of cells of the adaptive immune system and epithelial cells are also discussed, considering how they may aid in the clearance of *F. tularensis.* An overview of the functional roles of cell types and the effect of their depletion on host susceptibility to *F. tularensis* can be found in Figure 1.1. As previously discussed, the virulence of *F. tularensis* is dependent on the route of infection and this is also mirrored in the importance of certain cell types when confronted with pulmonary or cutaneous infection. As this PhD is focused on pneumonic *F. tularensis* infection, this is the primary route of infection discussed; however host response to other routes of infection is also mentioned.

1.2.4.1 Macrophages

F. tularensis is able to replicate *in vitro* in murine macrophages harvested from a variety of different tissues, including alveolar, peritoneal and bone marrow-derived macrophages (Anthony et al., 1991, Polsinelli et al., 1994). An important aspect of susceptibility and resistance to intracellular pathogens is conferred by natural resistance-associated macrophage protein (NRAMP), encoded by the *Slc11a1* gene (Govoni and Gros, 1998). The non-functional *Slc11a1* gene in C57Bl/6 mice is critical in conveying susceptibility to pulmonary *F. tularensis* (Powell and Frelinger, 2017), suggesting that macrophage NRAMP plays a crucial role in host defence against *F. tularensis.* Rapid intracellular replication within macrophages can lead to

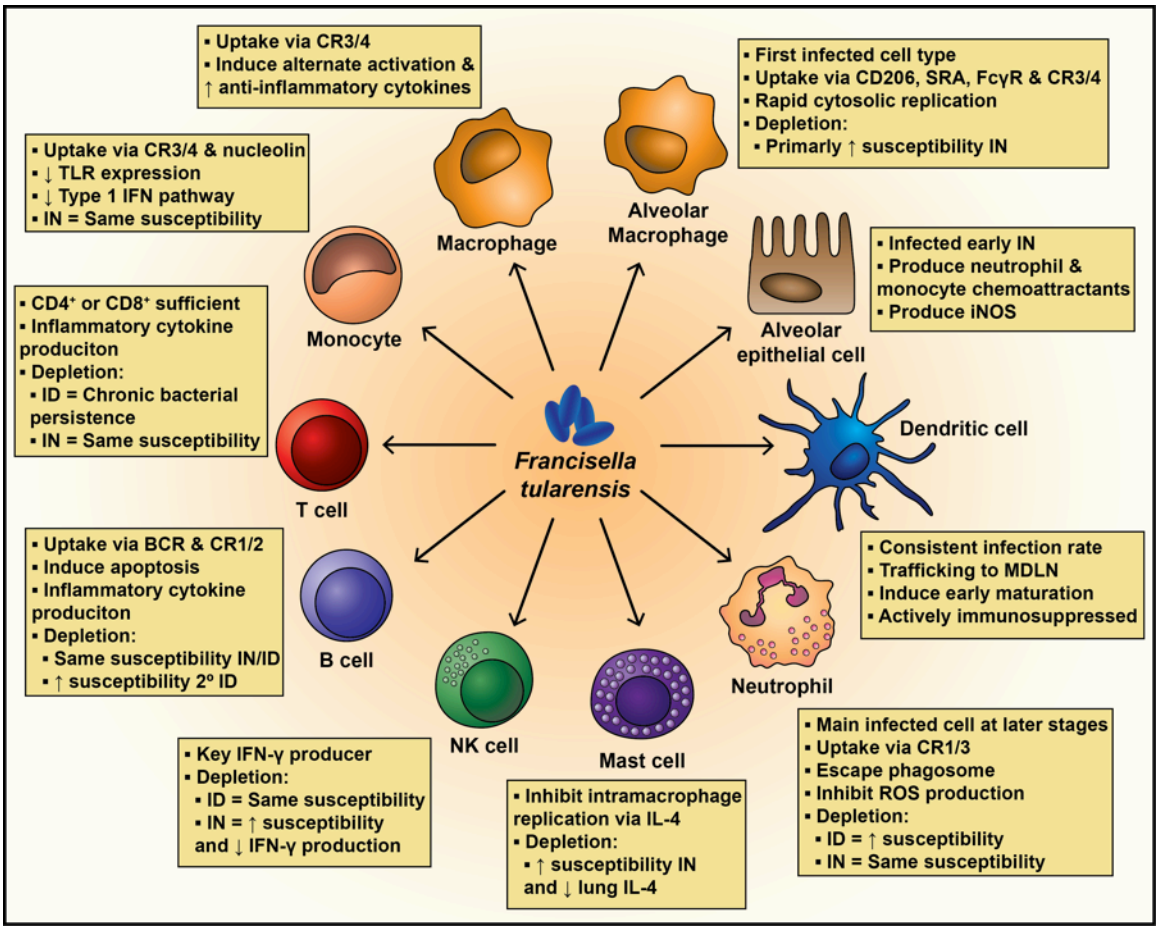

Figure 1.1 | Cell types involved in *F. tularensis* infection. *F. tularensis* has been shown to infect a variety of different cell types within the host. Alveolar macrophages are the first infected cell type following intranasal infection and represent a large, early replicative niche, with uptake mediated by a number of receptors. Depletion of alveolar macrophages has shown mixed results in response to intranasal *F. tularensis* infection but mice primarily show increased susceptibility to infection. Alveolar epithelial cells that line the alveolar space are also infected early on and are important initiators of the innate response through production of neutrophil and monocyte chemoattractant. Dendritic cells appear to be actively immunosuppressed during *F. tularensis*, but remain a relatively large proportion of infected cells and contribute to early dissemination and trafficking of the bacteria. *F. tularensis* is able to further dampen inflammatory responses in macrophages by inducing alternative activation, skewing macrophages towards an anti-inflammatory phenotype. Similarly, TLR expression is reduced on monocytes to reduce Type I IFN responses. Interestingly, depletion of monocytes had no effect on susceptibility to intranasal *F. tularensis* infection. Similarly, despite being the main infected cell type at later stages of infection, neutrophil depletion also shows no altered susceptibility to intranasal infection. *F. tularensis* is able to escape the neutrophil phagosome and evade killing by inhibiting ROS production. Mast cells play an important role in IL-4 production and depletion leads to increased susceptibility to intranasal infection. Similarly, depletion of NK cells leads to increased susceptibility intranasal due to their crucial production of IFNγ. Depletion of the adaptive response, T and B cells, does not increase susceptibility to intranasal infection, but can lead to chronic bacterial persistence and increased susceptibility to secondary infection.

apoptosis *in vitro* (Lai and Sjostedt, 2003). It has been shown that the primary *F. tularensis*-target cell type in the lungs for 24 hours post-infection with intranasal *F. tularensis* LVS infection are alveolar macrophages (Hall et al., 2008), which is not surprising considering alveolar macrophages make up 90% of the leukocytes in the alveolar lumen (Snelgrove et al., 2011).

Interestingly, depletion of alveolar macrophages has given mixed results in respect to outcome of *F. tularensis* infection. One method of depleting alveolar macrophages is by administering clodronate intratracheally, resulting in non-specific depletion of >90% of all airway antigen presenting cells in mice (Van Rooijen and Sanders, 1994, Bosio and Dow, 2005). Following intranasal *F. tularensis* LVS infection, alveolar macrophage-depleted mice survived for significantly longer with significantly lower bacterial burden in the lung up to 3 days post infection, as well as having significantly fewer bacteria in peripheral organs such as the spleen suggesting reduced bacterial dissemination (Bosio and Dow, 2005).

In contrast, a more recent study using a lower infectious dose of *F. tularensis* LVS suggested that clodronate-mediated alveolar macrophage depletion increases susceptibility of mice to pulmonary *F. tularensis* LVS infection (Steiner et al., 2017). Similarly, a more specific depletion of alveolar macrophages using diphtheria toxin (DT) treatment of CD11c.DOG mice led to increased lung burden and an increased inflammatory response. However, DT treatment significantly altered lung homeostasis prior to infection so this may have contributed to changes seen during *F. tularensis* LVS infection (Roberts et al., 2015).

The pro-inflammatory response elicited by macrophages has been shown to be important in protection against *F. tularensis* infection and will be discussed in more detail; however *F. tularensis* may induce the alternative activation of macrophages to diminish the production of pro-inflammatory cytokines and macrophage effector mechanisms. Macrophages are induced to produce IL-4 and IL-13 during *F. tularensis* infection, which amplifies the anti-inflammatory phenotype through autocrine and paracrine mechanisms (Shirey et al., 2008). The process of alternative activation of macrophages from an inflammatory ‘M1’-like phenotype to an anti-inflammatory ’M2’-like phenotype and its role during infection with intracellular pathogens has been reviewed extensively (Gordon, 2003, Gordon and Martinez, 2010).

The literature presents mixed findings regarding the direct importance of macrophages during *F. tularensis* infection. Interestingly, *F. tularensis* mutant

Δ*pyrF*, deficient in *de novo* pyrimidine biosynthesis and unable to replicate in macrophages, showed no decrease in virulence in animal models (Horzempa et al., 2010). This suggests that *F. tularensis* is able to replicate and survive in other cell types while still inducing pathogenesis. Therefore, macrophages by not be directly involved in bacterial clearance, however as they may be playing an important role in orchestrating the subsequent response to infection.

1.2.4.2 Monocytes

Monocytes are important in dealing with *F. tularensis* infection (Hall et al., 2008), with much work *in vitro* being conducted in human monocytes. Following infection with virulent *F. tularensis* Schu S4, primary monocytes downregulate transcripts of TLR2 and an important co-receptor CD14 (Butchar et al., 2008), both important in mounting an inflammatory response against *F. tularensis* (Malik et al., 2006, Chase and Bosio, 2010). *F. tularensis* also downregulates type I IFN signalling in human monocytes (Butchar et al., 2008, Cremer et al., 2011). Yet at the same time, human monocytes produce IL-23 in response to *F. tularensis* in order to induce NK cells to produce IFNγ (Butchar et al., 2007).

The chemokine receptor CCR2 is essential in the migration of monocytes from the bone marrow to sites of bacterial infection (Serbina and Pamer, 2006). Thus, systemic *F. tularensis* challenge in $CCR2^{-/-}$ mice led to a decreased expansion of splenic monocytes and increased bacterial burdens in the spleen compared to wild type (WT) mice (Pietras et al., 2011). Similarly, CX3CR1 has been shown to be important in monocyte homeostasis (Landsman et al., 2009). Interestingly, although $CX3CR1^{-/-}$ mice exhibit increased monocyte recruitment during pulmonary *F. tularensis*, there is no difference in bacterial burdens compared to WT mice (Hall et al., 2009). In the same way, depletion of monocytes and neutrophils in mice via anti-Gr-1 antibody treatment led to no differences in susceptibility to pulmonary *F. tularensis* infection (Conlan et al., 2002).

As with macrophages, the direct role of monocytes in bacterial clearance is unclear. Although these data are from studies that will have effects on cells other than monocytes, they do suggest that monocytes are important in eliciting the subsequent inflammatory response towards *F. tularensis*, but may not be as important during pulmonary infection.

1.2.4.3 Neutrophils

Another important cell type recognised as one of the first responders to *F. tularensis* infection is neutrophils. Extensive neutrophil recruitment occurs in the lung at day 3 post-infection, making up around 50% of total LVS-infected cells (Hall et al., 2008). Neutrophils are key innate immune cells that are able to kill invading pathogens by ingesting them following capture in neutrophil extracellular traps (NETs) and through the production of reactive oxygen species (ROS) (Nguyen et al., 2017, Papayannopoulos, 2018). However, unlike other intracellular pathogens, *F. tularensis* is able to escape the neutrophil phagosome and replicate in the cytosol. Furthermore, it has been shown that *F. tularensis* LVS can evade ROS-dependent killing by human neutrophils through disruption of NADPH oxidase assembly (McCaffrey and Allen, 2006, McCaffrey et al., 2010). Thus neutrophils may in fact provide a safe replicative niche for *F. tularensis* persistence.

Although it is clear that neutrophils play a role during *F. tularensis* infection, whether they are critical for defence against the infection remains unclear. The effect of neutrophil depletion on *F. tularensis* infectious outcome is dependent on the route of infection. Neutrophils appear critical in response to primary systemic infection; neutrophil-depleted mice succumb to otherwise sub-lethal *F. tularensis* LVS doses when administered via intravenously or intradermallly (Sjöstedt et al., 1994, Conlan et al., 2002). In contrast, the effect of neutrophil depletion during pulmonary infection is much less evident, with only a minor increase in bacterial burden in peripheral organs observed following neutrophil depletion (Conlan et al., 2002).

Interestingly, a recent study suggested that timing of the neutrophil depletion was an important factor. Depletion of neutrophils at day 3 post-infection, as opposed to at the time of infection, rendered mice highly susceptible to pulmonary *F. tularensis* infection (Steiner et al., 2017). This suggests that depleting neutrophils once they have become the main replicative niche for the bacteria leads to an exacerbated infectious outcome. However, in this study, susceptibility was only determined by the percentage survival of mice and not bacterial burden, which could potentially be a better indicator of direct infectious outcome. Interestingly, excessive neutrophil recruitment may also directly contribute to *F. tularensis* pathogenesis in the lung. Mice deficient in an important producer of neutrophil chemoattractants, metalloproteinase 9, exhibited reduced neutrophil recruitment in the lung, as well as decreased bacterial burden, pro-inflammatory cytokine production and

histopathology (Malik et al., 2007). These studies highlight the fine balance involved in neutrophil-mediated protection and the exacerbation of *F. tularensis* pathology.

The fact that neutrophils become the most infected cell type during *F. tularensis* infection highlights the role of neutrophils as a replicative niche for the bacteria. Furthermore, this is supported by the ability of *F. tularensis* to target a key neutrophil effector function through dampening ROS-dependent killing, as well as the mixed infectious outcome following neutrophil depletion.

1.2.4.4 Dendritic cells

There is a large shift in the percentage of *F. tularensis*-infected macrophages and neutrophils during the first 3 days of pulmonary infection, yet this is not the case for dendritic cells (DCs). The percentage of infected DCs remains consistently at around 10% throughout the first 3 days of infection with *F. tularensis* LVS (Hall et al., 2008). Interestingly, it was shown that *F. tularensis* LVS is able to induce early maturation of airway DCs, but not alveolar macrophages, with increased expression of MHC-II and CD86 within 24 hours of infection *in vivo* (Bosio and Dow, 2005). Yet at the same time, *F. tularensis*-infected DCs are actively immunosuppressed and show decreased production of pro-inflammatory cytokines (Bosio et al., 2007, Chase et al., 2009). Furthermore, DCs have been linked with trafficking of bacteria to the draining mediastinal lymph node during the early stages of *F. tularensis* infection (Bar-Haim et al., 2008). These data suggest that DCs may serve to facilitate early bacterial dissemination by inhibiting the elicitation of an inflammatory response and acting as a replicative niche throughout early infection.

1.2.4.5 Natural killer cells

Natural killer (NK) cells are important in protection against various microbial pathogens (Horowitz et al., 2011); however, studies investigating their role during *F. tularensis* infection has shown mixed results. NK cell depletion using an anti-asialo GM1 antibody showed no difference in bacterial burden in the lungs of mice infected intradermally with *F. tularensis* LVS (Bokhari et al., 2008). On the other hand, depletion of NK cells before intranasal infection with *F. tularensis* LVS led to a decreased number of IFNγ secreting cells and reduced mouse survival (Lopez et al., 2004). Difficulties in fully depleting NK cells without affecting other cell types *in vivo* may contribute to varying results (Nishikado et al., 2011).

Regardless of the direct role of NK cell during protection against *F. tularensis*, it has become evident that these cells are one of the primary sources of IFNγ during *F. tularensis* infection. *In vitro* infection of mouse hepatic mononuclear cells with *F. tularensis* LVS showed that approximately half of the cells that contributed to the increase in secretion of IFNγ were NK cells (Wickstrum et al., 2007). Similarly, the source of IFNγ produced in mice in response to *F. tularensis* LVS infection was also shown to primarily be NK cells in liver and the lung (Lopez et al., 2004, De Pascalis et al., 2008). Furthermore, NK cell depletion led to a 50% reduction in hepatic serum IFNγ levels compared to non-depleted mice (Bokhari et al., 2008). Although these data highlight the importance of NK cells in their production of IFNγ during *F. tularensis* infection, the minimal effect of depletion on infectious outcome suggests that other cell types are able to effectively compensate.

1.2.4.6 Mast cells

Mast cells are most prominently known in their role in allergic inflammation, but also have varying roles in controlling bacterial infections (Amin, 2012, Johnzon et al., 2016). Mice deficient in mast cells showed increased susceptibility to pulmonary *F. tularensis* infection compared to WT mice and this was accompanied by reduced levels of IL-4 production in the lung of infected mice (Ketavarapu et al., 2008). Furthermore, mast cells were able to inhibit intra-macrophage growth of *F. tularensis in vitro* in an IL-4 and TLR2-dependent manner (Ketavarapu et al., 2008, Rodriguez et al., 2012). Interestingly, FcεRI-associated vesicles from mast cells directly interact with macrophages via trogocytosis and subsequently upregulate expression of caspase-1 in macrophages during *F. tularensis* infection *in vitro* (Rodriguez et al., 2016). These data further illustrate the importance of mast cells in helping to orchestrate the immune response against *F. tularensis* infection.

1.2.4.7 T cells

The majority of T cells express the αβ T cell receptor (TCR), with these being subdivided into various T cell subsets dependent on the expression of CD4, CD8 and the production of signature cytokines (Broere et al., 2011). Mice deficient in αβ-TCR, thus the majority of T cells, initially control a sublethal intradermal *F. tularensis* infection, but a high bacterial burden is maintained and they eventually succumb to the infection. Furthermore, specific deletion of either $CD4^+$ or $CD8^+$ T cells leads to efficient clearance of the bacteria, suggesting both $CD4^+$ and $CD8^+$ T cells are individually sufficient to clear *F. tularensis* infection (Cowley et al., 2005). In fact, expansion of antigen-specific $CD8^+$ T cells occurred between days 5-9 p.i.

following intranasal challenge, with the peak $CD8^+$ T cell response thought to occur between days 9 and 14 (Place et al., 2017). Interestingly, mice simultaneously depleted of $CD4^+$ and $CD8^+$ T cells, unlike αβ-TCR-deficient mice, survive but develop a long-term chronic *F. tularensis* infection. In this case control of bacterial infection is attributed to a specific population of $CD4^-$ $CD8^-$ T cells (Cowley et al., 2005). Unfortunately, the role of T cells during pulmonary *F. tularensis* has been studied much less. Thymectomized mice (removal of the thymus and subsequently no T cell development) and SCID mice (deficient in functional T and B cells) are no more susceptible to intranasal *F. tularensis* challenge than WT mice, with all succumbing equally to infection (Chen et al., 2004b). However, virulent type A *F. tularensis* has been shown to induce depletion of αβ T cells in the lung and lead to thymic atrophy (Chen et al., 2005a, Sharma et al., 2011), suggesting that it may be able to disrupt T cell-mediated immunity to pulmonary infection.

1.2.4.8 B cells

B cells are an important part of the adaptive immune response and can be crucial in the defence of pathogens, as well as being manipulated by some pathogens to enhance survival (Nothelfer et al., 2015). *F. tularensis* effectively replicates within B cells, via B cell receptor-mediated uptake. Intracellular replication within B cells eventually leads to apoptosis of infected cells, as well as causing nuclear fragmentation and membrane blebbing of neighbouring uninfected B cells (Krocova et al., 2008, Plzakova et al., 2015). These data suggest that *F. tularensis* may target B cells during infection. In fact, *F. tularensis* infects peritoneal B cells during early intraperitoneal infection that subsequently produce a number of inflammatory cytokines (Plzakova et al., 2014). This suggests that B cells may play a role in the protective response during *F. tularensis* infection. However, B cell-deficient mice were no more susceptible than WT mice following intranasal or intradermal infection with *F. tularensis*, although they showed increased susceptibility to secondary intradermal infection (Elkins et al., 1999, Chen et al., 2004b).

1.2.4.9 Alveolar epithelial cells

As well as alveolar macrophages, alveolar epithelial cells are a dominant cell type within the alveolar space and line the majority of the alveolar surface. Therefore, it is interesting to note that *F. tularensis* interacts with type II alveolar epithelial (ATII) cells 2 hours following intranasal infection. Furthermore, primary human ATII cells stimulated with *F. tularensis in vitro* produced high levels of neutrophil and monocyte chemoattractants IL-8 and MCP1 respectively (Gentry et al., 2007). This

suggests that ATII cells may play a role in aiding the development of the innate immune response against *F. tularensis*. They may also play a direct role in protection against the pathogen, as murine epithelial cells have been shown to produce iNOS *in vivo* following intranasal *F. tularensis* infection and can inhibit intracellular growth *in vitro* via reactive nitrogen intermediates (Maggio et al., 2015).

1.2.5 Intracellular life cycle

It is clear that *F. tularensis* is an opportunistic bacterium that is able to infect and replicate within a variety of different cell types. The intracellular life cycle of *F. tularensis* is fairly similar regardless of the cell type infected, from cellular uptake, phagosomal escape, cytosolic replication and finally transmission to uninfected cells (Figure 1.2). Here, various aspects of the intracellular life cycle are discussed, along with how *F. tularensis* is able to manipulate host cell machinery to increase bacterial survival.

1.2.5.1 Cell entry

It is known that *F. tularensis* predominantly infects host mononuclear phagocytes, macrophages and neutrophils in particular, using them as a replicative niche (Hall et al., 2008). The mode of uptake, along with the intracellular interactions between the bacteria and host cell machinery, are important in determining bacterial virulence (Clemens and Horwitz, 2007). Entry into macrophages appears to be via a recently identified process of looping phagocytosis involving pseudopod loops (Figure 1.2), a process that is strongly dependent on complement receptors (CRs). Different CRs have been further implicated in the internalisation of *F. tularensis* LVS into different cell types. CR1 and CR2 are involved in uptake of *F. tularensis* LVS into B cells (Plzakova et al., 2015), CR1 and CR3 in the uptake of serum-opsonised *F. tularensis* LVS into neutrophils (Schwartz et al., 2012b), while CR3 and CR4 are thought to be the main receptors for the uptake of serum-opsonized LVS to enter monocyte-derived macrophages and dendritic cells (DCs) (Clemens et al., 2005). Thus, antibody inhibition of CR3 and CR4 significantly inhibited the uptake of *F. tularensis* LVS by monocyte-derived macrophages (MDM) (Clemens et al., 2005).

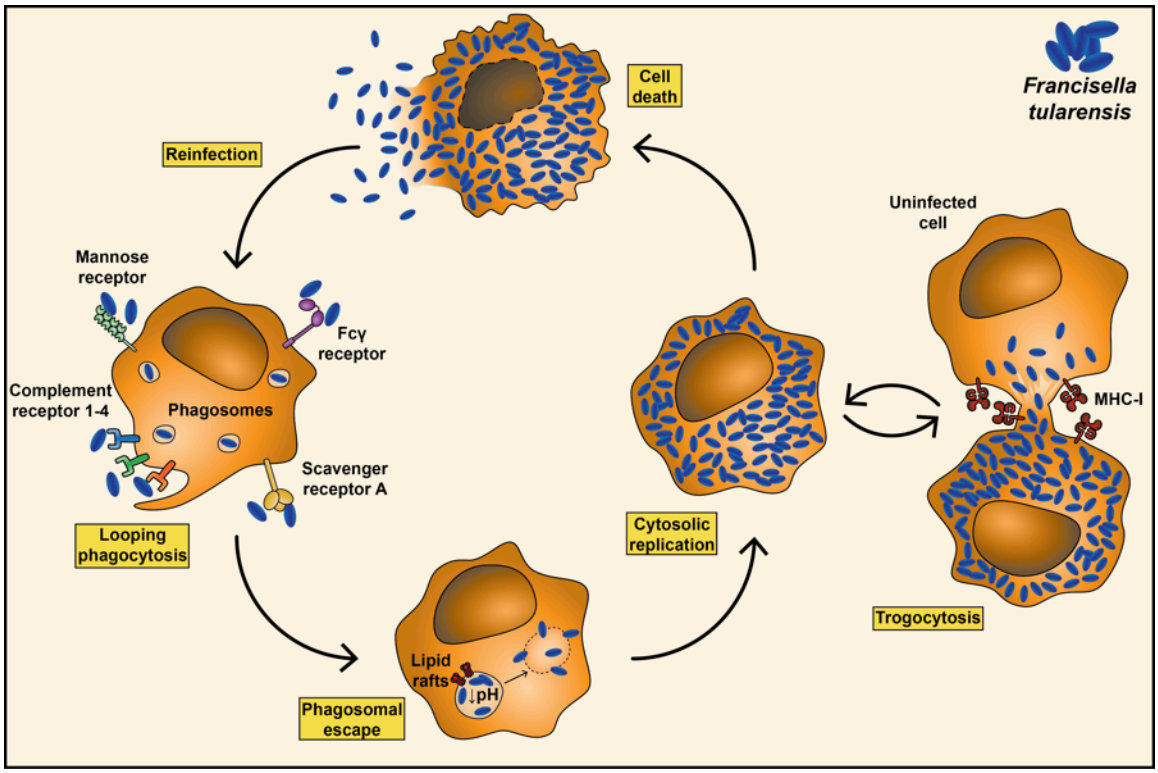

Figure 1.2 | The *in vitro* intracellular life cycle of *F. tularensis*. As previously discussed, *F. tularensis* is able to infect multiple cell types. Uptake across a number of cell types is mediated by complement receptors (CR) 1-4. Macrophages have been shown to internalise bacteria via looping phagocytosis and incorporate them into phagosomes through interactions with a number receptors such as scavenger receptor A, Fcγ receptor and the mannose receptor. At this point *F. tularensis* is able to escape the phagosome within 1-4 hours by inhibiting phagosomal maturation and lysosomal fusion, as well as disrupting the phagosomal membrane through acidification and by using lipid rafts. *F. tularensis* then undergoes exponential cytoplasmic replication, ultimately leading to cell death and release of bacteria which are able to reinfect other cells. Interestingly, a novel process of bacterial transmission to uninfected cells independent trogocytosis has been described. This involves the direct transfer of cytoplasmic bacteria and plasma membrane fragments between live cells, including acquisition of functional major histocompatibility complex I. Adapted from (Chong and Celli, 2010).

The mannose receptor (CD206) has also been implicated in the uptake of *F. tularensis*, but it appears to be more important in the uptake of non-opsonised *F. tularensis* LVS. Inhibition of the mannose receptor with soluble mannan showed significantly decreased phagocytosis of non-opsonised *F. tularensis* LVS by MDM (Schulert and Allen, 2006). Interestingly, no significant difference was seen in the uptake of both opsonised and non-opsonised *F. tularensis* LVS by J774 murine macrophage-like cells following mannan treatment (Schulert and Allen, 2006, D'Elia et al., 2011a), suggesting that different cells types used *in vitro* may have differing responses to infection with *F. tularensis* LVS. Opsonisation significantly increased bacterial uptake by MDM, with mannan treatment only providing minimal inhibition

(Schulert and Allen, 2006). Taken together, these results indicate that opsonised bacteria are greatly dependent on CR3 and CR4 for uptake, with the mannose receptor being dispensable. The opposite can be said for non-opsonised *F. tularensis* LVS with blockade of CR3 having no effect on MDM uptake of non-opsonised bacteria (Schulert and Allen, 2006). Other receptors such as scavenger receptor A and the Fcγ receptor have also been implicated in various uptake mechanisms, each altering the intracellular fate of *F. tularensis* (Pierini, 2006, Jones et al., 2014). Interestingly, nucleolin has also been shown to traffic from the nucleus to act as a cell surface receptor for uptake of *F. tularensis* into human monocytes (Barel et al., 2010). Deletion or blockade of any one receptor does not lead to complete inhibition of *F. tularensis* internalisation, suggesting that multiple pathways may be used depending on the circumstances of infection, adding to the adaptability of this bacterium.

1.2.5.2 Phagosomal escape and cytosolic replication

The intracellular phase of *F. tularensis* infection begins with the bacteria residing in non-acidified phagosomes, followed by rapid escape into the cytoplasm where replication can occur (Santic et al., 2006). The bacterium is able to achieve this through prevention of full maturation, acidification and lysosomal fusion of the phagosome. This is supported by the findings that dead *F. tularensis* and latex beads, but not live *F. tularensis*, are located within phagosomes that stain with lysosomal markers such as cathepsin D and have a much lower pH of 5.5 compared to 6.7 for live *F. tularensis* (Clemens et al., 2004). Interestingly, prevention of acidification with weak bases chloroquine and NH_4Cl and the Na^+/H^+ pump inhibitor ouabain has been shown to significantly inhibit *F. tularensis* LVS replication in macrophage cytoplasm, suggesting that early maturation and acidification may be required for efficient bacterial growth (Fortier et al., 1995). Although this finding contradicts the previous study concerning phagosomal acidification, blocking acidification would also affect the levels of available intracellular iron that dissociates from transferrin at lower pH of 5.5 (Steiner et al., 2014). The importance of iron for the survival of *F. tularensis* LVS was shown with mutants deficient in the ferrous iron (feo) and ferric-siderophore (fsl) uptake systems. These double deletion mutants of *F. tularensis* LVS were unable to replicate in the murine macrophage-like cells J774A.1 and had attenuated virulence in mice (Perez and Ramakrishnan, 2014). The impaired replication of *F. tularensis* LVS after blocking acidification could have been indirectly due to the lack of available iron in the cell. Yet this then raises the issue that if *F. tularensis* inhibits

phagosome maturation and acidification as suggested in the first study mentioned, it must sequester iron once it has escaped the phagosome.

What can be agreed upon is that after entry into the cell, *F. tularensis* is able to disrupt the phagosomal membrane and escape into the cytoplasm after 1 to 4 hours (Golovliov et al., 2003, Chong et al., 2008, Clemens et al., 2009). The exact mechanism by which *F. tularensis* escapes the phagosome is unknown. However it has been described that *F. tularensis* LVS is able to gain entry into macrophages via lipid rafts (Tamilselvam and Daefler, 2008), which is also a characteristic of other intracellular bacteria such as *Listeria monocytogenes*. This mechanism suggests that *F. tularensis* may have unidentified cholesterol-targeted proteins, such as Listeriolysin O in *L. monocytogenes*, that can be used to escape the phagosome (Kayal and Charbit, 2006, Meibom et al., 2009).

Regardless, the importance for *F. tularensis* LVS in finding a replicative niche has been demonstrated *in vitro*. Inhibition of *F. tularensis* LVS uptake into lung cells with LY294002, wortmannin (PI3-kinase inhibitors) and MG132 (inhibitor of proteosome activity) produced reduced levels of inflammatory cytokines such as IL-6 and α when compared to non-inhibited cells. To support the *in vitro* findings, wortmannin treatment in mice infected intranasally with *F. tularensis* LVS caused significant reductions in secreted levels of IL-6, TNFα and IFNγ in the lung compared to untreated infected mice (D'Elia et al., 2011a).

There is also evidence to show that during cytoplasmic replication *F. tularensis* can modulate the autophagy pathway. During the cytoplasmic replication phase of *F. tularensis* LVS infection, a portion of bacteria appear to become enclosed within large autophagy-derived vacuoles that have been termed *Francisella*-containing vacuoles (FCVs) (Checroun et al., 2006). These vacuoles co-localised with the autophagy marker LC3 and were significantly reduced when autophagy was inhibited using 3-methyladenine (3-MA). Yet, the reduced number of FCV following 3-MA treatment did not affect the viability and replication of *F. tularensis* LVS (Checroun et al., 2006). These results directly contradict more recent findings that 3-MA treatment significantly decreases *F. tularensis* LVS growth in fibroblasts and bone marrow-derived macrophages (BMDM) (Steele et al., 2013). However, in the later study, double the concentration of 3-MA was used and it was also given at an earlier time point, suggesting comparison between the two results must be taken with caution.

Thus, there is clearly much deliberation over many aspects of the entry and intracellular life cycle of *F. tularensis* and how the bacterium manipulates the host cell. Nevertheless, it is clear that *F. tularensis* is able to selectively modulate aspects of host cell machinery to its advantage.

1.2.5.3 Cell-cell transmission

A characteristic of *F. tularensis* infection is rapid replication and infection of numerous cell types, particularly during pulmonary infection (Hall et al., 2008, Roberts et al., 2014). Once in the cytoplasm, *F. tularensis* is able to quickly replicate up to 1000-fold and induce apoptosis within 12-24 hours (Lai and Sjostedt, 2003). *In vitro* there is no decrease in bacterial burden following apoptosis, suggesting that host cell apoptosis is not a protective mechanism and is induced by the increasing bacterial number (Lai et al., 2001). However, mice deficient in key components of the apoptotic pathway, caspase-1 and ASC, exhibit increased mortality and *F. tularensis* burdens compared to WT mice, suggesting that apoptosis does play a role in defence against the pathogen (Mariathasan et al., 2005). Furthermore, it has been shown that *F. tularensis* is able to inhibit apoptosis pathways in human neutrophils, prolonging its time within the cytosol to increase bacterial replication (Schwartz et al., 2012a). It is evident that *F. tularensis* can interfere with host apoptotic pathways, dictating when cell death and subsequent bacterial spread to other cells can occur.

Dampening the apoptotic response to increased bacterial burdens early during *F. tularensis* infection would be beneficial to the pathogen in order to avoid detection by the host (Green et al., 2009). Despite this there is still significant bacterial spread to other cell types (Hall et al., 2008), and recently a novel mechanism of cell to cell spread has been suggested. Thus, it has been proposed that *F. tularensis* is able to directly transfer from infected cells to uninfected macrophages (Steele et al., 2016) via trogocytosis, which involves the transfer of plasma membrane fragments between two live cells independent of phagocytosis of apoptotic bodies (Joly and Hudrisier, 2003). Trogocytosis was upregulated in infected cells *in vitro* and bacterial transfer between cells was also accompanied by the exchange of functional major histocompatibility complex 1 (MHC-I) (Steele et al., 2016). Trogocytosis may be a way for rapid bacterial dissemination to other cells early during infection with *F. tularensis*, while increasing chances of immune evasion.

1.3 Immune response to *F. tularensis*

An important characteristic of *F. tularensis* is the ability to evade immune detection and dampen host immune responses during the early stages of infection. Firstly, important host mechanisms of bacterial detection through the complement pathway and pattern recognition receptors (PRRs) are introduced. Furthermore, the mechanisms of how *F. tularensis* is able to manipulate these pathways to hinder immune signalling are explored. The ability of *F. tularensis* to evade or avoid detection by host protection mechanisms subsequently contribute to the suppression, or perhaps more appropriately the postponement, of appropriate innate immune responses to infection. Thus, key pro-inflammatory cytokines and chemokines involved in defence against *F. tularensis* infection are outlined, as well as regulatory cytokines that may play a role in regulating the excessive inflammatory response characteristic of later *F. tularensis* infection. The effects of murine depletion models of key PRRs and cytokines on susceptibly to *F. tularensis* infection are discussed throughout this section (Table 1.1).

1.3.1 Complement and pattern recognition receptors

1.3.1.1 Complement and antibody

Complement has long been considered an important first line of defence against microbial pathogens through direct microbial killing, as well as orchestrating immunological and inflammatory processes during infection (Ricklin et al., 2010). It has been well established that during the initial stages of inhalational infection *F. tularensis* is able to suppress the induction of the immune response. Mechanisms by which *F. tularensis* achieve this are not fully understood, but progress has been made to elucidate certain aspects of innate immune response modulation. As was mentioned earlier, *F. tularensis* is able to interact with complement receptors in order to promote internalisation by phagocytic cells such as macrophages. It has been shown that C3 complement components, such as C3b and more importantly iC3b, are deposited on the surface of the bacteria and this is correlated with increased phagocytosis by host cells (Ben Nasr and Klimpel, 2008). This depositionof C3b is required to form C5 convertases, leading to the recruitment of the membrane attack complex (MAC) that forms pores in the bacterial membrane and ultimately causes lysis (Sarma and Ward, 2011).

Table 1.1 | The effect of depletion/knockout* of immune response components on murine infection with *F. tularensis* LVS

Component	Intradermal	Dose (CFU)	Intranasal	Dose (CFU)	References
Pattern Recognition Receptors					
TLR-2	↑ Susceptibility (~60% survival vs 100% WT)	~38,680	↑ Susceptibility (~20% survival vs 100% WT)	~4330	Abplanalp et al., 2009
MyD88	↑ Susceptibility (0% survival vs 100% WT)	~45,000	↑ Susceptibility (0% survival vs ~80% WT)	~5360	Abplanalp et al., 2009
TLR-4	Slight susceptibility increase at very high dose (~25% survival vs ~50% WT)	~1.1 x 10^7	No change (High dose = 0% survival KO & WT; Low dose = 100% survival KO & WT)	~2000 (HD) ~100 (LD)	Chen et al., 2004a; Chen et al., 2005b
Cytokines & Chemokines					
IFNγ	↑↑ Susceptibility - Lethal at very low dose	~20	↑ Susceptibility at very low dose (~40% survival vs 100% WT)	~100	Chen et al., 2004b
TNFα	↑↑ Susceptibility - Lethal at very low dose	~20	↑ Susceptibility at very low dose (~20% survival vs 100% WT)	~100	Chen et al., 2004b
IL-12p35	Delayed bacterial clearance but survive	~3 x 10^6	↑ Susceptibility (~0% survival vs 100% WT)	~1000	Elkins et al., 2002; Duckett et al., 2005
IL-12p40	All survive but never clear bacteria	~3 x 10^6	↑ Susceptibility (~0% survival vs 50% WT)	~1000	Elkins et al., 2002; Duckett et al., 2005
IL-12Rβ2	↑ Susceptibility (~20% survival vs 100% WT)	~1 x 10^5	↑↑ Susceptibility - Lethal at very low dose	~100	Melillo et al., 2013
IL-23p19	No change - Same LD_{50} as WT	> 10^6	No significant change (~50% survival vs ~70% WT)	~1000	Kurtz et al., 2014
IL-17	↑ Susceptibility only at high dose (0% survival vs ~80% WT)	~7 x 10^6	↑ Susceptibility at low dose (~40% survival vs 100% WT)	~500	Cowley et al., 2010
IL-6	↑ Susceptibility (~10% survival vs 80% WT)	~10000	↑ Susceptibility (~0% survival vs 100% WT)	~2000	Kurtz et al., 2013
IL-4	No change - Trend towards decreased susceptibility (LD50 = 9 x 10^5 vs 2 x 10^5 WT) †	N/A	↑ Susceptibility (~30% survival vs ~75% WT)	~3000	Leiby et al., 1992; Ketavarapau et al., 2008
IL-10	↓ Susceptibility (~90% survival vs 0% WT)	~2 x 10^6	↑ Susceptibility (~15% survival vs ~75% WT)	~1600	Metzger et al., 2013
TGF-β††	**?**	N/A	No change in organ bacterial burden by day 4 p.i	~1 x 10^4	Vautier et al. unpublished observations
MIG	Comparable bacterial clearance at multiple doses	~10^4 - 10^7	**?**	N/A	Park et al., 2002
CX3CR1	**?**	N/A	No change in organ bacterial burden by day 3 & 7 p.i	1000	Hall et al., 2009

* Data represent the effect of *in vivo* knockouts unless otherwise stated

† Data for intradermal infection represents effect of depletion by anti-IL4 (11B1) blocking mAb

†† Data represent effect of depletion by anti-TGF-β blocking mAb

Interestingly, the level of MAC deposition on the surface of LVS was significantly decreased compared to the levels of C3b. This attenuation of lethal MAC recruitment by *F. tularensis* may be through the recruitment of a major complement regulator, glycoprotein factor H, to the bacterial surface (Ben Nasr and Klimpel, 2008). The generation of iC3b on the bacterial surface through cleavage of C3b by factor H leads to the inefficient assembly of the MAC, as well as serving as an opsonin through interactions with CR3 and CR4. Both CR3 and CR4 have been shown to promote efficient phagocytosis of LVS by macrophages and dendritic cells (Ben Nasr et al., 2006, Ben Nasr and Klimpel, 2008). These findings are a prime example of how *F. tularensis* is able to both negatively and positively exploit a cellular process to increase its survival. Similarly, *F. tularensis* has been shown to bind to the complement regulatory protein vitronectin that may further protect the bacterium from MAC-mediated lysis and promote internalisation (Singh et al., 2010, Madar et al., 2015). Furthermore, *F. tularensis* has been shown to bind surface plasminogen that can then be activated into plasmin (Clinton et al., 2010), as plasmin can also degrade soluble antibody, it may allow *F. tularensis* to prevent antibody mediated complement activation (Jones et al., 2012).

1.3.1.2 Toll-like receptors

An important characteristic of many successful pathogens is their ability to avoid engagement by PRRs, such as the membrane-anchored Toll-like receptors (TLRs) and cytosolic NOD-like receptors (NLRs). As *F. tularensis* resides in membrane-associated phagosomes before escaping into the host cytosol, it has developed mechanisms to avoid detection by both types of PRRs or to engage receptors to promote a weaker inflammatory response. An example of this mechanism is the unique lipopolysaccharide (LPS) expressed by *F. tularensis*. LPS is a large, conserved molecule found on the outer membrane of Gram-negative bacteria and is often responsible for a strong TLR4-dependent immune response in the host (Trent et al., 2006). The lipid A anchor portion of LPS is the main component recognised by TLR4, but *F. tularensis* lipid A differs by having three acyl chains instead of six, longer fatty acid chains and no phosphate groups, giving it poor TLR4 stimulatory activity (Phillips et al., 2004, Barker et al., 2016). In fact, $TLR4^{-/-}$ mice showed no significant difference in levels of IFNγ or IL-12p40 following intradermal or intranasal infection with *F. tularensis* LVS compared to WT mice (Chen et al., 2004a, Chen et al., 2005b). Survival rates for $TLR4^{-/-}$ mice infected intranasally with *F. tularensis* LVS was no different to that of WT mice (Chen et al., 2004a), while

intradermal infection of TLR4$^{-/-}$ mice only led to decreased survival at large doses (Chen et al., 2005b).

On the other hand, TLR2 has been shown to be a critical mediator of the innate immune response against *F. tularensis*. Following intranasal or intradermal infection with *F. tularensis* LVS, TLR2 and Myd88 (a TLR adaptor protein) deficient mice were both more susceptible, with impaired cytokine production towards *F. tularensis* and reduced ability to control growth and dissemination (Abplanalp et al., 2009). It was also shown that *F. tularensis* LVS co-localized with phagosomes that were positive for TLR2/MyD88 *in vitro* (Cole et al., 2007). Interestingly, *F. tularensis* LVS mutants unable to escape the phagosome and enter the cytoplasm showed greatly increased expression of TLR2-dependent pro-inflammatory cytokines such as TNFα (Cole et al., 2008). These findings suggest that although TLR2 is important in initiating an immune response against *F. tularensis*, the bacterium must be able to dampen TLR2-mediated responses earlier in infection when in the phagosome.

The possibility of other important pathways was supported through the finding that MyD88$^{-/-}$ mice showed increased susceptibility to lower doses of *F. tularensis* LVS compared to TLR2$^{-/-}$ mice, although both showed equal susceptibility to higher dose infection (Abplanalp et al., 2009). These data suggest another role for MyD88 beyond its clear importance as a TLR2 adaptor protein. However, other Myd88-dependent molecules, such as TLR4 and TLR9, have been shown to have no critical involvement in responses to *F. tularensis* (Collazo et al., 2006, Abplanalp et al., 2009). Nevertheless, further elucidation of the downstream signalling of TLR2/MyD88 has demonstrated that BMDMs infected with *F. tularensis* LVS induce splicing of the transcription factor XBP1 that is required for the production of inflammatory cytokines such as TNFα and IL-6 (Martinon et al., 2010). It was further shown that splicing of XBP1 was impaired in TLR2-deficient mice, which was accompanied with increase bacterial burden in infected organs, a finding reproduced in XBP1-deficient mice (Martinon et al., 2010).

Infection of MDMs with *F. tularensis* LVS has been shown to induce the increased expression of the micro-RNA miR-155 in a TLR2-dependent manner. This upregulation ultimately leads to the inhibition of Src homology 2-containing inositol phosphatase (SHIP) and MyD88 translation. However, overexpression or inhibition of miR-155 had no significant effect on bacterial uptake by MDMs or TNFα and IL-6 secretion (Bandyopadhyay et al., 2014). The miR-155-mediated regulation of the immune response during infection appears to be part of a complicated

feedback loop. Loss of SHIP induces activation of the PI3 kinase/Akt pathway that is important for cell survival and activation of pro-inflammatory responses, while loss of MyD88 would dampen the inflammatory response through dysregulation of TLR signalling (Bandyopadhyay et al., 2014). The complex role micro-RNAs play during *F. tularensis* infection needs to be studied further, but may be a way for *F. tularensis* LVS to both impair host defences while at the same time ensuring macrophage survival to enhance bacterial growth and dissemination.

1.3.1.3 NOD-like receptors

Once escaped from the phagosome, *F. tularensis* must then avoid detection by the cellular PRRs such as NLRs. It has been shown that macrophages with LVS infection in the cytosol eventually undergo apoptosis that is dependent on inflammasome assembly and inflammatory cytokine (e.g. IL-1β) release through caspase-1 and the adaptor protein ASC signalling. Mice deficient in these two proteins were more susceptible to *F. tularensis* infection, possibly due to the fact that both caspase-1 and ASC-deficient macrophages are resistant to *F. tularensis*-induced cell death (Mariathasan et al., 2005). Recently this pathway has been further elucidated through the identification of an NLR responsible for recognition of *F. tularensis* in the cytoplasm. Absent in melanoma 2 (AIM2) is an NLR that promotes inflammasome assembly and caspase-1 activation via interactions with ASC (Gavrilin and Wewers, 2011, Man et al., 2016). Activation of the AIM2 inflammasome specifically by *F. tularensis* has been shown to be dependent on the transcription factor IRF1 and expression of guanylate-binding proteins (GBPs) (Man et al., 2015). The *F. tularensis* gene *mviN*, encoding for a putative lipid II flippase, has been shown to be important in evading activation of the inflammasome and contributes to bacterial virulence (Ulland et al., 2010). Intraperitoneal infection of mice with an *mviN* mutant *F. tularensis* LVS improved survival and decreased bacterial burden compared to infection with WT bacteria. This decreased virulence was attributed to the increased activation of AIM2-dependent inflammasome activation (Ulland et al., 2010). These findings suggest that dampening or avoidance of AIM2 signalling by *F. tularensis* is important for bacterial survival and virulence.

1.3.2 Inflammatory cytokines

For the purpose of this thesis, the introduction into the role of specific cytokines in contributing to protection against *F. tularensis* infection is in isolation. However, it is important to remember the influence the inflammatory and regulatory cytokines discussed below have on the many cell types mentioned earlier. Many cellular

functions are driven by the secretion and subsequent response to cytokines {Arango Duque, 2014 #1390}{Nemeth, 2016 #1391}, thus the role of cytokines discussed here must be considered in the context of the overarching response to infection.

1.3.2.1 IFNγ and TNFα

The inflammatory Th1 cytokines IFNγ and TNFα are important in controlling the initial infection to many intracellular pathogens, including *F. tularensis.* However, as mentioned previously, a key characteristic of respiratory *F. tularensis* infection is the lack of a pro-inflammatory response during the first days of infection. Detectable levels of IFNγ and TNFα mRNA can be found in the skin following intradermal infection with *F. tularensis* LVS by 24 hours post-infection, with significant increases by 48 hours (Stenmark et al., 1999). Similarly, protein production of IFNγ and TNFα in liver homogenates following intradermal infection of LVS was detected by 24 hours post-infection, with significant increases by 48 hours post-infection (Golovliov et al., 1995). Following intranasal infection of sublethal *F. tularensis* LVS dose (1000 CFU), mice showed significant increase in IFNγ expression by lung lymphocytes by 96 hours post-infection, with detectable levels only apparent by 72 hours post-infection (Lopez et al., 2004). Another study using a similar sublethal dose of *F. tularensis* LVS for intranasal infection showed increases in IFNγ and TNFα protein production in lung homogenates as late as 5 days post-infection (Malik et al., 2006). Analysis of lung homogenates following a lethal intranasal dose (10,000 CFU) showed a large increase of IFNγ production 3 days post-infection (Duckett et al., 2005), suggesting a stronger, yet inadequate response to higher doses. Nevertheless, these inflammatory anti-microbial cytokines have been shown to be essential for the survival of the host during infection by either route. Knockout mice deficient in either IFNγ or TNFα, infected with *F. tularensis* LVS by both the intranasal or intradermal route, are extremely susceptible to infection (Elkins et al., 1996, Chen et al., 2004b).

Treatment of alveolar macrophages with recombinant IFNγ before infection with *F. tularensis* LVS allowed them to eliminate the bacteria by 48 hours post-infection, compared to continued replication over 5 days seen in untreated alveolar macrophages (Polsinelli et al., 1994). This could be due to IFNγ promoting inflammasome-independent anti-microbial activity of guanylate binding proteins and restricting cytosolic replication (Wallet et al., 2017). Production of TNFα was seen in IFNγ-stimulated alveolar macrophages in response to *F. tularensis* LVS; however, anti-TNFα treatment had no effect on the anti-*F. tularensis* LVS activity of alveolar

macrophages (Polsinelli et al., 1994). Although this latter result seems to contradict the importance of TNFα, it may also be the case that the pre-stimulation of alveolar macrophages with IFNγ, that would not occur naturally, creates an inflammatory environment that makes TNFα redundant.

Mice given recombinant IFNγ intravenously prior to *F. tularensis* LVS infection showed significantly lower bacterial burden and enhanced resistance compared to untreated mice (Anthony et al., 1989). In this case *F. tularensis* LVS was administered intravenously which is likely to elicit different types of responses to those seen in intradermal and intranasal infections. Nevertheless, as with the other two routes of infection, neutralization of TNFα and IFNγ with monoclonal antibodies rendered mice susceptible to normally sublethal intravenous doses of *F. tularensis* LVS (Sjostedt et al., 1996). Interestingly, treatment with the same monoclonal antibodies in *F. tularensis*-immune mice that had survived a primary *F. tularensis* LVS infection, had no effect on susceptibility to secondary infection of *F. tularensis* LVS (Sjostedt et al., 1996). This result suggests that primary and secondary *F. tularensis* infections may elicit different defence mechanisms. This may explain the redundancy of TNFα after stimulation of alveolar macrophages with IFNγ, as during secondary infection macrophages may well have had similar IFNγ stimulation. In spite of this, care must be taken when comparing these studies as the route of infection plays a pivotal role in the immune response elicited.

1.3.2.2 IL-12

The critical involvement of IFNγ in protection against *F. tularensis* raises the question whether regulators of this cytokine also play a role in protection from infection. It has been well documented that IL-12 is a key driver of Th1 differentiation and can induce the production of IFNγ (Trinchieri, 2003), yet the role IL-12 plays during *F. tularensis* infection seems to be more complex. It was initially noted that *F. tularensis* LVS-immune mice were able to control a secondary intradermal infection of *F. tularensis* LVS through high expression of IL-12 in the skin suggesting it played a role in protection (Stenmark et al., 1999). As IL-12 is a heterodimer made up of two subunits, p35 and p40, it was later found that deficiencies in these subunits had differing outcomes on LVS infection. Mice lacking the p40 subunit, as well as mice treated with neutralizing anti-IL-12 antibodies, were unable to clear intradermal *F. tularensis* LVS and developed a chronic infection. In contrast, $p35^{-/-}$ mice showed a delay in bacterial clearance but were able to do so with no impaired survival (Elkins et al., 2002). Interestingly, IL-12p40 can also

interact with the IL-23p19 subunit from the heterodimeric IL-23, possibly implicating this cytokine in protection against *F. tularensis*. However, recent work has dismissed this by showing that bacterial burdens, survival and cytokine production in IL-23p19$^{-/-}$ mice infected intradermally or intranasally with *F. tularensis* LVS were equivalent to WT mice (Kurtz et al., 2014). These findings show that IL-23 does not play an important role in immunity to *F. tularensis* and also suggests a novel function in protection from intradermal infection for IL-12p40, independent of the known cytokine associations. This is a possibility as IL-12p40 is excessively expressed when compared to IL-12 and IL-23 levels, and can also be present as a free monomer and homodimer (Trinchieri, 2003). Nevertheless, further investigation into the precise function of IL-12p40 with regards to protection against *F. tularensis* LVS is required.

In contrast to its apparent dispensability during intradermal infection, IL-12 plays a pivotal role during resistance to intranasal infection. Mice deficient in both IL-12 p35 and p40 subunits were susceptible to intranasal infection with *F. tularensis* LVS doses that are sublethal in WT mice (Duckett et al., 2005). To further illustrate the protective role of IL-12 in respiratory infection, exogenous IL-12 treatment prior to infection with a lethal dose of *F. tularensis* LVS allowed the mice to survive the infection. This survival was not seen in IFNγ$^{-/-}$ mice suggesting that IL-12 protection is dependent on IFNγ expression (Duckett et al., 2005). Taking both these findings into consideration, it is clear that the route of infection affects the immune response to *F. tularensis* LVS and the role IL-12 plays in this. Nevertheless, it cannot be excluded that IL-12p40 alone can play an important role in protection for both intradermal and intranasal infection. The IL-12 receptor subunit β2 (IL-12Rβ2) is critical for survival against primary *F. tularensis* LVS challenge by any route. IL-12Rβ2$^{-/-}$ mice infected intranasally or intradermally had an LD_{50} two log lower than that seen in WT mice (Melillo et al., 2013). The exquisite susceptibility of mice deficient in the IL-12Rβ2 compared to either of the IL-12 subunits suggests that the signalling by the IL-12Rβ2 may extend beyond the function of IL-12.

1.3.2.3 IL-17

Another cytokine implicated in the protection against *F. tularensis* is IL-17. Consistent with the lack of immune response early in respiratory *F. tularensis* infection, IL-17 can only be found in the lungs of infected mice by day 3 post-infection. Interestingly, IL-17 was not found in lung or spleen homogenates following sublethal intradermal *F. tularensis* LVS infection (Cowley et al., 2010).

IL-17 augments the polarization of the Th1 response through stimulation of IL-12 production *in vitro* in *F. tularensis*-infected DCs and both IL-12 and IFNγ induction in macrophages (Lin et al., 2009). IL-17 also appears to have a protective role later in infection, but as with many aspects of *F. tularensis* LVS infection, such an effect depends on the route of infection.

IL-17-deficient mice infected intranasally succumbed to much lower doses of *F. tularensis* LVS than if infected intradermally (1 x 10^3 compared to 7 x 10^6 respectively) (Cowley et al., 2010). When IL-$17^{-/-}$ mice were given a sublethal intradermal infection there was no significant difference in bacterial growth in the liver or lung, with only a slight increase seen in the spleen compared to WT. In contrast, intranasal *F. tularensis* LVS infection led to increased bacterial burdens in IL-$17^{-/-}$ mice in all organs at the peak of infection on day 7 and then further significantly increased, particularly the lung by day 10 (Cowley et al., 2010). Nevertheless, this significant increase in bacterial growth in IL-$17^{-/-}$ mice was not seen during earlier stages of the infection, suggesting that IL-17 may play a more prominent role in augmenting growth control later in infection. The induction of the IL-17/Th17 pathway was suggested to be induced by IL-23 (Lin et al., 2009); however as discussed earlier with the involvement of IL-23, it appears that the Th17 immune response to *F. tularensis* LVS is independent of IL-23 and remains functional in IL-23 $p19^{-/-}$ mice (Kurtz et al., 2014).

1.3.2.4 IL-6

Research has also demonstrated an important role for IL-6 during infection with *F. tularensis*. Following intradermal *F. tularensis* LVS infection, IL-6 was detected in liver homogenates by day 1, peaking by day 3 post-infection. Significantly reduced expression of IL-6 following *F. tularensis* LVS infection was seen in TLR2-deficient mice (Martinon et al., 2010), as well as in mice treated with wortmannin to inhibit bacterial uptake by lung cells (D'Elia et al., 2011a). Thus, following intranasal or intradermal infection, IL-$6^{-/-}$ mice showed significantly decreased survival when compared to WT, as well as increased bacterial burdens in the liver, lung and spleen (Kurtz et al., 2013).

1.3.3 Anti-inflammatory and regulatory cytokines

1.3.3.1 IL-4

In contrast to the pro-inflammatory cytokines, the importance of Th2 cytokines has been studied in less detail. Through measuring the kinetics of mRNA transcripts from pulmonary lymphocytes following intranasal infection of mice with *F. tularensis* LVS, it was shown that there was an early upregulation of Th2 cytokines. Thus, IL-4, IL-13 and IL-5 mRNA levels were significantly increased by day 2 post-infection, but returned to control levels by day 6 corresponding with the upregulation of IFNγ and IL-17. Interestingly, in the same study this increased mRNA expression did not lead to detectable protein levels of the Th2 cytokines (Markel et al., 2010). This discord between mRNA and protein could be due to the overbearing expression of Th1 cytokines that ultimately drive away from Th2 responses.

The role IL-4 plays in inhibiting differentiation towards a Th1 response would suggest that this cytokine has a negative effect on the protection against *F. tularensis* LVS that is reliant on a strong Th1 inflammatory response. Mice treated with an anti-IL-4 monoclonal antibody before being given an intradermal *F. tularensis* LVS infection showed a minimal decreased susceptibility and increased survival compared to WT mice. However, these results were not significant (Leiby *et al.*, 1992). This was supported by showing that *F. tularensis* LVS is able to induce alternate activation of macrophages to increase survival in an IL-4 dependent manner (Shirey et al., 2008). *F. tularensis* LVS failed to alternatively activate IL-4 receptor α-deficient mouse (IL-4Rα$^{-/-}$) macrophages and IL-4Rα$^{-/-}$ mice exhibited increased survival compared to WT mice following intraperitoneal *F. tularensis* LVS infection (Shirey et al., 2008). In contrast, IL-4$^{-/-}$ mice given an intranasal challenge exhibited significantly increased susceptibility compared with WT mice. Bacterial burdens in the lung and spleen were also significantly higher in IL-4$^{-/-}$ mice by day 3 after *F. tularensis* LVS infection, although burdens were not significantly different at day 6 post-infection (Ketavarapu et al., 2008). One proposed positive function for IL-4 in early protection against *F. tularensis* is in partnership with mast cells. Mast cells isolated from IL-4$^{-/-}$ mice were unable to inhibit bacterial replication when co-cultured with IL-4$^{-/-}$ macrophages (Ketavarapu et al., 2008). Taken together, more research is needed on the protective role of IL-4 against *F. tularensis* LVS infection, which may be dependent on the route and stage of infection.

1.3.3.2 IL-10

IL-10 is a cytokine with anti-inflammatory properties and is an important regulator of pro-inflammatory responses during infection (Kuhn et al., 1993, Hawrylowicz and O'Garra, 2005). The lack of an early immune response following intranasal *F. tularensis* infection suggests a role for regulatory cytokines that function to suppress inflammatory responses. IL-10 has been shown to play an interesting role in protection against *F. tularensis*, and not surprisingly its function is dependent on route of infection.

Mice deficient in IL-10 survived a lethal dose of intradermal *F. tularensis* LVS that killed WT mice within 9 days of infection. This protection from death was accompanied by decreased bacterial burdens in the spleen and effective bacterial clearance (Metzger et al., 2013). Levels of IL-10 mRNA in the spleen rapidly increased by day 1 post infection when infected intradermally, with protein levels showing a similar increase by day 3 (Metzger et al., 2013). Although not significant, IL-10 protein levels have also been shown to increase in the lungs following intranasal infection (Periasamy et al., 2011). Therefore, it is interesting that IL-10 KO mice were significantly more susceptible to intranasal *F. tularensis* LVS infection when compared to WT mice (Metzger et al., 2013). Similarly, others found significantly increased weight loss and increased systemic bacterial burdens by day 7 in IL-$10^{-/-}$ mice following intranasal *F. tularensis* LVS infection (Vautier et al., unpublished observations, University of Manchester). These opposing findings of route dependent negative and positive influence of IL-10 during protection against *F. tularensis* suggest complex modulation of regulatory systems during the various routes of infection.

As shown in other experimental models, IL-10 is able to suppress IL-17 expression (McKinstry et al., 2009). Thus, this mechanism may be a link between the differing roles during the two routes of infection. Levels of IL-17 were significantly increased in the spleen of IL-10 deficient mice compared to WT mice when infected intradermally with *F. tularensis* LVS. Such increased IL-17 expression is essential for the resistant phenotype seen in IL-$10^{-/-}$ mice, as neutralization of IL-17 caused the mice to succumb to *F. tularensis* LVS infection they had previously survived (Metzger et al., 2013). As discussed earlier, given that IL-17 levels are significantly increased in the lungs during respiratory *F. tularensis* LVS infections (Cowley et al., 2010), it would be interesting to see if IL-17 expression is increased in the lungs of IL-$10^{-/-}$ mice that are more susceptible following intranasal infection. If IL-17 were to

be increased in a similar manner, it may suggest that the overexpression of IL-17 could exacerbate pulmonary inflammation and IL-10 plays an important role in modulating the inflammatory response. However, further studies need to be undertaken to further investigate this possibility.

1.3.3.3 TGF-β

The difference in response to *F. tularensis* LVS administered via the respiratory route compared to the intradermal route suggests that regulation of immune cells in the lungs must play a pivotal role in protection. One important regulatory cytokine involved in maintaining lung homeostasis is TGF-β. Bronchial and alveolar epithelial cells express the integrin αvβ6 which binds and activates latent TGF-β (Munger et al., 1999). The interaction between alveolar macrophages and alveolar epithelial cells through TGF-β activation by αvβ6 appears to be important. Mice lacking the β6 subunit develop age-related emphysema through increased expression of MMP12 by macrophages, a phenotype rescued by the transgenic expression of TGF-β (Morris et al., 2003). As mentioned earlier, alveolar macrophages make up 90% of the leukocytes in the lung and are one of the primary cellular targets of respiratory *F. tularensis*. Thus, the action of TGF-β on alveolar macrophages during *F. tularensis* infection may also play a role in protection.

BMDMs and DCs infected *in vitro* with *F. tularensis* LVS showed increased expression of TGF-β, but this was only significant with macrophage infection. The same study showed similar results *in vivo*, with mice infected via the respiratory route with *F. tularensis* LVS having significantly elevated secretion of TGF-β from cells harvested in bronchoalveolar lavage (BAL) fluid of infected mice (Bosio and Dow, 2005). Although this study used an intratracheal route of infection, similar findings of significant upregulation of TGF-β by 24 hours p.i. have also been found in mice infected intranasally with *F. tularensis* LVS (Periasamy et al., 2011). However, no significant differences were seen in bacterial burdens of isotype and TGF-β antibody treated mice infected intranasally with *F. tularensis* LVS (Vautier et al., unpublished observations). The results from the studies using anti-TGF-β antibody suggest that TGF-β is not important for protection against *F. tularensis* infection. However, the increased expression of TGF-β seen after infection with *F. tularensis,* as well as its role in regulation of alveolar macrophages indicate that further research is needed to fully disregard TGF-β as player in protection against *F. tularensis.*

1.3.4 Other soluble immune mediators

Aside from the important regulatory signalling of cytokines, other secreted molecules have also been investigated to understand their role in protection against *F. tularensis.* The lipid mediator prostaglandin E_2 (PGE_2) has been shown to play some role in promoting a Th2-like response and inhibiting T cell proliferation (Woolard et al., 2007). PGE_2 expression increases slightly in the lungs of mice infected intradermally or intranasally with *F. tularensis* LVS by day 7. However, mice infected intranasally showed significantly increased expression of PGE_2 after a return to control levels in mice infected intradermally (Woolard et al., 2008). Increased PGE_2 production was shown to be important in dampening expression of IFNγ in mice following intranasal infection with *F. tularensis* LVS, as pharmacological inhibition of PGE_2 with indomethacin led to increased IFNγ levels and decreased bacterial burden in the lung (Woolard et al., 2008).

The importance of IFNγ for protection against *F. tularensis* also influenced the direction of research into the role of chemokines during infection. Monokine induced by IFNγ (Mig) is a chemokine induced by IFNγ that contributes to T cell infiltration into peripheral tissues during inflammation. However, apart from impairment in *F. tularensis*-specific antibody production in *mig*$^{-/-}$ mice infected with *F. tularensis* LVS, there was no effect on bacterial clearance compared to WT mice (Park et al., 2002). Similarly, CX3CR1-deficient mice also show no difference in susceptibility to intranasal infection, although they did have increased monocyte and neutrophil recruitment to the lungs following infection (Hall et al., 2009). This was surprising as CX3CR1 is known to facilitate binding of CX3CL1-expressing cells to endothelial cells during infiltration into infected tissue (Hall et al., 2009). From the current data it appears that the overall role for chemokines in protection against *F. tularensis* LVS is redundant (Cowley and Elkins, 2011). Most chemokines studied appear to play important roles in cellular recruitment during the inflammatory response against *F. tularensis* LVS, therefore further investigating the effects of multiple chemokine receptor and ligand deficiencies may provide better understanding of their roles.

1.4 *F. tularensis* subspecies tularensis - Schu S4

This PhD has used *F. tularensis* LVS, a strain which is attenuated in humans while maintaining virulence in mice, as the model of bacterial pulmonary infection. However, like many other models there are similarities and differences within the representative subspecies. Earlier the difficulties in working with *F. tularensis*

subspecies *tularensis* Type A strain Schu S4 were briefly touched upon. As Schu S4 is a CL3 pathogen, this increases the cost, time and safety precautions of working with the bacterium. For this reason, the use of Schu S4 has often been as a follow on study from findings in experiments with LVS. Here some of the differences and similarities regarding the life cycle and host response to Schu S4 compared to LVS will be briefly mentioned.

With regards to cell entry and intracellular replication, Schu S4 shows large similarities to LVS. The importance of CRs remains prominent in cell entry. It was shown that CR3 is important for the uptake of serum-opsonized Schu S4 in macrophages (Geier and Celli, 2011), with CR3 and CR1 needed for uptake into neutrophils (Schwartz et al., 2012b). Similarly, the mannose receptor plays a more prominent role in the internalisation of non-opsonized Schu S4 (Geier and Celli, 2011). Once internalised, prevention of acidification through the ATPase inhibitor bafilomycin has been shown to significantly delay phagosomal escape, suggesting that early maturation and acidification may be required for efficient escape of Schu S4 from the phagosome (Chong et al., 2008). Interestingly, unlike LVS, Schu S4 has been shown to actively avoid autophagy early after escape into the cytoplasm through protection by the *Francisella* O-antigen present in the bacterial LPS and capsule (Case et al., 2014). However, Schu S4 is still able to re-enter FCVs later during the cytoplasmic replication phase (Checroun et al., 2006); suggesting that the more virulent strain may avoid early autophagy detection when autophagy may play a role in eliminating cytoplasmic bacteria.

The host immune response elicited against Schu S4 has a more prominent pattern with a dampened early response, followed by hypercytokinemia that is often the cause of sepsis and death (Cowley, 2009). Infection with Schu S4 has a much shorter time frame compared to LVS, with mice often succumbing to the infection by day 5. Therefore, although the significant increase of inflammatory cytokines such as IFNγ, TNFα and IL-6 by day 3 post-infection with Schu S4 is similar to that of LVS, the shorter time frame of Schu S4 infection means the resolution of inflammation cannot occur (Sharma et al., 2011). Unlike LVS, Schu S4 does not induce an alternate activated macrophage phenotype earlier in infection (D'Elia et al., 2015). The more prominent classically activated macrophages that express high levels of iNOS may indeed contribute to excessive inflammation, tissue damage and death seen in Schu S4 infection. As would be expected, certain cytokines have differences in importance during the response to Schu S4. In contrast to LVS, IL-6$^{-/-}$

mice infected intranasally with Schu S4 showed no difference in bacterial burdens or survival rate compared to WT mice (Laws et al., 2013).

In the same way, IL-10$^{-/-}$ mice infected with Schu S4 showed no difference in survival kinetics compared to WT mice (Metzger et al., 2013). A study proposed a protective role for TGF-β during Schu S4 infection. They showed that mice treated with anti-TGF-β mAb prior to infection with Schu S4 significantly reduced bacterial burdens in the lung compared to untreated mice (Bosio et al., 2007). However, no difference was seen compared to isotype treated controls suggesting their conclusion must be considered with care. Taken together, these results indicate that there may be redundancy with the inflammatory response against Schu S4, with other cytokines able to influence the outcome of infection when IL-6 is not present. Similarly, the lack of difference in IL-10 and possibly TGF-β deficient mice suggests that the modulation of the immune response by these regulatory cytokines is not enough to impact protection against the more virulent Schu S4. Another possibility is that due to the shorter course of Schu S4 infection, these cytokines just do not have enough time to have an effect and influence the disease outcome. Furthermore, high-mobility group protein B1 (HMGB1) has been shown to be a late mediator of sepsis and pro-inflammatory responses to infection (Wang et al., 1999). It has been shown to be significantly upregulated during Schu S4 infection and may contribute to the subsequent cytokine storm seen during infection. This highlights potent mediators of inflammation during virulent *F. tularensis* infection that may be therapeutically targeted to reduce harmful cytokine response (D'Elia et al., 2013a).

1.5 Lung immune homeostasis

As has been extensively discussed, it is evident that *F. tularensis* is able to subvert the host immune response and convey high virulence via pulmonary infection. It is therefore important to understand how the lung maintains immune homeostasis at steady state and the changes that occur when an inflammatory response is mounted against pathogens.

1.5.1 Pulmonary airway

Immunity within the pulmonary airways relies on a network of interactions. Firstly, the physical barrier against airway infections consists of pulmonary epithelium cells, mucus-secreting goblet cells, ciliated cells and club (Clara) cells that secrete surfactant (Lloyd and Marsland, 2017). Similarly, mucus produced by

goblet cells is crucial in lining the pulmonary epithelium in order to trap pathogens and airway particulates, they are then removed by ciliary action and coughing (Wanner et al., 1996). Defects in mucus production and impaired mucus clearance can have severe consequences in disease such as cystic fibrosis and chronic obstructive pulmonary disease (Randell and Boucher, 2006). Interestingly, in addition to this protective barrier function, many of these airway constituents are pivotal in the regulation of immune responses in the lung.

1.5.1.1 Airway epithelial cells

Pulmonary epithelial cells line the airway and are in intimate contact with cells of the immune system, as well as inhaled innocuous antigens and pathogens. To this end, they express TLRs that are able to recognise pathogen-associated molecular patterns from a variety of pathogens (Lambrecht and Hammad, 2012). Similarly, they are able to provide negative regulatory signals to alveolar macrophages through the secretion of regulatory cytokines such as IL-10 and TGF-β (Munger et al., 1999, Lim et al., 2004), as well as through expression of CD200 inducing negative regulation via interactions with CD200R (Jiang-Shieh et al., 2010). This prevention of alveolar macrophage activity restricts their inflammatory function while still clearing particulates and cellular debris from the airways to maintain homeostasis. Airway epithelial cells have also been shown to directly contribute to the clearance of apoptotic cells and debris via the secretion of anti-inflammatory cytokines (Juncadella et al., 2013).

1.5.1.2 Dendritic cells

Airway mucosal dendritic cells are also closely linked with the airway epithelium and play a specialised role in immune surveillance. They are positioned below or within the epithelium, extending protrusions through intact epithelia into the airway lumen for antigen acquisition (Jahnsen et al., 2006). However, these DCs lack the capacity for efficient antigen presentation at rest and have been shown to stimulate an anti-inflammatory Th2 response until an inflammatory stimulus is present, suggesting that they promote airway tolerance (Stumbles et al., 1998). Similarly, plasmacytoid DCs (pDCs) have been shown to take up inhaled antigen in the lung and present it in a tolerogenic form to draining node T cells, with pDC depletion in mice leading to increased hypersensitivity to inert inhaled antigen (de Heer et al., 2004).

1.5.1.3 Neutrophils

Neutrophils are important cell types in the innate immune response and are the first cells to be recruited to the lung during infection (Burns et al., 2003, Craig et al., 2009). Interestingly, at steady-state the lung has a relatively large number of neutrophils compared to other organs. They are kept in the lung through CXCR4 signalling, driven by expression of its ligand CXCL12 by pulmonary epithelium cells (Devi et al., 2013). Positioning of neutrophils in close proximity to the airways and interstitium would allow for rapid infiltration during inflammation (Kreisel et al., 2010). Upon infection the host is able to increase the number of circulating neutrophils in the blood from the bone marrow, allowing them to then migrate out of the capillaries surrounding the site of infection (Marsh et al., 1967, Smith, 2000). Some important murine chemokines involved in neutrophil lung recruitment are KC, MIP-2, CXCL5 and lungkine (Baggiolini et al., 1994, Chen et al., 2001).

Once at the site of infection neutrophils are equipped with a number of mechanisms to kill invading pathogens. Neutrophils are efficient phagocytes that are able to engulf, and subsequently kill, invading pathogens by a number of mechanisms. Following phagocytosis, neutrophil granules are able to fuse with the phagosome, releasing a number of microbicidal factors such as myeloperoxidase (MPO) and neutrophil elastase (NE) (Kjeldsen et al., 1994, Kolaczkowska and Kubes, 2013, van Kessel et al., 2014). Furthermore, MPO from neutrophil granules is able to drive another anti-microbial function of neutrophils, the production of ROS through NAPDH oxidase activity (Eiserich et al., 1998, Nguyen et al., 2017). The importance of ROS in controlling invading pathogens is evident. Patients with chronic granulomatous disease (CGD), resulting from a defect in NADPH oxidase activity, suffer from recurrent, severe bacterial and fungal infections (Holmes et al., 1967, Segal et al., 2000). Finally, neutrophil extracellular trap (NET) formation is a mechanism by which neutrophils are able to capture and kill extracellular bacteria, while also preventing further microbial dissemination (Brinkmann et al., 2004, Branzk et al., 2014). As with ROS production being heavily dependent on MPO, NET formation is dependent on ROS production and the translocation of NE to the nucleus (Papayannopoulos et al., 2010).

1.5.1.4 Alveolar macrophages

Unlike traditional macrophages that develop from circulating bone-marrow monocytes, alveolar macrophages have been shown to develop into tissue resident cells from fetal monocytes during early stages of life (Guilliams et al., 2013).

Alveolar macrophages make up over 90% of leukocytes in the alveolar lumen and are crucial in maintaining airway homeostasis (Maus et al., 2006). Due to constant interaction with innocuous antigens in the airway, alveolar macrophage activation is tightly controlled through a number of cell-cell and soluble mediator interactions to limit unwanted inflammatory responses. Subsequently, alveolar macrophage depletion in mice increased susceptibility to T cell mediated inflammatory responses against normally innocuous inhaled antigen (Thepen et al., 1989). The robust regulation of alveolar macrophages is mostly through the expression of multiple negative regulatory receptors that interact with ligands and soluble mediators in the airspace, predominantly derived from epithelial cells (Hussell and Bell, 2014).

1.5.2 Negative immune regulators and *F. tularensis* infection

This thesis focused primarily on the negative immune regulator CD200 receptor (CD200R), which will be discussed in greater detail later, but some other negative regulatory receptors that dictate repression of alveolar macrophage activation will be discussed. Furthermore, the role these negative regulators may play during *F. tularensis* infection, either through direct research or interpretation from similar pathogens will also be explored (Figure 1.3).

1.5.2.1 SIRPα & pulmonary surfactant-associated proteins

An important mechanism by which alveolar macrophage can be modulated is by pulmonary surfactant proteins and signal inhibitory regulatory protein α (SIRPα). Surfactant proteins A and D (SP-A and SP-D) are able to bind SIRPα and initiate a signalling pathway to block the production of pro-inflammatory mediators (Gardai et al., 2003). This interaction has also been shown to dampen the phagocytic activity of alveolar macrophages towards apoptotic cells, with this inhibition achieved through SIRPα signalling to activate SHP-1 and RhoA (Janssen et al., 2008). However, another study showed enhanced phagocytosis of *M. tuberculosis* by human alveolar macrophages incubated with soluble SP-A, allowing the bacterium to enter its replicative niche (Gaynor et al., 1995). These opposing findings of inhibition and activation of phagocytosis may indicate how a bacterium can manipulate the host response. Similarly, it is not known whether the enhanced phagocytosis of *M. tuberculosis* is mediated through interaction with SIRPα, and was completely inhibited by blocking the mannose receptor before treatment with SP-A. *F. tularensis* has also been shown to infect type II alveolar epithelial cells as well as alveolar macrophages (Bradburne et al., 2013), infection with the bacteria may be able to upregulate secretion of SP-A from these epithelial cells.

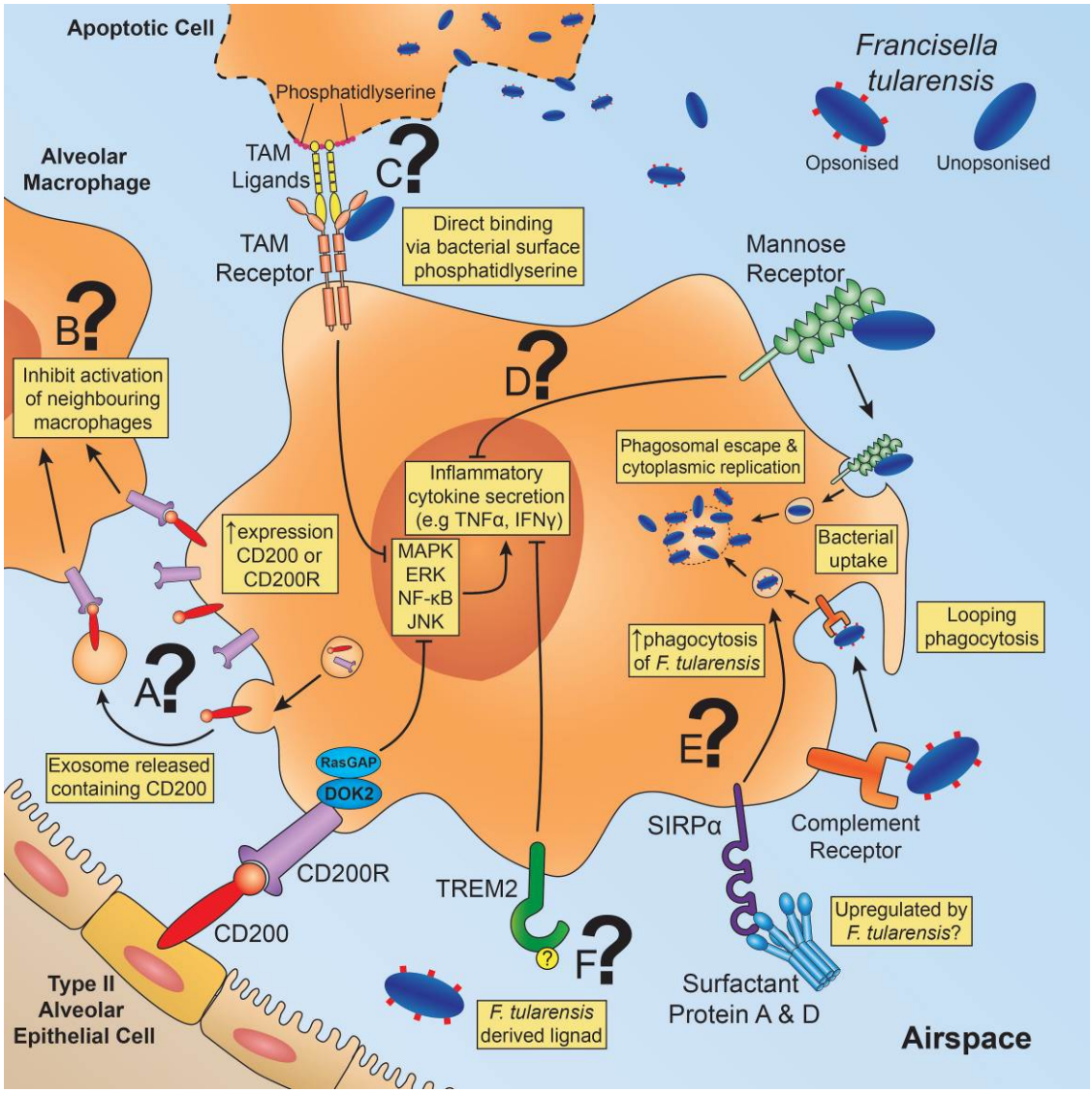

Figure 1.3 | Negative immune regulators potentially important during *F. tularensis* infection. During normal pulmonary homeostasis alveolar macrophage activity against innocuous antigens is inhibited by negative immune regulators. *F. tularensis* may modulate some of these negative immune regulators in order to dampen the host immune response during infection. A) Binding of CD200 to CD200R leads to the inhibition of pro-inflammatory MAPK, ERK and JNK pathways. Both CD200R and CD200 may be upregulated on alveolar macrophages during *F. tularensis* infection. It may also be possible that *F. tularensis* can induce the release of exosomes containing CD200 from macrophages. B) As CD200 is usually expressed on type II alveolar epithelial cells, the CD200 in exosomes and upregulation on macrophages may lead to the inhibition of neighbouring alveolar macrophages. C) Inhibition of MAPK, ERK and NF-κB pathways by TAM (Tyro3, Axl and Mertk) receptors may be through binding Gas6 and Protein S ligands that can bind to phosphatidylserine expressed by *F. tularensis*-induced apoptotic cells. Similarly, phosphatidylserine may be expressed on the bacterial membrane to induce binding to TAM receptors. D) Beyond its role in phagocytosis of unopsonised *F. tularensis,* binding the mannose receptor may also inhibit secretion of pro-inflammatory cytokines. E) Although binding of SP-A and SP-D to SIRPα inhibits the phagocytic activity of macrophages against apoptotic cells, it may increase the phagocytosis of *F. tularensis* to allow it to enter its replicative niche. F) TREM2 signalling can inhibit secretion of inflammatory cytokines and may be upregulated during *F. tularensis* infection. As the ligands for TREM2 are not fully characterised, *F. tularensis* may directly bind TREM2 in order to dampen the host immune response. Adapted from Hussell & Bell (2014).

1.5.2.2 TAM Receptors

The three TAM receptors, Tyro3, Axl and Mertk, are a receptor protein tyrosine kinase subfamily that play an important role in controlling innate immunity and regulating homeostatic phagocytosis through the clearance of apoptotic cells and membranes (Lemke and Rothlin, 2008). Binding of TAM receptor ligands Gas6 or protein S to phosphatidylserine on apoptotic cells has been shown to inhibit TLR-dependent signal transduction leading to inhibition of MAPK, ERK and NF-κB pathways (Lemke and Rothlin, 2008). Increased expression of phosphatidylserine on macrophages was noted following *F. tularensis* infection (Ireland et al., unpublished observations, Dstl), suggesting this may influence interactions with TAM signalling. Much of this suppression is mediated by activation of suppressor of cytokine signalling (SOCS) proteins SOCS1 and SOCS3 that are transcribed after STAT1 signalling (Rothlin et al., 2007). The importance of TAM receptors for apoptotic cell clearance has been shown in macrophages from *mertk*$^{-/-}$ mice that have severely impaired clearance of apoptotic thymocytes (Scott et al., 2001). Additionally, a disorder characterised by retinal dystrophy has been shown to be due to a mutation in Mertk leading to disrupted clearance of apoptotic cells in the retina (Duncan et al., 2003, Tschernutter et al., 2006). Interestingly, Mertk appears to be dispensable for the uptake and clearance of bacteria. The *F. tularensis* LVS burden in *mertk*$^{-/-}$ macrophages 6 and 24 hours after infection was similar to those in WT macrophages (Williams et al., 2009). Although an extracellular bacteria, no difference in phagocytosis or killing of *E. coli* was seen in macrophages lacking TAM receptors (Williams et al., 2009). These data suggest that Mertk is dispensable in the phagocytosis and killing of bacteria.

On the other hand, Axl protein levels in the lung were increased following influenza virus infection, particularly in BMDMs. Influenza-infected mice treated with anti-Axl mAb showed significantly increased survival and decreased lung pathology compared to untreated mice (Shibata et al., 2014). Investigating the immune response and lung pathology of Axl-deficient mice infected with *F. tularensis* would be interesting as the work previously mentioned was conducted *in vitro* (Williams et al., 2009). An important aspect of TAM receptor signalling that has been shown to be manipulated by certain intracellular pathogens is the exposure of phosphatidylserine. *L. amazonensis* has been shown to inhibit macrophage activation through the exposure of phosphatidylserine on their surface that also aids in the uptake of the parasite into macrophages. This interaction also induced the secretion of TGF-β and IL-10 (de Freitas Balanco et al., 2001). This may also be a

possible inhibitory mechanism employed by *F. tularensis* to inhibit macrophage activity.

1.5.2.3 TREM Family

The triggering receptor expressed on myeloid cells (TREM) family is a set of immunoregulatory receptors found on macrophages that consist of activating and inhibitory receptors. TREM1 is selectively expressed on neutrophils and alveolar macrophages, functioning to promote a pro-inflammatory response through the secretion of cytokines such as TNFα (Bouchon et al., 2000). On the other hand, TREM2 functions to regulate the development of DCs and other myeloid cells, as well inhibiting TLR-mediated macrophage inflammation (Colonna, 2003). TREM2 expression is significantly reduced on murine alveolar macrophages following LPS treatment, along with increased expression of inflammatory mediators. Silencing of TREM2 with shRNA led to the increased expression of TLR4 on alveolar macrophages and increased production of TNFα following LPS treatment (Gao et al., 2013). Following infection with respiratory pathogen *S. pneumoniae*, TREM2 expression was increased on alveolar macrophages. *Trem2*$^{-/-}$ mice showed increased bacterial clearance in the lungs and improved survival compared to WT mice (Sharif et al., 2014). This suggests that respiratory pathogens may be able to modulate the expression of TREM2 in order to inhibit inflammatory responses and increase survival.

1.5.2.4 Mannose Receptor

The mannose receptor is expressed by, among other cells, alveolar macrophages. It has been shown to be essential for the suppression of alveolar macrophages through the recognition of non-opsonised bacteria. Pre-treatment of alveolar macrophages with a mannose receptor-blocking agent as well as a targeted siRNA resulted in the increased expression of TNFα in response to non-opsonised *Pneumocystis*, a yeast-like fungus found in the lung, compared to untreated macrophages (Zhang et al., 2005). This suggests that the mannose receptor may function to prevent alveolar macrophages from initiating inappropriate inflammatory responses against commensal pathogens in the airways. As stated earlier, the mannose receptor has been shown to play an important role in the uptake of non-opsonised LVS and Schu S4 (Schulert and Allen, 2006, Geier and Celli, 2011). Perhaps the interaction of *F. tularensis* with the mannose receptor not only aids uptake, but may also be a method of dampening the immune response elicited towards the bacterium.

1.6 CD200:CD200 Receptor

The CD200:CD200R pathway is the primary regulatory pathway studied in this PhD thesis; therefore the role it plays in negatively regulating immune functions will be discussed in detail. The focus of this PhD thesis is to understand whether the characteristic delayed immune response seen during *F. tularensis* infection is due to manipulation of immunoregulatory pathways, in particular CD200:CD200R. Thus, various pathogens will be introduced that have been shown to disrupt the pathway in order to increase survival in the host. Furthermore, the effects of CD200 or CD200R deficiency on infectious outcome will be introduced, as well as therapeutic targeting of the CD200:CD200R pathway.

1.6.1 CD200:CD200R family and function

The CD200 (OX2) protein was first purified and characterised in rats in 1982 (Barclay and Ward, 1982) and has since been found to be expressed on numerous cell types including bronchial epithelial cells, neurons in the central nervous system and keratinocytes (Webb and Barclay, 1984, Dick et al., 2001, Rosenblum et al., 2004, Jiang-Shieh et al., 2010). Furthermore, the distribution of CD200 on these cell types is conserved in humans (Wright et al., 2001). Further characterisation of CD200 showed that it was a member of the immunoglobulin superfamily (IgSF) and that it contained a single transmembrane domain and a short cytoplasmic domain of 19 amino acids, suggesting an inability for intracellular signalling (Clark et al., 1985).

The receptor for CD200 (CD200R) was later identified as a protein with expression restricted to cells of myeloid lineage. There are high levels of CD200R expression on alveolar macrophages when compared to other lung and tissue-resident macrophages, as well as strong expression on neutrophils (Wright et al., 2003, Snelgrove et al., 2008). CD200R is similar in structure to CD200 but had a larger cytoplasmic domain that suggested an increased signalling capacity (Wright et al., 2000). Interestingly, unlike other inhibitory myeloid immune receptors, CD200R does not have an immunotyrosine-based inhibitory motif (ITIM) usually phosphorylated by Src family kinases such as SHPs and SHIP-1 as major initiator proteins (Ravetch and Lanier, 2000).

Genes closely related to CD200R were also characterised and termed CD200RLa-d, however their ability to bind CD200 remains controversial. Some findings suggests that CD200RL molecules do not bind to CD200, confirming that CD200 is the sole ligand for CD200R in the family (Wright et al., 2003, Hatherley et al., 2005).

However, another group has questioned these findings due to incomplete NH_2-terminal domains for CD200RLb-c, suggesting that the CD200RL family interact with CD200 (Gorczynski et al., 2004). Further elucidation of CD200 binding would provide interesting insight into alternate roles for CD200:CD200R signalling. Soluble forms of CD200 also exist that are produced by membrane shedding or mRNA splicing (Chen et al., 2008, Twito et al., 2013), therefore it would be interesting to determine difference in binding and signalling capabilities.

The downstream signalling of CD200:CD200R binding was first elucidated in mast cells, initiated through phosphorylation of a tyrosine motif on the cytoplasmic tail of CD200R (Zhang et al., 2004). This phosphorylation allows binding and phosphorylation of docking protein 2 (Dok2), that in turn recruits Ras GTPase-activating protein (RasGAP) and leads to the inhibition of pro-inflammatory signalling by ERK, JNK and MAPK pathways (Zhang et al., 2004, Mihrshahi et al., 2009). The inhibition of MAPK activation is responsible for the lack of mast cell degranulation and cytokine production following CD200R engagement (Zhang et al., 2004). Dok1 is also phosphorylated upon CD200R signalling, but is delayed and leads to less recruitment of RasGAP. Alternatively, Dok1 phosphorylation recruits the adaptor proteins CT10 sarcoma oncogene cellular homologue (Crk) and Crk-like (CrkL), initiating a negative feedback loop to regulate inhibition by CD200R (Mihrshahi and Brown, 2010).

The function of this receptor-ligand interaction has been shown to be heavily involved in myeloid regulation, with $CD200^{-/-}$ mice showing dysregulation of myeloid populations in the spleen and brain (Hoek et al., 2000). As the differences in $CD200^{-/-}$ mice were only seen on myeloid cells expressing CD200R, it was evident that the function of CD200 was dependent on binding to CD200R. It has been shown that CD200 in the follicular epithelium can attenuate inflammatory skin reactions and plays a role in maintaining immune tolerance (Rosenblum et al., 2004). Constitutive expression of CD200R represses pro-inflammatory Th1 cell activation both *in vitro* and *in vivo* (Gorczynski et al., 1999, Gorczynski et al., 2000). Similarly, CD200R has been shown to be a potent regulator of mast cell and human basophil function (Cherwinski et al., 2005, Shiratori et al., 2005). While reduced expression of monocyte CD200R in sarcoidosis leads to enhanced pro-inflammatory cytokine production (Fraser et al., 2016).

As well as dampening pro-inflammatory Th1 immunity, the CD200:CD200R pathway also plays an interesting role in regulation of Th2 immunity. Activation of CD200R

with the ligand CD200 increased production of IL-4 and IL-10 (Gorczynski et al., 2000). However, CD200$^{-/-}$ mice showed a pronounced increase in Th2-associated cytokines and enhanced tolerance to autoimmune uveitis (Taylor et al., 2005). Similarly, CD200R has also recently been shown to be upregulated on allergen-specific Th2 cells and is strongly correlated to Th2 pathology (Blom et al., 2017). This suggests that maintaining immune homeostasis via CD200R may be a fine balance between dampening Th1 responses and avoiding exacerbated Th2 immunity.

1.6.2 CD200:CD200R and infectious disease

1.6.2.1 Bacterial pathogens

CD200$^{-/-}$ mice have increased susceptibility to *Neisseria meningitides* compared to WT mice due an excessive inflammatory response. Although there was no difference in bacterial burden, CD200$^{-/-}$ mice had significantly increased levels of IL-6 and TNFα (Mukhopadhyay et al., 2010). *N. meningitides* has also been shown to push monocyte differentiation towards macrophages with higher CD200R expression. Upon meningococcal infection these macrophages are important in forming a homeostatic microenvironment through secretion of anti-inflammatory mediators (Wang et al., 2016). Similarly, infection with *Salmonella enterica* upregulates the expression of CD200 and CD200R on murine effector T cells, which also showed decreased TNFα and increased IL-4 production (Caserta et al., 2012). These data show the immunomodulatory role of the CD200:CD200R pathway in response to bacterial infections, and how the pathogen can manipulate the pathway to aid bacterial persistence. Nevertheless, more research is needed to understand the role of CD200R in the context of respiratory bacterial pathogens.

1.6.2.2 Parasitic pathogens

Infection with the encaphilitic parasite *Toxoplasma gondii* in WT mice led to increased expression of CD200R on microglia and CD200 on blood vessel endothelial cells (Deckert et al., 2006). Microglia exhibited increased activation, with increased production of TNFα inducible nitric oxide synthase (iNOS) production, during *T. gondii* infection in CD200$^{-/-}$ mice. This led to decreased parasitic burdens and increased survival in CD200$^{-/-}$ mice (Deckert et al., 2006).

In the same way, *Leishmania amazonensis* upregulates the expression of CD200 on macrophages, which contributes to its increased virulence over *L. major*. This is

supported by the findings that *L. amazonensis* shows decreased virulence and decreased intracellular replication in CD200$^{-/-}$ mice (Cortez et al., 2011). Furthermore, they showed that CD200 on macrophages inhibits iNOS and nitric oxide production following *L. amazonensis* infection, but not *L. major* infection that does not upregulate CD200. Interestingly, exogenous addition of CD200 increased the virulence of *L. major* infection (Cortez et al., 2011).

As CD200 is usually expressed by non-myeloid cells, upregulation on macrophages may imply that they could actually inhibit neighbouring macrophages by expressing both CD200R and CD200. It has been shown that macrophages infected with intracellular bacteria *Mycobacterium tuberculosis* can release exosomes to signal to neighbouring naive macrophages to stimulate a pro-inflammatory response in a TLR-dependent manner (Bhatnagar et al., 2007). Furthermore, these membrane vesicles contain lipoglycans that have been shown to inhibit T cell activation and provide a mechanism for immune evasion (Athman et al., 2017). It is possible that these vesicles may also contain CD200 that can then bind to CD200R on nearby macrophages to inhibit rather than activate macrophage activity and an inflammatory response. Although this has not been tested, it poses an interesting perspective for the methods of immune modulation used by various pathogens.

1.6.2.3 Viral pathogens

As with bacterial and parasitic pathogens, viruses show variation in infectious outcome upon removal of CD200R signalling. CD200$^{-/-}$ mice exhibited decreased viral replication and viral titers in response to mouse hepatitis corona virus (MHV) infection (Karnam et al., 2012). This was associated with increased levels of IFNα levels in CD200$^{-/-}$ mice, suggesting that the lack of immunomodulation by CD200R has a positive effect on MHV clearance. In contrast, although there were no differences in viral titers, CD200$^{-/-}$ mice are highly susceptible to influenza A infection compared to WT due to an exacerbated inflammatory response (Snelgrove et al., 2008). CD200R expression is increased on alveolar macrophages during influenza infection which may serve to control the inflammatory response to the virus, which as seen in the CD200 deficient mice is a major cause of mortality (Snelgrove et al., 2008). However, CD200R$^{-/-}$ mice actually showed the opposite infectious outcome compared to CD200$^{-/-}$ mice. CD200R$^{-/-}$ mice showed an enhanced inflammatory response, albeit less than CD200$^{-/-}$ mice, and exhibited decreased pathogenesis and viral load in response to influenza A infection compared to WT (Goulding et al., 2011). Furthermore, this enhanced influenza-

induced inflammatory response in CD200R$^{-/-}$ mice provided protection against secondary bacterial infection with *Streptococcus pneumoniae*, decreasing bacterial burden and preventing systemic dissemination (Goulding et al., 2011).

Mortality in murine herpes simplex virus 1-induced (HSV-1) encephalitis is strongly attributed to increased inflammatory cytokine responses in a TLR2-dependent manner (Kurt-Jones et al., 2004). Interestingly, CD200R$^{-/-}$ mice exhibited decreased HSV-1 titers and increased survival compared to WT mice. In this study it was suggested that dysfunctional TLR2 signalling in CD200R$^{-/-}$ mice led to protection against HSV-1 infection (Soberman et al., 2012).

The differences in infectious outcome to viral infection between CD200 and CD200R-deficient mice highlight the fine balance between a detrimental and beneficial excessive inflammatory response. Furthermore, it suggests there may be a more complex relationship between CD200R signalling beyond ligand binding to CD200.

1.6.3 Viral orthologues of CD200

Viruses have numerous methods of manipulating host inhibitory receptors in order to avoid immune detection (Ong et al., 2016), with some having evolved to express orthologs of CD200 in order to manipulate CD200R signalling. Kaposi's sarcoma-associated herpesvirus (KSHV) expresses a viral ortholog of CD200 (vOX2) on the surface of infected cells which binds to CD200R, but not related CD200R proteins, with similar avidity to CD200 (Foster-Cuevas et al., 2004, Amini et al., 2015, Kwong et al., 2016). vOX2 is able to decrease macrophage activity *in vitro*, as well as negatively regulating antigen-specific T cell response *in vivo* (Foster-Cuevas et al., 2004, Misstear et al., 2012). Furthermore, vOX2 has been shown to downregulate basophil function, as well as inhibiting oxidative bursts and IL-8 secretion in human neutrophils (Rezaee et al., 2005, Shiratori et al., 2005).

However, not all viral CD200 orthologues follow the same pattern. The CD200 orthologue expressed by cytomegalovirus e127 does not alter viral replication or inhibit myeloid activity, despite binding to CD200R with equivalent affinity to CD200 (Foster-Cuevas et al., 2011). Alternatively, M141 is the CD200 orthologue expressed by myxoma virus and has been shown to inhibit macrophage and lymphocyte activation leading to in increased pathology and viral dissemination in infected rabbits (Cameron et al., 2005). Nevertheless, it has been shown that M141

does not bind to CD200R, thus must be having immunomodulatory effects independent of CD200R signalling (Akkaya et al., 2016).

1.6.4 Therapeutic targeting of CD200:CD200R

Binding of CD200 to CD200R induces phosphorylation of downstream targets that ultimately leads to the inhibition of pro-inflammatory signalling (Zhang et al., 2004). Thus, a CD200 immunoadhesion (CD200-Fc) was developed to further study the therapeutic potential of activating CD200R signalling (Gorczynski et al., 1999). Much of the therapeutic research has been targeted towards controlling excessive inflammatory responses during disease. Treatment of influenza-infected mice with CD200-Fc fusion protein led to significantly decreased weight loss and influenza-induced inflammation (Snelgrove et al., 2008). Similarly, administration of CD200-Fc during ocular HSV infection reduced the incidence and severity of lesions compared to control, as well as reduced IFNγ production from isolated splenocytes (Sarangi et al., 2009).

As well as pathogen-induced inflammation, CD200-Fc can alleviate autoimmune disorders. Collagen-induced arthritis in DBA/1 mice induces severe arthritis within 30 days; however treatment with CD200-Fc stopped the development of arthritis (Gorczynski et al., 2001b, Simelyte et al., 2008). Furthermore, CD200-Fc treatment significantly reduced the expression of inflammatory cytokines and matrix metalloprotease 13 in joints of arthritic mice (Simelyte et al., 2008). In models of skin and renal transplantation, *in vivo* infusion of CD200-Fc promotes increased allograft and xenograft survival (Gorczynski et al., 1999). Interestingly, splenocytes from CD200-Fc treated mice exhibited polarisation towards production of the Th2 cytokines IL-4 and IL-10, suggesting the development of a more tolerogenic environment (Gorczynski et al., 2002). However, this is not the case for other graft rejection treatments. $CD200^{-/-}$ mice showed difference in corneal graft survival when compared to WT. Similarly, mice treated with CD200-Fc following corneal allografts showed no difference in allograft rejection time, suggesting that targeting the CD200R signalling pathway is not a useful therapeutic option for corneal graft rejection (Nicholls et al., 2015).

The CD200:CD200R pathway also plays an important role in neuroimmune regulation and could be a potential therapeutic target for neurodegenerative diseases. $CD200^{-/-}$ mice show enhanced activation of microglia in the brain and exhibit exacerbated inflammatory response in response to LPS or amyloid-β (Aβ) (Lyons et al., 2007, Costello et al., 2011). The production and deposition of Aβ

peptide is thought to drive pathogenesis of Alzheimer's disease (Murphy and LeVine, 2010). Treatment of aging rats with CD200-Fc decreases microglial activation, as well as inhibiting Aβ-induced inflammatory responses in mice (Cox et al., 2012, Lyons et al., 2012). Interestingly, recent evidence from the same group suggests that microglia from $CD200^{-/-}$ mice exhibit increase phagocytosis and lysosomal function and diminishes microglial activation in response to Aβ (Lyons et al., 2016). This contradicting data highlights the complexity of CD200R signalling.

Many therapeutic studies have increased CD200R signalling in order to inhibit inflammatory responses, however CD200R signalling has been shown to play a detrimental role in tumour progression and metastasis. It was originally shown that protection from growth of transplanted leukemic tumour cells in mice was abolished with CD200-Fc treatment and decreased further by the co-infusion of $CD200R^{+}$ macrophages (Gorczynski et al., 2001a). Further studies showed that CD200 expression on a breast cancer cell line EMT6 increased during growth in immunocompromised mice and subsequent neutralisation of CD200 led to decreased tumour metastasis and an increase in anti-tumour immune cells (Gorczynski et al., 2011). These findings were further supported by showing decreased EMT6 tumour metastasis in $CD200R^{-/-}$ mice and when using EMT6 cells with silenced CD200, potentially due to an increase activity of $CD8^{+}$ T cells (Podnos et al., 2012, Curry et al., 2017).

These data highlight a different aspect of CD200:CD200R therapeutic targeting, in that blocking rather than activating CD200R signalling can have beneficial effects on tumour progression. Similarly, blocking CD200 may also be beneficial indirectly through tumour-derived vaccines. Glioma-derived CD200 has been shown to supress anti-tumour immune responses to vaccination, while inhibiting CD200 significantly increased leukocyte infiltration, and cytokine production to the vaccine site (Xiong et al., 2016). Thus the complexity of therapeutically targeting the CD200:CD200R pathway is evident, trying to balance the reduction of excessive inflammatory response, while at the same time maintaining protective ones.

1.7 Aims

Research investigating infection with *Francisella tularensis* over the past decades has been extensive. The use of the attenuated *F. tularensis* LVS strain in mice has allowed for a deeper understanding of its life cycle and the immune response elicited against this bacterium. The strong pro-inflammatory response towards *F. tularensis* is a double-edged sword, with many cytokines such IFNγ, TNFα and IL-6 essential for protection, yet possibly the cause of sepsis and death later in infection if the response is exacerbated. An understudied area is the mechanisms by which *F. tularensis* is able to achieve initial immune suppression seen during respiratory infection. Understanding how the bacterium is able to achieve early immune suppression could have major implications for the development of treatments and vaccines for *F. tularensis* and possibly other respiratory pathogens. As the lung has the exceptional ability to maintain homeostasis between innocuous and harmful pathogens, the negative regulatory pathways seem an extremely likely target for evasive pathogens such as *F. tularensis*. Through the course of this thesis two overarching aims were investigated:

Does CD200R play a role in the early immune suppression during *F. tularensis* infection?

This aim was addressed in chapter 3, where the expression of negative immune regulators during *F. tularensis* infection was investigated, as well as the importance of CD200R signaling using *in vitro* and *in vivo* models of infection. At the end of chapter 3, and throughout chapter 4, the effect of lack of CD200R *in vivo* on susceptibility to intranasal *F. tularensis* infection was investigated. The aim was to characterise how cell populations and inflammatory cytokine responses changed within the lung throughout the course of infection.

What are the mechanisms by which CD200R influences infectious outcome?

Some interesting findings from chapter 4 paved the way for the investigation of this aim in terms of the role of CD200R in modulating neutrophil effector functions. Subsequently, the effect of neutrophil depletion during *F. tularensis* infection in WT and $CD200R^{-/-}$ mice was tested. Furthermore, there was a focus on understanding the mechanisms behind how lack of CD200R on neutrophils could alter effector functions, such as ROS production and NETosis, needed for efficient pathogen clearance.

Chapter 2

Materials & Methods

2.1 Bacteria

2.1.1 *Francisella tularensis* live vaccine strain

Francisella tularensis live vaccine strain (LVS) was derived from an original NDBR101 *Pasteurella tularensis* live vaccine, experimental lot 4. The LVS strain was originally derived from a culture obtained from the Gamaleia Institute, USSR, which was passaged five times through mice to decrease virulence before being cultured from the blood of moribund mice (Eigelsbach and Downs, 1961). The vial used has been stored at -20°C in the culture collection at the Defence Science and Technology Laboratory (Dstl, Porton Down). The vaccine contained 6 x 10^9 colony forming units (CFU) of lyophilized *F. tularensis* LVS.

2.1.2 Preparation of master stock

The lyophilized vaccine (2.1.1) was resuspended in 2 ml sterile water and 100 µl of the bacterial suspension was streaked onto 20 blood cysteine glucose agar (BCGA) plates (Oxoid, Thermo Fisher). Plates were incubated at 37°C for 48 hours and then all the bacterial lawns were scraped into cryopreservation liquid (Technical Service Consultants Ltd). Following this, 1 ml aliquots of the bacterial suspension were placed into vials containing cryopreservation beads (Technical Service Consultants Ltd) and stored at -80°C.

2.1.3 Preparation of an *in vitro* challenge dose

The bacterial challenge dose for *in vitro* experiments was often high and required large volumes; therefore a fresh challenge dose was used every time. A cryopreservation bead was taken from the master stock (2.1.2) with an inoculation loop and streaked onto a BCGA plate. The BCGA plate was incubated at 37°C for 48 hours. The bacteria from the LVS lawn was then resuspended in complete L-15 media until a spectrophotometer reading of optical density at 600 nm 0.20 was obtained. It was previously determined that OD_{600nm} 0.20 corresponded to ~1x10^9 CFU/ml. The required CFU was then obtained through further serial dilutions.

2.1.4 Preparation of an *in vivo* challenge dose

Initially challenge doses for *in vivo* experiments were obtained the same way as for *in vitro* experiments (2.1.3). However, it was later changed to working from a frozen *in vivo* challenge stock of *F. tularensis* LVS. This consisted of a preparation of ~1x10^9 CFU/ml (2.1.3) diluted down to make 100 µl aliquots of 1x10^6 CFU/ml which

were frozen at -80°C in cryopreservation liquid. When an *in vivo* challenge dose was required, an aliquot of $1x10^6$ CFU/ml was diluted in PBS (Sigma) to $2x10^4$ CFU/ml so that 1000 CFU could be given in 50 µl intranasal doses (described further in 2.3.2).

2.2 *In vitro* infection models

2.2.1 MH-S cells

In order to study alveolar macrophage responses to *F. tularensis* infection *in vitro*, the MH-S cell line (American Type Culture Collection, CRL-2019) was used. These cells were derived by transforming cells obtained from the bronchoalveolar lavage of Balb/c mice with simian virus 40 (SV40) (Mbawuike and Herscowitz, 1989). MH-S cell cultures were maintained in complete RPMI (Sigma) (10% FCS), splitting cells by scraping when 90% confluent every 2-3 days. Cultures were maintained until passage 25-30 before seeding a fresh vial.

2.2.2 Generation of bone marrow-derived macrophages

Hind legs were removed from WT and $CD200R^{-/-}$ mice, bones were cleaned and bone marrow was flushed from bones using sterile PBS. Cells were resuspended in 1 ml red blood cell lysis buffer for 3 minutes, before quenching with complete RPMI. Cells were then centrifuged for 5 minutes at 300 x g, before being resuspended in complete BMDM media (RPMI – 20% FCS, 20 mM HEPES, 20 ng/ml MCSF) (Sigma) and $6x10^6$ cells were seeded in 10cm non-treated culture dish. After 7 days, the supernatant was removed and adherent cells were carefully removed by gently scraping the culture dish. Cells were washed and resuspended in complete RPMI (10% FCS) to a concentration of $4x10^5$ cells/ml and seeded in a 24 well plate.

2.2.3 Primary neutrophil isolation

Bone marrow was isolated from hind legs of WT and $CD200R^{-/-}$ mice as described previously (2.2.2), and neutrophils were isolated by negative selection using MACS Neutrophil Isolation Kit (Miltenyi Biotec) as per the manufacturer's instructions. In short, the single cell suspension was incubated with a neutrophil biotin-antibody cocktail for 10 minutes at 4°C, washed with wash buffer and incubated for 15 minutes at 4°C with anti-biotin microbeads. Neutrophils were then isolated by magnetic separation with MS MACS columns and a MACS Separator (Miltenyi Biotec). Following isolation, $4x10^5$ cells/well were seeded for further downstream processing.

2.2.4 *F. tularensis* LVS *in vitro* infection assay

F. tularensis LVS inoculum was prepared as described previously. Multiplicity of infection (MOI) of 100 was achieved through serial dilutions in L15 media (10% FCS, 5 mM L-Glutamine) (Life Technologies). Actual inoculum MOI was determined by plate count on BCGA. Cells were incubated for 2 hours (MH-S cells and BMDM) or 4 hours (primary neutrophils) with the LVS inoculum at 37°C to allow for cellular uptake of the bacteria. LVS was removed and cells were washed with warm PBS, followed by 30 minute incubation with 10 µg/ml gentamicin (Sigma) to kill any extracellular bacteria. At this point cells were either lysed to determine bacterial burden (2.2.6) or culture medium replaced with complete L15 with 2 µg/ml gentamicin for 24 hours.

2.2.5 CD200-Fc treatment *in vitro*

For experiments involving CD200-Fc treatment, cells were treated with 10 ng/ml CD200-Fc or human IgG1 (R&D Systems) in complete L15 medium during incubation with LVS for 2 hours, as well as throughout the incubation with gentamicin (2.2.4). CD200-Fc recombinant protein is 49 kDa and consists of an N-terminal mouse CD200 (Gln31-Gly232) derived from the mouse myeloma cell line NS0, fused to human IgG1 (Pro100-Lys330) at the C-terminal by a polypeptide linker (IEGRMD).

2.2.6 Determining bacterial burden

To determine bacterial load at desired time points, the cells were lysed for 2-3 minutes with 1 ml of cold dH_20 while scraping. The neat lysates were immediately plated in triplicate 50 µl spots onto BCGA plates. Neat lysates were further diluted in PBS and plated in the same way. BCGA plates were incubated for 4-5 days at 37°C and single colonies were counted to determine *F. tularensis* LVS burden (CFU/ml).

2.3 *In vivo* infection models

2.3.1 Animals

All animal experiments were performed under the project license 40/03633 (Mark Travis - immunoregulation during pathogen infection). Female WT C57BL/6 mice (Charles River, UK) and $CD200R^{-/-}$ mice, bred on a C57BL/6 background (Boudakov et al., 2007), were kept in specific pathogen–free conditions according to institutional and UK Home Office guidelines in the Biological Services Facility at The

University of Manchester. They were provided with autoclaved food, water and bedding. All procedures were performed in accordance with the Home Office Scientific Procedures Act (1986) and under the DERFA license.

2.3.2 *F. tularensis* LVS *in vivo* intranasal infection

Eight- to twelve-week old WT or CD200R$^{-/-}$ mice were put under light anesthesia with isoflurane and infected intranasally with 50 µl PBS containing ~1000 CFU LVS. Actual dose was determined by plating dilutions of the challenge dose on BCGA plates (2.2.6). Mouse weights were recorded daily, clinical scoring was monitored and mice were culled when needed by cervical dislocation or intraperitoneal overdose of 20% weight/volume sodium pentobarbitone (Animalcare Ltd, York, UK).

2.3.3 CD200-Fc treatment

Female WT mice were treated intraperitoneally with 200 µl PBS or 10 µg CD200-Fc or hIgG in 200 µl PBS one day before intranasal challenge with *F. tularensis* LVS. They were further dosed at day 1, 3 and 5 p.i., before being culled at day 7 p.i. (Figure 4.7A).

2.3.4 Antibiotic treatment

Female WT mice were treated intraperitoneally with a sham injection of 200 µl ddH_2O or 100, 10 or 1 mg/kg gentamicin in 200 µl ddH_2O at day 1, 3 and 5 following intranasal challenge with *F. tularensis* LVS. Mice were culled at day 7 p.i. (Figure 4.10A).

2.3.5 Antibody-mediated neutrophil depletion

WT C57BL/6 and CD200R$^{-/-}$ mice were treated intraperitoneally with 50µg *InVivo*Plus anti-mouse Ly6G (clone 1A8) (Bio X Cell, #BP0075-1) or *InVivo*Plus rat IgG2a isotype control (Bio X Cell, #BP0089) in 200 µl PBS one day before intranasal challenge with *F. tularensis* LVS. They were further dosed at day 1, 3 and 5 p.i., before being culled at day 7 p.i.

2.3.6 Determining organ bacterial burden

The lung, liver and spleen of *F. tularensis* LVS infected mice were removed and weighed, before pressing organs through a 40 µM cell sieve in 1 ml PBS containing protease inhibitor cocktail (Roche). Organ homogenates were plated in triplicate 50 µl spots at appropriate dilutions up to 10^{-6} on BCGA plates and incubated at 37°C

for 4-5 days. Once colonies had grown sufficiently, single colonies were counted and final bacterial burden was calculated using corresponding organ weights (CFU/g).

2.4 Flow cytometry

2.4.1 *In vitro* cell preparation

The supernatant was removed and adherent cells were washed twice with PBS. Cells were then dislodged by scraping the well in 200 µl PBS and processed for flow cytometry as described in 2.4.4.2.

2.4.2 Lung single cell suspension

The right lobes of the lung were dissected, placed in 1 ml Hank's Balanced Salt Solution (HBSS, Sigma) and processed for flow cytometry analysis. Lung tissue was finely chopped and 100 µg/ml Liberase TM (Roche) and 100 µg/ml DNase I (Roche) were added to the HBSS. Samples were shaken at 37°C for 30 minutes. HBSS containing 5 mM EDTA was added to stop the digest and samples were placed on ice. Digested tissue was then passed through a 40 µM cell sieve and centrifuged at 300 x g for 5 minutes. This was followed by resuspension in red blood cell lysis buffer (Sigma) for 3 minutes at room temperature, before quenching with complete RPMI. Samples were centrifuged at 300 x g for 5 minutes, washed in PBS, and centrifuged again before staining for flow cytometry.

2.4.3 Bronchoalveolar lavage (BAL)

In order to retrieve cells from the alveolar airway, bronchoalveolar lavage (BAL) was performed on mice. Briefly, following death by intraperitoneal overdose of 20% w/v sodium pentobarbitone, the trachea was exposed and a small incision was made. A 21g needle attached to plastic tubing was inserted into the trachea and 1ml of HBSS with 0.05 M EDTA (BAL fluid) was inserted into the lungs and washed out twice. BAL samples were then centrifuged at 300 x g for 5 minutes and supernatants removed. The cell pellet was resuspended in 1 ml red blood lysis buffer for 3 minutes a room temperature, before quenching with complete RPMI. The suspension was then centrifuged at 300 x g for 5 minutes and processed for flow cytometry.

2.4.4 Antibodies

2.4.4.1 Anti-*F. tularensis* LVS antibody

For intracellular detection of *F. tularensis* LVS by flow cytometry was initially achieved by using a FITC-labelled anti-*F. tularensis* lipopolysaccharide (LPS) (clone F20.29) monoclonal antibody made by the Detection Department, Dstl (Porton Down). However, due to a supply shortage of the previous antibody, this was subsequently changed to using an anti-*F. tularensis* LPS monoclonal antibody (clone FB11, Abcam) labelled in house with an APC Conjugation Kit (Abcam) to a stock concentration of 1.5 mg/ml.

2.4.4.2 Cell staining protocol for flow cytometry

Cells from the macrophage infection assays and those prepared from organ digestion were both used for flow cytometry analysis. Cells were stained with LIVE/DEAD® Fixable Blue Dead Cell Stain kit (Table 2.1, Invitrogen) and incubated for 10 minutes at 4°C. Cells were washed in FACS buffer (0.5% FCS in 1x PBS) and incubated with an Fc receptor blocking CD16/32 antibody (eBiosciences) at 5 µg/ml for 20 minutes at 4°C. Subsequently, cells were stained with antibodies against extracellular markers (Table 2.2) for 30 minutes at 4°C. For intracellular staining, cells were washed, centrifuged and resuspended in Fixation/Permeabilisation buffer (concentrate:diluent, 1:3) (eBioscience) and incubated at 4°C overnight. Cells were then washed in permeabilisation buffer (concentrate:dH_20, 1:9) (eBioscience), centrifuged and incubated with antibodies against intracellular markers (Table 2.3) in permeabilisation buffer for an additional 30 minutes at 4°C. Appropriate isotype controls were used for all intracellular markers and extracellular gating was originally established using fluorescence minus one (FMO) stained samples. Finally, the cells are washed, resuspended in FACS buffer and analysed on a BD LSR Fortessa (BD Biosciences) unless otherwise stated. Data was further analysed using FlowJo software (Tree Star, Ashland, Oregon).

Table 2.1 | Specifications for fluorescent viability dyes.

Viability Stain	Fluorochrome	Concentration	Company
Annexin V	Pacific Blue	1/100	Invitrogen
LIVE/DEAD Blue	UV450	1/200	Invitrogen
SYTOX-Orange	PE	5 µM	Invitrogen
TO-PRO-3	APC	1 µM	Invitrogen

Table 2.2 | Specifications of fluorochrome-conjugated antibodies for extracellular targets.

Antibody Target	Fluorochrome	Concentration	Clone	Company
CD11b	APC-Cy7	1 µg/ml	M1/70	BioLegend
CD11c	PE-eFluor 610	1 µg/ml	N418	eBioscience
CD200R	PE	1 µg/ml	OX-110	BioLegend
CD4	BV650	1 µg/ml	RM4-5	BioLegend
CD45	FITC BV510	1 µg/ml	30-F11	BioLegend
CD63	PE-Cy7	1 µg/ml	NVG-2	BioLegend
CD64	PE-Cy7	1 µg/ml	X54-5/7.1	BioLegend
CD8	BV785	1 µg/ml	53-6.7	BioLegend
I-A/I-E (MHC-II)	AlexaFluor 700	1 µg/ml	M5/114.15.2	BioLegend
Gr1 (Ly6C and Ly6G)	FITC	1 µg/ml	RB6-8C5	BioLegend
LAMP-1	FITC	1 µg/ml	1D4B	BioLegend
Ly6C	BV421	1 µg/ml	HK1.4	BioLegend
Ly6G	BV711 PE-Cy7	1 µg/ml	1A8	BioLegend
Myeloperoxidase (MPO)	FITC	1 µg/ml	2D4	Abcam
Siglec-F	PerCP-eFluor 710	1 µg/ml	1RNM44N	eBioscience
TCR-β	BV605	1 µg/ml	H57-597	BioLegend

Table 2.3 | Specifications of fluorochrome-conjugated antibodies for intracellular targets and corresponding isotype controls.

Antibody Target	Fluorochrome	Concentration	Clone	Company
F. tularensis LPS	FITC	1 µg/ml	F30.29	Dstl
F. tularensis LPS	APC	2.5 µg/ml	FB11	Abcam
IFNγ	BV711	1 µg/ml	XMG1.2	BioLegend
IL-6	PE	2 µg/ml	MP5-20F3	eBioscience
TNFα	PerCP-eFluor710	1 µg/ml	MP6-XT22	eBioscience
Rat IgG1	BV711/PE/ PerCP-eFluor710	1 µg/ml	eBRG1	eBioscience
Rat IgG2a	APC	2.5 µg/ml	RTK2758	BioLegend

2.5 Image Stream

Samples were processed the same as would be for flow cytometry analysis (2.4.4.2). Samples were placed in a round-bottom 96-well plate and analysed on an Amnis ImageStream^X Mark II (Millipore). Data was further analysed on the analysis software IDEAS® (Amnis).

2.6 Measurement of cytokines and chemokines

2.6.1 Cytokine stimulation

Lungs were processed to a single cell suspension as described previously (2.4.2). Cells were placed in a round-bottom 96-well plate and incubated at 37°C for 4 hours with complete RPMI containing Cell Stimulation Cocktail (plus protein transport inhibitors (1X, eBioscience). The cocktail consisted of phorbol 12-myristate 13-acetate (PMA) and ionomycin to induce activation of cells to produce cytokines, and brefeldin A and monensin to allow secreted proteins to accumulate in the endoplasmic reticulum and Golgi apparatus. Following the incubation, cells were processed for flow cytometry as described previously (2.4.4.2).

2.6.2 Measuring *ex vivo* organ cytokines

Neat organ homogenates from the lung used to determine bacterial burden (2.3.6) were used to measure organ cytokine concentrations. The levels of cytokines IFNγ, TNFα, IL-17A, IL-6, IL-1β and KC were measured via the LEGENDplex Multiplex Immunoassay (Biolegend) according to the manufacturer's instructions. Briefly, organ homogenate supernatants were incubated for 2 hours at room temperature

with beads conjugated to specific antibodies that could be distinguished by size and internal fluorescence intensities. Following a wash step, a biotinylated detection antibody cocktail was added for 1 hour at room temperature to bind to the specific analyte-bound capture beads. Streptavidin-phycoerythrin (SA-PE) was subsequently added for 30 minutes at room temperature, binding to the biotinylated detection antibodies and providing PE fluorescence that was quantified in reference to a standard curve using a BD FACS Verse and the LEGENDplex Software (VigeneTech). Final cytokine was determined by normalising to original lung weight.

2.7 Histology

2.7.1 Lung dissection and inflation

Mice were culled by intraperitoneal overdose of 20% w/v sodium pentobarbitone and the lungs and trachea were exposed. The left lobe of the lung was tied off with thread at the primary bronchus and removed. A small incision was made in the trachea and a 21g needle attached to plastic tubing was inserted into the trachea. Following this, 2-3 ml of 10% formalin was injected into the lung until the right lobe was fully inflated. The inflated lung was removed and placed in a 50 ml centrifuge containing 20 ml of 10% formalin and left overnight. The following day, the lung was cleaned of excess tissue, placed into a histology cassette and stored in 70% ethanol until needed.

2.7.2 Tissue processing and haematoxylin and eosin (H&E) staining

All tissue processing took place in the Histology facility (University of Manchester). Histology cassettes were removed from 70% ethanol and placed in a Shandon Citadel 2000 automated tissue processer (Thermo Scientific). The automated program consisted of passing samples through various stations including: increasing ethanol concentrations to dehydrate the sample, clearing agents such as xylene to remove ethanol and finally embedded by infiltration of molten paraffin wax.

Processed lung tissue was then manually embedded in paraffin wax blocks using a Shandon Histocentre2 (Thermo Scientific). Tissue blocks were sectioned using a Microm HM 330 (Thermo Scientific) and placed onto microscopy slides. Paraffin sections were dewaxed by placing slides in xylene solutions, rehydrated with reducing concentrations of ethanol (100%, 95%, 80% and 75%) and finally washed with distilled water. Subsequently, samples were H&E stained using Shandon Linistain GLX (Thermo Scientific).

2.7.3 Sample imaging and image analysis

H&E stained samples were imaged using a Pannoramic 250 Flash III (3DHistech) in the Bioimaging facility (University of Manchester). Images were further analysed using CaseViewer (3DHistech) and representative images were taken at 20x magnification. Scale bar represents 50 μm. Quantification of cell infiltration was determined using particle analysis in ImageJ with one detectable nucleus equating to one cell (Schneider et al., 2012), then normalised to the surface area of lung tissue in the image by manually removing all bronchial and vascular lumen area.

2.8 RNA

2.8.1 RNA extraction

Cells were lysed with 350 μl of RLT Buffer (Qiagen) and stored at -80°C until required. RNA was isolated using the RNeasy Mini Kit (Qiagen) according to the manufacturer's instructions. Briefly the steps between spins involved: adding 350 μl of 70% ethanol, a DNase digestion, adding 700 μl RW1 Buffer, two steps of 500 μl RPE Buffer, a drying step and finally eluting in 30 μl RNase-free water. RNA concentration was measured using a NanoDrop 2000c (Thermo Scientific) and RNA purity was assess by the ratio of absorbance at 260/280 nm.

2.8.2 Preparation of complementary DNA (cDNA)

cDNA was generated from extracted RNA using the High-Capacity RNA-to-cDNA™ Kit (Applied Biosystems - Thermo Fisher) according to the manufacturer's instructions. The reverse transcription (RT) reaction mix contained 10 μl 2X RT Buffer, 1 μl 20X RT Enzyme and up to 9 μl RNA sample after normalising concentrations; making up a total 20 μl reaction mix. RT was performed using a Chromo4 thermocycler (Bio-Rad) with three steps: 37°C for 60 minutes, 95°C for 5 minutes and 4°C indefinitely. Typically, cDNA was used immediately for real-time qPCR or stored at -20°C.

2.8.3 Real-time qPCR

Quantitative real-time PCR was performed on the Quant Studio 12K Flex system (Applied Biosystems). Each reaction mixture contained 10 ng of cDNA, 2X Fast SYBR Green Master Mix (Applied Biosystems) and 0.6 μM of forward and reverse primers (see Table 2.4 for mouse primer sequences). Samples were incubated at 95°C for 5 minutes, followed by a denaturing step at 95°C for 5 seconds and a

combined annealing/extension step at 60°C for 30 seconds repeated for 40 cycles. Values of target mRNA were normalized to the housekeeping gene β-actin. Data were analysed using the 2-ΔΔCT method (Livak and Schmittgen, 2001) and presented in-terms of fold change in relation to uninfected control.

Table 2.4 | Primer sequences for detection of mouse genes by qPCR.

Gene	Sequence (5'-3')
CD200R	Forward: ATCAGTGGCTTCAGAAAATGCAA
	Reverse: GCCTCCACCTTAGTCACAGT
CD206	Forward: TTCAGCTATTGGACGCGAGG
	Reverse: GAATCTGACACCCAGCGGAA
SIRPα	Forward: CACATCACCTTGGATAGAAGCC
	Reverse: CAGCCAGATCAGCTGGAGATC
TREM2	Forward: GCACCTCCAGGAATCAAGAG
	Reverse: GGGTCCAGTGAGGATCTGAA

2.9 Apoptosis/necrosis assays

Primary neutrophil were isolated as described previously (2.2.3). To monitor the progression of cell death in WT and CD200R$^{-/-}$ neutrophils, 2-colour viability staining was performed with annexin V and TO-PRO-3 (Table 2.1) (Jiang et al., 2016). Briefly, cells were washed with PBS and stained for 20 minutes with annexin V at 4°C for 20 minutes, before adding TO-PRO-3 for an additional 10 minutes. Samples were washed with PBS and analysed immediately on a BD FACSCanto II.

2.10 Measurement of reactive oxygen species

2.10.1 ROS in response to PMA or *F. tularensis* LVS

Primary neutrophil were isolated as described previously (2.2.3). WT and CD200R$^{-/-}$ primary neutrophils were incubated for 15 minutes with Dihydrorhodamine 123 (DHR123) (25 ng/ml), followed by 1-hour stimulation with PMA (100 ng/ml). Alternatively, primary neutrophils were infected with LVS MOI 100 and incubated with DHR123 for 24 hours. DHR123 is able to diffuse into the cell where it is oxidized by ROS to cationic rhodamine 123, which in turn emits green fluorescence (FITC) that can be measured by flow cytometry.

2.10.2 Detection by flow cytometry

At the desired time point, cells were washed in PBS labelled with α-Ly6G antibody for 20 minutes and FITC DHR123 expression was then measured using a BD FACSCanto II. Oxidative index was quantified using the following equation: MFI Stimulated/MFI Unstimulated. DHR ratio was quantified using the following equation: MFI DHR^{+}/MFI DHR^{-}.

2.11 Measuring neutrophil extracellular trap formation

Primary neutrophil were isolated as described previously (2.2.3), and stimulated with 100 ng/ml PMA for 1 hour at 37°C. Cells were washed in PBS and stained for the MPO (Table 2.2) and the viability dye SYTOX-Orange (Table 2.1) for 20 minutes at 4°C. Cells were analysed immediately on a BD FACSCanto II and NET formation was determined by MPO and SYTOX positivity (Masuda et al., 2017).

2.12 Statistical analysis

All graphs and statistical analysis were produced using GraphPad Prism 6 for Windows, version 6.04. Data was expressed as the mean ± standard deviation (SD). Figure legends display the number of experiments undertaken, as well as the number of repeats per group. Normality was determined using the D'Agostino-Pearson and Shapiro-Wilk normality tests. If any data set within the samples showed normal distribution, the data was subsequently analysed parametrically. Statistical analysis was performed by one-way ANOVA, two-way ANOVA and Tukey's multiple comparison test or unpaired t-tests. Significance was considered at $p<0.05$.

Chapter 3

Determining the role of CD200R in the early immune suppression during *Francisella tularensis* infection

3.1 Introduction

Francisella tularensis exhibits increased virulence when contracted via the inhalational route in humans and in animal models (Gurycova, 1998). However, *F. tularensis* LVS is attenuated in humans while maintaining full virulence in mice, allowing research on the bacterial life cycle, host immune response against the pathogen and mechanisms of virulence in murine models (Eigelsbach and Downs, 1961, Roberts et al., 2014, Golovliov et al., 1995, Conlan et al., 2002). Of particular interest is the ability of *F. tularensis* LVS to evade and dampen the host immune response during early stages of pulmonary infection, aiding in rapid replication and dissemination of the bacterium (Bosio, 2011). During this early stage of infection, the primary infected cell type is the alveolar macrophage due to their abundance in the pulmonary airway (Hall et al., 2008).

Alveolar macrophages play a crucial role in the maintenance of airway immune homeostasis through the expression of numerous negative regulatory receptors such as CD200R, SIRPα and TREM2. These receptors interact with ligands and soluble mediators present in the alveolar lumen to dampen alveolar macrophage activity, preventing inappropriate inflammatory response to innocuous antigens (Hussell and Bell, 2014). An array of pathogens have been shown to manipulate these regulatory pathways, and thus alveolar macrophage activity, in order to increase pathogen survival (Gaynor et al., 1995, Cortez et al., 2011, Sharif et al., 2014). Therefore, it was hypothesised that *F. tularensis* was able to modulate negative immune regulatory receptors on alveolar macrophages to dampen inflammatory activity and evade immune detection during early infection.

In Chapter 3, this hypothesis was initially explored using *in vitro* models, before investigating the early response to *F. tularensis* LVS using a knockout mouse model. A preliminary RNA screening highlighted CD200R as a promising target, allowing research to be focused on CD200R. The negative regulator CD200R has very high expression on alveolar macrophages and functions to downregulate ERK, JNK and MAPK inflammatory signalling (Zhang et al., 2004). Thus, it was hypothesised that lack of negative signalling by CD200R would offer protection from infection by increasing the early immune response against *F. tularensis*, a hypothesis tested by characterising the early response to *F. tularensis* infection in $CD200R^{-/-}$ mice.

3.2 Results

3.2.1 Developing an *in vitro* model for *F. tularensis* LVS infection

The initial goal was to optimise an appropriate *in vitro* infection model in order to investigate the effects of *F. tularensis* infection. The overarching focus was to investigate pulmonary *F. tularensis* infection, and alveolar macrophages have been shown to be the first infected cell type in mice via this route (Hall et al., 2008). Therefore, it was important to obtain an initial, basic understanding of how *F. tularensis* growth occurred in alveolar macrophages and how the bacterium influenced regulatory pathways in these cells. This would be achieved by studying *in vitro* models before moving onto the more complex *in vitro* environment.

To this end, MH-S cells were chosen, an SV40-transformed alveolar macrophage-like cell line (Mbawuike and Herscowitz, 1989), for the *in vitro* model. These cells have been shown to have similar receptor expression and particle binding properties to primary alveolar macrophages (Mbawuike and Herscowitz, 1989), and have been used in the study of macrophage interaction with other intracellular pathogens such as *Legionella pneumophila* and *Mycobacterium tuberculosis* (Melo and Stokes, 2000, Matsunaga et al., 2001).

Firstly, a method to consistently incubate cells with the same infectious dose was developed. Thus, the bacterial concentration of *F. tularensis* LVS resuspended in cell culture media was determined by measuring the optical density (OD) of the media at a wavelength of 600 nm. There was an exponential increase in the bacterial count in media of OD_{600} 0.05, 0.10, 0.15 and 0.20, with an OD of 0.20 correlating to a bacterial concentration of approximately $1x10^9$ CFU/ml (Figure 3.1A). From these results an accurate estimate of the multiplicity of infection (MOI) used during *in vitro* assays was achieved, prior to determining the actual dose.

Following this, the effect of different *F. tularensis* LVS MOI on infection kinetics in MH-S cells was determined. To this end, cells were incubated with the appropriate MOI for 2 hours to allow the bacteria to be phagocytosed by the cells. After 2 hours, cells were washed with culture media and treated with 10 µg/ml gentamicin for 30 minutes to kill extracellular bacteria not taken up by the cells. At this point, cells were either taken for further downstream processing (i.e. enumeration of bacterial burden, flow cytometry, RNA extraction) or maintained in culture media with 2 µg/ml gentamicin (to kill remaining extracellular bacteria and focus counts on intracellular bacteria only) and cells analysed at 6 or 26 hours post-infection (Figure 3.1B).

Infecting MH-S cells with different *F. tularensis* LVS MOI of 1, 10 and 100 (average MOI of 1.6, 22 and 147 respectively), all showed a consistent pattern of infection throughout the 26 hours post-infection (p.i.) (Figure 3.1C). As expected there were increased bacterial burden between MOI 1, 10 and 100 at 2, 6 and 26 hours p.i., but the infection dynamics remained the same for each condition. At each challenge dose there was no change in bacterial burden between 2 and 6 hours p.i., whereas by 26 hours p.i. a large two-log increase in bacterial burden was observed regardless of MOI (Figure 3.1C). However, there were only significant differences during infection with an MOI 100 compared to 1 and 10 at 6 and 26 hours p.i. (Figure 3.1C), therefore MOI 100 was used in all future *in vitro* experiments in order to try and elicit the biggest response from the cells.

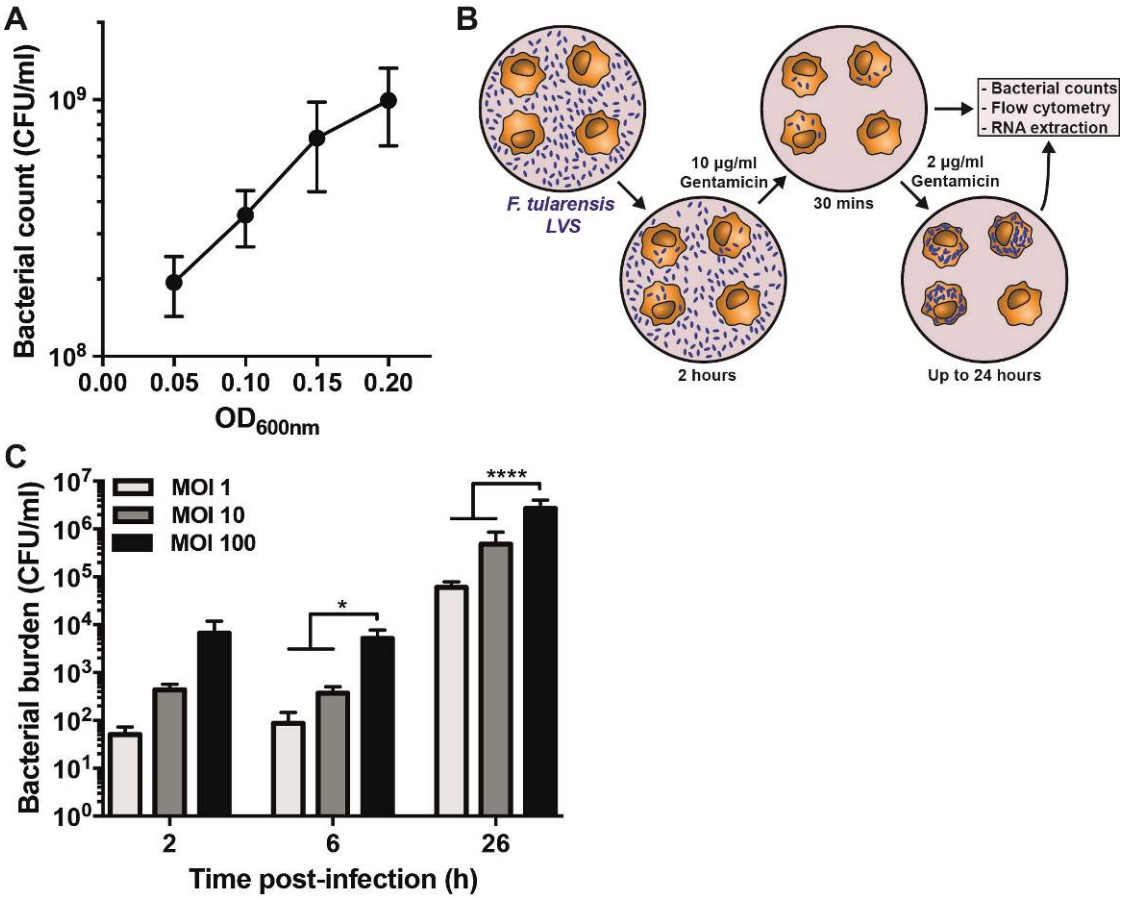

Figure 3.1 | Optimising an *in vitro* macrophage infection model for *F. tularensis* LVS. A) *F. tularensis* LVS grown on BCGA plates for 48 hours was resuspended in L-15 culture media and the bacterial concentration (CFU/ml) was determined from media at OD_{600nm} 0.05, 0.10, 0.15 and 0.20 measured on a spectrophotometer. B) Schematic diagram explaining the methodology of the *in vitro* macrophage infection assay (further description in Methods 2.2.4). C) MH-S cells were incubated with an average *F. tularensis* LVS MOI 1.9 (■), MOI 22 (■) or MOI 147 (■), and then lysed at 2, 6 and 26 hours p.i. to determine bacterial burden. Data are representative of two independent experiments and is shown as mean ± SD (n=6, 3/group). Statistical analysis was performed between MOI using a two-way ANOVA (*p<0.05, ****p<0.0001).

To better understand the timecourse of infection within macrophages, the timepoints post-infection when bacterial burden was measured were increased. This allowed better understanding of infection kinetics between 6 and 26 hours p.i. where a large increase in bacterial replication was observed. MH-S cells were infected with *F. tularensis* LVS and bacterial burden was measured at 2, 6, 10, 14, 20 and 26 hours p.i. As was previously observed, there was no significant difference in bacterial burden at 2 and 6 hours p.i. (Figure 3.2A). However, there was an exponential increase in burden from 10 hours up to 26 hours p.i., reaching significance at 20 and 26 hours p.i. (Figure 3.2A). These data suggest that there was very little net growth of bacteria until between 6-10 hours p.i., but once the bacteria began to replicate they did so continuously until 26 hours p.i.

3.2.2 Analysing *in vitro F. tularensis* LVS infection by flow cytometry

Next, the kinetics of *F. tularensis* LVS infection in MH-S cells was investigated further using flow cytometry. To determine the percentage of infection, cells were pre-gated on single, live cells (Figure 3.2B). It was interesting to note that incubation of MH-S cells with LVS did not affect the viability of the cells throughout the time course of infection when compared to uninfected controls (Figure 3.2C). The percentage of infected cells was measured at 2, 6, 10, 14, 20 and 26 hours p.i. using a FITC-conjugated monoclonal antibody against *F. tularensis* LVS (Figure 3.2D). Results showed that only ~1% of cells were infected at 2 and 6 hours p.i., significantly increasing to ~3% at 10, 14 and 20 hours p.i., before reaching ~4% at 26 hours p.i. that was significantly higher than other timepoints (Figure 3.2D & E). These results suggested that despite a high MOI, few cells were infected.

Results obtained by flow cytometry showing low percentage cell infection was surprising considering the high bacterial burden seen when enumerating CFU in MH-S cells. Therefore a different antibody was tested to determine whether a better representation of infection in MH-S cells could be observed. The FITC-*F. tularensis* antibody was compared to a new APC-conjugated monoclonal antibody against *F. tularensis* LVS. When measuring percentage of *F. tularensis* LVS infection in MH-S cells at 26 hours p.i., the APC-*F. tularensis* antibody was able to provide a more distinct population of infected cells compared to the FITC antibody (Figure 3.3A). Subsequently, this allowed the measurement of significantly more infected cells, at 26 hours p.i. when using the APC-*F. tularensis* antibody (Figure 3.3B). Thus, these data suggest that the APC-*F. tularensis* antibody was more effective at labelling the bacteria and provided a more sensitive quantification of infected cells.

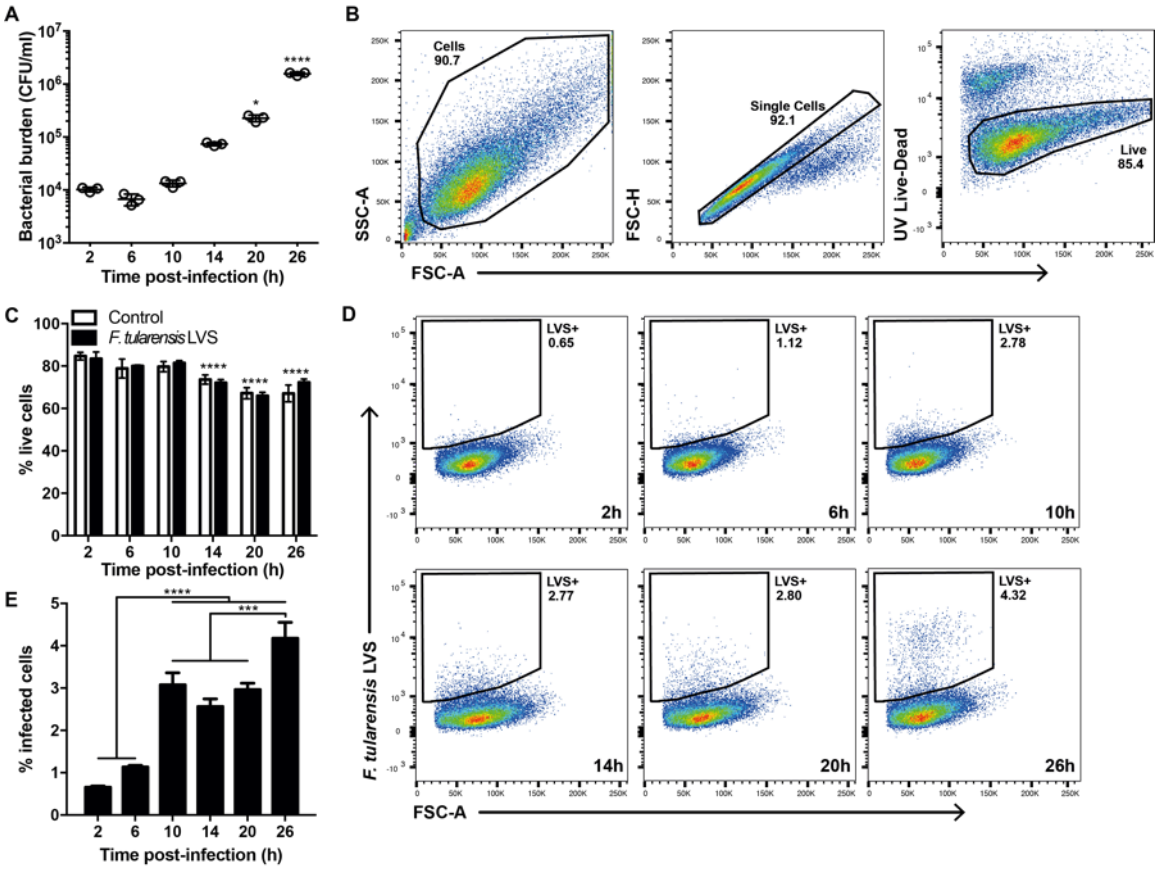

Figure 3.2 | Exponential increase in *F. tularensis* burden from 6 to 26 hours post-infection in MH-S cells. MH-S cells were incubated with *F. tularensis* LVS MOI 95 and analysed at 2, 6, 10, 14, 20 and 26 hours p.i. A) Bacterial burden (CFU/ml) was enumerated in infected MH-S cells. B) Gating strategy for flow cytometry analysis, showing samples initially pre-gated on live, single cells. C) Percentage of live cells of uninfected and infected MH-S cells at 2, 6, 10, 14, 20 and 26 hours p.i. D) Representative dot plots of infected MH-S cells at 2, 6, 10, 14, 20 and 26 hours p.i., determined by *F. tularensis* LVS-FITC monoclonal antibody expression (E) Quantification of percentage infection in MH-S cells infected with *F. tularensis* LVS. Data is from one experiment shown as mean ± SD (n=3). Statistical analysis was performed using a one-way ANOVA (***p<0.001, ****p<0.0001).

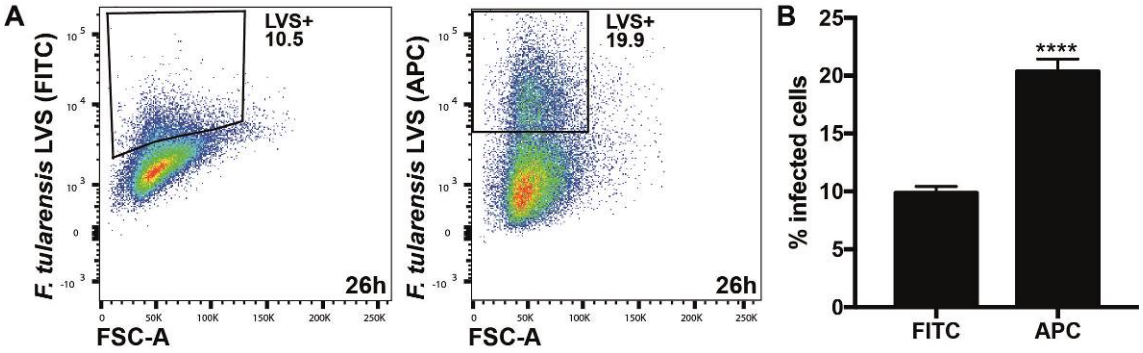

Figure 3.3 | APC-conjugated *F. tularensis* LVS antibody provides a more sensitive detection of infected cells. MH-S cells were incubated with LVS MOI 100 and analysed by flow cytometry at 26 hours p.i. A) Representative dot plots comparing the percentage of *F. tularensis* LVS-infected cells using FITC and APC *F. tularensis* LVS monoclonal antibodies. B) Quantification percentage of infected MH-S cells at 26 hours p.i. Data represents on experiment and is shown as mean ± SD (n=3). Statistical analysis was performed using a student t-test (****p<0.0001).

3.2.3 Analysing *F. tularensis* LVS infection *in vitro* by ImageStream

Despite the increased sensitivity of the APC-*F. tularensis* antibody, there was still interest in better understanding the relatively low percentage of infection in MH-S cells and additional information about the localisation of infection within macrophages was explored. Thus, infected MH-S cells were analysed using an ImageSteam that was able to combine the phenotyping abilities of flow cytometry with the detailed imagery of microscopy (Phanse et al., 2012, Jenner et al., 2016). MH-S cells were infected with *F. tularensis* LVS and analysed at 2, 6 and 26 hours p.i. with the ImageStream. Cells were initially gated on single and in focus cells (Figure 3.4A), before looking at the percentage of infected cells (Figure 3.4B). As previously observed, there was no difference between the percentage infection seen at 2 and 6 hours p.i., while there was a significant increase in infected cells at 26 hours p.i. (Figure 3.4C). Similar results were also observed when measuring maximum pixel intensity of APC, with a significant increase in APC intensity at 26 hours p.i. (Figure 3.4D).

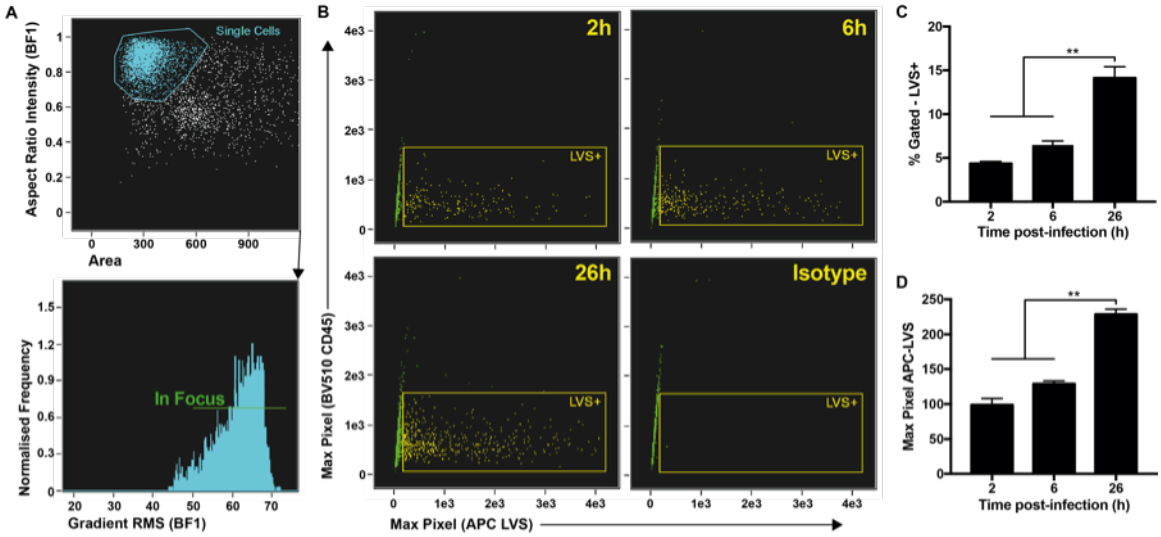

Figure 3.4 | ImageStream analysis of *F. tularensis* LVS-infected MH-S cells. MH-S cells were incubated with *F. tularensis* LVS MOI 66 and analysed by ImageStream at 2, 6 and 26 hours p.i. A) Samples were pre-gated on single, in focus cells B) Infected MH-S cells were analysed at 2, 6 and 26 hours p.i. (C & D) Quantitative data presented as (C) percentage of LVS-infected cells and (D) max pixel intensity of APC-*F. tularensis* LVS at 2, 6 and 26 hours p.i. Data represents on experiment and is shown as mean ± SD (n=3). Statistical analysis was performed using a one-way ANOVA (n=3) (**p<0.01).

The novel aspect of this technique was the ability to have high-resolution images of individual infected cells, to understand how percentage infection and max pixel intensity correlates to the number of *F. tularensis* within the cells. Representative images of infected cells (Figure 3.5) at 2 and 6 hours p.i. confirmed that there was

no net growth during this time as the number of bacteria remained at ~2-4 per cell. In contrast, there was a large congregation of *F. tularensis* LVS within the cell at 26 hours p.i., but unfortunately it was difficult to determine exact numbers of bacteria within the cell. Furthermore, the percentage of infected cells seen previously (Figure 3.4C) was supported by observations that the majority of cells imaged showed no infection (data not shown). For this reason, percentage of infected cells by flow cytometry and CFU was used as a measurement of bacterial burden in future *F. tularensis* LVS infections.

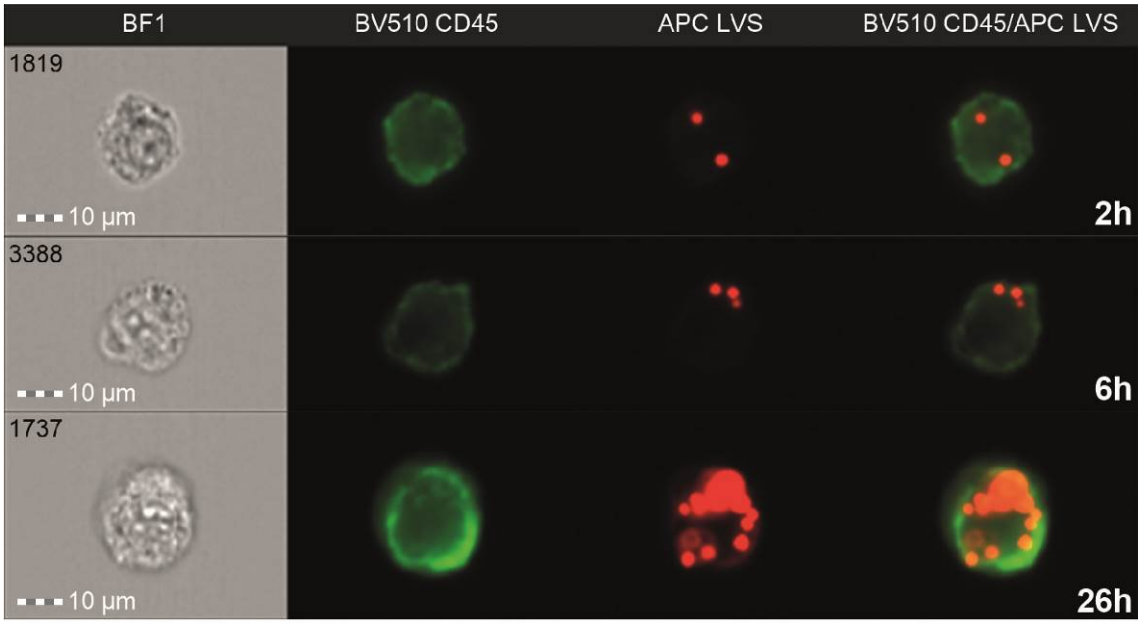

Figure 3.5 | Visualising internalised *F. tularensis* LVS in MH-S cells by ImageStream. Representative images of one experiment taken by ImageStream of *F. tularensis* LVS-infected MH-S cells at 2, 6 and 26 hours p.i. Channels shown from left to right are brightfield, CD45, *F. tularensis* LVS and a merge of CD45/LVS. Scale bar = 10 µm.

3.2.4 CD200R mRNA expression is significantly upregulated during *F. tularensis* LVS infection

After setting up assays to detect *F. tularensis* infection *in vitro,* the aim was to better understand how *F. tularensis* LVS is able to subvert the immune response early in infection. To this end, the effect of *F. tularensis* LVS infection on pulmonary immune regulators was investigated *in vitro* using MH-S cells. RNA was extracted from *F. tularensis* LVS-infected MH-S cells at 2, 6, 10, 14, 20 and 26 hours p.i., and gene expression for a number of potential immune regulatory molecules known to control alveolar macrophage responses (Figure 1.3) quantified by Real-Time (RT) PCR and normalised to uninfected controls. There was a gradual increase in the expression of *cd200r* during the course of infection, reaching significance over all other time

points at 20 hours p.i. with a ~7-fold increase in expression (Figure 3.6A). Although not as striking, there was also a significant ~3-fold upregulation of *sirpα* at 20 hours p.i. (Figure 3.6B). On the contrary, no significant change in mRNA expression of *trem2* or *cd206* throughout the course of infection was observed (Figure 3.6C & D). These data suggest that CD200R in particular could play an important role during *F. tularensis* LVS infection.

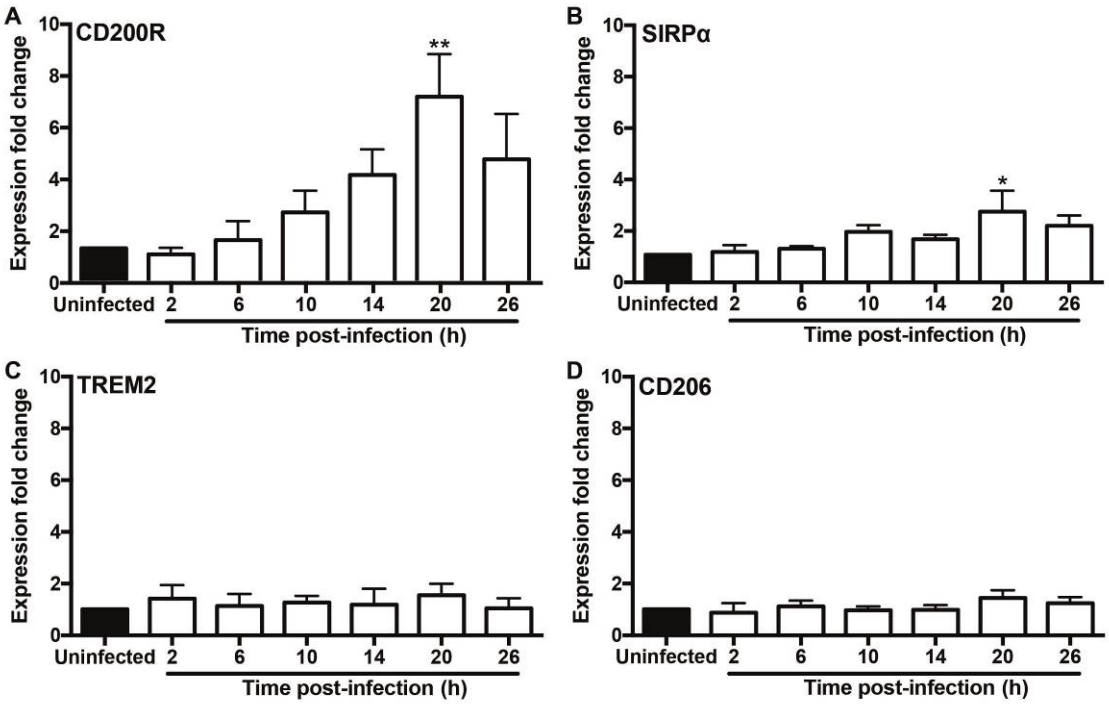

Figure 3.6 | *F. tularensis* LVS infection upregulates CD200R mRNA expression in MH-S cells. Quantitative real-time PCR of A) *cd200r*, B) *sirpα*, C) *trem2* and D) *cd206* mRNA expression in MH-S cells following *F. tularensis* LVS infection at 2, 6, 10, 14, 20 and 26 hours p.i. Results are presented as fold change in relation to uninfected MH-S cells after normalizing to β-actin mRNA levels. Data represents three independent experiments and data is shown as mean ± SD (n=9, 3/group). Statistical analysis was performed using two-way ANOVA (*p<0.05, **p<0.01).

3.2.5 The CD200R pathway is protective during *in vitro F. tularensis* LVS infection

Binding of CD200 to CD200R induces phosphorylation of downstream targets that ultimately leads to the inhibition of pro-inflammatory signalling (Zhang et al., 2004). Thus, using the CD200R-activating immunoadhesin CD200-Fc (Gorczynski et al., 2001b, Gorczynski et al., 2002, Lyons et al., 2012, Gorczynski et al., 1999), would allow for the investigation of the role of CD200R signalling during *F. tularensis* LVS infection.

MH-S cells were treated with CD200-Fc, or human IgG (hIgG) as a control, prior to and during *F. tularensis* LVS infection for 26 hours. Cells were taken at 2, 6 and 26 hours p.i. and analysed by flow cytometry (Figure 3.7A). There were no significant differences in percentage of infected cells (Figure 3.7B) or bacterial burden (Figure 3.7C) at 2 and 6 hours p.i. between cells treated with hIgG and CD200-Fc. However, there was a significant reduction in percentage of infected cells and the overall bacterial burden at 26 hours p.i. in cells treated with CD200-Fc compared to hIgG control treated (Figure 3.7B & C). These results indicated that activation of the CD200R pathway can decrease infection of MH-S cells by *F. tularensis* LVS. Thus, instead of CD200R signalling promoting immune evasion as hypothesised initially, it appears that this pathway may play a protective role during infection.

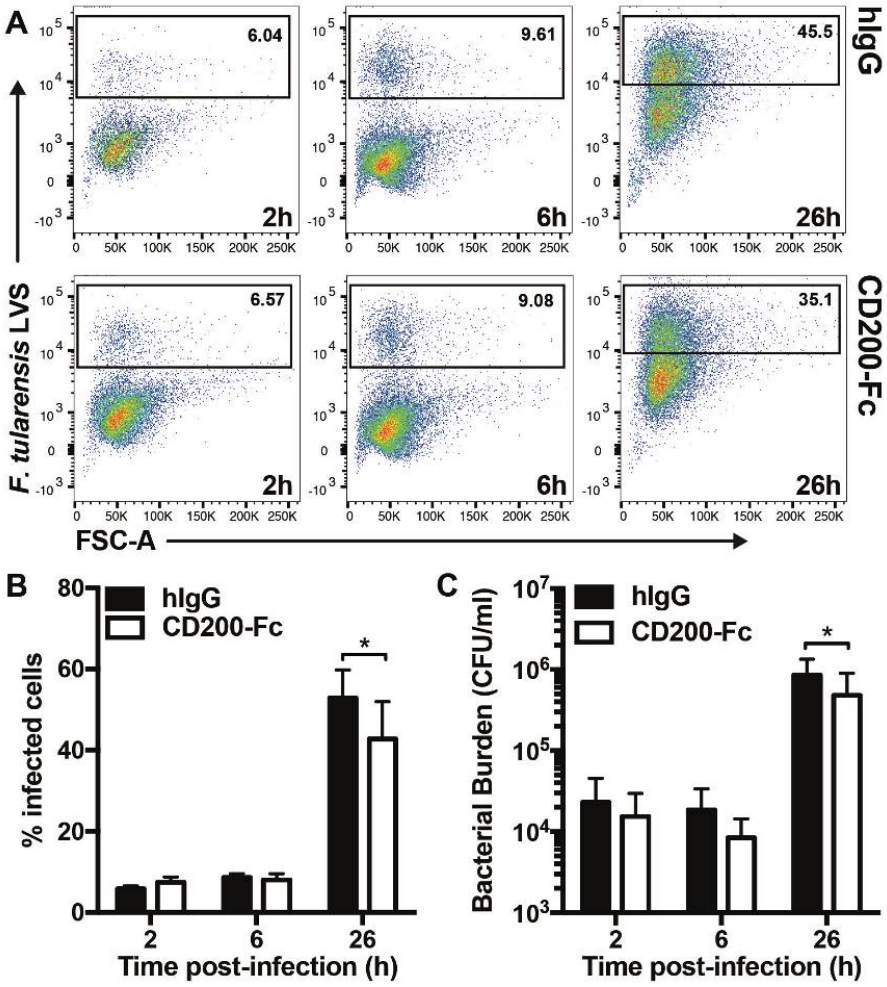

Figure 3.7 | Activating CD200R reduces *F. tularensis* LVS burden in MH-S cells. MH-S cells were treated with 10 ng CD200-Fc or hIgG and incubated with an average *F. tularensis* LVS MOI 74 and analysed at 2, 6 and 26 hours p.i. A) Representative dot plots showing percentage of infected MH-S cells at 2, 6 and 26 hours p.i. following CD200-Fc or hIgG treatment. B) The percentage of LVS infected CD200-Fc- and hIgG-treated MH-S cells was calculated at 2, 6 and 26 hours p.i. C) Total bacterial burden was enumerated by counting CFU and presented as CFU/ml. Data represents two independent experiments and data is shown as mean ± SD (n=6, 3/group). Statistical analysis was performed using two-way ANOVA (*p<0.05).

To further explore the potential protective role for CD200R signalling during *F. tularensis* LVS infection, bone marrow-derived macrophages (BMDM) from wild type (WT) and CD200R$^{-/-}$ mice were cultured and infected with *F. tularensis* LVS. Upon characterising the BMDM for phenotypic markers by flow cytometry, it was noted that WT and CD200R$^{-/-}$-derived BMDM had very low expression of MHC-II and high expression of CD11c and CD11b (Figure 3.8). Interestingly, while WT BMDM mostly expressed low levels of Gr-1, there were two distinct populations of CD200R$^{-/-}$ BMDM that had differing Gr-1 expression. One population was similar to WT BMDM with low Gr-1 expression, while the other had high expression of Gr-1. As expected CD200R$^{-/-}$ BMDM had no expression of CD200R, while the WT BMDM showed high expression (Figure 3.8). These results confirm that BMDM from CD200R$^{-/-}$ mice did indeed lack CD200R, while secondly supporting a successful culture of BMDM.

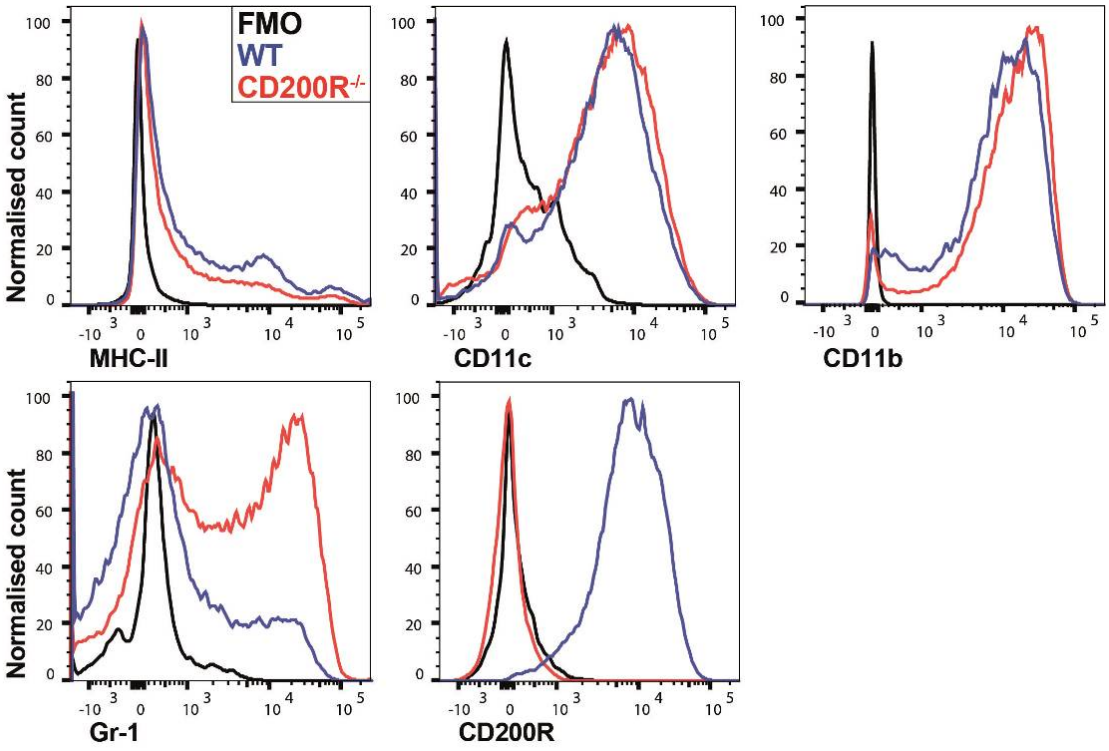

Figure 3.8 | Phenotypic characterisation of WT and CD200R$^{-/-}$-derived BMDM. Primary BMDM were cultured for 7 days from WT and CD200R$^{-/-}$ mice as described in Methods 2.2.2 and characterized by flow cytometry. Representative histograms show expression of MHC-II, CD11c, CD11b, Gr-1 and CD200R in WT (blue) and CD200R$^{-/-}$ (red) derived BMDM. Expression with fluorescence minus-one (FMO) control (black) is also presented.

After characterising the BMDM, their response to *F. tularensis* infection was determined. WT and CD200R$^{-/-}$-derived BMDM were infected with *F. tularensis* LVS for 2, 6 or 26 hours and bacterial burden determined via bacteriology or flow cytometry (Figure 3.9A). As seen previously with MH-S cells, no significant differences were observed in percentage infection or bacterial burden early during infection at 2 and 6 hours p.i. (Figure 3.9B & C respectively). However, at 26 hours p.i. there was a significant increase in *F. tularensis*-infected CD200R$^{-/-}$ BMDM compared to WT (Figure 3.9B), as well as a significantly enhanced bacterial burden when compared to WT BMDM (Figure 3.9C). These findings indicate that that lack of CD200R exacerbates *F. tularensis* LVS infection *in vitro.*

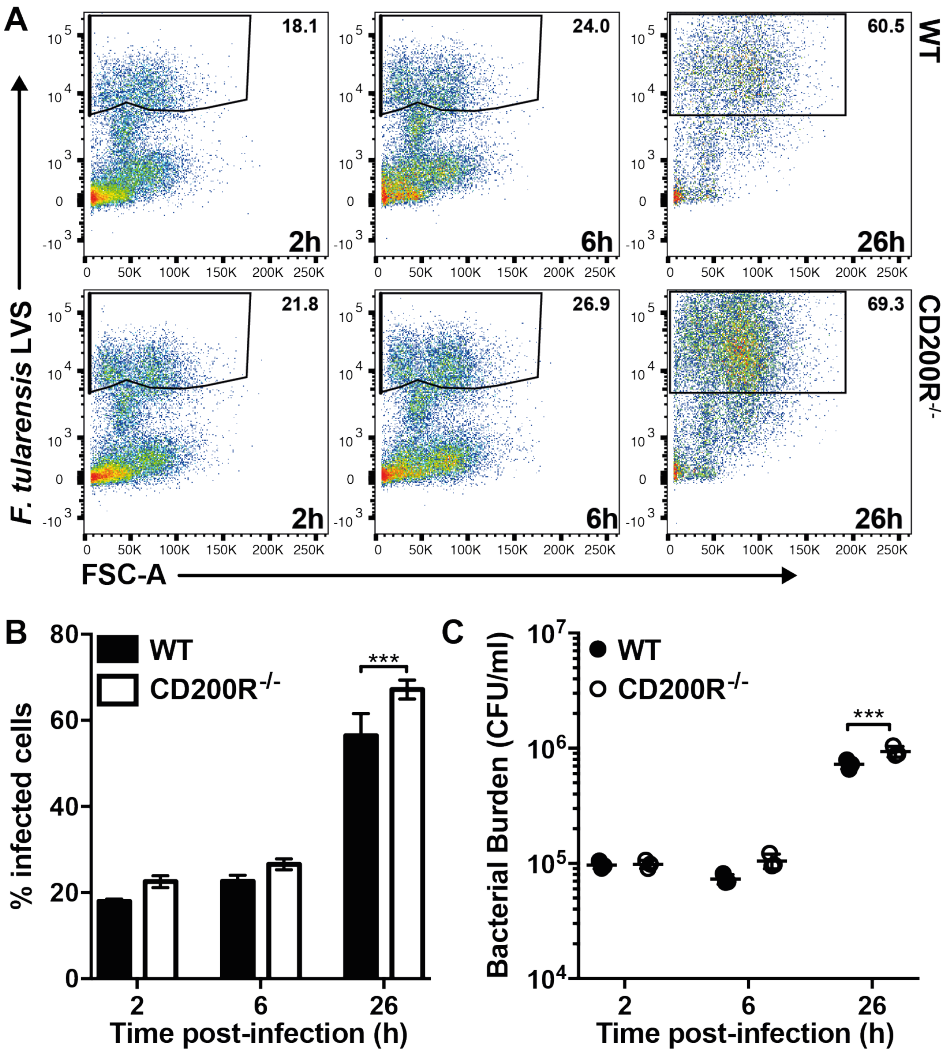

Figure 3.9 | Increased *F. tularensis* LVS burden in CD200R$^{-/-}$-derived BMDM. Primary BMDM from WT and CD200R$^{-/-}$ mice were incubated with an average *F. tularensis* LVS MOI 71 and analysed at 2, 6 and 26 hours p.i. A) Representative dot plots showing levels of *F. tularensis* LVS infection WT and CD200R$^{-/-}$ BMDM at 2, 6 and 26 hours p.i. B) The percentage of LVS infected WT and CD200R$^{-/-}$ BMDM was calculated at 2, 6 and 26 hours p.i. C) Total bacterial burden was enumerated by counting CFU and presented as CFU/ml. Data is representative of two experiments and is shown as mean ± SD (n=3/group). Statistical analysis was performed using two-way ANOVA (***p<0.001).

It was next determined whether activating the CD200R pathway in WT BMDM with CD200-Fc could protect against *F. tularensis* LVS-infection as seen in MH-S cells (Figure 3.7). WT-derived BMDM were treated with CD200-Fc recombinant protein or hIgG control prior to, as well as during, *F. tularensis* LVS infection for 26 hours. Interestingly, unlike with MH-S cells, there was no significant difference in percentage infection or overall bacterial burden throughout the course of the infection upon CD200-Fc treatment (Figure 3.10A & B respectively). These data suggest that there may be some differences between CD200R signalling in MH-S cells and BMDM.

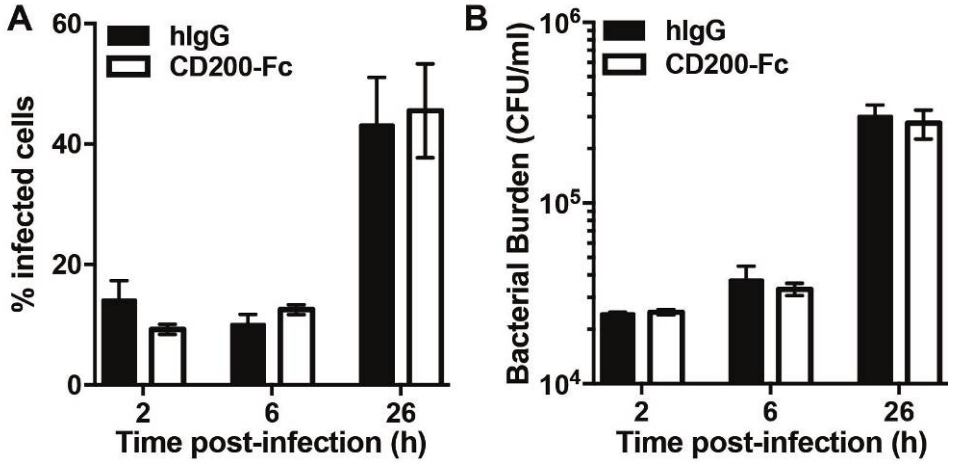

Figure 3.10 | Activation of CD200R on BMDM does not alter *F. tularensis* LVS burden. Primary BMDM from WT mice were treated with 10 ng CD200-Fc or hIgG, incubated with *F. tularensis* LVS MOI 81 and analysed at 2, 6 and 26 hours p.i. Level of LVS infection was determined by A) flow cytometry as percentage of infected cells and B) total bacterial burden (CFU/ml) enumerated by counting CFU. Data represents one experiment and is shown as mean ± SD (n=3). Statistical analysis was performed using two-way ANOVA.

3.2.6 Determining the bacterial burden in WT and CD200R$^{-/-}$ mice during early pulmonary *F. tularensis* LVS infection *in vivo*

With *in vitro* findings showing that CD200R may play a protective role during *F. tularensis* LVS infection, it was investigated whether this would also be the case during a lethal pulmonary infection *in vivo*. 8-12-week old WT and CD200R$^{-/-}$ mice were intranasally infected with a lethal *F. tularensis* LVS dose of 1000 CFU, and their weight was monitored before sacrificing the mice 4, 24, 48 and 72 hours p.i.

There was no percentage weight change in any of the mice during the course of the 72 hour *F. tularensis* LVS infection (Figure 3.11A). Therefore, the bacterial burden (CFU/g of tissue) of the lung, liver and spleen of infected mice was determined to understand how this correlated with weight loss (Figure 3.11B). Firstly, there was a

rapid, exponential increase in bacterial replication in the lung up to 72 hours p.i. Despite high bacterial burdens in the lung already by 24 hours p.i., dissemination of the bacteria to the peripheral organs of the liver and spleen did not appear to take place until 48 hours p.i. At this point there was extensive bacterial burden was observed in the peripheral organs up to 72 hours p.i. Nevertheless, there was no significant difference in LVS burden in the lung, liver or spleen between WT and CD200R$^{-/-}$ mice at these early timepoints (Figure 3.11B).

These data suggested that CD200R may not play a direct role in controlling the early response to *F. tularensis* LVS infection *in vivo*. However, it was important to further investigate the potential differences in lung cell population dynamics of WT and CD200R$^{-/-}$ mice that were responding to *F. tularensis* LVS infection.

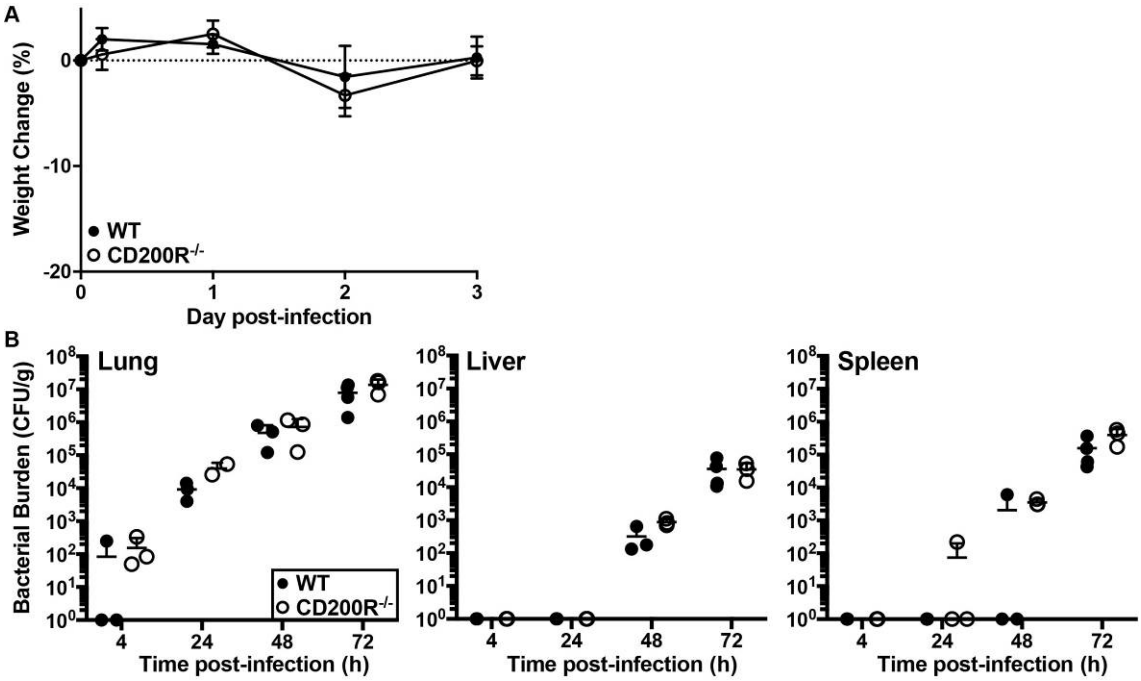

Figure 3.11 | No differences in early *F. tularensis* LVS burden in WT and CD200R$^{-/-}$ mice. WT and CD200R$^{-/-}$ C57BL/6 mice were infected intranasally with *F. tularensis* LVS CFU 600 and culled at 4, 24, 48 and 72 hours p.i. A) Mouse weights were monitored daily and data shows weight change plotted as percentage weight loss. B) Bacterial burdens (CFU/g) in the lung, liver and spleen of WT and CD200R$^{-/-}$ mice were enumerated at 4, 24, 48 and 72 hours p.i. Data is from one experiment and is shown as mean ± SD (n=3-4). Statistical analysis was performed using two-way ANOVA.

3.2.7 Characterising the early response to *F. tularensis* LVS infection in the lung

As previously discussed, pulmonary *F. tularensis* infection is characterised by increased virulence and a dampened immune response. In order to understand the phenotypic changes of cell populations within the lung during this period of *F. tularensis* LVS infection, a gating strategy was developed to detect cells types of interest. The primary cell types of interest were those that had previously been shown to be involved in responding to pulmonary *F. tularensis* infection and that express CD200R, such as lung macrophages and neutrophils (Hall et al., 2008).

Lung cells were isolated following bronchoalveolar lavage (BAL) and analysed by flow cytometry, and initially gated on single, live, $CD45^+$ lymphocytes (Figure 3.12A). At this point $CD11b^+$ $Ly6G^+$ neutrophils were gated out, and then CD64 and Siglec-F were used to distinguish between alveolar macrophages ($CD64^+$ Siglec-F^+), lung macrophages ($CD64^+$ Siglec-F^-) and eosinophils ($CD64^-$ Siglec-F^+). Lung macrophages could then be further divided by their expression of CD11b and CD11c into interstitial macrophages ($CD11b^+$ $CD11c^+$) and inflammatory monocytes/macrophages ($CD11b^+$ $CD11c^-$ $Ly6C^+$). $CD4^+$ and $CD8^+$ T cell populations previously gated as $CD64^-$ Siglec-F^- $TCR\beta^+$, as well as lung dendritic cells ($CD64^-$ Siglec-F^- MHC-II^+). The dendritic cells (DCs) were further divided into $CD11b^-$ $CD11c^+$ DCs and $CD11b^+$ $CD11c^+$ DCs (Figure 3.12A).

The surface expression of CD200R on various cells was determined (Figure 3.12B). As expected, there was reduced CD200R expression on any cell type in the $CD200R^{-/-}$ mice compared to WT. There was high CD200R expression on WT alveolar macrophages and robust expression on neutrophils, with reduced expression on interstitial macrophages (Figure 3.12B).

Following the development of an adequate flow cytometry gating strategy, the shifts in cell populations and the infected cell types through the course of *F. tularensis* LVS infection in WT and $CD200R^{-/-}$ mice could be monitored. Interestingly, the alveolar macrophage population was significantly reduced in $CD200R^{-/-}$ mice compared to WT at 48 hours p.i., with the WT population being reduced to similar levels by 72 hours p.i. (Figure 3.13A). It was observed that the percentage of *F. tularensis* LVS-infected alveolar macrophages remained low up to 24 hours p.i. From 48 hours p.i. there was an increase in the percentage of infected cells, with significantly more infected alveolar macrophages present in $CD200R^{-/-}$ mice at

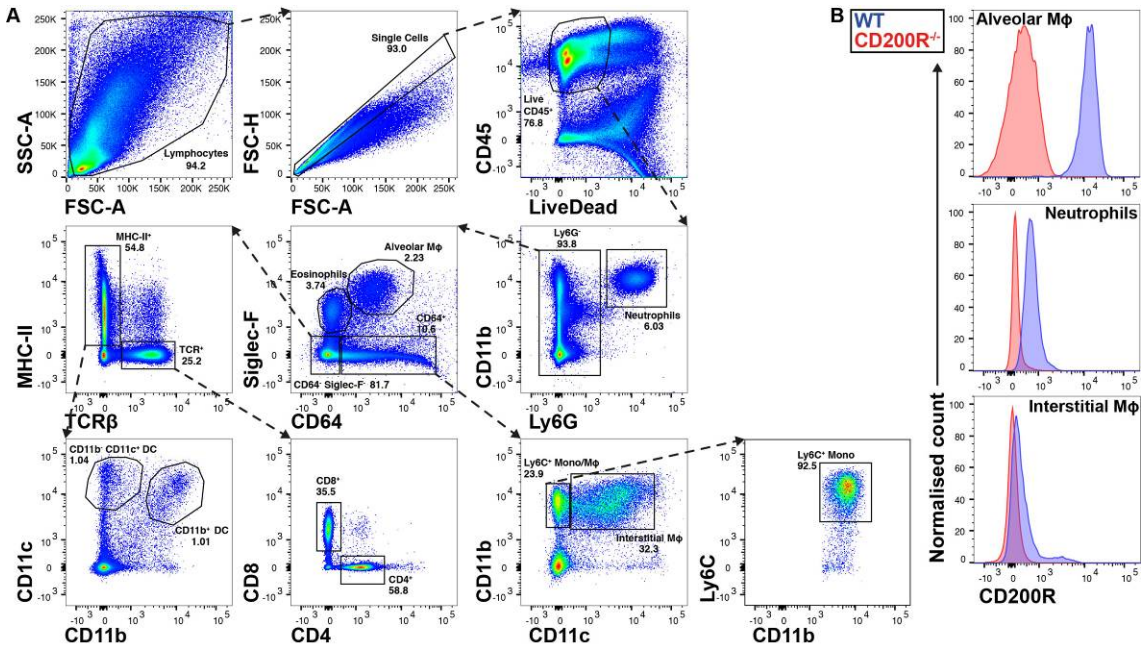

Figure 3.12 | Gating strategy for lung cell populations. Bronchoalveolar lavage was performed prior to lung digestion and lungs were processed to give a single cell suspension before staining for flow cytometry. A) Samples were initially gated on single, live $CD45^+$ lymphocytes. $CD11b^+$ $Ly6G^+$ neutrophils were gated out and CD64 and Siglec-F was used to distinguish between alveolar macrophages, eosinophils and lung macrophages. Lung macrophages were further split into interstitial macrophages ($CD11b^+$ $CD11c^+$) and inflammatory monocytes/macrophages ($CD11b^+$ $CD11c^-$ $Ly6C^+$). The $CD64^-$ $Siglec\text{-}F^-$ population was subdivided to look at $CD4^+$ and $CD8^+$ T cell populations ($TCR\beta^+$), as well as lung dendritic cells ($CD64^-$ $Siglec\text{-}F^-$ $MHC\text{-}II^+$). Dendritic cells were further divided by expression of CD11b and CD11c. B) Representative (n=4) histograms of CD200R expression in alveolar macrophages, neutrophils and interstitial macrophages from WT (blue) and $CD200R^{-/-}$ (red) mice.

48 and 72 hours p.i compared to WT (Figure 3.13A). These data could point towards an *F. tularensis* LVS-induced depletion of alveolar macrophages, occurring earlier in $CD200R^{-/-}$ mice due to increased infection in alveolar macrophages compared to WT. Nevertheless, the reduction in alveolar macrophage populations at 72 hours p.i. suggested that these cells were contributing little to the bacterial burden seen in the lung.

As it seemed unlikely alveolar macrophages were contributing significantly to the bacterial burden in the lung, other cell types were investigated. These included interstitial macrophages, $Ly6C^+$ monocytes/macrophages and neutrophils (Figure 3.13B, C & D respectively), all of which shared very similar kinetics during *F. tularensis* LVS infection both in terms of proportion of $CD45^+$ cells and percentage of *F. tularensis* LVS-infected cells. Very little change in the proportion of $CD45^+$ cells was observed from WT mice for all three cell types from 0 to 48 hours

p.i., followed by a large increase in cells at 72 hours p.i. (Figure 3.13B-D). Interestingly however, there was a significantly higher proportion of Ly6C$^+$ monocytes/macrophages and neutrophils in CD200R$^{-/-}$ mice compared to WT at 72 hours p.i. (Figure 3.13C & D respectively).

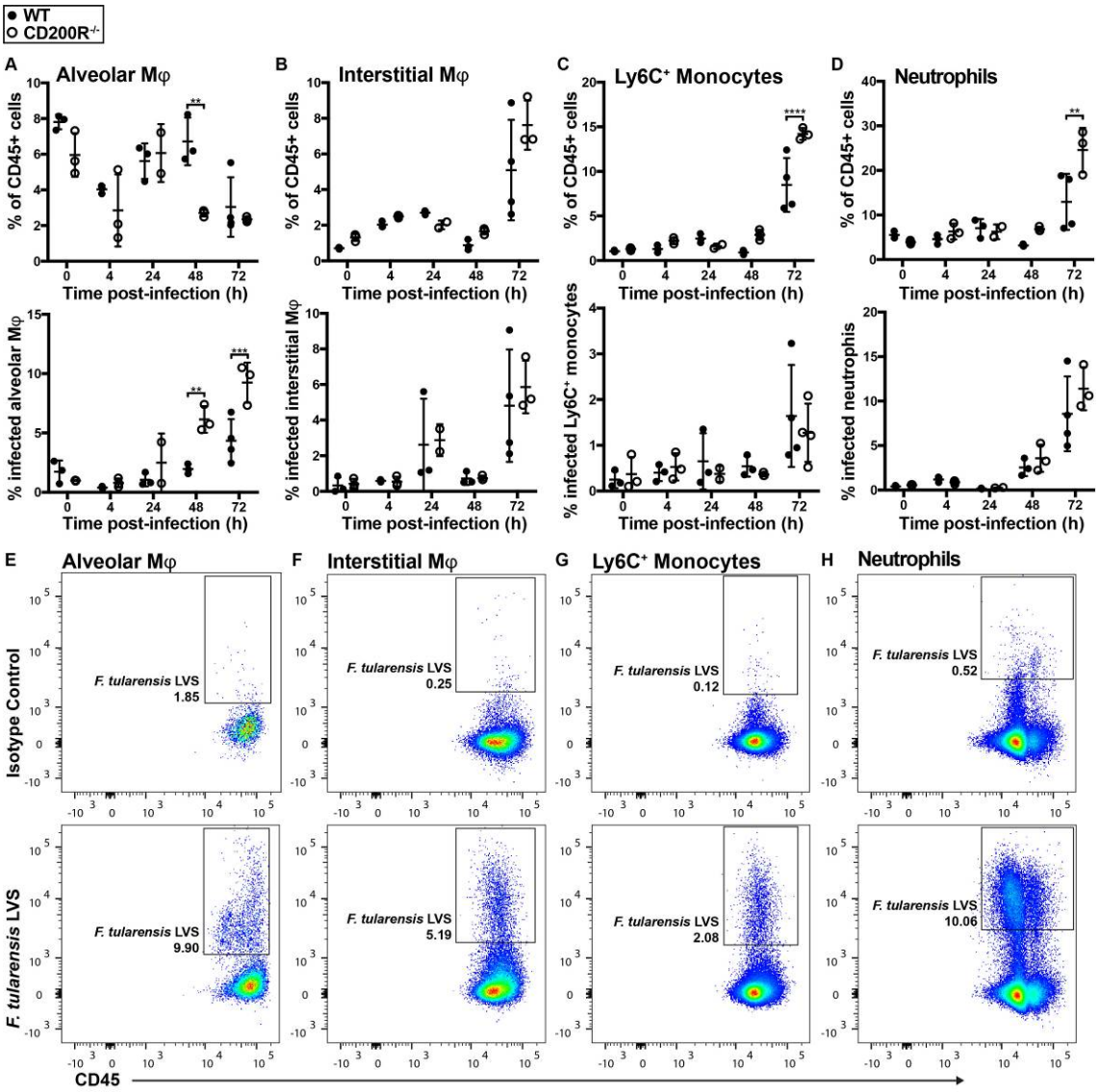

Figure 3.13 | Characterising lung cell populations during early stage *F. tularensis* LVS infection in WT and CD200R$^{-/-}$ mice. WT and CD200R$^{-/-}$ C57BL/6 mice were infected intranasally with *F. tularensis* LVS CFU 600 and culled at 4, 24, 48 and 72 hours p.i. Uninfected and infected lungs were analysed by flow cytometry as described in figure 3.13. Data is presented as percentage of live, CD45$^+$ cells and percentage of infected cells for A) alveolar macrophages, B) interstitial macrophages, C) Ly6C$^+$ monocyte/macrophages and D) neutrophils. Representative dot plots of infection level at 72 hours p.i. with *F. tularensis* LVS measured with IgG2a isotype control or anti-*F. tularensis* LVS antibody for E) alveolar macrophages, F) interstitial macrophages, G) Ly6C$^+$ monocyte/macrophages and H) neutrophils. Data represents one experiment and is shown as mean ± SD (n=3-4). Statistical analysis was performed using two-way ANOVA (**p<0.01, ***p<0.001).

Similarly, there was little change in the percentage of *F. tularensis* LVS-infected interstitial macrophages and Ly6C$^+$ monocytes/macrophages up to 48 hours p.i. (Figure 3.13B & C respectively). It was not until 72 hours p.i. an increase in percentage infection was observed, however there were no significant differences between WT and CD200R$^{-/-}$ mice. Neutrophils showed a similar infection pattern; however they became infected at 48 hours p.i., increasing to even higher percentage of infected cells at 72 hours p.i. (Figure 3.13D). Representative flow cytometry dot plots demonstrate the level of *F. tularensis* LVS infection in alveolar macrophages, interstitial macrophages, Ly6C$^+$ monocytes/macrophages and neutrophils (Figure 3.13E-H respectively). This showed the sensitivity of the APC anti-*F. tularensis* LVS antibody *in vivo* compared to the IgG2a isotype antibody.

Together these data suggest that there is an influx of inflammatory cells, such as neutrophils and Ly6C$^+$ monocytes/macrophages, in response to *F. tularensis* LVS infection. Yet this is subsequently accompanied by an increase in *F. tularensis* LVS infection in the cells that are recruited to deal with the infection.

3.2.8 Characterising the early response to *F. tularensis* LVS infection in BAL fluid

This thesis focuses on *F. tularensis* LVS infection via the intranasal route; so much of the initial bacteria will reside in the airways before entering lung tissue. Therefore, it was important to understand if there were differences in the cell populations and infection rates in the BAL fluid of WT and CD200R$^{-/-}$ mice.

Cells were isolated from BAL fluid of uninfected mice and LVS-infected mice at 4, 24, 48 and 72 hours p.i. and analysed by flow cytometry. The gating strategy used started similar to the lung by gating on single, live, CD45$^+$ lymphocytes. However, following this less markers were needed due to the reduced diversity of cell populations in the BAL fluid. Alveolar macrophages (Ly6G$^-$ TCRβ$^-$ CD11b$^-$ CD11c$^+$) were the dominant population, but CD11b$^+$ CD11c$^+$ (Ly6G$^-$ TCRβ$^-$) cells and neutrophils (Ly6G$^+$) were also present (Figure 3.14A & B).

As expected, alveolar macrophages were the main cell type in the BAL fluid of uninfected mice and during *F. tularensis* LVS infection (Figure 3.14C). There was a slight decrease in the proportion of alveolar macrophages at 72 hours p.i., however there was no difference between WT and CD200R$^{-/-}$ mice. Similarly, although the percentage of infected alveolar macrophages increased during infection, there were no significant differences between WT and CD200R$^{-/-}$ mice (Figure 3.14C).

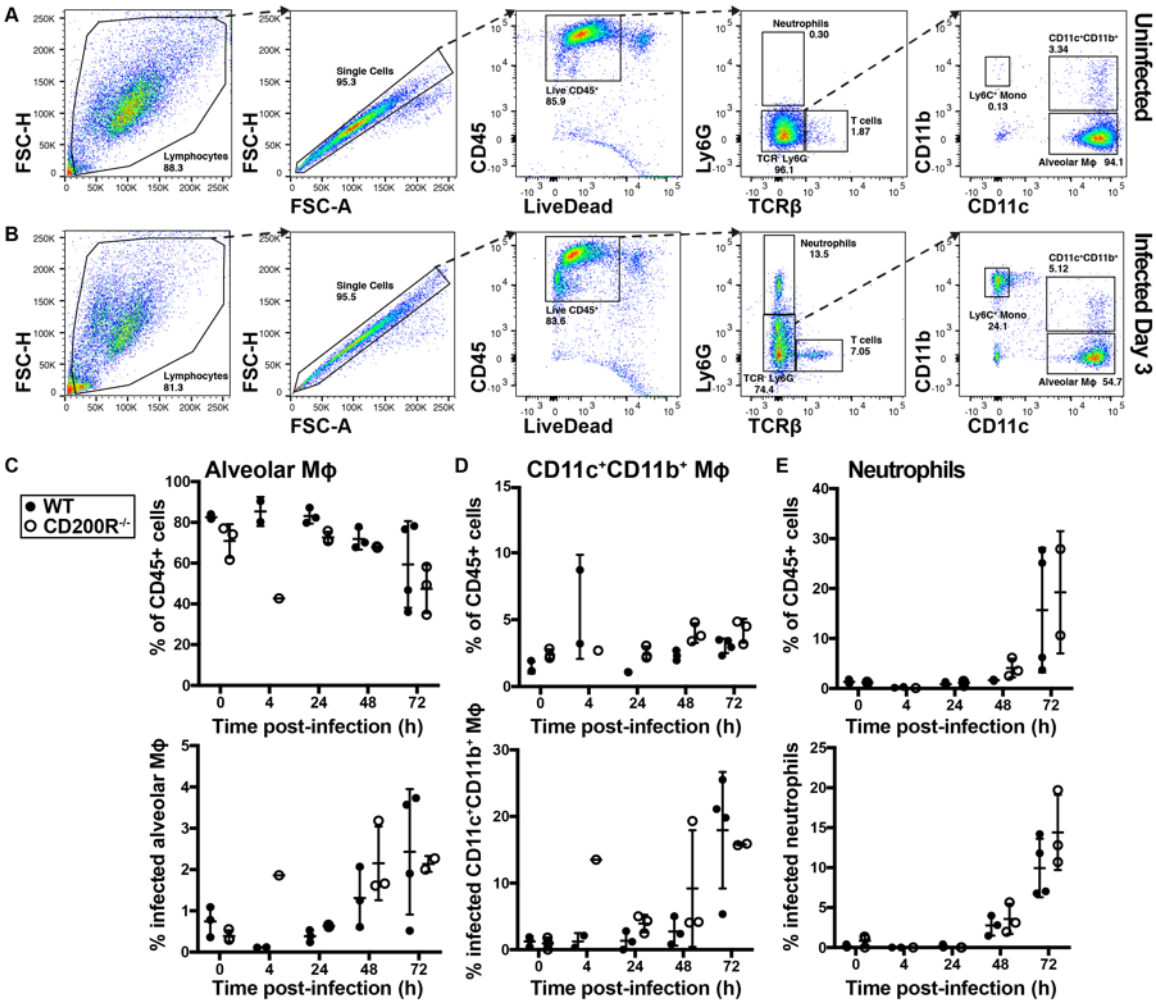

Figure 3.14 | Characterising BAL fluid cell populations during early stage *F. tularensis* LVS infection in WT and CD200R$^{-/-}$ mice. WT and CD200R$^{-/-}$ C57BL/6 mice were infected intranasally with *F. tularensis* LVS CFU 600 and a bronchoalveolar lavage (BAL) was performed prior to culling at 4, 24, 48 and 72 hours p.i. Cells were isolated from BAL fluid and stained for flow cytometry. Uninfected (A) and day 3 *F. tularensis* infected (B) Samples were gated on single, live CD45$^+$ lymphocytes. Neutrophils (Ly6G$^+$) and T cells (TCRβ$^+$) were gated out, with the double negative population divided further. CD11b and CD11c were used to distinguish alveolar macrophages (CD11c$^+$ CD11b$^-$) from CD11c$^+$ CD11b$^+$ cells. Data is presented as percentage of live, CD45$^+$ cells and percentage of infected cells for C) alveolar macrophages, D) CD11c$^+$ CD11b$^+$ cells and E) neutrophils. Data represents one experiment and is shown as mean ± SD (n=1-4). Statistical analysis was performed using two-way ANOVA.

It was also of interest to monitor less common cell types in the BAL fluid and to see how the population dynamics shifted during the *F. tularensis* LVS infection. The CD11b$^+$ CD11c$^+$ population remained constant throughout the course of infection in WT and CD200R$^{-/-}$ mice; however there was a large increase in the percentage of infected cells at 72 hours p.i. (Figure 3.14D). The population kinetics of neutrophils were very similar to those seen in the lung (Figure 3.14E). In the BAL fluid there was a small influx of neutrophils at 48 hours p.i., with this increasing further at 72 hours p.i. (Figure 3.14E). Similarities could also be seen in the

percentage of infected cells, with some infected neutrophils noticeable at 48 hours p.i. and increasing significantly by 72 hours p.i. However, there was no difference in cell proportions or percentage of infected cells between WT and CD200R$^{-/-}$ mice (Figure 3.14E).

These data suggest that, as with the lung, an increasing *F. tularensis* LVS burden is accompanied by the influx of inflammatory cells such as neutrophils, which in turn reduces the proportion of alveolar macrophages within the airway. Nevertheless, there were no significant differences between the BAL fluid from WT and CD200R$^{-/-}$ mice, Due to this, it was decided to not separate BAL and lung tissue in future experiments in order to get a better picture of the lung environment as a whole during *F. tularensis* LVS infection.

3.3 Discussion

3.3.1 Developing a reliable *in vitro* model of *F. tularensis* infection

3.3.1.1 Appropriate cell types

As the aim in this thesis was to investigate pulmonary *F. tularensis* infection, an appropriate *in vitro* model was required to understand whether *F. tularensis* was able manipulate negative immune regulators. To this end, MH-S cells, an immortalised murine alveolar macrophage cell line, were used as an *in vitro* model for early pulmonary *F. tularensis* infection. Although, MH-S cells have been shown to be an effective *in vitro* model for other intracellular pathogens (Melo and Stokes, 2000, Matsunaga et al., 2001), it must be noted that MH-S cells lack some features of alveolar macrophages. MH-S cells do not express Siglec-F and CD116, both present on WT alveolar macrophages. Furthermore, they do not support mouse pneumovirus replication, which is a feature seen in wild-type alveolar macrophages, (Brenner et al., 2016). Nevertheless, even the use of primary alveolar macrophages *in vitro* would have disadvantages. Firstly, upon adherence to tissue culture surfaces alveolar macrophages exhibit increased activation and a more inflammatory phenotype, which is not indicative of an alveolar macrophage at steady-state in the airway (Standiford et al., 1991, Bang et al., 2011, Tomlinson et al., 2012). Secondly, obtaining equivalent numbers of alveolar macrophages via murine BAL as were required for *in vitro* experiments poses ethical and technical issues due to increased mouse numbers.

Similarly, when looking at the consequences of lack of CD200R on macrophages during *F. tularensis* infection, BMDM were chosen instead of primary alveolar macrophages. *F. tularensis* efficiently replicates within BMDM, with BMDMs behaving similarly to MH-S cells in some aspects of responses to *F. tularensis* infection (Griffin et al., 2013, Shakerley et al., 2016). BMDM cultured from WT and CD200R$^{-/-}$ mice expressed characteristic markers also determined by others such as CD11c and CD11b, as well as low MHC-II expression (Wang et al., 2013, Na et al., 2016). Interestingly, BMDM from CD200R$^{-/-}$ mice were not a homogenous population with two distinct groups of Gr-1^{+} and Gr-1^{-}, as opposed to WT BMDM that all had low Gr-1 expression. Differentiated BMDM express Gr-1 (Wang et al., 2013), however it has been suggested that Gr-1 expression is lost as monocytes differentiate into mature macrophages (Francke et al., 2011). Regardless, there was no difference in the percentage of *F. tularensis* LVS-infected BMDM between the Gr-1^{+} and Gr-1^{-} population from CD200R$^{-/-}$ (data not shown), suggesting that this heterogeneity within the cultured BMDM did not affect the overall results seen during experiments.

3.3.1.2 Infectious dose and measuring *F. tularensis* infection

A recurring challenge during this thesis was maintaining a consistent infectious dose between experiments, both *in vitro* and *in vivo*. MOI 100 was used for all *in vitro* experiments; however variation in actual challenge dose used to infect cells was often encountered. This was due to the initial process of obtaining a challenge dose through making an *F. tularensis* LVS suspension of OD_{600nm} 0.20, before further diluting to the appropriate bacterial concentration. This method left some margin for error, from the accuracy of the spectrophotometer to the number of dilutions. It is true that in working with bacteria a log scale is often used; therefore small variations within the same log scale (i.e. 10^2 or 10^3) may not have a critical influence on the overall outcome of the experiment. Nevertheless, to allow for more reliable comparisons between experiments, a more accurate method of determining challenge dose before the start of the experiment would be advantageous.

The variability in infectious dose may also have been a factor in the lower percentage of infected cells in earlier experiments. However, changing from the anti-*F. tularensis* LVS-FITC to the anti-*F. tularensis* LVS-APC antibody for bacterial detection by flow cytometry provided a significant increase in the sensitivity of detection. Regardless, it was interesting to see that even with a high *F. tularensis* LVS MOI of 100, only approximately 5-20% of cells uptake the bacterium *in vitro*

and become infected. This low percentage of infected cells is characteristic of *F. tularensis* infections *in vitro* (D'Elia et al., 2011b), and may be a method of avoiding immune detection early during infection by reducing the number of cells available to elicit an inflammatory response. Furthermore, it was shown by ImageStream that of the cells that become infected, up to 4 bacteria are taken up by MH-S cells, followed by large net growth from 6 to 26 hours p.i. that rendered counting individual bacterium difficult (Figure 3.5). These data suggest that as well as a low percentage of infected cells, those infected cells also uptake a low number of bacterium considering the high infectious dose.

3.3.2 A protective role for CD200R against *F. tularensis* LVS

In this chapter it was hypothesised that a reduction in negative immune regulatory signalling would allow for a faster immune response against *F. tularensis* and decrease susceptibility to infection. It was shown that CD200R expression is significantly upregulated in the alveolar macrophage cell line MH-S cells during *F. tularensis* infection (Figure 3.6). Similarly, other intracellular pathogens, such as *T. gondii* and *L. amazonensis*, upregulate components of the CD200R pathway on host macrophages to promote virulence (Deckert et al., 2006, Cortez et al., 2011). Therefore, it was surprising to find that upon activation of CD200R signalling with CD200-Fc, a significant reduction in *F. tularensis* bacterial burden was observed (Figure 3.7). These results were further supported by data showing that bacterial burden was significantly increased in CD200R$^{-/-}$ BMDM when compared to WT (Figure 3.9). Together these data suggested that, opposed to the original hypothesis, CD200R function actually conveyed protection against *F. tularensis* infection *in vitro*.

The significant differences seen in CD200-Fc-treated MH-S cells and CD200R$^{-/-}$ BMDM were at 26 hours p.i. in both experiments, with no differences seen up to 6 hours p.i. Having previously shown that net bacterial growth occurs exponentially from 6 to 26 hours p.i., these data suggest that CD200R is unlikely to be functioning in the uptake of *F. tularensis* infection and more likely involved in controlling bacterial replication within the cell. However, it must also be considered that *F. tularensis* has a lag phase to allow preparations for exponential growth as seen in *Salmonella enterica* {Rolfe, 2012 #1392}. This could explain the initial delay in net bacterial growth, however it could also be the case that CD200R acts on this phase of growth to ultimately influence rate of exponential growth.

Interestingly, there was no difference in the *F. tularensis* burden in WT BMDM following treatment with CD200-Fc as observed in MH-S cells (Figure 3.10). One reason for the different response to CD200-Fc treatment could be due to the different genetic origins of the two cell types. MH-S cells are an immortalised alveolar macrophage cell line from BALB/c mice (Mbawuike and Herscowitz, 1989), whereas the BMDM used were derived from C57BL/6 mice. There is evidence of varying susceptibility to *F. tularensis* infection in different inbred mouse strains, with C57BL/6 mice showing increased susceptibility to aerosol challenge compared to BALB/c mice following immunisation with *F. tularensis* LVS (Chen et al., 2003), yet showing increased resistance when compared to A/J mice (Fink et al., 2016).

Thus, the effect of activating CD200R could be different between and C57BL/6 and BALB/c mice. It would therefore be interesting to investigate whether similar results were obtained from BALB/c-derived BMDM. Similarly, due to the increased susceptibility of both BALB/c and C57BL/6 mice to intracellular bacteria due to a non-functional Nramp {Powell, 2017 #1349}, investigating *F. tularensis* infection in macrophages derived from other mouse strains with functional Nramp such as DBA/2 may provide differing outcomes. Nevertheless, as there was a significantly increased *F. tularensis* burden in CD200R$^{-/-}$ BMDM compared to WT in our infection model, this suggested that CD200R still played an important role during *F. tularensis*.

3.3.3 Early changes *in vivo* during pulmonary *F. tularensis* infection

3.3.3.1 No clear role for CD200R during early *F. tularensis* infection

After finding a protective role for CD200R *in vitro*, it was hypothesised that this would also be the case *in vivo*. Due to a particular interest in determining whether CD200R on alveolar macrophages played a role in protection against pulmonary *F. tularensis* infection, the earlier stage of infection was investigated as this is where any differences were predicted to be seen.

Initially it was noted that despite rapid bacterial replication within the lung, as well as dissemination to the liver and spleen by 48-72 hours p.i., no weight loss in mice was observed (Figure 3.11A). It has been shown that *F. tularensis* is characterised by a lack of inflammatory immune response during early infection (Lopez et al., 2004, Duckett et al., 2005, Malik et al., 2006), thus the onset of weight loss may correlate to the start of the host inflammatory response, something explored further in Chapter 4.

There were no significant differences in *F. tularensis* burden during the 72 hours p.i. between WT and CD200R$^{-/-}$ mice (Figure 3.11B), suggesting that CD200R may not be important in controlling *F. tularensis* infection during the early stages of infection. Nevertheless, when looking more specifically at cell populations within the lung (Figure 3.13), it was evident that CD200R$^{-/-}$ mice had altered responses to *F. tularensis* that could potentially lead to differences in infectious outcome compared to WT. Lack of CD200R led to a significant increase in inflammatory cells such as neutrophils and Ly6C^{hi} monocyte/macrophages in the lung, with these populations becoming the most prominent in the lung at 72 hours p.i. Nevertheless, the limitations of looking at cell proportions as a percentage of CD45^{+} cells, as oppose to total cell numbers, must be considered. The significant reduction in alveolar macrophage populations at 72 hours p.i. may solely be due to large influx of other cell types, thus using total cell numbers would provide a greater insight into cell dynamic during infection.

Although there was an increase in infected CD200R$^{-/-}$ alveolar macrophages over WT as seen in previous *in vitro* experiments, this was only following the loss of a large proportion of alveolar macrophages, perhaps due to increased LVS-induced cell death. Thus, unless alveolar macrophages populations are able to replenish during infection, any differences seen in CD200R$^{-/-}$ mice during later *F. tularensis* infection are unlikely to be directly due to alveolar macrophage.

3.3.3.2 Distinguishing between BAL and lung tissue

In this chapter BAL cells were isolated from lung tissue in order to better investigate alveolar macrophage function within the context of CD200R and *F. tularensis* infection. Consistent with the literature, the majority of cell types within the BAL fluid were alveolar macrophages (Snelgrove et al., 2011). However, alveolar macrophages were also present in the lung tissue suggesting that the BAL protocol was not effective in removing all the cells from the airway. Furthermore, unlike with the whole lung tissue, there were no significant differences between cell populations and infection percentage in the BAL of WT and CD200R$^{-/-}$ mice; albeit the sample size for sections of this experiment was low. Nevertheless, similar patterns were observed between BAL and lung tissue in the reduction in alveolar macrophage populations at 72 hours p.i., most likely due to cell death and the recruitment of inflammatory cells, particularly neutrophils into the airways. The lack of differences between BAL and lung tissue, as well as the minimal contribution of alveolar macrophages during the later stages of *F. tularensis* infection, led to the decision to

not distinguish between the two in future experiments conducted in Chapter 4 and 5.

3.4 Conclusion

Chapter 3 demonstrated that CD200R plays a protective role during *F. tularensis* infection *in vitro*, but does not directly influence infectious outcome during early pulmonary infection *in vivo*. Nevertheless, investigation into the cell populations in the lung during early *F. tularensis* infection suggests that the significant increase in recruitment of inflammatory cells in CD200R$^{-/-}$ mice compared to WT may lead to differences in infectious outcome later in infection, something explored in more depth in Chapter 4 and 5.

Chapter 4

The role of CD200R *in vivo* during *Francisella tularensis LVS* infection

4.1 Introduction

In Chapter 3, the protective role of the CD200R pathway against *F. tularensis* LVS *in vitro* was explored. Following this, the early stages of *F. tularensis* LVS infection in WT and CD200R$^{-/-}$ mice *in vivo* was investigated to determine whether CD200R was involved in the early immune suppression characteristic of *F. tularensis* LVS infection. Despite seeing no differences in overall bacterial burden (Figure 3.11B), further investigation of cell populations in the lung showed an influx of inflammatory cells in CD200R$^{-/-}$ mice compared to WT at 72 hours p.i. Figure 3.13C & D). For this reason, Chapter 4 aimed to identify whether these cellular differences in CD200R$^{-/-}$ mice would lead to altered infectious outcomes to *F. tularensis* LVS in the latter stages of infection. Based on results in chapter 3, it was hypothesised that CD200R$^{-/-}$ mice would show an enhanced *F. tularensis* burden in the later stages of infection when compared to WT following an intranasal challenge.

Furthermore, in Chapter 3 it was demonstrated that activation of CD200R *in vitro* through treatment with CD200-Fc led to significantly decreased *F. tularensis* LVS burden (Figure 3.7). Thus, in Chapter 4 the potential use of CD200-Fc as a treatment for *F. tularensis* infection *in vivo* was investigated. CD200-Fc treatment alleviates pathogen-induced inflammation in influenza and ocular HSV infection models (Snelgrove et al., 2008, Sarangi et al., 2009); as well as reducing inflammation in autoimmune disorders, such as collagen-induced arthritis and transplantation, potentially driving a more tolerogenic environment (Gorczynski et al., 1999, Simelyte et al., 2008). Building from findings in Chapter 3, it was hypothesised that inducing CD200R signalling via treatment with CD200-Fc could ameliorate *F. tularensis* LVS disease.

4.2 Results

4.2.1 Exacerbated pulmonary *F. tularensis* LVS burden in CD200R$^{-/-}$ mice

In order to understand the latter stages of *F. tularensis* LVS infection in WT and CD200R$^{-/-}$ mice, the time scale of the infection was extended from experiments detailed in Chapter 3. WT and C200R$^{-/-}$ mice were challenged intranasally with an average lethal dose of 1275 CFU *F. tularensis* LVS and culled at day 1, 3, 5 and 7 p.i. As previously observed when monitoring the weights of mice during *F. tularensis* LVS infection (Figure 3.12A), there was no weight loss within the first 3 days of infection (Figure 4.1A). However, from day 4 p.i. there was rapid weight loss until the endpoint of the study at day 7 p.i. Day 7 was chosen as the humane endpoint due to excessive weight loss and clinical scoring beyond this point. Interestingly, there was no significant difference in weight change between WT and CD200R$^{-/-}$ mice throughout the course of infection (Figure 4.1A). The level of splenomegaly was also measured over the course of *F. tularensis* LVS infection as a marker of disease severity (Chiavolini et al., 2008). There was a steady increase in splenomegaly throughout the course of infection, with a significant increase in spleen weight in CD200R$^{-/-}$ mice compared to WT at day 7 p.i. (Figure 4.1B). Thus, this latter result suggests that CD200R$^{-/-}$ mice may be more susceptible to infection later in infection.

Bacterial burden were enumerated in the lung, liver and spleen of WT and CD200R$^{-/-}$ mice at day 1, 3, 5 and 7 p.i. to track the dynamics of *F. tularensis* LVS infection. In the lung, it was interesting to note that at day 3 p.i. mice had already reached peak bacterial burden despite not displaying any weight loss (Figure 4.1C). *F. tularensis* LVS burden in the lung remained high at day 5 p.i., yet there was no significant difference in burden between WT and CD200R$^{-/-}$ mice. However, at day 7 p.i. a significantly enhanced bacterial burden was observed in the lungs of CD200R$^{-/-}$ mice compared to WT (Figure 4.1C). These results suggest that lack of CD200R expression in the lung significantly exacerbates later stages of *F. tularensis* LVS infection.

Monitoring the bacterial burden in peripheral organs such as liver and spleen confirmed that full bacterial dissemination from the lung occurs at day 3 p.i., with peak bacterial burden in the liver and spleen reached at day 5 p.i. (Figure 4.1D & E respectively). Interestingly, at this time point there was no difference in liver burden

between WT and CD200R$^{-/-}$ mice, however a significantly increased bacterial burden in CD200R$^{-/-}$ spleens was observed (Figure 4.1D & E respectively). This significant difference was not observed at day 7 p.i., with a levelling off of bacterial burdens seen in the peripheral organs.

Overall these data propose that, as suggested from *in vitro* in Chapter 3, the CD200R pathway is also protective *in vivo* during *F. tularensis* LVS infection. Lack of CD200R causes an exacerbated bacterial burden in the lungs of CD200R$^{-/-}$ mice and enhanced splenomegaly in the later stages of infection, as well as showing increased bacterial burden in the spleen.

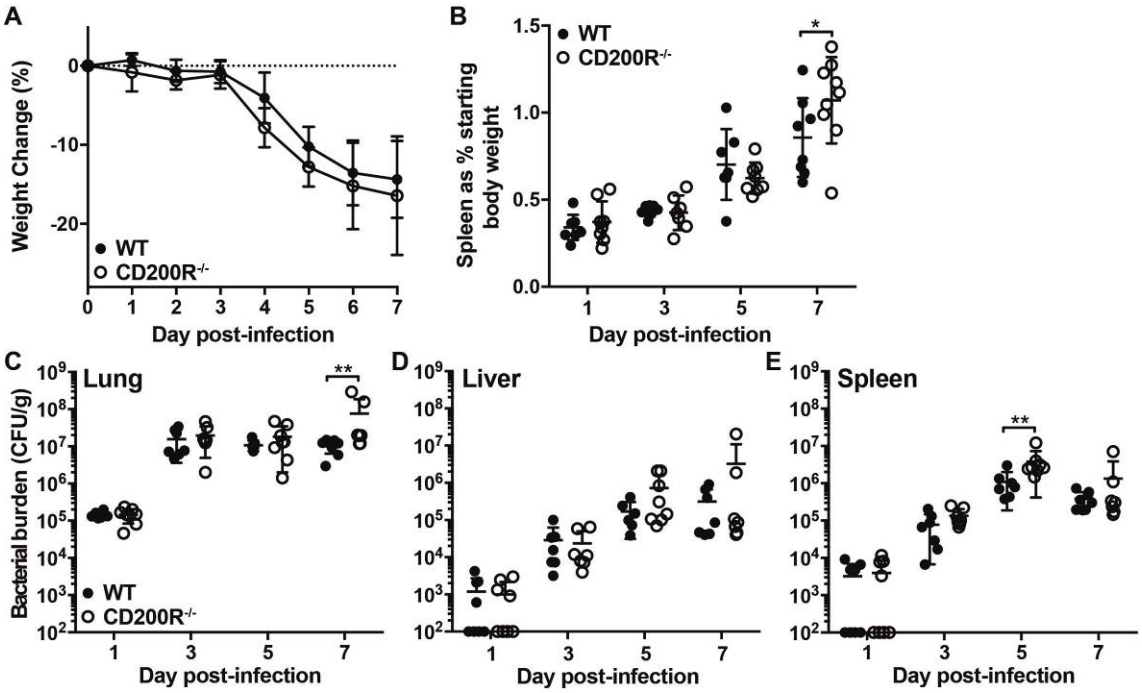

Figure 4.1 | Lack of CD200R results in an exacerbated pulmonary *F. tularensis* LVS burden. WT and CD200R$^{-/-}$ mice were infected intranasally with an average of 1275 CFU *F. tularensis* LVS and were culled at day 1, 3, 5 and 7 p.i. A) Mouse weights were monitored daily and are represented as percentage weight change. B) Splenomegaly was determined by presenting spleen weight as a percentage of starting body weight prior to infection. Bacterial burden (CFU/g) was enumerated at day 1, 3, 5 and 7 p.i. in the C) lung, D) liver and E) spleen of WT and CD200R$^{-/-}$ mice. Data represents two independent experiments and is shown as mean ± SD (n=6-8, 3-4/group). Statistical analysis was performed using two-way ANOVA (*p<0.05, **p<0.01).

4.2.2 Increased neutrophil influx and *F. tularensis* LVS-infected neutrophils in lungs of CD200R$^{-/-}$ mice

After showing an increased *F. tularensis* LVS burden in CD200R$^{-/-}$ mouse lungs, the cell dynamics in the lung during the course of infection was investigated. Cells were isolated from uninfected and *F. tularensis* LVS-infected lungs at day 1, 3, 5 and 7

p.i., stained for flow cytometry and gated as described previously (Figure 3.13A). It must also be noted that flow cytometry staining of cell populations remained stable throughout the course of infection (data not shown).

Initially populations of interest were investigated as a percentage of live $CD45^+$ cells to determine how these changed through the course of *F. tularensis* LVS infection. There were no differences between alveolar macrophage populations at day 5 and 7 p.i. in WT and $CD200R^{-/-}$ mice (Figure 4.2A). Similarly, there were no significant differences in percentage of interstitial macrophages and Ly6C+ monocyte/macrophage populations between WT and $CD200R^{-/-}$ mice (Figure 4.2B & C respectively). However, these populations increased as *F. tularensis* infection progressed. Interestingly, there was a significant increase in neutrophil percentage in $CD200R^{-/-}$ mice compared to WT at day 5 and 7 p.i. (Figure 4.2D). With little differences between WT and $CD200R^{-/-}$ mice in other cell types through the course of infection, these data suggest that this enhanced influx of neutrophils may be a factor in the increased *F. tularensis* LVS burden seen in lungs of $CD200R^{-/-}$ mice.

To understand how specific cell types contributed to overall bacterial burden, the percentage of *F. tularensis* LVS-infected cells within the lung were determined. There was an increase in percentage of infected alveolar macrophages at day 5 and 7 p.i.; however there were no significant differences between WT and $CD200R^{-/-}$ mice (Figure 4.2E). In the same way, there was a gradual increase in infected interstitial macrophages and $Ly6C^+$ monocyte/macrophages up to day 5 p.i., before a slight decrease at day 7 p.i. (Figure 4.2F & G respectively). However, no significant differences between WT and $CD200R^{-/-}$ mice were seen. Consequently, it was investigated whether the increased influx of neutrophils in $CD200R^{-/-}$ was accompanied by an increase in *F. tularensis* LVS infection in neutrophils. *F. tularensis* LVS-infected neutrophils were present at day 3 p.i, with the highest neutrophil infection seen at day 5 p.i., before reduced percentage infection at day 7 p.i. (Figure 4.2H). Interestingly, there were significantly increased *F. tularensis* LVS-infected neutrophils at both day 5 and 7 p.i. in $CD200R^{-/-}$ mice (Figure 4.2H). An alternative gating strategy was used to determine the infected cell types at day 7 p.i. as a percentage of total $CD45^+$ *F. tularensis* infected cells (Figure 4.2I). It was noted that neutrophils were the most infected cell type, followed by interstitial macrophages. Other cell types such as alveolar macrophages and $Ly6C^+$ monocyte/macrophages constituted only a small percentage of the total infected cells.

Overall these data indicate that neutrophils are playing a key role in exacerbating *F. tularensis* LVS infection in the lung of CD200R$^{-/-}$ mice. In the later stages of infection there was significantly enhanced neutrophilia in CD200R$^{-/-}$ mice, as well as a significant increase in *F. tularensis* LVS-infected neutrophils. As there were few differences in other cell types, the observed neutrophil phenotype seen in CD200R$^{-/-}$ may be directly contributing to the significantly exacerbated LVS burden seen in the lung. Thus, the functional significance of CD200R$^{-/-}$ neutrophils in exacerbated *F. tularensis* LVS infection was investigated further in Chapter 5.

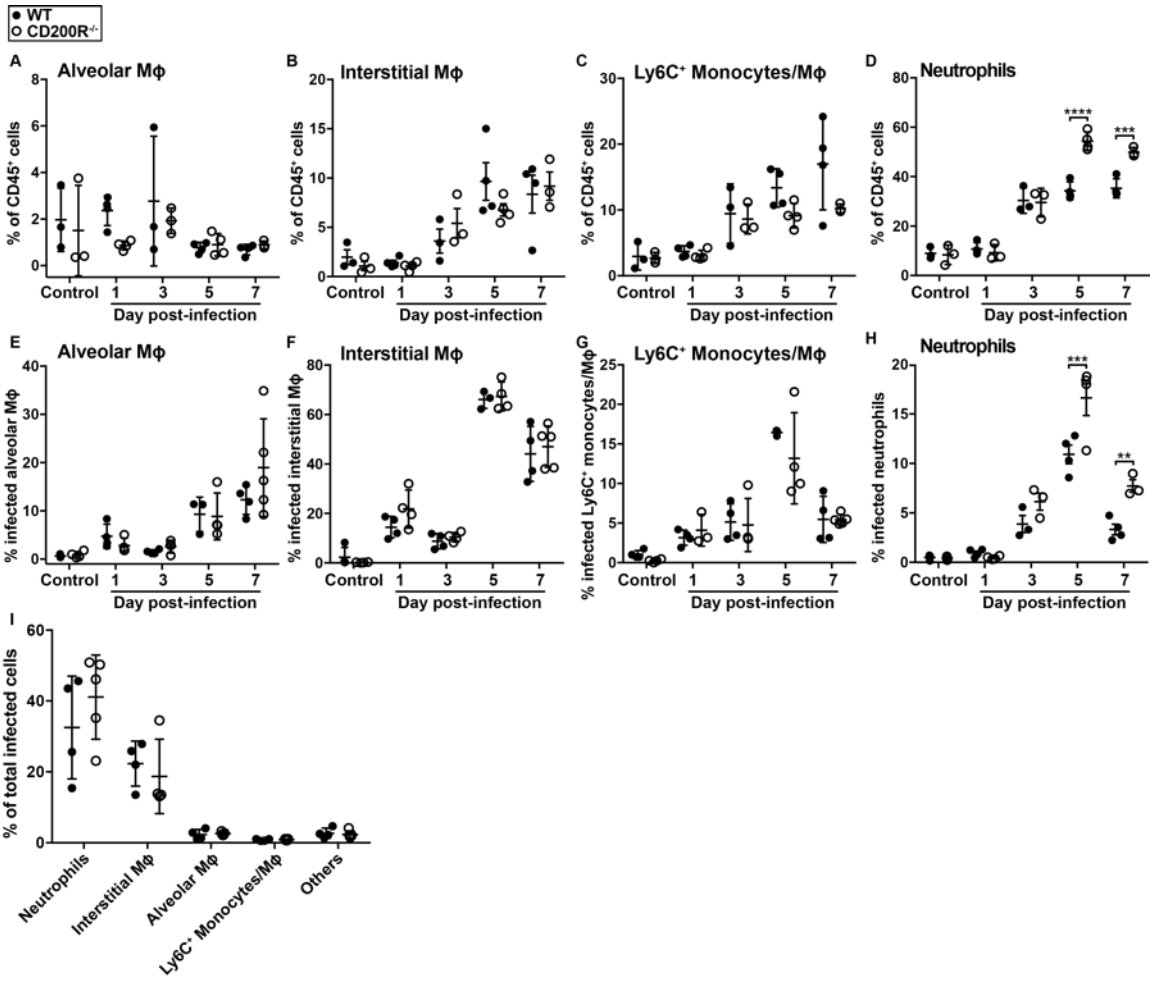

Figure 4.2 | Increased neutrophilia and *F. tularensis* LVS-infected neutrophils in lungs of CD200R$^{-/-}$ mice at later timepoints post-infection. WT and CD200R$^{-/-}$ mice were infected intranasally with an average of 1275 CFU *F. tularensis* LVS and culled at day 1, 3, 5 and 7 p.i. Cells were isolated from the lung, processed for flow cytometry and stained as described previously (Figure 3.13A). Data is presented as percentage of live, CD45^{+} cells for A) alveolar macrophages, B) interstitial macrophages, C) Ly6C^{+} monocyte/macrophages and D) neutrophils. The percentage of infected cell was determined for E) alveolar macrophages, F) interstitial macrophages, G) Ly6C^{+} monocyte/macrophages and H) neutrophils. I) Infected cell types at day 7 p.i. as a percentage of total infected CD45^{+} cells. Data is representative of two independent experiments and is shown as mean ± SD (n=3-4/group). Statistical analysis was performed using two-way ANOVA (**p<0.01, ***p<0.001).

4.2.3 Delayed and exacerbated pro-inflammatory cytokine response in CD200R$^{-/-}$ mice during *F. tularensis* LVS infection

Next, it was important to determine whether the bacterial burden and alterations in lung cell populations correlated with the hosts cytokine response against *F. tularensis* LVS infection. Thus, the expression of various pro-inflammatory cytokines was determined from lung homogenate through the course of *F. tularensis* LVS infection in WT and CD200R$^{-/-}$ mice.

No pro-inflammatory cytokines were detected within the first 3 days of *F. tularensis* LVS infection in either WT or CD200R$^{-/-}$ mice (Figure 4.3), as has been documented previously (D'Elia et al., 2013b) for WT mice. Increased levels of pro-inflammatory cytokines were observed at day 5 p.i., but there were no significant differences in the levels of IFNγ, TNFα and IL-17A between WT and CD200R$^{-/-}$ mice (Figure 4.3A-C respectively). Interestingly, there was significantly less IL-6, IL-1β and KC production in lung homogenates of CD200R$^{-/-}$ at day 5 p.i. compared to WT mice (Figure 4.3D-F respectively).

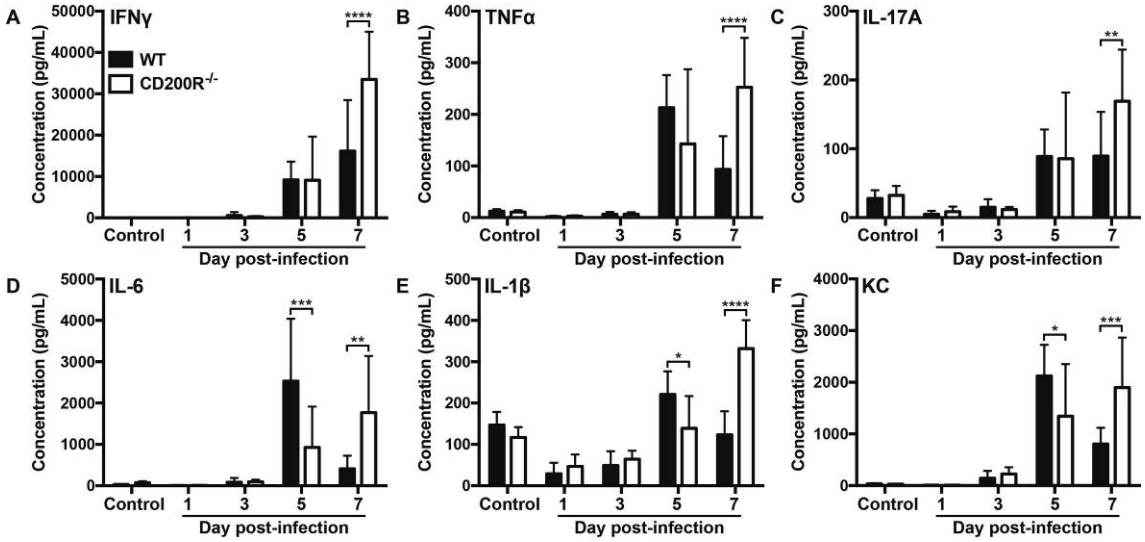

Figure 4.3 | Delayed and exacerbated pro-inflammatory cytokine response in CD200R$^{-/-}$ mice during *F. tularensis* LVS infection. WT and CD200R$^{-/-}$ mice were infected intranasally with an average of 1275 CFU *F. tularensis* LVS and lung homogenate collected from uninfected mice and at day 1, 3, 5 and 7 p.i. Pro-inflammatory cytokines IFNγ, TNFα, IL-17A, IL-6, IL-1b and KC (A-F respectively) were detected in lung homogenate using the BioLegend LEGENDplex immunoassay. Data represents two independent experiments and is shown as mean ± SD (n=6-8, 3-4/group). Statistical analysis was performed using two-way ANOVA (*p<0.05, **p<0.01, ***p<0.001, ****p<0.0001).

However, following this initial delayed response to *F. tularensis* LVS infection, the pro-inflammatory cytokine signature was enhanced later during infection in mice lacking CD200R expression, with IFNγ, TNFα, IL-17A, IL-6, IL-1β and KC production in the lung all significantly upregulated in CD200R$^{-/-}$ mice at day 7 p.i. (Figure 4.3A-F respectively). Thus, there appeared to be a delay in the initial pro-inflammatory cytokine response, followed by an exacerbated response in the absence of CD200R. This delayed response could be contributing to the increased bacterial burden seen in lungs of CD200R$^{-/-}$ mice, with the delayed cytokine response resulting in a delayed immune response to *F. tularensis* LVS infection.

4.2.4 No gross changes in lung pathology following *F. tularensis* LVS infection in WT and CD200R$^{-/-}$ mice

Following findings of increased *F. tularensis* LVS burden and an exacerbated pro-inflammatory cytokine response in the lungs of CD200R$^{-/-}$ mice, it was examined how this affected the gross pathology of the lung of *F. tularensis* LVS-infected mice at day 7 p.i. Thus, histopathological analysis was carried out for uninfected and infected lungs from WT and CD200R$^{-/-}$ mice by inflating and fixing lung tissue with 10% formalin, before processing and staining with hematoxylin and eosin (H&E) (Methods 2.7).

As expected, uninfected lungs showed normal histology and there were no differences between WT and CD200R$^{-/-}$ mice (Figure 4.4A & B). On the contrary, at day 7 p.i. with *F. tularensis* LVS there were evident signs of inflammation in the lungs. There was thickening of the airway epithelium, mild collapse of the alveolar space and a large amount of peri-vascular and peri-bronchial mononuclear cell infiltration (black arrows, Figure 5.4C & D). Nevertheless, overall there were no gross differences in lung pathology between *F. tularensis* LVS-infected WT and CD200R$^{-/-}$ mice.

To investigate the differences further, the level of inflammation and cellular infiltration in lung samples was quantified. The number of cells within the tissue were counted using ImageJ software to quantify the extent of cell infiltration. However, there was no significant difference in cell infiltrate between WT and CD200R$^{-/-}$ mice following *F. tularensis* LVS infection (Figure 4.4E). These data suggest that although there was an increased *F. tularensis* LVS burden and exacerbated pro-inflammatory cytokine response in CD200R$^{-/-}$ mice, subsequent effects on lung pathology are less evident.

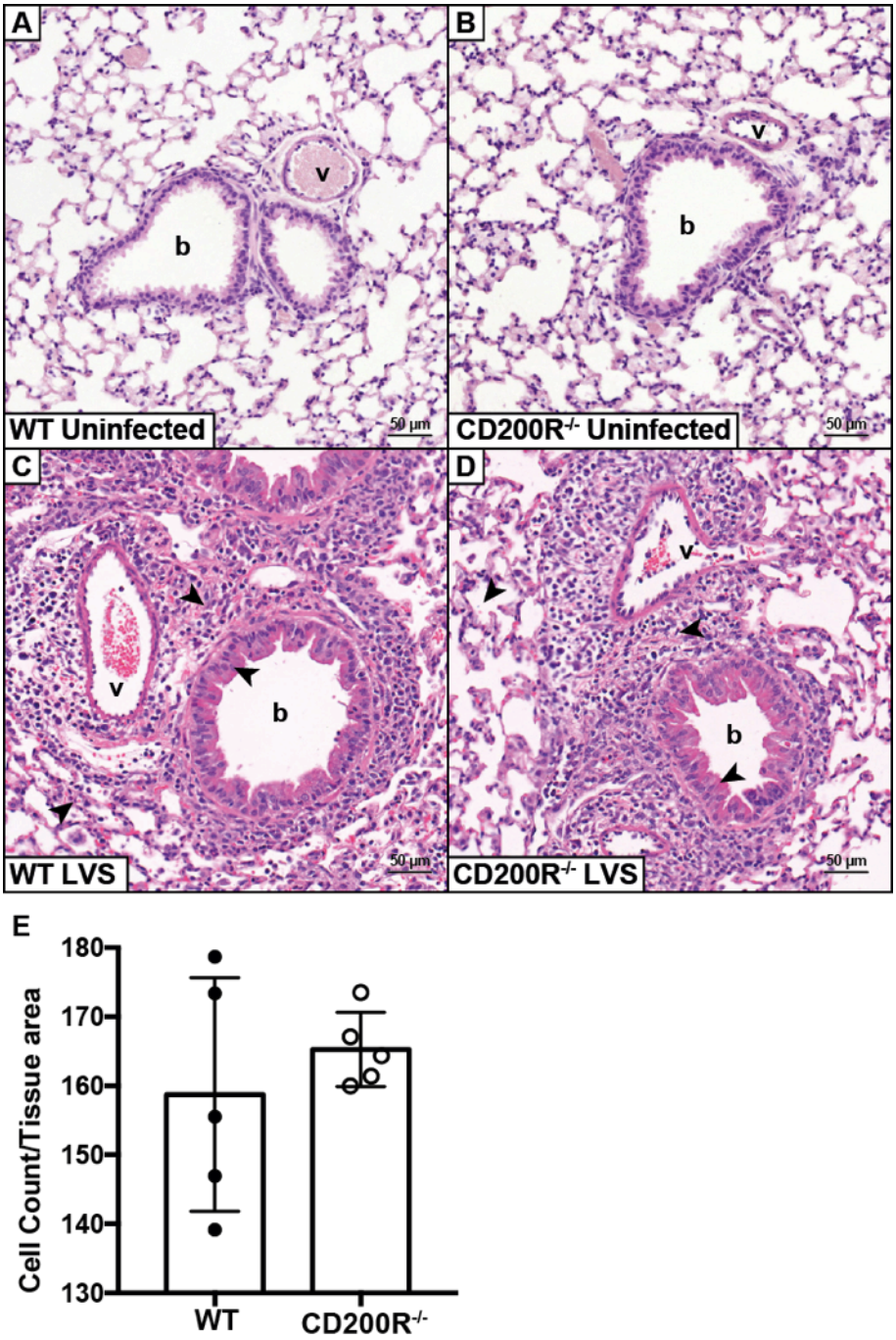

Figure 4.4 | H&E-stained lung of WT and CD200R$^{-/-}$ mice following *F. tularensis* LVS infection. Lung tissue was taken from uninfected WT and CD200R$^{-/-}$ and at day 7 p.i. with *F. tularensis* LVS. H&E-stained lung sections were processed as described in methods 2.7. Representative images display bronchioles (b) and blood vessels (v) within the lung of uninfected (A & B) and LVS-infected (C & D) WT and CD200R$^{-/-}$ mice. Thickening of the airway epithelium, mild collapse of the alveolar space, peri-bronchial and peri-vascular mononuclear cell infiltration (black arrows, C & D). E) Quantitative analysis of cell infiltration using ImageJ. Cells were counted and normalised to total tissue area (tissue minus bronchial and vascular lumen). Images shown are at 20x magnification and scale bar represents 50 µm. Data is representative of one experiment and is shown as mean ± SD (E, n=5, 4-10 images per group). Statistical analysis was performed using unpaired t-tests.

4.2.5 CD200R$^{-/-}$ mice exhibit a delayed resolution of *F. tularensis* LVS infection

Having seen an exacerbated bacterial burden in CD200R$^{-/-}$ at day 7 p.i. following a lethal dose of *F. tularensis* LVS, it was next investigated whether CD200R played a role in the resolution of infection. Thus, WT and CD200R$^{-/-}$ mice were infected intranasally with a lower dose of 450 CFU *F. tularensis* LVS in order to increase chances of survival and recovery. Weights were monitored daily and the experiment end-point was reached once all mice had reached their original starting weight prior to infection, in this case day 17 p.i. Unfortunately, two WT mice had to be culled prior to the experiment endpoint on humane grounds due to excessive weight loss and clinical scoring, therefore statistical analysis on these data was not possible.

When looking at weight change over the course of infection, weight loss started to occur at day 3 p.i. and begin to level off at day 7 p.i as was expected (Figure 4.5A). The period between day 7 and 10 p.i. was a crucial point in determining recovery, as weights were maintained during this time and it was at this point where two WT mice had to be culled. From day 10 p.i. there was a steady increase in weight gain until mice reached their starting weight at day 17 p.i. There was a trend of slower recovery in CD200R$^{-/-}$ mice as the remaining WT mice had almost reached their starting weight by day 15 p.i. (Figure 4.5A).

As mice had fully recovered from the weight they had lost due to the *F. tularensis* LVS infection, it could be assumed that mice had successfully cleared the bacteria. However, when bacterial burden were enumerated in the lung, liver and spleen in WT and CD200R$^{-/-}$ at day 17 p.i. it was surprising to still see bacteria present (Figure 4.5B). Interestingly, there was an increased bacterial burden in the lungs of CD200R$^{-/-}$ compared to WT. Similarly, WT mice had cleared the burden from the liver while CD200R$^{-/-}$ mice still harboured some bacteria. Both WT and CD200R$^{-/-}$ had failed to fully clear the bacteria from the spleen and there were no differences in burden (Figure 4.5B).

These data suggest that even though mouse weights would suggest recovery from *F. tularensis* LVS, bacteria is still abundant in the host. Interestingly, an increased bacterial burden in lungs of CD200R$^{-/-}$ mice, as well as a trend of slower weight gain compared to WT mice, points towards a role for CD200R in the clearance of *F. tularensis* LVS infection. However, as there was no possibility of conducting statistical tests due to low WT sample size assumptions from these findings must be taken with caution.

4.2.6 Characterising lung cell populations following recovery from *F. tularensis* LVS infection

After showing an increased *F. tularensis* LVS burden in CD200R$^{-/-}$ mice compared to WT after recovery, despite weight gains suggesting full recovery from infection, it was important to see how cell populations in the lung had been affected by *F. tularensis* LVS infection. Cells were isolated from the lungs of WT and CD200R$^{-/-}$ mice at day 17 p.i., stained for flow cytometry and gated as described previously (Figure 3.13A).

Initially, it was noted that percentages of cell populations had returned to levels similar to those seen very early in *F. tularensis* LVS infection (Figure 4.2). Interestingly, there were trends of decreased neutrophil percentages in CD200R$^{-/-}$ mice (Figure 4.6A). There were no differences in the percentage of alveolar and interstitial macrophages between WT and CD200R$^{-/-}$ mice (Figure 4.6B & C respectively). However, there was a trend towards increased percentage of Ly6C^{hi} monocyte/macrophages and CD4^{+} T cells in CD200R$^{-/-}$ mice (Figure 4.6D & E respectively).

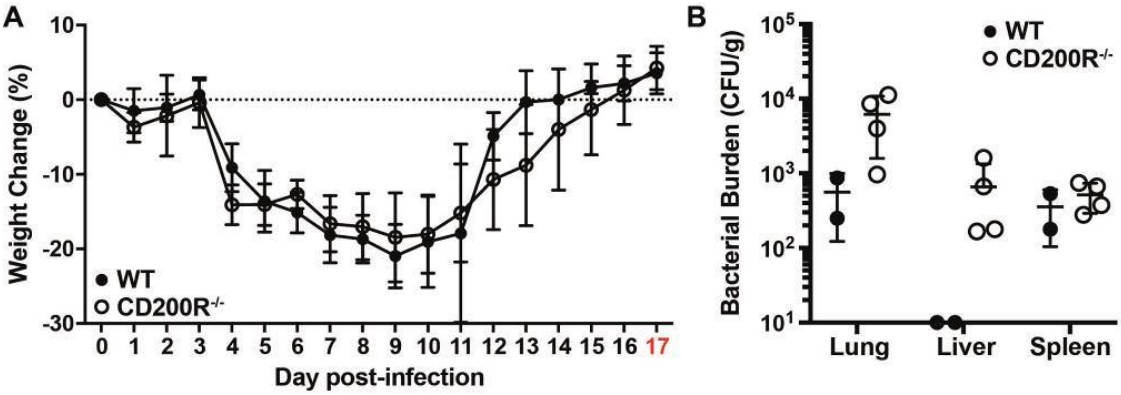

Figure 4.5 | Characterising recovery from *F. tularensis* LVS infection in WT and CD200R$^{-/-}$ mice. WT and CD200R$^{-/-}$ mice were infected intrasally with 450 CFU *F. tularensis* LVS and were culled at day 17 p.i. A) Mouse weights were monitored daily and are represented as percentage weight change. B) Bacterial burden (CFU/g) was enumerated at day 17 p.i. in the lung, liver and spleen of WT and CD200R$^{-/-}$ mice. Data represents one independent experiment and is shown as mean ± SD (n=2-4).

Furthermore, percentage of infection within the cells was determined and it showed that *F. tularensis* LVS-infected neutrophils in CD200R$^{-/-}$ mice were increased compared to WT mice (Figure 4.6F). There were no differences in the percentage of infected alveolar macrophages, interstitial macrophages and Ly6C^{hi} monocyte/macrophages between WT and CD200R$^{-/-}$ mice (Figure 4.6G-I respectively). When looking at *F. tularensis* LVS-infected total live, CD45^{+} cells there was no difference in WT and CD200R$^{-/-}$ mice (Figures 4.6J).

Taken together these results suggest that the persistence of *F. tularensis* LVS in CD200R$^{-/-}$ neutrophils may be contributing to a delay in bacterial clearance. However, without statistical tests firm conclusions from this data cannot to be made.

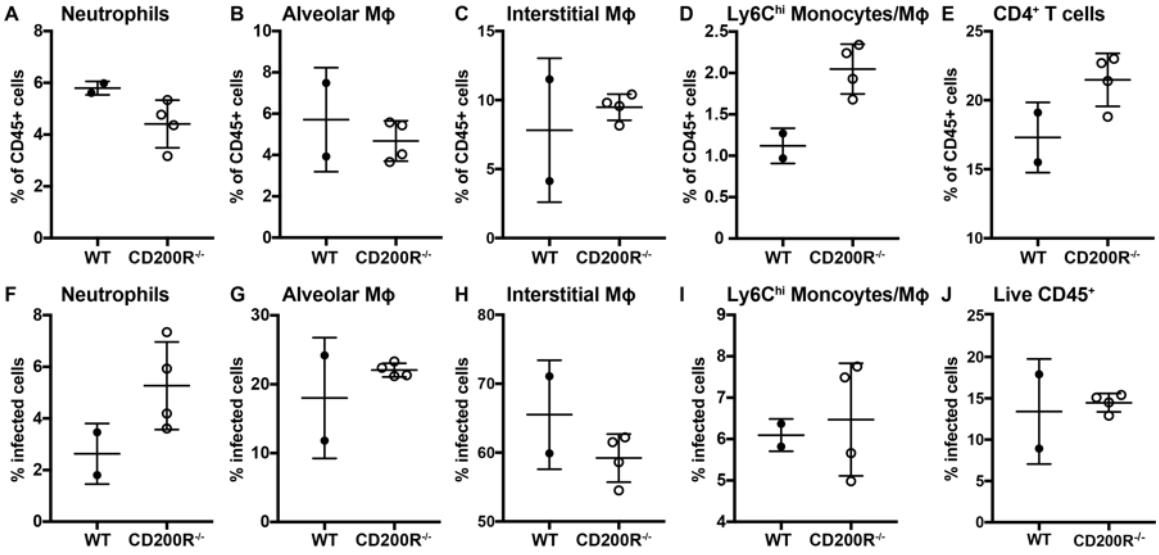

Figure 4.6 | Characterising lung populations in WT and CD200R$^{-/-}$ mice following recovery from *F. tularensis* LVS infection. WT and CD200R$^{-/-}$ mice were infected intranasally with 450 CFU *F. tularensis* LVS and were culled at day 17 p.i. Cells were isolated from the lung, processed for flow cytometry and stained as described previously (Figure 3.13A). Data is presented as percentage of live, CD45^{+} cells for A) neutrophils, B) alveolar macrophages, C) interstitial macrophages, D) Ly6C^{+} monocyte/macrophages and E) CD4^{+} T cells. The percentage of infected F) neutrophils, G) alveolar macrophages, H) interstitial macrophages, I) Ly6C^{+} monocyte/macrophages and J) total live CD45^{+} cells were determined. Data is representative of one independent experiment and is shown as mean

4.2.7 Investigating the CD200R pathway as a therapeutic target against *F. tularensis* LVS infection

The previous data suggests that lack of CD200R in mice exacerbates pulmonary *F. tularensis* LVS infection and may lead to impaired bacterial clearance during recovery. Therapeutically targeting the CD200R pathway has previously been shown beneficial in alleviating influenza-induced illness, reducing severity of arthritis and modulating microglial activation in neurodegenerative disease (Simelyte et al., 2008, Snelgrove et al., 2008, Lyons et al., 2012). Therefore, the question was asked whether activating CD200R signalling, through treatment with the receptor agonist CD200-Fc, could improve outcome during *F. tularensis* LVS infection.

Thus, WT mice were treated intraperitoneally with 10 µg CD200-Fc, hIgG or PBS one day prior to intranasal challenge with an average of 1731 CFU *F. tularensis* LVS, then again at day 1, 3 and 5 p.i. before culling animals at day 7 p.i. (Figure 4.7A). Weight loss maintained the characteristic pattern during *F. tularensis* LVS infection with very little weight change within the first 3 days of infection. When mice began to lose weight, there was no significant difference in percentage weight loss between PBS, hIgG and CD200-Fc-treated mice (Figure 4.7B).

Following this, bacterial burden was enumerated in the lung, liver and spleen of PBS, hIgG and CD200-Fc-treated mice. It was found that CD200-Fc treatment significantly reduced the bacterial burden in the lung compared to PBS-treated mice; however there was no significant difference when compared to hIgG treatment (Figure 4.7C). It must also be noted that there was no significant difference in burden between PBS- and hIgG- treated mice. Furthermore, CD200-Fc treatment had no significant effect on the bacterial burden in the liver and spleen compared to either control treatment (Figure 4.7C).

Although there was a beneficial effect of CD200-Fc treatment against *F. tularensis* LVS infection compared to PBS treatment, this was not the case when compared to an appropriate hIgG control. The fact that hIgG treatment showed no significant difference compared to PBS treatment would point towards some positive effects of CD200-Fc treatment. Nevertheless, these data would indicate that perhaps the hIgG portion of the recombinant CD200-Fc protein is also influencing *F. tularensis* LVS infectious outcome.

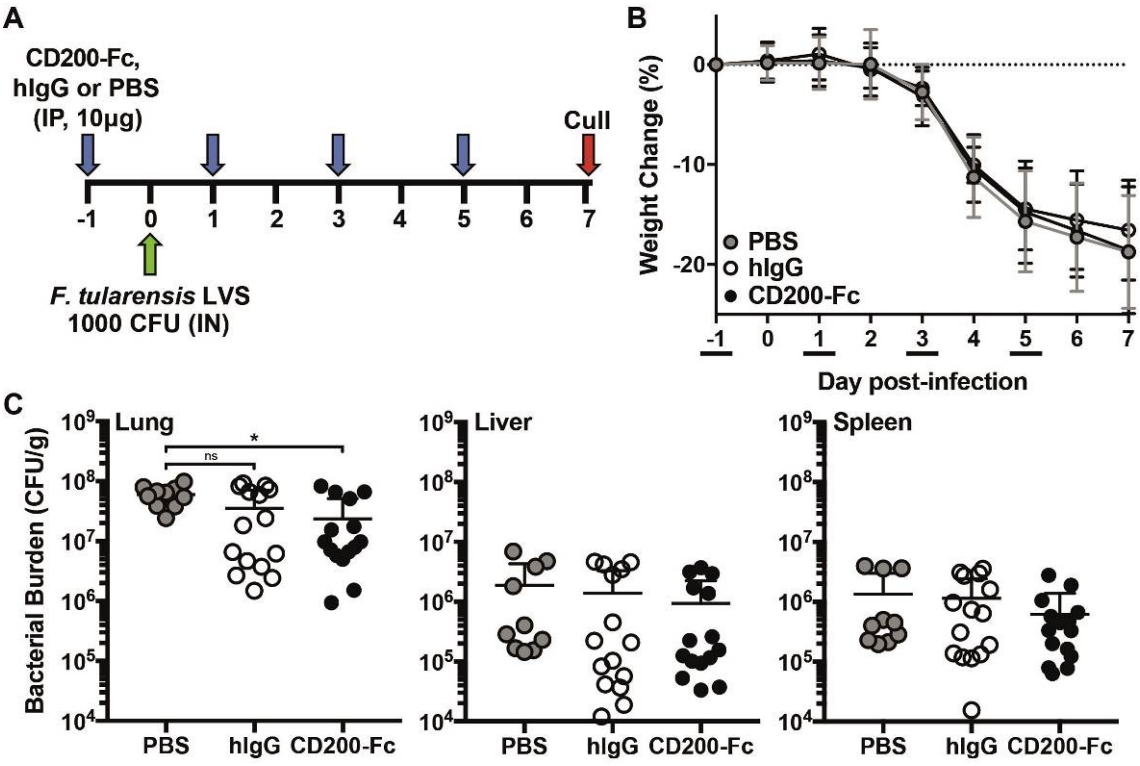

Figure 4.7 | Minimal positive effect of CD200-Fc treatment on *F. tularensis* LVS infection. A) WT mice were treated intraperitoneally with 10 µg CD200-Fc, hIgG or PBS at day -1, 1, 3 & 5 of *F. tularensis* LVS infection, before culling at day 7 p.i. The mean challenge dose of 1731 CFU *F. tularensis* LVS was administered intranasally. B) Mouse weights were monitored daily and are represented as percentage weight change. C) Bacterial burden (CFU/g) of the lung, liver and spleen was enumerated at day 7 p.i. Data represents three independent experiments and is shown as mean ± SD (n=15, 5/group). Statistical analysis was performed using one-way ANOVA (ns = not significant, *p<0.05).

4.2.8 Characterising lung cell populations following CD200-Fc treatment of *F. tularensis* LVS infection

Despite there being no significant differences in bacterial burden following CD200-Fc treatment of *F. tularensis* LVS infection compared to hIgG, changes in cell populations within the lung were also investigated. Cells were isolated from the lungs of WT mice at day 7 p.i. following the dosing regimen described in figure 4.7A, stained for flow cytometry and gated as described previously (Figure 3.13A).

There were no significant differences in any of the cell populations investigated. No significant differences were observed in the percentage of alveolar and interstitial macrophages, Ly6C^{hi} monocyte/macrophages and neutrophils following CD200-Fc treatment (Figure 4.8A-D).

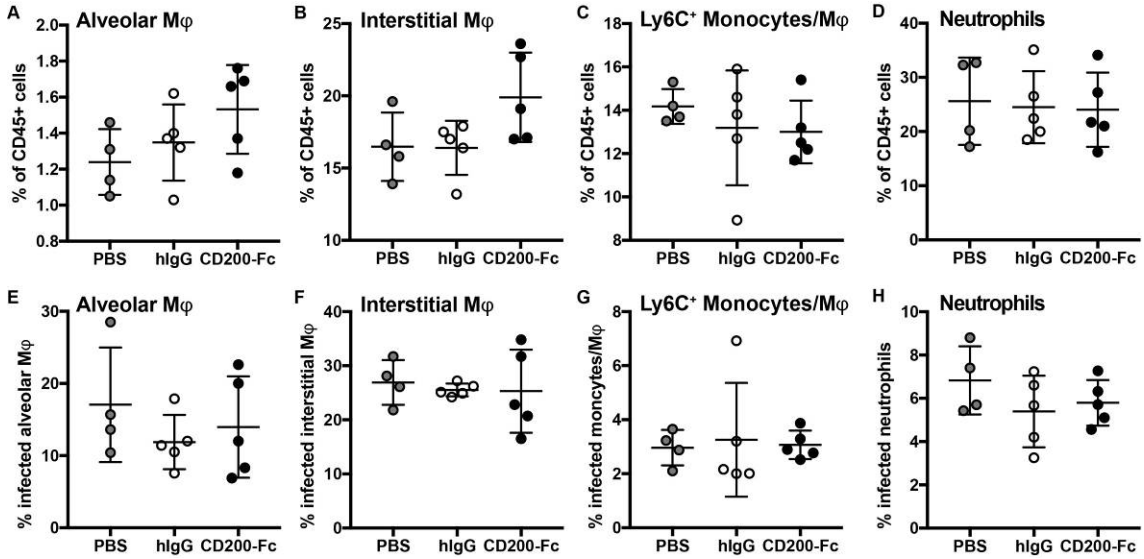

Figure 4.8 | Characterising lung populations following CD200-Fc treatment of *F. tularensis* LVS infection. WT mice were treated IP with 10 µg CD200-Fc, hIgG or PBS at day -1, 1, 3 & 5 of *F. tularensis* LVS infection, before culling at day 7 p.i. The mean challenge dose of 1731 CFU *F. tularensis* LVS was administered intranasally. Cells were isolated from the lung, processed for flow cytometry and stained as described previously (Figure 3.13A). Data is presented as percentage of live, $CD45^+$ cells for A) alveolar macrophages, B) interstitial macrophages, C) $Ly6C^+$ monocyte/macrophages and D) neutrophils. The percentage of infected E) alveolar macrophages, F) interstitial macrophages, G) $Ly6C^+$ monocyte/macrophages and H) neutrophils was also determined. Data is representative of three independent experiments and is shown as mean ± SD (n=5). Statistical analysis was performed using one-way ANOVA.

When investigating the percentage of infection within the cells, there were no significant differences in the percentage of *F. tularensis* LVS-infected alveolar macrophages, interstitial macrophages and $Ly6C^{hi}$ monocyte/macrophages following CD200-Fc treatment (Figure4.8E-G respectively). Although there was no significant difference in *F. tularensis* LVS-infected neutrophils, the results mirrored that of the overall bacterial burden with hIgG and CD200-Fc-treated mice having similar effects compared to PBS-treated (Figure 4.8H). Nevertheless, these data show that there were no significant differences in the cell populations within the lung following CD200-Fc treatment compared to controls.

4.2.9 Characterising the cytokine response in the lung following CD200-Fc treatment of *F. tularensis* LVS infection

CD200-Fc has been shown to reduce the production of pro-inflammatory cytokines by agonising the CD200R pathway in other studies (Simelyte et al., 2008, Snelgrove et al., 2008). As $CD200R^{-/-}$ mice exhibit an exacerbated inflammatory cytokine

response (Figure 4.3), it was hypothesised that CD200-Fc treatment could reduce the levels of pro-inflammatory cytokines. Thus, the expression of various lung pro-inflammatory cytokines and chemokines were measured following treatment of *F. tularensis* infection with PBS, hIgG and CD200-Fc.

Overall there the data points towards reduced pro-inflammatory cytokine levels following CD200-Fc treatment. Reduction of IL-6, IL-17A and IL-12p40 levels with CD200-Fc were not significant (Figure 4.9A-C respectively). However, the concentration of TNFα was significantly reduced in CD200-Fc-treated lungs compared to hIgG-treated (Figure 4.9D). Interestingly, there was a significant reduction in the concentration of KC and MCP1 following CD200-Fc treatment compared to hIgG, but not against PBS-treated (Figure 4.9E & F respectively).

As with previous *in vivo* data with CD200-Fc treatment of *F. tularensis* LVS infection, these data show significant reduction TNFα, KC and MCP1 production reduced production of pro-inflammatory cytokines following CD200-Fc treatment. This highlights the potential use of CD200-Fc as treatment in dampening the exacerbated pro-inflammatory cytokine response induced by *F. tularensis* LVS infection.

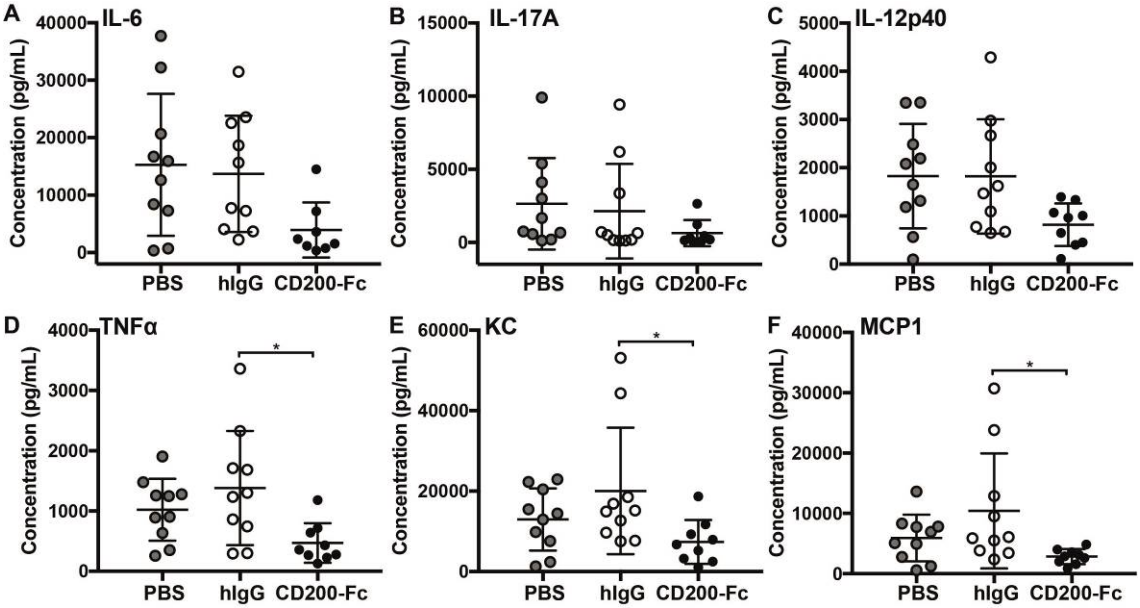

Figure 4.9 | General reduction in cytokine responses in the lung following CD200-Fc treatment of *F. tularensis* LVS infection. WT mice were treated IP with 10 µg CD200-Fc, hIgG or PBS at day -1, 1, 3 & 5 of *F. tularensis* LVS infection, before culling and collecting lung homogenated at day 7 p.i. The mean challenge dose of 1731 CFU *F. tularensis* LVS was administered intranasally. Pro-inflammatory cytokines IL-6, IL-17A, IL-12p40, TNFα, KC and MCP1 (A-F respectively) were detected in lung homogenate using the BioLegend LEGENDplex immunoassay and subsequent analysis software. Data represents two independent experiments and is shown as mean ± SD (n=10, 5/group). Statistical analysis was performed using one-way ANOVA (*p<0.05).

4.2.10 Developing a sub-optimal *in vivo* antibiotic treatment for *F. tularensis* LVS infection

Following CD200-Fc treatment during *F. tularensis* LVS infection, a suboptimal antibiotic model was developed to investigate the use of CD200-Fc in a combined antibiotic-immunomodulatory therapy do try and increase the effects of CD200-Fc treatment. This type of treatment could potentially extend the window for successful antibiotic-induced bacterial clearance during acute disease (Klimpel et al., 2008, D'Elia et al., 2013b).

Consequently, WT mice were treated intraperitoneally with 1, 10 and 100 mg/kg gentamicin, or a sham injection, at day 1, 3 and 5 p.i. with 643 CFU *F. tularensis* LVS administered intranasally (Figure 4.10A). When monitoring weight change it was noted that mice treated with 1 mg/kg gentamicin showed the same weight loss seen in sham treated mice. On the contrary, both 10 and 100 mg/kg treatments led to almost no weight loss (Figure 4.10B).

With such drastic differences in weight loss between the gentamicin doses, it was of interest to determine how these correlated with bacterial burden in the lung, liver and spleen of infected mice. Although treatment with 1 mg/kg gentamicin led to no difference in weight loss compared to sham-treated mice, there was a log reduction in bacterial burden in the lung, liver and spleen (Figure 4.10C). Interestingly, while 10 and 100 mg/kg treatment resulted in no weight loss in infected mice, the bacterial burdens highlighted differences within the two doses. The bacterial burden in the lung following 10 mg/kg gentamicin was only reduced by less than a log compared to 1 mg/kg treatment, while the bacteria was almost fully cleared following 100 mg/kg treatment (Figure 4.10C). Similarly, 100mg/kg treatment was sufficient to fully clear bacteria from the liver, while 10 mg/kg treatment led to a two-log reduction in liver burden compared to sham treatment (Figure 4.10C). The spleen appeared to be the least affected organ in terms of antibiotic-induced bacterial clearance. Both 10 and 100 mg/kg gentamicin treatment only led to a further log reduction in bacterial burden when compared to 1 mg/kg treatment (Figure 4.10C).

These data highlight the fine balance between overall bacterial burden and subsequent weight loss. Although there were differences in weight loss between sham and 1 mg/kg treatment, as well as 10 and 100 mg/kg treatment, overall bacterial burdens tended to follow a log-dependent decrease in accordance with the log increase in dose. Therefore, when designing a suboptimal antibiotic model for

CD200-Fc experiments, the lack of correlation between bacterial burden and weight loss needs to be considered.

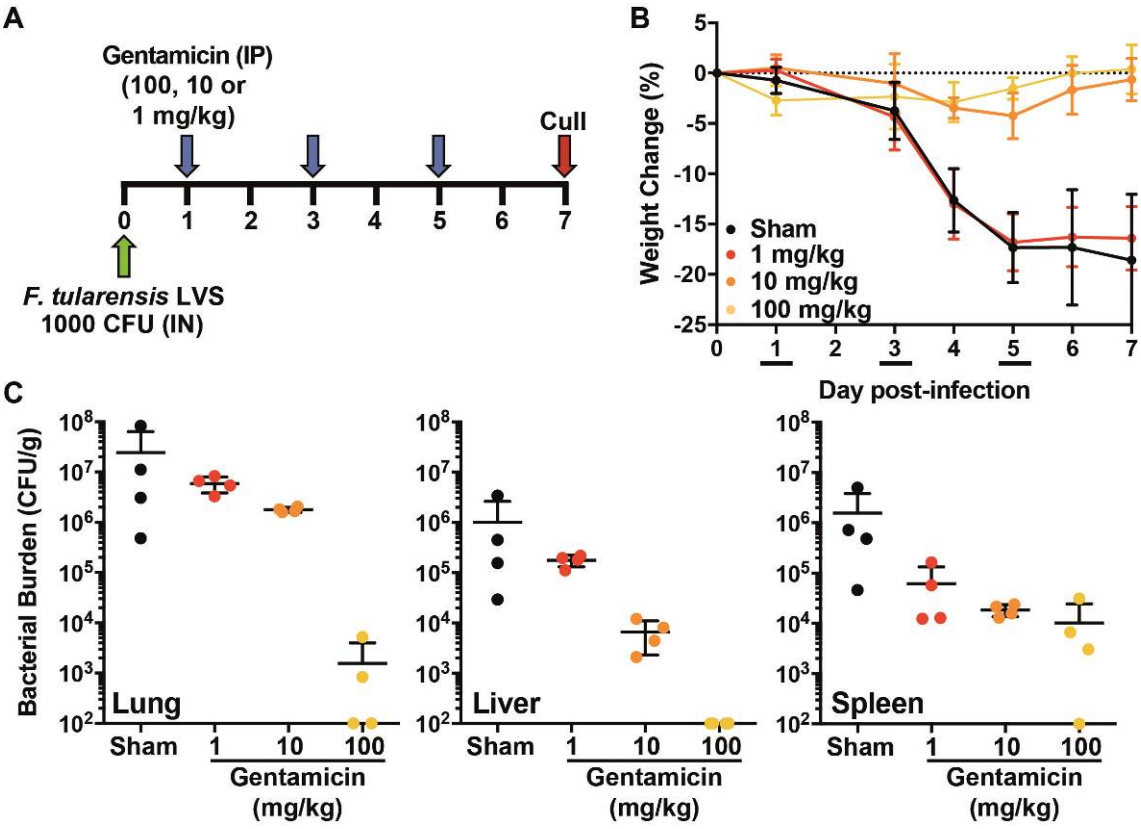

Figure 4.10 | Developing a sub-optimal *in vivo* antibiotic treatment for *F. tularensis* LVS infection. WT mice were treated intraperitoneally with a sham injection or 100, 10 or 1 mg/kg gentamicin at day 1, 3 & 5 of *F. tularensis* LVS infection, before culling at day 7 p.i. The challenge dose of 643 CFU LVS was administered intranasally. B) Mouse weights were monitored daily and are represented as percentage weight change. C) Bacterial burden (CFU/g) of the lung, liver and spleen was enumerated at day 7 p.i. Data represents one independent experiment and is shown as mean ± SD (n=4).

4.3 Discussion

4.3.1 Protective role for CD200R during later stages of pulmonary *F. tularensis* infection

4.3.1.1 Exacerbated *F. tularensis* burden and pro-inflammatory response in CD200R$^{-/-}$ mice

In this chapter the role of CD200R during the later stages of pulmonary *F. tularensis* infection was investigated. As was hypothesised, CD200R$^{-/-}$ mice exhibited significantly increased bacterial burden in the lung later in *F. tularensis* LVS infection following intranasal challenge compared to WT (Figure 4.1C). Similarly, there was a significantly increased bacterial burden in the spleen of CD200R$^{-/-}$ compared to WT at day 5 p.i. (Figure 4.1E). This overall increase in bacterial burden was also associated with significantly increased splenomegaly in CD200R$^{-/-}$ mice compared to WT, which is characteristic of increased disease severity (Feldman, 2003, Chiavolini et al., 2008). Interestingly, a general reduction in bacterial burden was seen in the liver and spleen, but not the lung, at day 7 p.i. suggesting that bacterial clearance in the peripheral organs occurred before clearance at the primary site of infection. The bacterial persistence and significantly increased burden in the lung of CD200R$^{-/-}$ mice compared to WT was one of the reasons only the lung was investigated further in terms of cell population dynamics, cytokine levels and pathology.

Despite this, there was no significant difference in weight loss and survival between WT and CD200R$^{-/-}$ mice following *F. tularensis* infection, which could bring into question the biological significance of an increased lung bacterial burden in CD200R$^{-/-}$ mice. Nevertheless, the long-term consequences of increased bacterial burdens were briefly investigated and suggested a persistent infection in CD200R$^{-/-}$ mice. Understanding how CD200R$^{-/-}$ mice previously infected with *F. tularensis*, deal with co-infection or secondary infections could shed greater light on the biological significance of these findings.

Furthermore, although findings from the experiment looking at recovery from *F. tularensis* infection must be interpreted with caution due to low sample size, it highlights important aspects of *F. tularensis* infection dynamics. It was interesting to note that even at day 17 p.i. where surviving mice had fully recovered to their original weight, extensive bacterial burden was still present in the lungs and peripheral organs (Figure 4.5). Although two WT mice had to be culled due to

excessive weight loss that would presumably have shown higher bacterial burden than surviving WT mice, there was a trend of increased bacterial burden in CD200R$^{-/-}$ mice. This was evident in the lung, as well as in the liver where bacteria had been fully cleared in WT mice. Low n numbers in this experiment severely underpower the results obtained and thus brings into question any conclusions made. Repeating this experiment with increased numbers of mice would provide greater reliability in these findings, nevertheless when taken together it is evident that CD200R plays an important role in the controlling *F. tularensis* LVS infection.

4.3.1.2 Delayed and exacerbated pro-inflammatory cytokine response in CD200R$^{-/-}$ mice

Many studies have shown that pulmonary *F. tularensis* LVS infection is characterised by a delayed inflammatory cytokine response (Lopez et al., 2004, Malik et al., 2006, Cowley et al., 2010). Similarly, the data in this chapter showed that levels of pro-inflammatory cytokines such as IFNγ, TNFα and IL-6 were only detectable in lung homogenates at day 5 p.i. Interestingly, a delayed but exacerbated cytokine response was observed in CD200R$^{-/-}$ mice compared to WT in response to *F. tularensis* LVS (Figure 4.3). The pro-inflammatory cytokines IFNγ and TNFα are essential in controlling *F. tularensis* infection, with mice deficient in these cytokines showing extreme susceptibility to intranasal infection (Chen et al., 2004b). Thus, a more robust pro-inflammatory response could be considered beneficial for the clearance of *F. tularensis* LVS.

Nevertheless, in the case of mice lacking CD200R signalling, there is an uncontrolled and exacerbated response that has also been seen in other infectious models, such as influenza and *N. meningitides*. Interestingly, in these cases the excessive inflammatory response leads to increased weight loss, while bacterial/viral burdens remain unchanged (Snelgrove et al., 2008, Mukhopadhyay et al., 2010). On the contrary, despite the significantly increased bacterial burden in CD200R$^{-/-}$ mice, there was no difference in weight loss between WT and CD200R$^{-/-}$ mice. Similarly, H&E staining of LVS-infected lungs showed no gross differences in lung pathology between WT and CD200R$^{-/-}$ mice (Figure 4.4). As the excessive pro-inflammatory cytokine response in *F. tularensis* infection has been shown to drive pathology and susceptibility to infection (Malik et al., 2006, Cowley, 2009), findings in this chapter suggest that the exacerbated cytokine response in CD200R$^{-/-}$ mice was not contributing to increased susceptibility to infection. Thus, the

significantly increased *F. tularensis* LVS burden seen in the lung is more likely to be driven by other factors.

4.3.1.3 The role of neutrophils in CD200R$^{-/-}$ mice during *F. tularensis* infection

Following on from findings in Chapter 3 where there was increased infiltration of inflammatory cells into the lung at day 3 p.i. in CD200R$^{-/-}$ mice compared to WT, in the longer time course of infection over 7 days there were similar cell population kinetics. Increased infiltration of inflammatory cells were observed at day 3 p.i., albeit there was no significant difference between WT and CD200R$^{-/-}$ mice which could be explained by the fact BAL and lung tissue were not separated in these experiments. Nevertheless, the most striking finding was the significantly increased neutrophilia in CD200R$^{-/-}$ mice compared to WT, accompanied by significantly increased percentage of *F. tularensis* LVS-infected neutrophils (Figure 4.2). As there were no significant differences in the infection rate of any other cell types, neutrophils could be considered to be a key contributor to the increased bacterial burden of CD200R$^{-/-}$ mice lungs.

Neutrophils have been shown to be the most infected cell type in the lung from day 3 p.i. following pulmonary *F. tularensis* LVS challenge (Hall et al., 2008), perhaps due to the fact that infection induces a large influx of neutrophils to the infection site as part of the innate response (Marsh et al., 1967, Craig et al., 2009). As *F. tularensis* successfully infects neutrophils, this increased influx of neutrophils in CD200R$^{-/-}$ mice may be providing a larger replicative niche compared to WT.

Disruption of CD200R signalling in CD200$^{-/-}$ mice leads to dysregulation of myeloid populations (Hoek et al., 2000), while activation of the CD200R pathway has been shown to inhibit the production of the neutrophil chemoattractant IL-8 in a human monocytic cell line (Mihrshahi et al., 2009). Similarly, the data in this chapter shows that CD200R$^{-/-}$ mice express higher levels of KC, the murine IL-8 homolog, in the lung following *F. tularensis* LVS infection. This would suggest that perhaps the lack of CD200R on other cell types, such as macrophages that are one of the major sources of KC (De Filippo et al., 2008), might be contributing to the increased neutrophil influx in CD200R$^{-/-}$ mice. It would be interesting to investigate cell-specific CD200R deficient mice to further elucidate the influence of CD200R signalling during *F. tularensis* infection.

Alternatively, as there was only increased KC in CD200R$^{-/-}$ mice at day 7 p.i. and the increased neutrophilia was seen as early as day 5 p.i., the contribution of CD200R on other cell types towards the increase in *F. tularensis* LVS-infected neutrophils may be minimal. Neutrophils have been shown to drive pathology in *F. tularensis* infection (Malik et al., 2007), and it has been shown that *F. tularensis* can inhibit ROS-dependent killing by neutrophils though disruption of NADPH oxidase assembly (McCaffrey and Allen, 2006, McCaffrey et al., 2010). Therefore, it may also be the case that lack of CD200R signalling directly on neutrophils is further affecting their ability to deal with *F. tularensis* infection. This is something that was explored extensively in Chapter 5.

4.3.2 Maintaining a consistent *in vivo* infectious model

As with maintaining a consistent challenge dose for *in vitro* experiments discussed in Chapter 3.3, similar issues were encountered when preparing challenge doses for intranasal infections *in vivo*. The importance of challenge dose, time of infection end point and mouse strain/sex were all considered. From previous studies undertaken in the lab (data not shown), C57Bl/6 mice were the strain chosen due to increased susceptibility to the infection, as well as using only female mice to avoid sex bias. A high dose of 1000 CFU *F. tularensis* LVS was chosen as this has previously been shown to be around the LD_{50} for *F. tularensis* LVS intranasal infection (Fortier et al., 1991, Periasamy et al., 2016). It can be noted throughout this chapter that the average *F. tularensis* LVS CFU of intranasal challenge doses varied between experiments. This variation in challenge dose was primarily due to the variations in the accuracy of the spectrophotometer when preparing an LVS suspension of OD_{600nm} 0.20 being amplified during serial dilutions to achieve a final challenge dose of 1000 CFU.

Attempts to rectify this problem were achieved through creating frozen stocks specifically for *in vivo* challenges which solved some of the issues (Methods 2.1.4); however small variations between challenge doses still remained. Nevertheless, as the intranasal challenge doses all remained within the same log scale (10^3), the different doses most likely did not have a major impact on the overall results presented in this thesis. Furthermore, variation in the uptake of bacteria during the procedure of intranasal challenge itself would provide variability between mice and experiments, regardless of similar challenge doses. Nevertheless, enhanced burden in the lung of CD200R$^{-/-}$ mice was consistent between different experiments despite

variation in challenge does, strongly supporting a role for CD200R signalling in regulating responses to *F. tularensis* infection.

4.3.3 CD200R as a therapeutic target against *F. tularensis* infection

4.3.3.1 Minimal effect of CD200-Fc treatment *in vivo*

Despite showing evidence of CD200-Fc decreasing *F. tularensis* LVS burden *in vitro* in Chapter 3, experiments *in vivo* show minimal effects of CD200-Fc treatment. When compared to PBS-treated mice, CD200-Fc treatment led to a significant reduction in *F. tularensis* LVS burden in the lung; however there was no significant difference when compared to hIgG control-treated mice (Figure 4.7). Furthermore, there was also no difference in bacterial burden found in peripheral organs. Similarly, when looking at the cell populations in the lung, no significant differences between any of the treatments were observed (Figure 4.8). Nevertheless, it must be noted that there was no significant difference in lung bacterial burden between PBS and hIgG treatment, suggesting that CD200-Fc did have a slight independent effect. This was perhaps more notable when looking at the cytokine production in the lung following treatment of *F. tularensis* infection (Figure 4.9). There was a significant reduction in TNFα, KC and MCP1 production following CD200-Fc treatment compared to hIgG-treated mice. As introduced previously, CD200-Fc is a beneficial treatment for various inflammatory states in mice such as influenza, ocular HSV infection and autoimmune disorders through the reduction of pro-inflammatory cytokine responses (Gorczynski et al., 1999, Simelyte et al., 2008, Snelgrove et al., 2008, Sarangi et al., 2009). However, findings in this chapter suggest that the inflammatory response may not be playing a direct role in influencing infectious outcome with regards to bacterial burden, pathology and weight loss. Thus, the reduction in inflammatory responses induced by CD200-Fc may not be sufficient to influence *F. tularensis* LVS infectious outcome.

The similarities in *F. tularensis* burden between hIgG and CD200-Fc treated mice suggest that the hIgG portion of the recombinant protein may be having off-target effects. IgGs can bind to Fcγ receptors on myeloid cells and can lead to a variety of downstream effector functions (Unkeless and Eisen, 1975, Bournazos et al., 2016). It has been shown that human IgGs can bind to mouse FcγR with similar affinities to mouse IgGs and may have similar FcγR-mediated biological activities in mice (Dekkers et al., 2017). This is the case for the anti-angiogenic cancer drug bevacizumab, where anti-angiogenic effect of the drug was abolished through

disruption of the IgG-FcγR interaction, suggesting that the anti-angiogenic function is in part dependent on the hIgG (Bogdanovich et al., 2016).

Alternatively, it could also be a case of altering the dosing regimen of CD200-Fc treatment to reduce the chances of off-target affects. However, 10 μg CD200-Fc was administered per dose which has been used as a therapeutic dose multiple times in the literature (Gorczynski et al., 1999, Snelgrove et al., 2008, Yin et al., 2016). Furthermore, increasing dose does not guarantee a response as some studies have used 40 μg CD200-Fc per dose to treat corneal graft rejection, an inflammatory disorder, with no effect (Nicholls et al., 2015). The days in which dosing took place were also similar to others, with treatment administered in either one or two-day intervals. Due to the short nature of the infection, it was decided to dose every other day. Furthermore, the experiments in this chapter included a pre-treatment prior to infection, which may not be representative of real-life treatment of tularemia which would only be treated upon onset of symptoms after 3-4 day incubation period (Feldman, 2003). As there were differences in *F. tularensis* LVS burden later in infection in CD200R$^{-/-}$ mice, it would be interesting to see whether starting CD200-Fc treatment when *F. tularensis* infection has developed would provide a difference treatment outcome. Another aspect to consider is the route of treatment. Intranasal administration of CD200-Fc, as oppose to intraperitoneal dosing, would ensure the treatment reaches its target organ of the lung and perhaps enhance the therapeutic effect. This was difficult to achieve to the severity of infection in mice and Home Office regulations, but would be interesting to peruse in the future.

4.3.3.2 Combined antibiotic-immunomodulatory therapy

In the final part of the chapter the effects of different doses of gentamicin treatment in pulmonary *F. tularensis* LVS infection were investigated, in the hope of developing a combined antibiotic-immunomodulatory therapy with CD200-Fc. The efficiency of antibiotic treatment during *F. tularensis* infection is highly dependent on the time after infection that the treatment is given, with increased success from earlier treatment (Russell et al., 1998, Steward et al., 2006, Klimpel et al., 2008). Therefore, developing a therapeutic strategy where the window for efficient treatment is increased, in this case reducing the inflammatory response via CD200-Fc administration, could be beneficial for *F. tularensis* infection.

Gentamicin was chosen as the antibiotic for *in vivo* treatment as it had previously been used during *in vitro* experiments, and more importantly it has been shown to

be an effective treatment for tularemia (Jackson and Lester, 1978, Mason et al., 1980). However, ciprofloxacin and levofloxacin have been shown to have a lower minimum inhibitory concentration (MIC) range against *F. tularensis* when compared to gentamicin (Caspar and Maurin, 2017). Thus, in determining a combination therapy, it would be beneficial to compare the effectiveness of CD200-Fc with antibiotics of varying bactericidal activity.

Furthermore, it must also be taken into account how infectious outcome of *F. tularensis* can be monitored and measured in mice. As has been experienced in previous experiments, weight loss and bacterial burden do not necessarily correlate during infection (Figure 4.10). It was determined that mice treated with 1 mg/kg gentamicin exhibited an increased bacterial clearance compared to sham treated, but interestingly there was no difference in weight loss. On the contrary, mice treated with 10 and 100 mg/kg gentamicin showed equally minimal weight loss, yet 100 mg/kg gentamicin treatment led to significantly increased bacterial clearance when compared to the 10 mg/kg dose. It is important to realise in these antibiotic models that although no weight loss occurs, there can still be considerable changes in bacterial burden. Thus, in future experiments it would be important to choose an optimal gentamicin dose that would allow *F. tularensis* infection to be monitored by weight loss as well as bacterial burden.

4.4 Conclusion

In Chapter 4 it was determined that CD200R is important in controlling *F. tularensis* LVS in the later stages of infection, demonstrated by a significantly increased bacterial burden in the lung of $CD200R^{-/-}$ mice compared to WT. Furthermore, $CD200R^{-/-}$ mice exhibited a delayed, but exacerbated, pro-inflammatory response to infection; however this did not appear to be contributing to increased pathology. This was further supported by the findings that a reduction in pro-inflammatory cytokine responses in the lung through treatment with CD200-Fc did not influence bacterial burdens.

It was later demonstrated that this elevated burden was associated with increased neutrophilia in $CD200R^{-/-}$ lungs, leading to increased *F. tularensis*-infected neutrophils that appeared to be the main contributors to elevated lung burdens. Chapter 5 will go on to extensively investigate the importance of CD200R signalling on neutrophils and the role this plays during pulmonary *F. tularensis* LVS infection.

Chapter 5

Determining the functional role of neutrophils during *Francisella tularensis* LVS infection

5.1 Introduction

Chapters 3 and 4 explored the importance of CD200R during pulmonary *F. tularensis* LVS infection. It was determined that CD200R plays a protective role in the lung during the later stages of infection, and data showed that this phenotype was linked to excessive neutrophilia and increased *F. tularensis* LVS-infected neutrophils in CD200R$^{-/-}$ mice compared to WT. Thus, this chapter aimed to further investigate the importance of neutrophils during *F. tularensis* LVS infection in CD200R$^{-/-}$ mice, as well as elucidating the functional mechanisms by which CD200R signalling on neutrophils can influence infectious outcome.

The role of neutrophils during *F. tularensis* infection is evident by the fact that following pulmonary infection, neutrophils account for around 50% of total infected cell types at day 3 p.i (Hall et al., 2008). However, previous studies in which neutrophils have been depleted during pulmonary *F. tularensis* infection have provided mixed results. Data from one group showed that neutrophil depletion had no effect on bacterial burdens and infectious outcome to *F. tularensis* (Conlan et al., 2002); while another demonstrated high susceptibility to infection when neutrophils were depleted at day 3 p.i. (Steiner et al., 2017). Nevertheless, this chapter looked at neutrophil depletion in CD200R$^{-/-}$ mice during pulmonary *F. tularensis* LVS infection. It was hypothesised that as neutrophils may be primary contributors to the increased pulmonary bacterial burden in CD200R$^{-/-}$ mice compared to WT and depleting neutrophils in this model would lead to a reduction in bacterial burden in CD200R$^{-/-}$ mice.

As well as investigating the effects of neutrophil depletion during *F. tularensis* LVS infection in CD200R$^{-/-}$ mice, this chapter also aimed to understand mechanistic functions of neutrophils that lack of CD200R signalling affected. As neutrophils had enhanced *F. tularensis* LVS burden in CD200R$^{-/-}$ mice compared to WT, it was hypothesised that neutrophils lacking CD200R were defective in key effector functions that serve to control bacterial infection.

Thus, it is clear that neutrophils play an important role in controlling pathogen clearance, with multiple effector functions that are critical in maintaining neutrophil activity. The findings in this thesis so far suggest that neutrophils in CD200R$^{-/-}$ mice are key contributors to an elevated *F. tularensis* LVS burden in the lungs and have a reduced ability to deal with infection. This chapter aimed to understand what is driving this dysfunctional neutrophil activity in CD200R$^{-/-}$ mice.

5.2 Results

5.2.1 Antibody-mediated neutrophil depletion abrogates increased *F. tularensis* LVS lung burden in CD200R$^{-/-}$ mice

Chapter 4 determined that an exacerbated *F. tularensis* LVS burden in the lungs of CD200R$^{-/-}$ mice was associated with increased neutrophilia and an increase in *F. tularensis* LVS-infected neutrophils (Figure 4.1 & 4.2). To further investigate whether this neutrophil phenotype was directly contributing to increased susceptibility to *F. tularensis* LVS in CD200R$^{-/-}$ mice, it was important to understand how depleting neutrophils during *F. tularensis* LVS infection altered the infectious outcome. Thus, mice were treated with an α-Ly6G monoclonal antibody to specifically deplete neutrophils during pulmonary *F. tularensis* infection.

Firstly, it was important to determine to what extent neutrophils were depleted and if they could replenish after α-Ly6G antibody treatment to determine an appropriate dosing regimen. WT mice were treated intraperitoneally with 50 µg α-Ly6G antibody or IgG2a control and neutrophil populations were monitored. The α-Ly6G antibody (clone 1A8) had previously been used to identify neutrophils in the lung by flow cytometry; however, this was no longer possible as Ly6G was the target for antibody-mediated killing of neutrophils. Therefore, in order to avoid masking a neutrophil population a combination of Ly6C and Gr-1 was used to identify neutrophils by flow cytometry.

The α-Gr-1 antibody reacts strongly with Ly6G (RB6-8C5 clone) expressed by neutrophils, but also weakly with Ly6C that is expressed by monocytes. Subsequently, the strong binding of the Ly6C antibody to monocytes was used to distinguish between these two populations (Figure 5.1A). Cells were isolated from the lung and analysed by flow cytometry, initially being gated on single, live CD45^{+} lymphocytes as described in figure 3.12. Ly6G^{+} neutrophils were demonstrated to overlap with Gr-1^{hi} Ly6C^{int} cells and can be comfortably distinguished from Gr-1^{hi} Ly6C^{hi} cells (Figure 5.1A). This confirmed that Gr-1^{hi} Ly6C^{int} cells were indeed neutrophils and provided an accurate way to determine efficient neutrophil depletion.

Consequently, it was demonstrated that treatment with 50 µg α-Ly6G effectively depleted neutrophils in the lung after 1 day. At day 2 and 3 post-treatment there was a slight replenishment of neutrophils, but there was still significant depletion when compared to IgG2a control treated mice (Figure 5.1B). To further confirm neutrophil

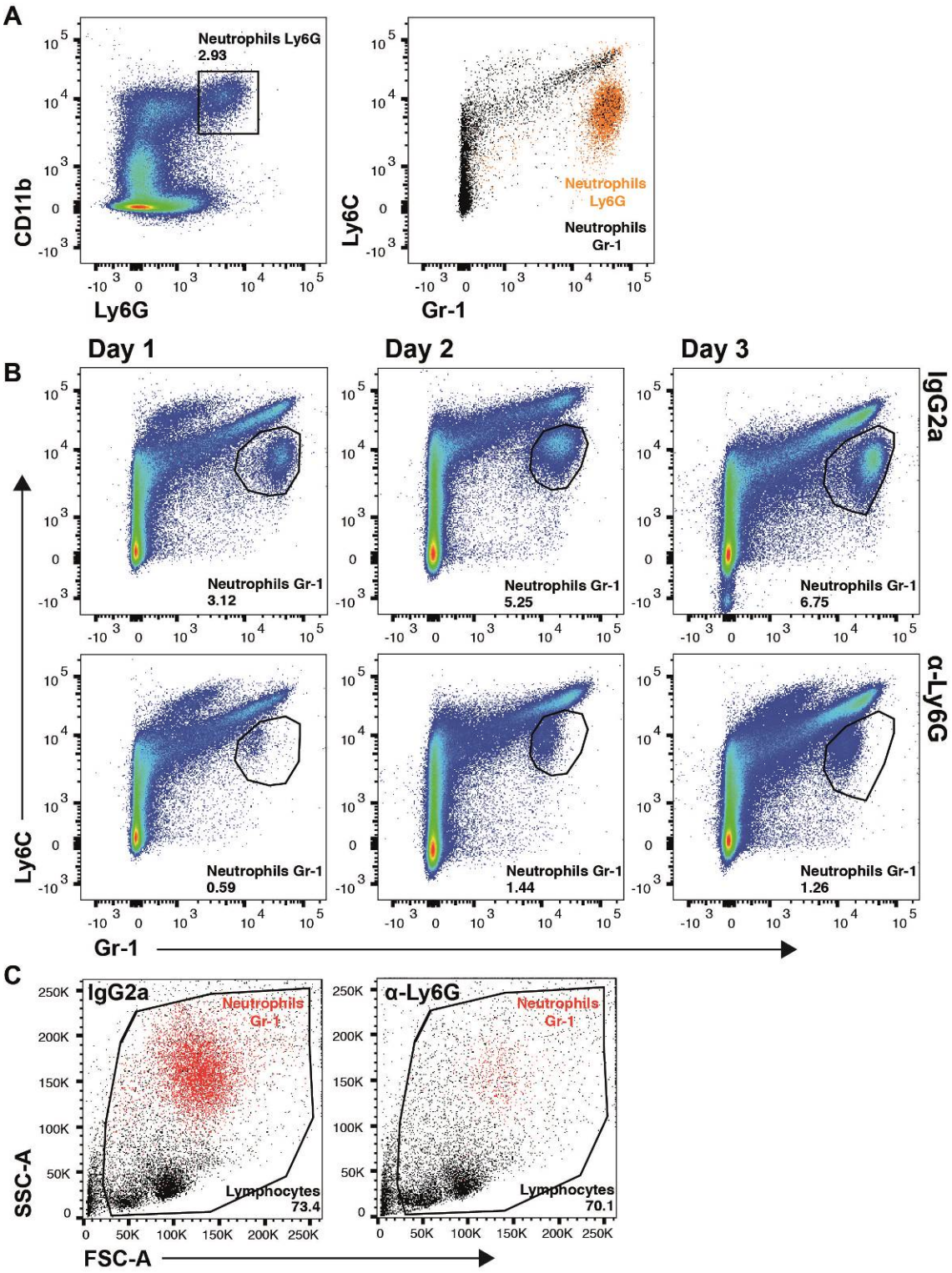

Figure 5.1 | **Confirmation of antibody-mediated neutrophil depletion *in vivo*.** WT C57BL/6 mice were treated intraperitoneally with 50 µg α-Ly6G or IgG2a control, then lung neutrophil populations monitored by flow cytometry at day 1, 2 and 3 post-treatment. A) Representative dot plots of IgG2a-treated lungs showing the overlap of live, $CD45^{+}$, $CD11b^{+}$ $Ly6G^{+}$ neutrophils with $Gr1^{hi}$ $Ly6C^{int}$ cells. B) Representative dot plots of $Gr\text{-}1^{hi}$ $Ly6C^{int}$ neutrophil populations at day 1, 2 and 3 post-treatment with α-Ly6G or IgG2a confirming neutrophil depletion in the lung. C) Representative back gating of $Gr\text{-}1^{hi}$ $Ly6C^{int}$ neutrophils (red) for FSC-A and SSC-A at day 1 post-treatment with α-Ly6G or IgG2a.

depletion, the increased granularity of neutrophils was used to identify the depleted population by forward and side scatter. The neutrophil population with high SSC-A in IgG2a treated mice was not present in mice treated with α-Ly6G (Figure 5.1C). It was determined that 50 µg α-Ly6G effectively depleted neutrophils *in vivo*, however due to the slight replenishment of neutrophils by day 2 post-treatment, it was decided to dose mice every other day during future studies.

Having confirmed successful neutrophil depletion, the next step was to deplete neutrophils during *F. tularensis* LVS infection in WT and CD200R$^{-/-}$ mice. The dosing regimen consisted of a pre-treatment with α-Ly6G or IgG2a one day prior to intranasal challenge with an average of 984 CFU *F. tularensis* LVS, followed by further treatments at day 1, 3 and 5 p.i. (Figure 5.2A). Weight change was monitored in WT and CD200R$^{-/-}$ mice throughout the course of the infection, and as seen previously weight loss only began at day 3 p.i. (Figure 5.2B). Interestingly, there appeared to be a slight increase in weight loss in WT and CD200R$^{-/-}$ mice treated with α-Ly6G consistently compared to those treated with IgG2a (Figure 5.2B). This suggested that by solely looking at weight change, neutrophil depletion had a detrimental effect on pulmonary *F. tularensis* LVS infectious outcome.

When enumerating the bacterial burden in infected lungs at day 7 p.i., there was the characteristic increased burden in CD200R$^{-/-}$ mice versus WT when treated with IgG2a (Figure 5C). However, neutrophil depletion in CD200R$^{-/-}$ mice led to a significant reduction in the lung bacterial burden, rescuing the phenotype by returning burdens back to levels of the WT mice (Figure 5.2C). Interestingly, neutrophil depletion had no effect on the bacterial burden of WT mice (Figure 5.2C). There was no significant difference in *F. tularensis* LVS burden in the liver at day 7 p.i. regardless of the condition (Figure 5.2D). Neutrophil depletion led to significantly reduced *F. tularensis* LVS burden in the spleen of WT and CD200R$^{-/-}$ mice when compared to WT IgG2a treated mice. Surprisingly, there was a significantly reduced bacterial burden in the spleen of CD200R$^{-/-}$ mice compared to WT treated with IgG2a, yet this difference was lost when treated with α-Ly6G (Figure 5.2E).

Together these data show the importance of neutrophils in driving increased lung *F. tularensis* LVS burdens in CD200R$^{-/-}$ mice, with neutrophil depletion in CD200R$^{-/-}$ mice rescuing the phenotype of exacerbated bacterial burden in the lungs. This would indicate that neutrophils play a detrimental role during *F. tularensis* LVS infection in CD200R$^{-/-}$ mice.

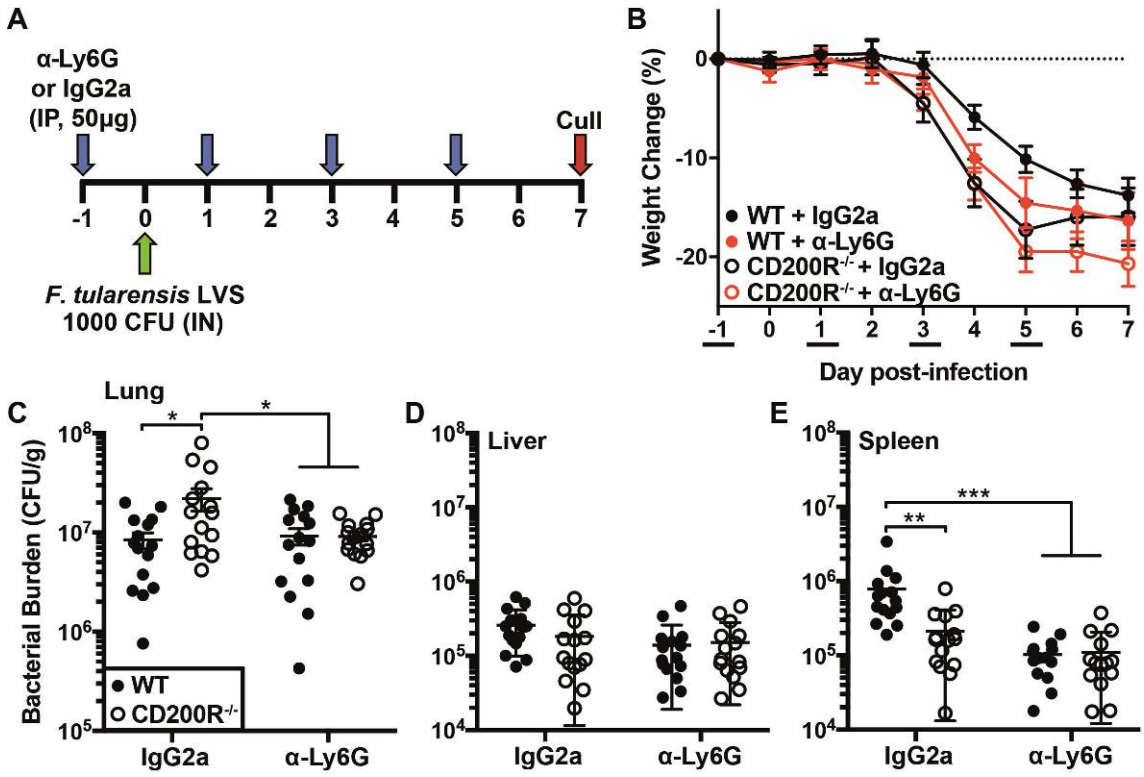

Figure 5.2 | Antibody-mediated neutrophil depletion abrogates increased *F. tularensis* LVS lung burden in CD200R$^{-/-}$ mice. A) WT and CD200R$^{-/-}$ mice were treated intraperitoneally with 50 µg α-Ly6G or IgG2a at day -1, 1, 3 & 5 of *F. tularensis* LVS infection, before culling at day 7 p.i. The mean challenge dose of 984 CFU *F. tularensis* LVS was administered intranasally. B) Mouse weights were monitored daily and are represented as percentage weight change. C) Bacterial burden (CFU/g) of the lung, liver and spleen was enumerated at day 7 p.i. Data represents three independent experiments and is shown as mean ± SD (n=15, 5/group). Statistical analysis was performed using two-way ANOVA (*p<0.05, **p<0.01, ***p<0.001).

5.2.2 Characterisation of pulmonary cell populations following neutrophil depletion during *F. tularensis* LVS infection

The bacterial burden data presented previously demonstrated that depleting neutrophils in CD200R$^{-/-}$ mice during pulmonary *F. tularensis* LVS infection rescues the exacerbated burden seen in lungs of untreated mice. It was important to pursue this phenotype and see how the population dynamics in the lung had shifted following neutrophil depletion. Furthermore, this would help determine if any other cell types may be contributing to the reduced burden in CD200R$^{-/-}$ mice following neutrophil depletion, or if the absence of neutrophils alone was sufficient to reduce the *F. tularensis* LVS burden.

Cells were isolated from the lung, stained them for flow cytometry and applied the same gating strategy as described previously (Figure 3.12), with the exception of using Ly6C and Gr-1 instead of Ly6G as markers to identify neutrophils (Figure 5.1). It was initially determined whether cell populations of interest had changed in WT and CD200R$^{-/-}$ mice. As expected, there was a significant increase in the percentage of neutrophils in IgG2a-treated CD200R$^{-/-}$ mice, with very few neutrophils present following neutrophil depletion (Figure 5.3A). There was no significant difference in the percentage of alveolar macrophages between any of the conditions (Figure 5.3B). Interestingly, there was a significant reduction in the percentage of interstitial macrophages and Ly6C^{hi} monocyte/macrophages in IgG2a-treated CD200R$^{-/-}$ mice compared to WT (Figure 5.3C & D respectively). Neutrophil depletion led to an increase in interstitial macrophage populations, abolishing the significant difference between WT and CD200R$^{-/-}$ mice (Figure 5.3C). In contrast, , a significant reduction in Ly6C^{hi} monocyte/macrophages population percentage was observed in IgG2a-treated CD200R$^{-/-}$ mice compared to WT (Figure 5.3D). These data suggest neutrophil depletion may be contributing to resurgence of interstitial macrophages populations in CD200R$^{-/-}$ mice.

Following this the percentage of infection within the cell populations described above was determined. Firstly, there was a significant increase in the percentage of *F. tularensis* LVS-infected neutrophils in IgG2a treated CD200R$^{-/-}$ mice compared to WT, whereas α-Ly6G treated mice showed very little neutrophil infection when presented as a percentage of total CD45+ cells (Figure 5.3E). Interestingly, there was no significant difference in WT and CD200R$^{-/-}$ mice regardless of the treatment when looking at the percentage of infected alveolar macrophages, interstitial macrophages and Ly6C^{hi} monocyte/macrophages (Figure 5.3F, G & H respectively).

Overall, the data points towards the detrimental effect of infected neutrophils during *F. tularensis* LVS infection in CD200R$^{-/-}$ mice. The lack of significant differences in the percentage infection of other cell types regardless of the condition indicates that the depletion of neutrophils, and the subsequent loss of an important replicative niche, is sufficient to reduce the overall lung bacterial burden in CD200R$^{-/-}$ mice.

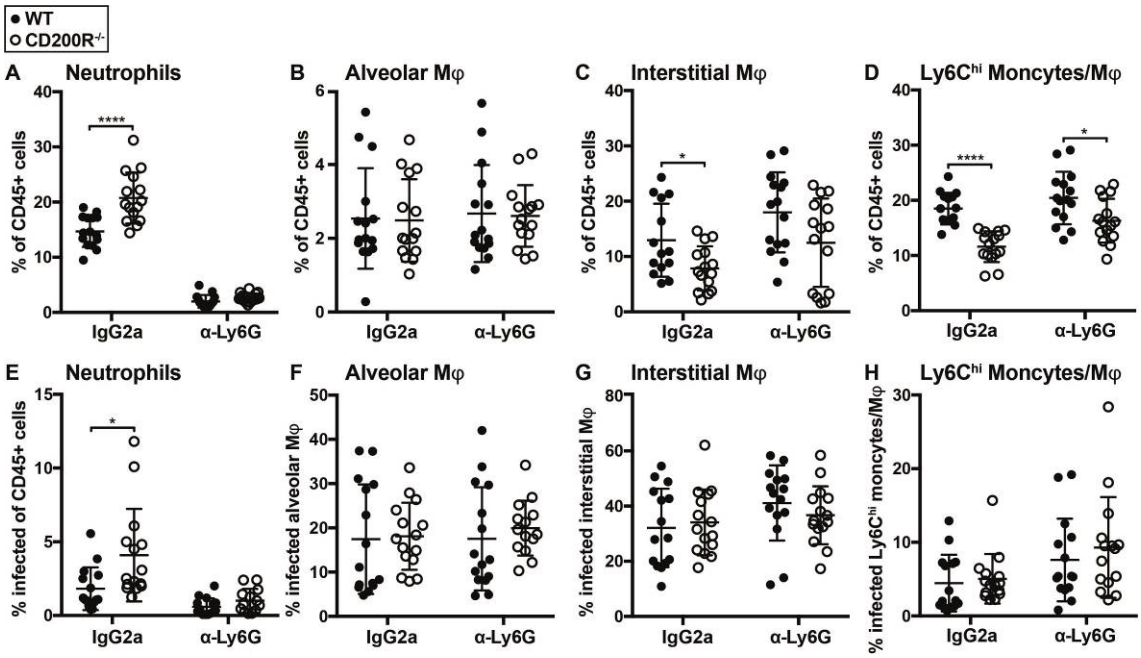

Figure 5.3 | Characterising lung cell populations following antibody-mediated neutrophil depletion, during *F. tularensis* LVS infection in WT and CD200R$^{-/-}$ mice. WT and CD200R$^{-/-}$ mice were treated as described in figure 5.2A. Infected lungs were analysed by flow cytometry as described in figure 3.13. Data is presented as percentage of live, CD45^{+} cells for A) neutrophils, B) alveolar macrophages, C) interstitial macrophages and D) Ly6C^{+} monocyte/macrophages. E) *F. tularensis* LVS-infected neutrophils are shown as a percentage of live, CD45^{+} cells. Similarly, percentage of *F. tularensis* LVS-infected F) alveolar macrophages, G) interstitial macrophages and H) Ly6C^{+} monocyte/macrophages are shown. Data represents three independent experiments and is shown as mean ± SD (n=15, 5/group). Statistical analysis was performed using two-way ANOVA (*p<0.05, ****p<0.0001).

5.2.3 No gross lung histopathology differences in WT and CD200R$^{-/-}$ mice following neutrophil depletion

As well as determining overall bacterial burden in the lung and further investigating the cell populations of interest by flow cytometry, it was also of interest to explore how neutrophil depletion affected the gross pathology of the lung during *F. tularensis* LVS infection in WT and CD200R$^{-/-}$ mice. Thus, histopathological analysis of infected lungs was conducted by inflating and fixing lung tissue with 10% formalin, before processing and staining with hematoxylin and eosin (HE).

Overall there were no gross differences in lung pathology between WT and CD200R$^{-/-}$ mice treated with IgG2a or α-Ly6G during LVS infection (Figure 5.4A-D). Nevertheless, signs of inflammation were evident in all the samples. Observations showed peri-vascular and peri-bronchial mononuclear cell infiltration, thickening of the airway epithelium and mild collapse of the alveolar space (black arrows, Figure 5.4A-D). To provide a quantitative measure of inflammation, number of cells within the tissue were counted using ImageJ to quantify the extent of cell infiltration. There were no significant differences in the cell count/tissue area between WT and

CD200R$^{-/-}$ mice treated with IgG2a or α-Ly6G during LVS infection (Figure 5.4E). These data suggest that although neutrophil depletion reduced lung bacterial burden in CD200R$^{-/-}$ mice, it did not impact lung pathology.

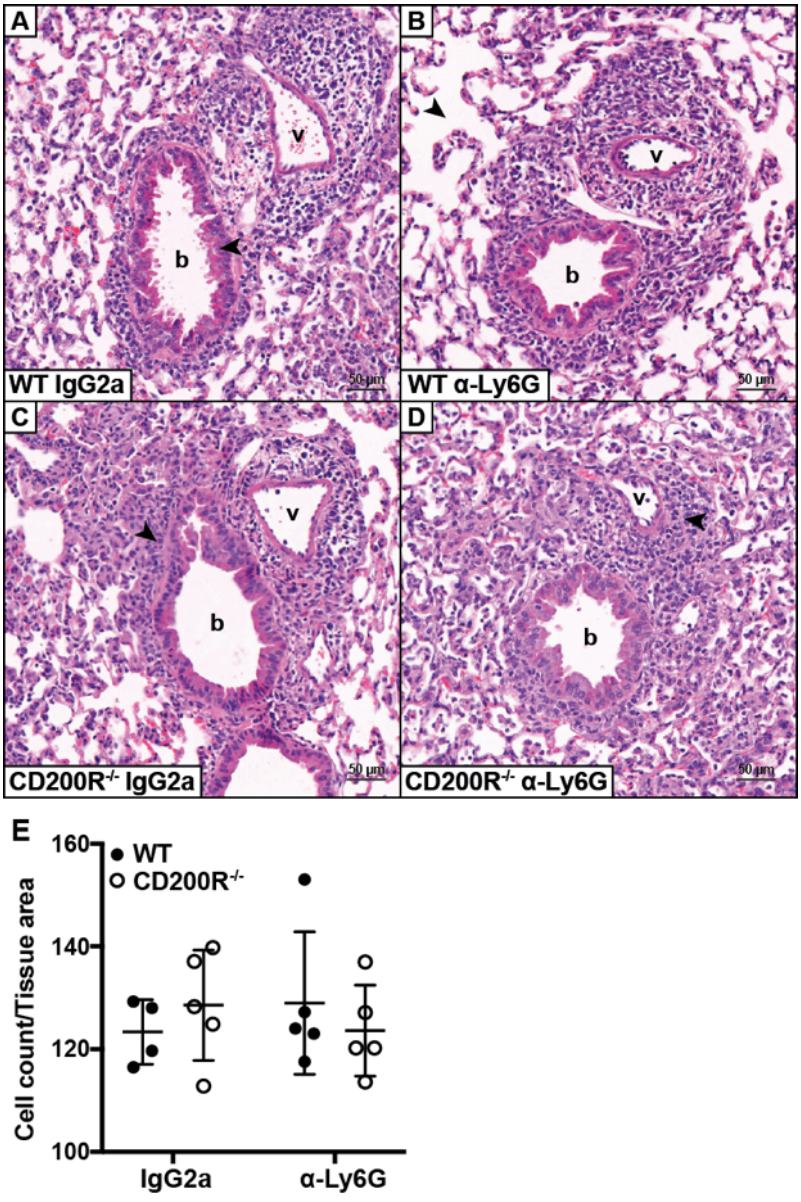

Figure 5.4 | H&E-stained lung of WT and CD200R$^{-/-}$ mice following antibody-mediated neutrophil depletion during *F. tularensis* LVS infection. Lung tissue was taken from IgG2a and α-Ly6G-treated WT and CD200R$^{-/-}$ at day 7 p.i. with *F. tularensis* LVS. H&E-stained lung sections were processed as described in methods 2.7. Representative images display bronchioles (b) and blood vessels (v) within the lung of IgG2a and α-Ly6G-treated WT (A & B) and CD200R$^{-/-}$ (C & D) mice. Black arrows represent thickening of the airway epithelium (A), mild collapse of the alveolar space (B), peri-bronchial (C) and peri-vascular (D) mononuclear cell infiltration. E) Quantitative analysis of cell infiltration using ImageJ. Cells were counted and normalised to total tissue area (tissue minus bronchial and vascular lumen). Images shown are at 20x magnification and scale bar represents 50 µm. Data is representative of one experiment and is shown as mean ± SD (E, n=4-5, 4-10 images per group). Statistical analysis was performed using two-way ANOVA.

5.2.4 Determining the pro-inflammatory cytokine response to *F. tularensis* LVS infection following neutrophil depletion

Although there was no difference in lung pathology following neutrophil depletion, it was important to determine if the pro-inflammatory cytokine response changed as it is known to play a role in controlling *F. tularensis* LVS infection, as well as in driving pathogenesis under certain conditions (Cowley, 2009, D'Elia et al., 2013a).

Total cytokine concentrations were measured in lung homogenate of WT and CD200R$^{-/-}$ mice treated with IgG2a or α-Ly6G during *F. tularensis* LVS infection. The most interesting observation was a significant increase in IL-17A production in α-Ly6G-treated WT mice that was not observed in CD200R$^{-/-}$ mice or any IgG2a-treated mice (Figure 5.5A). However, there was no significant difference in the concentration of KC between any of the conditions (Figure 5.5B). As IL-17A and KC play a role in neutrophil recruitment (De Filippo et al., 2008, Flannigan et al., 2017), it was interesting that neutrophil depletion only affected IL-17A. There was no significant difference in TNFα, IFNγ, IL-6 and IL-1β production in WT and CD200R$^{-/-}$ mice treated with IgG2a or α-Ly6G (Figure 5.5C-F respectively). These data indicated that apart from significant differences in IL-17A production, there was very little difference in the production of pro-inflammatory cytokines in the lungs of WT and CD200R$^{-/-}$ mice treated with IgG2a or α-Ly6G during *F. tularensis* LVS infection.

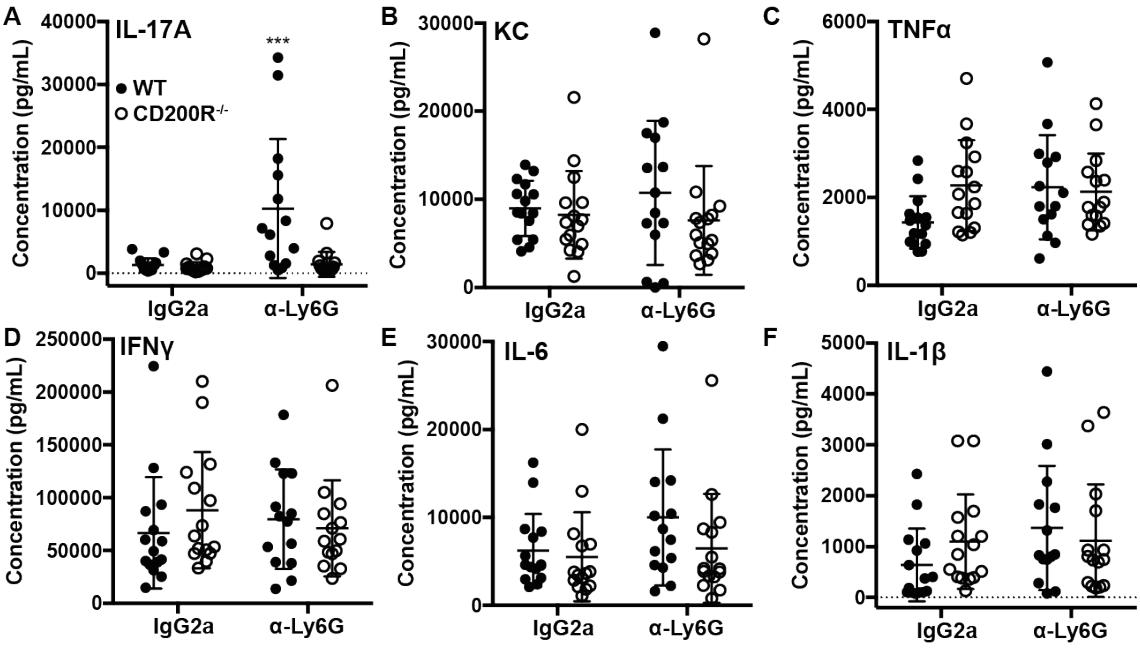

Figure 5.5 | No differences in cytokine response in neutrophil depleted WT and CD200R$^{-/-}$ mice following *F. tularensis* LVS infection. Lung homogenate was taken from IgG2a and α-Ly6G-treated WT and CD200R$^{-/-}$ at day 7 p.i. with *F. tularensis* LVS. IL-17A, KC, TNFα, IFNγ, IL-6 and IL-1β (A-F) were detected using the BioLegend LEGENDplex immunoassay. Data represents three independent experiments and is shown as mean ± SD (n=15, 5/group). Statistical analysis was performed using two-way ANOVA (***p<0.001).

To give a more detailed picture of cell-specific cytokine secretion in the lung, the production of IFNγ, TNFα and IL-6 in specific cell types in WT and CD200R$^{-/-}$ mice treated with IgG2a or α-Ly6G during *F. tularensis* LVS infection was determined. Thus, single cell suspension of *F. tularensis* LVS-infected lung was stimulated for 4 hours at 37°C with a cocktail of PMA and ionomycin to induce cytokine production, as well as brefeldin A and monensin to prevent protein transport out of the cell. Cells were then stained for flow cytometry and gated as described in figure 3.12.

Upon determining cytokine production in total live CD45^{+} cells there was a significant reduction in IFNγ, TNFα and IL-6 producing cells in CD200R$^{-/-}$ mice compared to WT when treated with IgG2a (Figure 5.6A). Upon treatment with α-Ly6G, there was a significant reduction in IFNy and IL-6 production in CD200R$^{-/-}$ mice compared to WT. However, there was no significant difference in TNFα-producing cells in neutrophil-depleted CD200R$^{-/-}$ mice compared to WT due to an increase in TNFα production in CD200R$^{-/-}$ CD45^{+} cells (Figure 5.6A).

Additionally, IFNy-producing, but not TNFα and IL-6-producing neutrophils were significantly reduced in IgG2a-treated CD200R$^{-/-}$ mice compared to WT. Neutrophil depletion meant that neutrophils became a minimal source of cytokine production (Figure 5.6B). Similarly, there was a significant reduction in IFNy-producing, but not TNFα and IL-6-producing, interstitial macrophages and Ly6C^{hi} monocyte/ macrophages in IgG2a-treated CD200R$^{-/-}$ mice compared to WT (Figure 5.6C and D respectively). Interestingly, IFNy and TNFα production in interstitial macrophages, but not Ly6C^{hi} monocyte/macrophages, was also significantly reduced in α-Ly6G-treated CD200R$^{-/-}$ mice compared to WT (Figure 5.6C and D respectively). There was no significant difference in IL-6-producing interstitial macrophages between WT and CD200R$^{-/-}$, but a significant reduction in α-Ly6G-treated CD200R$^{-/-}$ mice compared to IgG2a-treated was observed (Figure 5.6C). On the contrary, there was no significant difference between any conditions when looking at IL-6-producing Ly6C^{hi} monocyte/macrophages (Figure 5.6D).

These data show how the pro-inflammatory cytokine response within the lung in response to *F. tularensis* LVS infection varies in a cell-type specific manner. Overall the data shows a significant reduction in the percentage of cytokine-producing cells in IgG2a-treated CD200R$^{-/-}$ mice compared to WT. Nevertheless, as a whole the cytokine data does not provide evidence for the pro-inflammatory cytokine response playing an important role in the phenotype seen in CD200R$^{-/-}$ mice during neutrophil depletion.

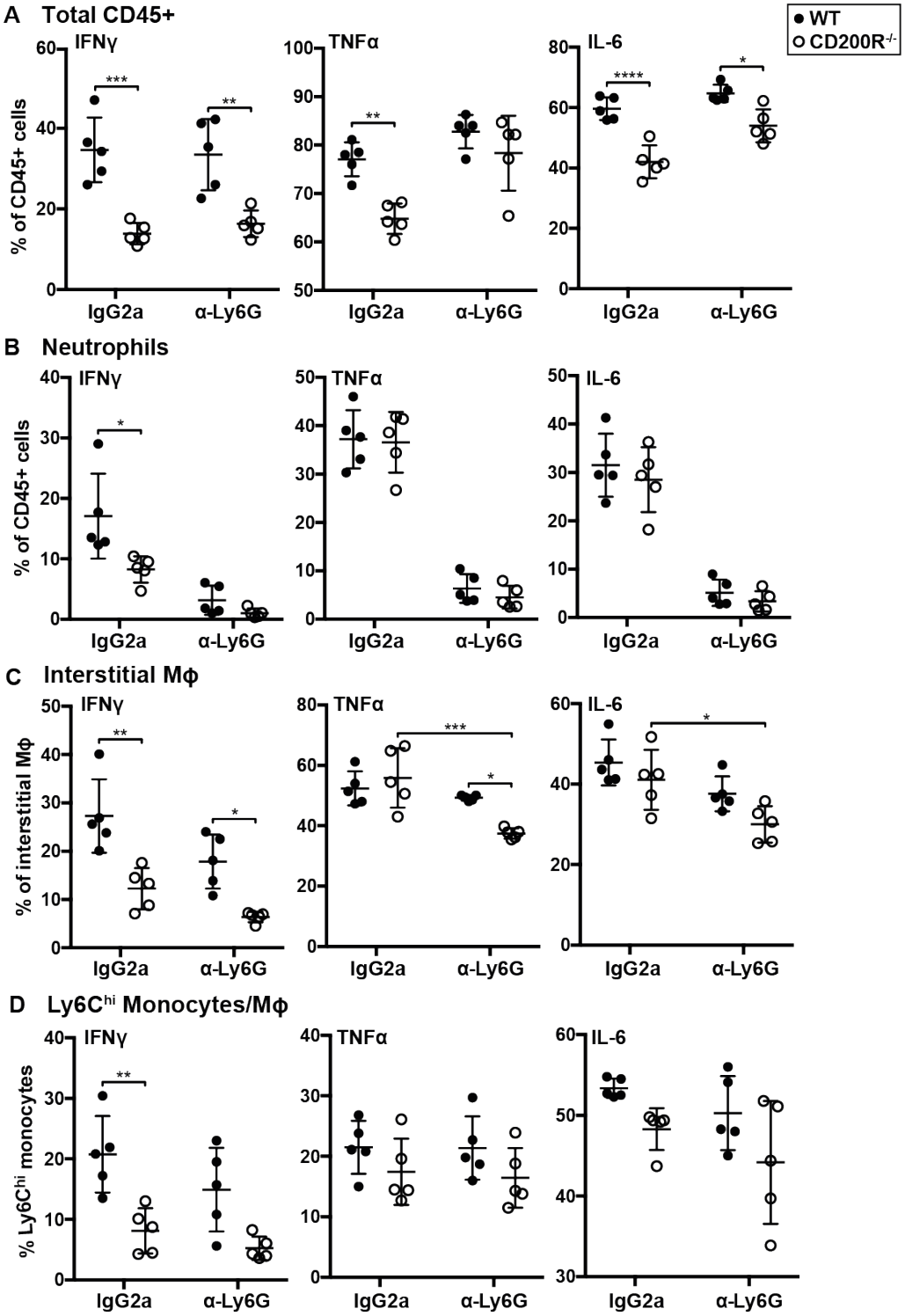

Figure 5.6 | Characterising cytokine-producing lung cells in neutrophil-depleted WT and CD200R$^{-/-}$ mice following *F. tularensis* LVS infection. Cells were isolated from lungs of IgG2a and α-Ly6G-treated WT and CD200R$^{-/-}$ at day 7 p.i. with *F. tularensis* LVS. Single cell suspension was then incubated for 4 hours at 37°C with a cocktail of PMA, ionomycin, brefeldin A and monensin. Samples were stained and analysed by flow cytometry as described in figure 3.13, with the addition of antibodies against IFNγ, TNFα and IL-6. Cytokine production in A) total live, CD45^{+} cells and B) neutrophils are presented as a percentage of live CD45^{+} cells. The percentage of cytokine-producing C) interstitial macrophages and D) Ly6Chi monocyte/macrophages was also determined. Data is representative of two independent experiments and is shown as mean ± SD (n=5). Statistical analysis was performed using two-way ANOVA (*p<0.05, **p<0.01, ***p<0.001).

5.2.5 Lack of CD200R on primary neutrophils increases susceptibility to *F. tularensis* LVS infection *in vitro*

After showing that neutrophils play a detrimental role during *F. tularensis* LVS infection in CD200R$^{-/-}$ mice, the next aspect to be explored was the intrinsic differences between WT neutrophils and those that lack CD200R expression. Thus, neutrophils were isolated from the bone marrow of WT and CD200R$^{-/-}$ mice by negative selection. There was an increase in the purity of the sample, with an enrichment of neutrophils in samples post-isolation (Figure 5.7A). There was no significant difference in the percentage neutrophils isolated from WT and CD200R$^{-/-}$ mice (Figure 5.7B). As shown previously in lung neutrophils (Figure 3.13B), bone marrow neutrophils isolated from WT mice showed stronger CD200R expression when compared to neutrophils from CD200R$^{-/-}$ mice (Figure 5.7C).

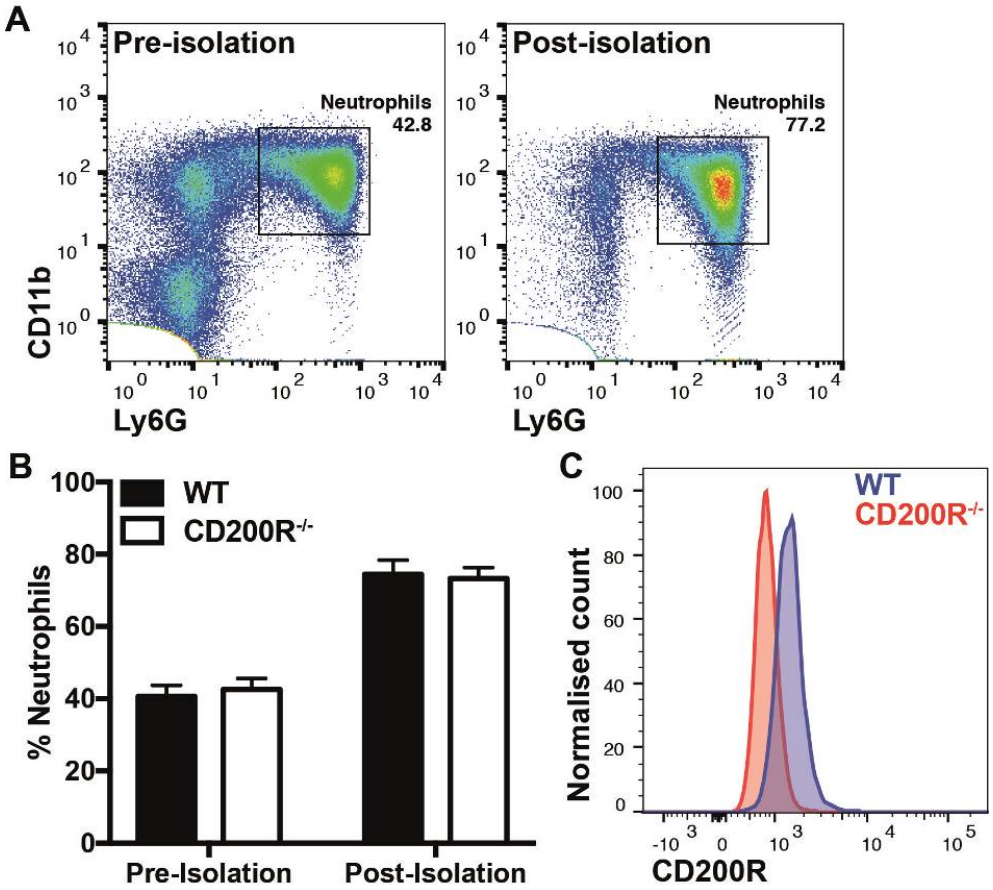

Figure 5.7 | Confirmation of neutrophil isolation from WT and CD200R$^{-/-}$ mouse bone marrow. Neutrophils were isolated by negative selection from WT and CD200R$^{-/-}$ mouse bone marrow (n=3). Cells were labelled and analysed by flow cytometry to determine the extent of isolation. A) Representative dot plots show CD11b^{+} Ly6G^{+} neutrophil population pre and post-isolation. B) Quantification of percentage neutrophils in WT and CD200R$^{-/-}$ bone marrow pre- and post-isolation. C) Histogram with representative CD200R expression on WT (blue) and CD200R$^{-/-}$ (red) neutrophils. Data represent one experiment and is shown as mean ± SD (B, n=3). Statistical analysis was performed using two-way ANOVA.

Having previously established that CD200R$^{-/-}$ neutrophils have significantly increased levels of *F. tularensis* LVS infection *in vivo* (Figure 4.2H and 5.3E), it was of interest to see whether this was also the case in isolated primary neutrophils *in vitro*. The neutrophil infection assay used was very similar to that used for macrophages described earlier (Figure 3.1 & Methods 2.2.3), although there was a change in the initial *F. tularensis* LVS incubation time from 2 to 4 hours to cater for the reduced phagocytic ability of neutrophils compared to macrophages (Silva and Correia-Neves, 2012).

WT and CD200R$^{-/-}$ neutrophils were incubated with an average *F. tularensis* LVS MOI 97, cells were processed at 4 and 24 hours p.i. and stained for flow cytometry to determine LVS infection within the neutrophils (Figure 5.8A). There was no significant difference in the percentage of infection at 4 hours p.i. between WT and CD200R$^{-/-}$ neutrophils. However, at 24 hours p.i. there was a significantly enhanced percentage of *F. tularensis* LVS-infected CD200R$^{-/-}$ neutrophils compared to WT (Figure 5.8B). No significant difference in burden between WT and CD200R$^{-/-}$ neutrophils was observed (Figure 5.8C). Together these data suggest that primary CD200R$^{-/-}$ neutrophils are more susceptible to LVS infection *in vitro*. Although there was no significant difference in overall *F. tularensis* LVS burden when determining CFU, this could be partly due to technical issues that will be discussed further.

5.2.6 No significant difference in *F. tularensis* LVS-induced cell death in WT and CD200R$^{-/-}$ neutrophils

Neutrophil cell death is an important part of the neutrophil response to infection and subsequently to the development of organ dysfunction (Iba et al., 2013). Given that *F. tularensis* has been shown to delay neutrophil apoptosis (Schwartz et al., 2012a), the apoptotic/necrotic rate of WT and CD200R$^{-/-}$ neutrophils during *F. tularensis* LVS infection was subsequently investigated. It was hypothesised that lack of CD200R expression may decrease neutrophil cell death, which may help explain the increased neutrophils seen in CD200R$^{-/-}$ mice during *F. tularensis* LVS infection.

To test this hypothesis, primary WT and CD200R$^{-/-}$ neutrophils were infected with an average MOI *F. tularensis* LVS of 97 for 4 and 24 hours, followed by 2-colour viability staining with annexin V to stain for apoptotic cells and the cell-impermeable dye TO-PRO-3 to stain dead cells. This staining method allowed the identification of cells at different stages of cell death (Jiang et al. 2016). By flow cytometry it was possible to distinguish between live (TO-PRO-3^{-} Annexin V^{-}), pre-apoptotic

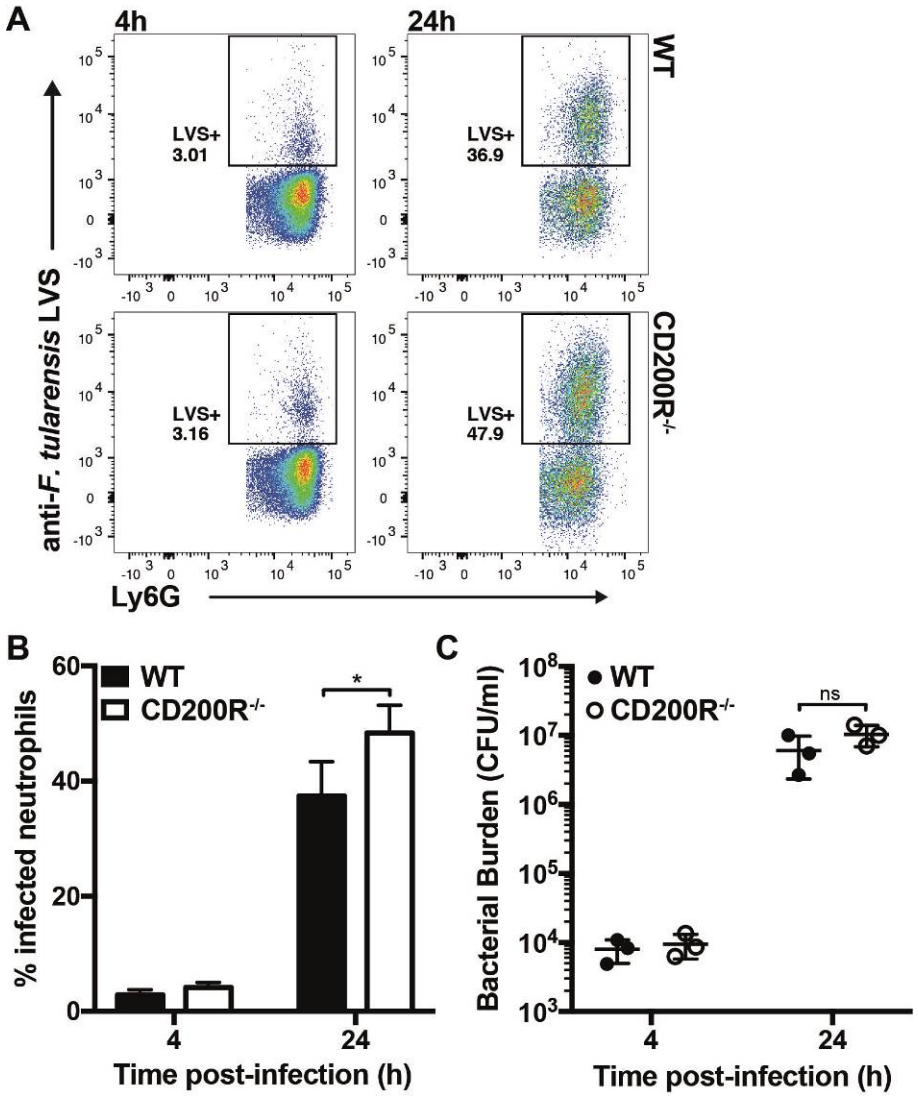

Figure 5.8 | Increased *F. tularensis* LVS burden in primary CD200R$^{-/-}$-derived neutrophils. Primary bone marrow neutrophils were isolated from WT or CD200R$^{-/-}$ mice and infected with a mean *F. tularensis* LVS MOI 97 for 4 and 24 hours. A) Representative dot plots of *F. tularensis* LVS-infected neutrophils at 4 and 24 hours p.i. Samples were pre-gated on live, single, CD11b^{+}Ly6G^{+} cells. D) Quantification of *F. tularensis* levels in neutrophils at 4 and 24 hours p.i. Data in B represents two independent experiments (n=6, 3/group), while data in C represent one experiment (n=3). Data is shown as mean ± SD. Statistical analysis was performed using two-way ANOVA (*p<0.05, ns = p>0.05).

(TO-PRO-3^{-} Annexin V^{+}), apoptotic (TO-PRO-3^{low} Annexin V^{+}) and necrotic cells (TO-PRO-3^{hi} Annexin V^{+}) in WT and CD200R$^{-/-}$ neutrophils at 4 and 24 hours p.i. (Jiang et al., 2016)(Figure 5.9A and B respectively).

There was no significant difference in percentage of live cells between uninfected and infected WT and CD200R$^{-/-}$ neutrophils at 4 hours p.i (Figure 5.9A and C). Similarly, there was no significant difference in percentage of pre-apoptotic or apoptotic cells between uninfected and infected WT and CD200R$^{-/-}$ neutrophils at 4 and 24 hours p.i. (Figure 5.9B, D and E). Nevertheless, it was interesting to note

that there was a shift from pre-apoptotic cells at 4 hours p.i to apoptotic cells at 24 hours p.i. (Figure 5.9A, B, D and E). Finally, no necrotic neutrophils were observed at 4h p.i.; however, there was a significant increase in necrotic *F. tularensis* LVS-infected WT neutrophils at 24 hours p.i compared to uninfected (Figure 5.9B and F).

These data highlight an interesting aspect of *F. tularensis* LVS infection, with a high infectious dose only causing a small but significant increase in cell death when compared to uninfected neutrophils. This further supports the ability of *F. tularensis* LVS to prolong neutrophil lifespan in order to potentially increase immune evasion with the neutrophil. Nevertheless, these data show that there is no significant difference in cell death progression between WT and CD200R$^{-/-}$ neutrophils when infected with *F. tularensis* LVS, suggesting that other factors are contributing to an elevated LVS burden in CD200R$^{-/-}$ neutrophils.

5.2.7 Primary WT and CD200R$^{-/-}$ neutrophils show no difference in degranulation responses after *F. tularensis* LVS infection

Neutrophils are extremely efficient professional phagocytes, able to engulf and kill pathogens by various mechanisms (Segal et al., 1980, van Kessel et al., 2014). One method is via phagosomal fusion with neutrophil granules that release anti-microbial proteins to kill engulfed pathogens. To further investigate the functional differences between WT and CD200R$^{-/-}$ neutrophils contributing to exacerbated *F. tularensis* burden, the expression of degranulation markers was used to broadly distinguish between granule subsets. LAMP-1 is expressed on late endosomes involved in the fusion of secretory vesicles to the plasma membrane, CD63 is expressed on primary granules and CD11b enhances degranulation of secondary and tertiary granules (Lacy, 2006, Ramadass and Catz, 2016).

Expression of LAMP-1, CD63 and CD11b (Lacy, 2006, Naegelen et al., 2015) (Figure 5.10A, B & C respectively) was determined in primary WT and CD200R$^{-/-}$ neutrophils at 4 and 24 hours p.i.. There was no significant difference in mean fluorescence intensity (MFI) of degranulation markers in WT and CD200R$^{-/-}$ neutrophils at 4 hours p.i. There was an increase in MFI of LAMP-1, CD63 and CD11b at 24 hours p.i. (Figure 5.10A, B & C respectively), however there was no significant difference between WT and CD200R$^{-/-}$ neutrophils. This suggests that there were no differences in WT and CD200R$^{-/-}$ neutrophil degranulation in response to *F. tularensis* LVS infection *in vitro*.

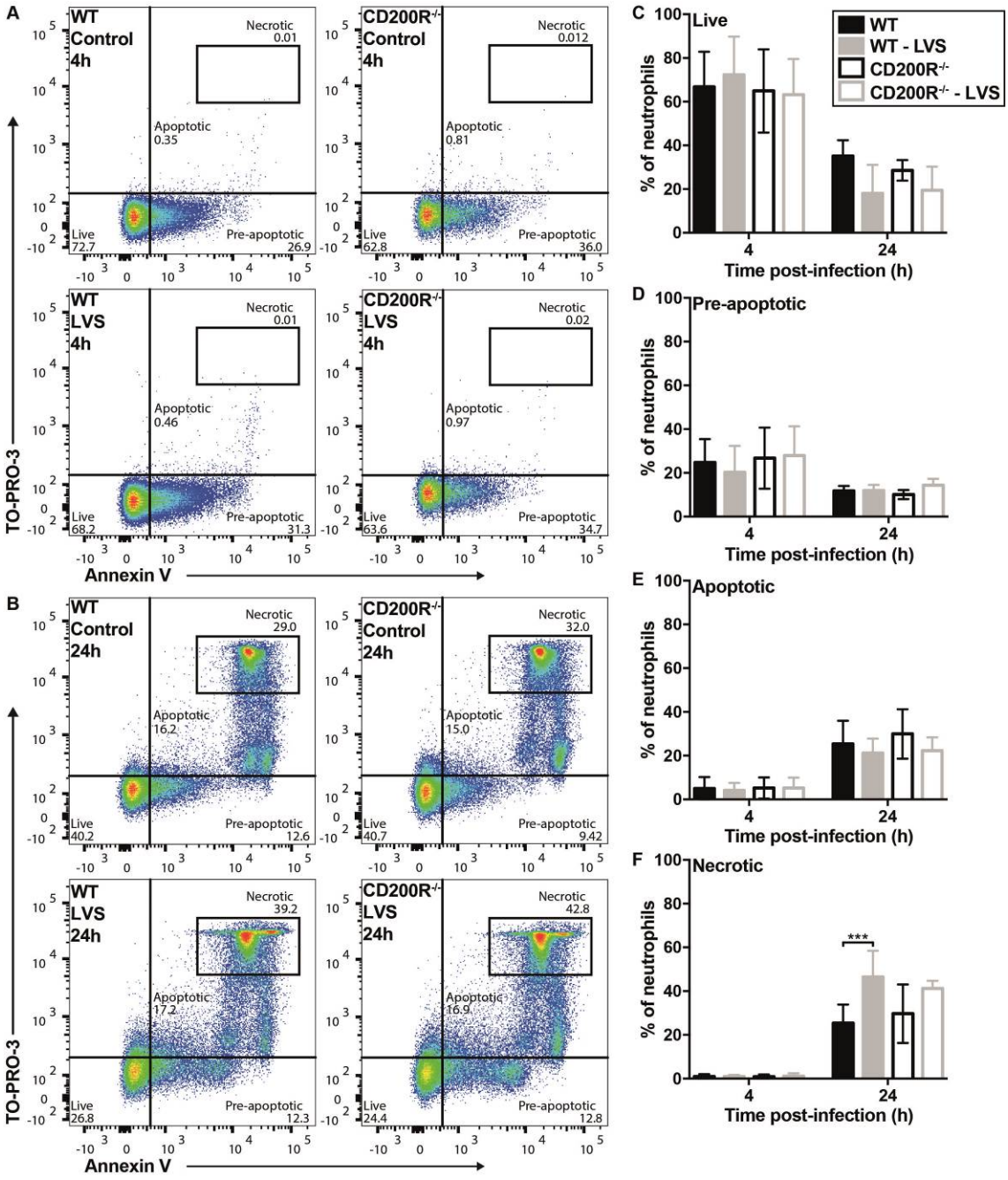

Figure 5.9 | Monitoring the progression of cell death in WT and CD200R$^{-/-}$ neutrophils in response to F. tularensis LVS infection. Primary bone marrow neutrophils were isolated from WT or CD200R$^{-/-}$ mice and infected with a mean LVS MOI 97 for 4 and 24 hours. Cells were stained with annexin V for 20 minutes, followed by another 10 minutes with the addition of a TO-PRO-3 stain. By flow cytometry we were able to distinguish at A) 4 and B) 24 hours p.i. between live (TO-PRO-3^{-} Annexin V^{-}), pre-apoptotic (TO-PRO-3^{-} Annexin V^{+}), apoptotic (TO-PRO-3^{low} Annexin V^{+}) and necrotic cells (TO-PRO-3^{hi} Annexin V^{+}) in WT and CD200R$^{-/-}$ neutrophils. Quantification of percentage C) live, D) pre-apoptotic, E) apoptotic and F) necrotic neutrophils at 4 and 24 hours p.i. Data represents two independent experiments and is shown as mean ± SD (n=6, 3/group). Statistical analysis was performed using two-way ANOVA (**p<0.01, ***p<0.001).

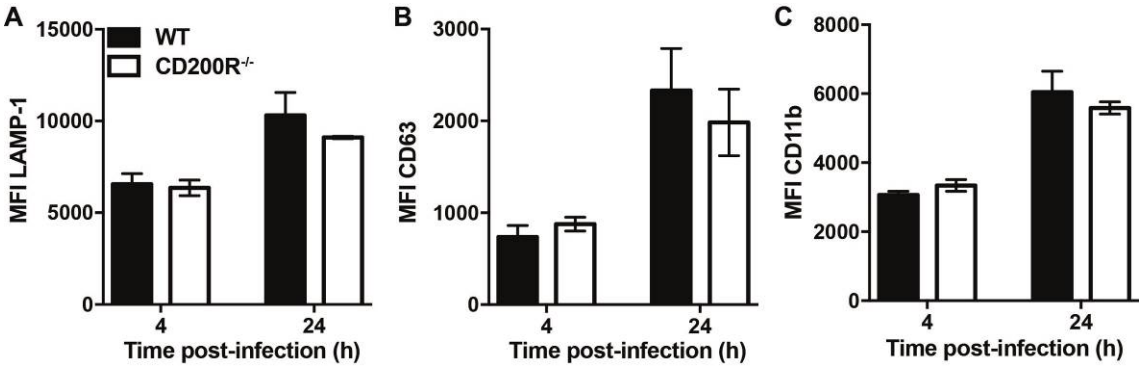

Figure 5.10 | No differences in WT and CD200R$^{-/-}$ neutrophil degranulation in response to *F. tularensis* LVS infection. Primary bone marrow neutrophils were isolated from WT or CD200R$^{-/-}$ mice and infected with a mean *F. tularensis* LVS MOI 97 for 4 and 24 hours. Cells were labelled with neutrophil degranulation markers and analysed by flow cytometry. Mean fluorescence intensity (MFI) was measured for A) LAMP-1, B) CD63 and C) CD11b on WT and CD200R$^{-/-}$ neutrophils at 4 and 24 hours p.i. Data is representative of two independent experiments and is shown as mean ± SD (n=3). Statistical analysis was performed using two-way ANOVA.

5.2.8 CD200R$^{-/-}$ neutrophils show aberrant ROS production in response to *F. tularensis* LVS and PMA

One of the key effector functions of neutrophils is their ability to produce powerful oxidative bursts through the production of reactive oxygen species (ROS). Oxygen is reduced through the NADPH oxidase complex which is assembled at the membrane following neutrophil activation, producing superoxide and hydrogen peroxide (Cross and Segal, 2004). As *F. tularensis* LVS has previously been shown to inhibit neutrophil reactive oxygen species (ROS) production through disruption of NADPH oxidase assembly (McCaffery & Allen 2006), the question was asked whether ROS production in response to stimuli was altered in CD200R$^{-/-}$ neutrophils.

The ability of primary neutrophils to produce ROS in response to PMA stimulation was initially investigated. Primary WT and CD200R$^{-/-}$ neutrophils were treated with PMA (100 ng/ml) and dihydrorhodamine 123 (DHR123) (25 ng/ml) for 1 hour. DHR123 is able to diffuse into the cell where it is oxidized by ROS to cationic rhodamine 123, which in turn emits green fluorescence that can be measured by flow cytometry (Figure 5.11A). In order to allow for correct normalisation of results across experiments, data was presented as an oxidative index (MFI unstimulated / MFI stimulated) (O'Gorman and Corrochano, 1995). The data showed that CD200R$^{-/-}$ neutrophils had a significantly lower oxidative index, suggesting that these cells produce significantly less ROS in response to PMA than WT neutrophils (Figure 5.11B).

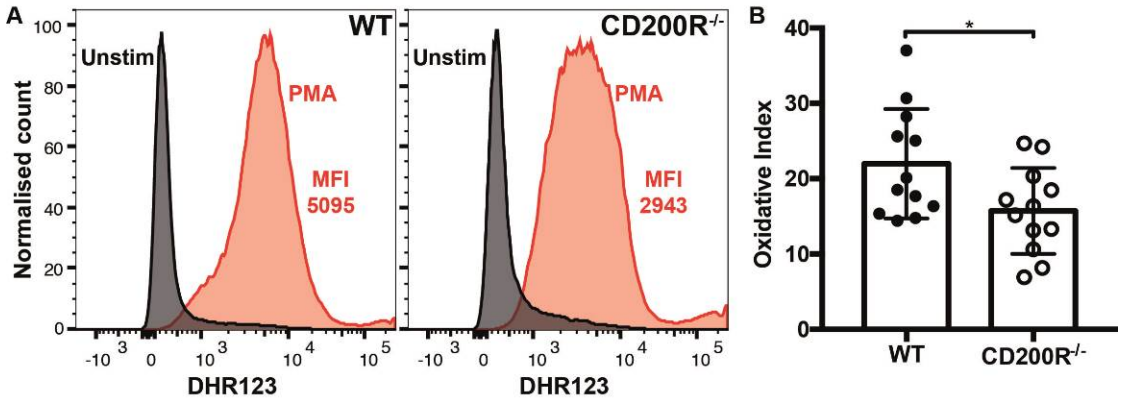

Figure 5.11 | CD200R$^{-/-}$ bone marrow neutrophils exhibit reduced ROS production in response to PMA. Primary bone marrow neutrophils were isolated from WT or CD200R$^{-/-}$ mice. Cells were incubated for 15 minutes with Dihydrorhodamine 123 (DHR123) (25 ng/ml), followed by 1 hour stimulation with PMA (100 ng/ml). DHR123 is oxidized by ROS to cationic rhodamine 123, which in turn emits green fluorescence that can be measured in the FITC channel by flow cytometry. A) Representative histograms of FITC DHR123 expression in unstimulated (black) or PMA treated (red) neutrophils. B) Oxidative index was quantified using the following equation: MFI Stimulated/MFI Unstimulated. Data represents four independent experiments and is shown as mean ± SD (n=12, 3/group). Statistical analysis was performed using unpaired t-test (*p<0.05).

As PMA has been shown to be a strong augmenter of neutrophil ROS production (Tyagi et al., 1988), it was important to investigate ROS production in the more specific context of *F. tularensis* LVS infection. WT and CD200R$^{-/-}$ neutrophils were infected with an average *F. tularensis* LVS MOI 113 and treated with DHR123, before measuring ROS production at 24 hours p.i. Unlike with PMA treatment, upon measuring DHR123 MFI it was noted that there were two distinct peaks of DHR positive and negative populations (Figure 5.12A). Therefore it was not possible to use oxidative index as described previously as a measure of ROS production. Instead DHR ratio (MFI DHR^{-} / MFI DHR^{+}) was used to determine ROS production. With this method it was observed that that the DHR ratio in CD200R$^{-/-}$ neutrophils was significantly lower compared to WT at 24 hours p.i. with *F. tularensis* LVS (Figure 5.12B). Interestingly, there was no significant difference in the percentage of DHR^{+} cells between WT and CD200R$^{-/-}$ neutrophils (Figure 5.12C); suggesting that the same amount of neutrophils are able to produce ROS, but subsequently produce less.

Taken together, these findings suggest that neutrophils lacking CD200R exhibit dysfunctional ROS production in response to a stimulus such as PMA and *F. tularensis* LVS infection. Thus, reduced ROS production is likely contributing to the CD200R$^{-/-}$ neutrophils reduced ability to deal with *F. tularensis* LVS infection.

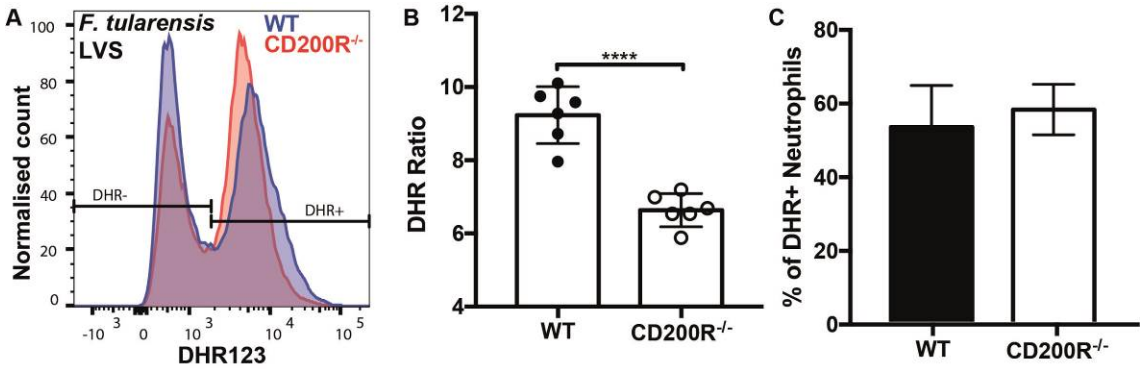

Figure 5.12 | CD200R$^{-/-}$ bone marrow neutrophils exhibit reduced ROS production in response to *F. tularensis* LVS. Primary bone marrow neutrophils were isolated from WT or CD200R$^{-/-}$ mice and infected with a mean *F. tularensis* LVS MOI 113 for 24 hours and incubated with Dihydrorhodamine 123 (DHR123) (25 ng/ml) throughout the infection. A) Representative histograms of FITC DHR123 expression in infected WT (blue) and CD200R$^{-/-}$ (red) neutrophils. B) Quantitative analysis of the DHR123 ratio (MFI DHR+/MFI DHR-) for LVS-infected WT and CD200R$^{-/-}$ neutrophils. C) The percentage of DHR+ WT and CD200R$^{-/-}$ neutrophils at 24 hours p.i. with *F. tularensis* LVS. Data represents two independent experiments and is shown as mean ± SD (n=6, 3/group). Statistical analysis was performed using unpaired t-test (****p<0.0001).

5.2.9 No difference in NET formation in WT and CD200R$^{-/-}$ neutrophils following 1 hour PMA stimulation

Having concluded that CD200R$^{-/-}$ neutrophils show dysfunctional ROS production in response to PMA and *F. tularensis* LVS infection, other neutrophil functions that are associated with ROS were investigated. Neutrophil extracellular traps (NETs) have been described as an important mechanism by which neutrophils are able to capture and kill bacteria (Brinkmann et al. 2004); with further studies showing that NET formation (NETosis) is a ROS-dependent process (Fuchs et al. 2007). Thus, it was hypothesised that reduced ROS production in CD200R$^{-/-}$ neutrophils could also lead to a reduction in NETosis.

WT and CD200R$^{-/-}$ neutrophils were incubated with PMA for 1 hour, before staining with the plasma membrane-impermeable DNA-binding dye SYTOX-Orange to detect the extracellular chromatin structures characteristic of NETs. The anti-microbial protein myeloperoxidase (MPO) was also used as a NET marker and would co-localise with SYTOX-Orange (Masuda et al. 2017). Thus MPO and SYTOX-Orange positive neutrophils were producing NETs (Figure 5.13A); however, there was no significant difference in the percentage of NETosis in WT and CD200R$^{-/-}$ neutrophils treated with PMA for 1 hour (Figure 5.13B).

These data suggest that despite showing decreased ROS production in CD200R$^{-/-}$ neutrophils compared to WT, this does not influence other neutrophil effector

functions of degranulation and NETosis. Thus, results in this chapter demonstrate that neutrophils are contributing to the enhanced *F. tularensis* burdens in lungs of CD200R$^{-/-}$ mice. This exacerbation is caused by an increased influx of neutrophils in CD200R$^{-/-}$ mice, which demonstrate a reduced ability deal with *F. tularensis* infection due to dysfunctional ROS production.

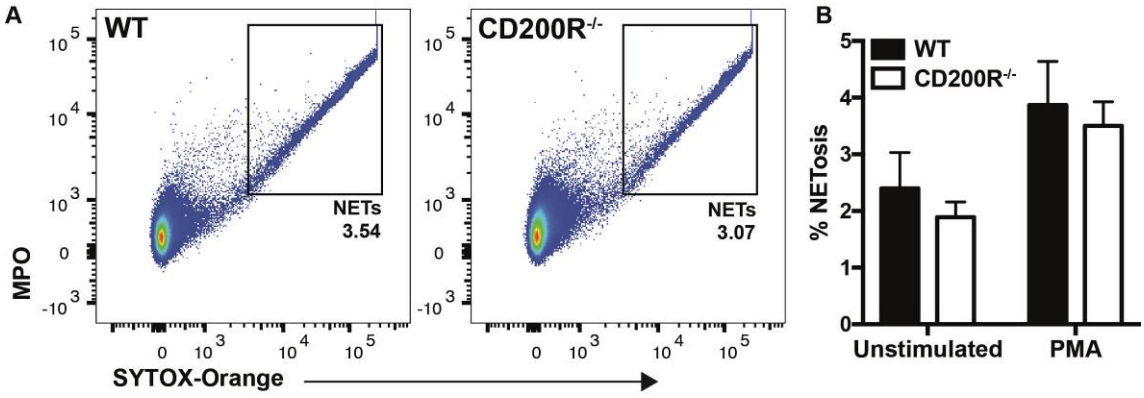

Figure 5.13 | No differences in WT and CD200R$^{-/-}$ neutrophil NET formation in response to one hour PMA stimulation. Primary bone marrow neutrophils were isolated from WT or CD200R$^{-/-}$ mice and stimulated for 1 hour with PMA (100 ng/ml). Cells were labelled with the plasma membrane-impermeant DNA-binding dye SYTOX-Orange and myeloperoxidase (MPO) to detect NET formation (NETosis) by flow cytometry. A) Representative dot plots of PMA-stimulated WT and CD200R$^{-/-}$ neutrophils, NETs are determined as MPO^{+} SYTOX^{+}. B) Quantification of NETosis as percentage of MPO^{+} SYTOX^{+} WT and CD200R$^{-/-}$ neutrophils following 1 hour PMA stimulation. Data represents one experiment and is shown as mean ± SD (n=3). Statistical analysis was performed using two-way ANOVA.

5.3 Discussion

5.3.1 Neutrophil depletion in CD200R$^{-/-}$ mice during *F. tularensis* LVS infection

5.3.1.1 Neutrophil depletion abrogates the increased *F. tularensis* LVS lung burden in CD200R$^{-/-}$ mice

Chapter 4 suggested that neutrophils were the key contributors to an increased *F. tularensis* LVS burden in the lungs of CD200R$^{-/-}$ mice compared to WT. Thus, in Chapter 5 it was hypothesised that depletion of neutrophils in CD200R$^{-/-}$ mice would reduce the *F. tularensis* LVS burden seen in the lung. To this end, it was shown that α-Ly6G-mediated neutrophil depletion abrogated the significantly increased *F. tularensis* LVS burden in the lung seen in control IgG2a-treated CD200R$^{-/-}$ mice compared to WT (Figure 5.2C).

Interestingly, neutrophil depletion in WT mice had no significant effect on bacterial burden in the lung. Furthermore, although α-Ly6G-treated mice exhibited increased weight loss compared to IgG2a-treated mice, this was not significant so cannot be considered as a sign of increased susceptibility to infection. These data are similar to findings of others who have showed that neutrophil depletion does not increase susceptibility to pulmonary *F. tularensis* LVS infection at day 4 p.i. (Conlan et al., 2002). In contrast, a more recent study has shown that depleting neutrophils at day 3 p.i. with pulmonary *F. tularensis* LVS leads to high susceptibility to infection, with neutrophil-depleted mice succumbing to infection at day 8 p.i. compared to 50% survival in untreated mice (Steiner et al., 2017).

Although published data regarding the effect of neutrophil depletion on pulmonary *F. tularensis* LVS infection appears contradictory, interpreting the results as a whole must be done with caution due to the differences in methodology. Conlan et al. determined susceptibility to infection through measuring bacterial burdens at day 4 p.i. (Conlan et al., 2002), which is much earlier than Steiner et al. who allowed the infection to run until as late as day 21 (Steiner et al., 2017). It is known that neutrophils are the prominent infected cell type the lung at day 3 p.i. with *F. tularensis* LVS (Hall et al., 2008); therefore depleting neutrophils at day 3 p.i. as Steiner et al. did, would kill a large population of infected cells and potentially lead to the simultaneous release of a large number of bacterium. The precise mechanism of antibody-mediated neutrophil depletion has not been well defined, however it has been suggested that phagocytosis of neutrophils by macrophages plays a central

role (Bucher et al., 2015, Bruhn et al., 2016). Thus, findings taken from depleting neutrophils during *F. tularensis* LVS infection may not fully represent the importance of neutrophils, but more so the response of macrophages to rapidly increased infection rates. It would be interesting to monitor the shift in infected cell populations when neutrophils are depleted at various times during *F. tularensis* LVS infection.

Nevertheless, in the context of neutrophil depletion in CD200R$^{-/-}$ mice, the data in this chapter highlight the detrimental role that CD200R$^{-/-}$ neutrophils play in the lung during pulmonary *F. tularensis* LVS infection. There was significantly increased neutrophilia in IgG2a-treated CD200R$^{-/-}$ mice compared to WT, as well as elevated percentage of *F. tularensis* LVS infected neutrophils (Figure 5.3).

Data was presented showing neutrophil infection as percentage of CD45^{+} cells rather than percentage of infected parent cells (as for other cell populations) to fully represent the extent of infection in neutrophil-depleted mice. Regardless, the lack of differences in rates of infection in other cell types following neutrophil depletion suggests that neutrophils are the key contributors to the infection phenotype seen in CD200R$^{-/-}$ mice. Furthermore, the small population of neutrophils that remained following depletion showed similar percentage of infection to the non-depleted neutrophil populations (data not shown), suggesting that neutrophil infection kinetics remain consistent regardless of quantity. Thus, this further suggests a dysfunction in CD200R$^{-/-}$ neutrophil effector functions driving the increased infection rate compared to WT.

An important consideration to make is the limitations of using cell proportions as a percentage of CD45^{+} cells, rather than total cell numbers. Following neutrophil depletion, the proportion of cell populations will change dramatically due to the loss of neutrophils. Thus, the direct comparison of cell populations between IgG2a and α-Ly6G-treated must be taken with caution when only using cell proportions. Using total cell numbers would have provided a better representation on how cell populations changed during infection following neutrophil depletion

5.3.1.2 Decreased bacterial dissemination following neutrophil depletion

As well as the fascinating findings in the lungs following neutrophil depletion in CD200R$^{-/-}$ mice, it must also be noted that there was a significantly reduced bacterial burden in the spleen of neutrophil-depleted WT mice (Figure 5.2E). Interestingly, although Conlan et al. showed no difference in *F. tularensis* LVS

burden in the lungs of neutrophil-depleted mice, they did see a significant decrease in the bacterial burden in the liver and spleen following neutrophil depletion (Conlan et al., 2002). These data suggest that neutrophil depletion may also aid in controlling the dissemination of *F. tularensis* LVS to peripheral organs.

This is interesting, as neutrophils have been shown to be important in stopping the dissemination of other respiratory bacterial infections. Lymph node neutrophils have been shown to intercept invading *Staphylococcus aureus* from the lung in order to prevent dissemination to the blood and peripheral organs (Bogoslowski et al., 2018). Similarly, neutrophil depletion led to increased susceptibility to *Acinetobacter baumannii* infection, characterised by elevated bacterial burdens in the lung and spleen (van Faassen et al., 2007). Interestingly, although not a respiratory infection model, another group have shown that neutrophils can aid in the dissemination of *Streptococcus pyogenes* through the formation of platelet-neutrophil complexes. Induced thrombocytopenia, a large reduction in platelet numbers, prior to infection led to a reduction in the formation of platelet-neutrophil complexes and subsequently significantly reduced bacterial dissemination (Kahn et al., 2013).

Thrombocytopenia has been documented to occur in only a small number of patients suffering from *F. tularensis* infection (Weber et al., 2012); however the role of platelets during *F. tularensis* infection has not been studied. In the context of pulmonary *F. tularensis* infection, platelets have been shown to promote the recruitment of neutrophils to the lung during septic infections (Zarbock et al., 2006, Asaduzzaman et al., 2009). Therefore, it would be interesting to look at the platelet populations and their activity during pulmonary *F. tularensis* LVS infection following neutrophil depletion. Perhaps the reduced occurrence of thrombocytopenia in *F. tularensis* infection is increasing the formation of platelet-neutrophil complexes, aiding bacterial dissemination to peripheral organs.

5.3.1.3 No gross changes in histopathology and pro-inflammatory cytokine response following neutrophil depletion

Neutrophils have been shown to drive pathology during pulmonary *F. tularensis,* potentially through the expression of MMP-9 (Malik et al., 2007). However, upon depletion of neutrophils there was no significant difference in the severity of lung pathology in WT and CD200R$^{-/-}$ mice following *F. tularensis* LVS infection (Figure 5.4). Furthermore, there was no difference in the majority of lung cytokines measured following neutrophil depletion in WT and CD200R$^{-/-}$ mice (Figure 5.5). However, one striking difference was the significant increase in IL-17A production in

WT, but not CD200R$^{-/-}$ mice, following neutrophil depletion during *F. tularensis* LVS infection. IL-17A is a strong mediator of neutrophil recruitment in response to respiratory infection (Miyamoto et al., 2003). Therefore, these data could suggest in WT mice, but not CD200R$^{-/-}$, the lack of neutrophils is driving pathways to compensate. However, this elevated expression of IL-17A does not correspond to any increased immune response or clearance of *F. tularensis* infection in WT mice. Similarly, others have found that IL-17 only contributes to neutrophil recruitment and not viral clearance during adenovirus type 1 respiratory infection (McCarthy et al., 2014). Thus, the relevance of increased IL-17A expression following neutrophil depletion in the context of CD200R and *F. tularensis* LVS infection remains unclear. Nevertheless, the data in this chapter does highlight that pro-inflammatory cytokines may not be contributing significantly to changes in bacterial burden seen between WT and CD200R$^{-/-}$ mice.

5.3.2 Mechanisms of CD200R$^{-/-}$ neutrophil effector functions

5.3.2.1 *F. tularensis* LVS infection in primary CD200R$^{-/-}$ neutrophils

To investigate the potential dysfunction in neutrophils that was causing this increased *F. tularensis* LVS infection rate in CD200R$^{-/-}$ mice compared to neutrophils in WT mice, neutrophils were isolated from the bone marrow in order to study them in an *in vitro* setting. Data in this chapter showed that although there was no difference in the initial uptake of *F. tularensis* LVS between WT and CD200R$^{-/-}$ neutrophils *in vitro*, there was a significant increase in the percentage of infected CD200R$^{-/-}$ neutrophils compared to WT at 24 hours p.i. (Figure 5.8). These data mirrored *in vivo* findings by showing a reduced ability of CD200R$^{-/-}$ neutrophils to deal with *F. tularensis* LVS infection. They also suggested that CD200R was not playing a role in the initial uptake of the bacteria in neutrophils, but was important during the phase of cytosolic replication and bacterial clearance. However, as discussed in previous chapters, it cannot be excluded that CD200R is interfering with the lag phase od *F. tularensis* growth in vitro that ultimately influences net bacterial growth.

A similar trend was also observed when enumerating bacterial burden in neutrophils. However, these changes were not significant, potentially due to technical issues in the lysing of cells. Initially, neutrophils were lysed with normal distilled water in order to release intracellular bacteria, but this was yielding much lower bacterial counts than anticipated. This was later resolved by lysing neutrophils with distilled water at pH11 (Decleva et al., 2006), which provided a more accurate

measurement of internalised bacterial burdens. If this methodology was used from the start, significance as seen in flow cytometry analysis of infection may have been reached.

It could also be argued that bone marrow-derived neutrophils are not a representative model of lung neutrophils. Indeed, it has been shown that the transcriptional profile of neutrophils is significantly changed during the transition from the bone marrow to sites of infection (Lakschevitz et al., 2015). These findings would suggest that bone marrow neutrophils might respond differently to lung neutrophils when challenged *in vitro* by *F. tularensis* LVS. Nevertheless, isolation of neutrophils from the lung would require digestion that could increase the activation of the neutrophils and alter natural responses to infection. Furthermore, the differences in neutrophil transcriptional profiles during infection and steady-state conditions must also be considered. It would be interesting to investigate differences in the responses to *F. tularensis* LVS between bone marrow-derived neutrophils isolated from healthy or *F. tularensis* LVS-infected mice. It could be explored whether neutrophils isolated from *F. tularensis* LVS-infected mice are more primed to deal with the infection, as well as determining whether this affected the dysfunctional response of CD200R$^{-/-}$ neutrophils.

5.3.2.2 Dysfunctional effector functions in CD200R$^{-/-}$ neutrophils

Findings from Chapter 4 and the start of Chapter 5 have strongly pointed towards a dysfunction in the ability of neutrophils lacking expression of CD200R to deal with *F. tularensis* LVS infection. Thus, in the latter parts of Chapter 5 the differences in neutrophil effector functions from WT and CD200R$^{-/-}$ mice were explored to determine the mechanisms behind the enhanced bacterial burden in CD200R$^{-/-}$ neutrophils.

As discussed previously, there was no difference in the phagocytic ability of WT and CD200R$^{-/-}$ neutrophils against *F. tularensis* LVS. Thus, differences between WT and CD200R$^{-/-}$ neutrophils were likely to be involved in the control of net growth of *F. tularensis* LVS. As *F. tularensis* LVS has been shown to prolong the life of human neutrophils in order to increase survival and cytosolic replication (Kinkead and Allen, 2016, Kinkead et al., 2017), it was investigated whether lack of CD200R affected neutrophil viability during infection. Using a novel flow cytometric protocol to monitor the progression of cell death (Jiang et al., 2016), it was determined that there was no difference in apoptosis or necrosis progression in WT and CD200R$^{-/-}$ neutrophils.

As survival of CD200R$^{-/-}$ neutrophils was not affecting *F. tularensis* LVS burdens (Figure 5.9), the main effector functions used by neutrophils to kill invading pathogens were investigated. The data demonstrated that CD200R$^{-/-}$ neutrophils exhibit significantly reduced ROS production in response to PMA stimulation and *F. tularensis* LVS infection compared to WT (Figure 5.11 & 5.12). This was determined by the oxidative index of a sample, by calculating the ratio between the DHR123 MFI of stimulated versus unstimulated neutrophils. This method has been used clinically to diagnose patients with CGD that are characterised by the reduced ability of their neutrophils to produce ROS, leading to recurrent infections (O'Gorman and Corrochano, 1995).

Further investigations are required to elucidate the direct effect of CD200R on ROS, as it may not be influencing production but could be altering ROS clearance and scavenging. This could potentially be a more appropriate role for CD200R in line with maintaining cellular homeostasis, rather than driving production (Minas and Liversidge, 2006). This role for regulation of oxidative stress by CD200R is supported by findings that reduced expression of CD200 was accompanied by decreased oxidative stress in the brains of mice infected with Venezuelan equine encephalitis virus following melatonin treatment (Montiel et al., 2015).

With regards to measuring ROS production during *F. tularensis* LVS infection, issues were encountered when determining the oxidative index as described previously. As uninfected and *F. tularensis* LVS-infected neutrophils were incubated with DHR123 for 24 hours, the uninfected neutrophils exhibited a single peak with a right shift in DHR MFI that suggested increased activation and increased ROS production (personal observation – data not shown). In contrast, *F. tularensis* LVS infection produced two distinct positive and negative neutrophil populations that had produced ROS. This finding was opposed to PMA stimulation where all neutrophils had produced ROS, and likely results from the ability of *F. tularensis* LVS to inhibit ROS production in neutrophils through disruption of NADPH oxidase assembly (McCaffrey et al., 2010). Thus, when calculating the 'oxidative index' for *F. tularensis* LVS infected neutrophils the DHR MFI of DHR+ and DHR- neutrophil populations was used, hence why it was subsequently renamed as the DHR ratio. Regardless, the data showed that CD200R$^{-/-}$ neutrophils produced significantly less ROS in response to 24 hours of *F. tularensis* LVS infection when compared to WT neutrophils.

Additionally, there was no significant difference between the percentage of ROS-producing WT and CD200R$^{-/-}$ neutrophils. This was also an interesting finding, as it suggested that although the same proportion of CD200R$^{-/-}$ neutrophils are able to produce ROS compared to WT, they produce significantly less. Unfortunately, due to the protocol not allowing for fixation of neutrophils, the ability to simultaneously determine neutrophil bacterial burden by flow cytometry was not possible. This would have allowed better understanding of the distribution of *F. tularensis* LVS within neutrophils and their ability to produce ROS. As CD200R$^{-/-}$ neutrophils display a significantly enhanced bacterial burden *in vitro* compared to WT, it is most likely not as simple as infected neutrophils produce ROS.

ROS production is one of the main microbicidal effector functions of neutrophils, with the other two important ones being degranulation and NETs. Given the heavy interactions between the three processes (Kolaczkowska and Kubes, 2013), it was interesting that there were no differences in expression of granule markers and NET formation between WT and CD200R$^{-/-}$ neutrophils. However, although the rate of degranulation does not seem to be affected (Figure 5.10), it could be that there is a difference in granule content between WT and CD200R$^{-/-}$ neutrophils. Granule subsets are classified by which granule proteins they contain (Kjeldsen et al., 1994). Primary granules contain MPO and neutrophil elastase (NE) that directly and indirectly crucial for neutrophil microbial activity (Eiserich et al., 1998, Klebanoff et al., 2013). Furthermore, tertiary granules contain matrix metalloproteinase 9 (MMP-9) to aid in the degradation of extracellular matrix and increase neutrophil transmigration (Hager et al., 2010, Kolaczkowska and Kubes, 2013). Therefore, determining the levels of granule components may elucidate other factors influencing effector function in CD200R$^{-/-}$ neutrophils.

NETosis has been shown to be heavily dependent on ROS production to trigger the translocation of NE to the nucleus and subsequently disrupt chromatin packaging (Papayannopoulos et al., 2010). Therefore it was surprising to see that reduced ROS production in CD200R$^{-/-}$ neutrophils did not lead to reduced NET formation when compared to WT neutrophils (Figure 5.13). Although this may suggest that NET formation was not altered in CD200R$^{-/-}$ neutrophils, NETs have been shown to take up to 3 hours to form (Fuchs et al. 2007), so increasing the PMA incubation time from 1 hour may yield different results. Additionally, recent studies have highlighted that certain respiratory pathogens may employ NET evasion strategies, through inhibition of NETosis, NET degradation and NET resistance, in order to confer increased immune protection form the host (Storisteanu et al., 2017).

Therefore, it would be interesting to investigate the formation of NETs in response to *F. tularensis* LVS to see whether such evasion strategies are used.

5.4 Conclusion

This final chapter demonstrated that that neutrophils were directly contributing to an increased *F. tularensis* LVS lung burden in CD200R$^{-/-}$ mice compared to WT. This was achieved through antibody-mediated neutrophil depletion abrogating the increased bacterial burden seen in the lungs of CD200R$^{-/-}$ mice. The mechanistic dysfunction of CD200R$^{-/-}$ neutrophil effector functions were explored, with such cells producing significantly less ROS in response to *F. tularensis* LVS infection compared to WT neutrophils. A reduced ability to produce ROS, and subsequently reduced microbicidal activity, would leave CD200R$^{-/-}$ neutrophil more susceptible to *F. tularensis* LVS infection. This dysfunctional effector function in CD200R$^{-/-}$ neutrophils, coupled with an excessive neutrophilia in CD200R$^{-/-}$ mice, provides a large replicative niche in the lungs of CD200R$^{-/-}$ mice to aid *F. tularensis* LVS replication and survival.

Chapter 6

General Discussion

6.1 General Discussion

Pulmonary homeostasis is essential in maintaining a balance between inflammatory response to harmful pathogens and tolerance to innocuous airborne antigens. Negative immune regulatory receptors play a critical role in controlling cellular responses in the airway by interacting with a variety of ligands and soluble factors, which make up the unique microenvironment in the airway lumen. This thesis aimed to investigate the role of negative immune regulators during *F. tularensis* infection, a highly virulent respiratory bacterium characterised by a dampened response during early stages of pulmonary infection. Preliminary studies highlighted CD200R, a potent negative regulator of alveolar macrophage activity, as potentially important during *F. tularensis* infection. Thus, it was hypothesised that *F. tularensis* was able to manipulate CD200R to elicit immune evasion and lack of this receptor would improve *F. tularensis* infectious outcome.

Interestingly, data in Chapter 3 and 4 determined that CD200R did not influence early infectious outcome to *F. tularensis*, but in fact offered protection during the later stages of infection both *in vitro* and *in vivo*. CD200R$^{-/-}$ mice exhibited exacerbated pulmonary bacterial burdens compared to their WT counterparts, with alveolar macrophage activity initially predicted to be the most affected immune cell type in CD200R$^{-/-}$ mice due to high CD200R expression on WT alveolar macrophages. However, observations in Chapter 4 showed excessive neutrophilia and increased rates of neutrophil infection in CD200R$^{-/-}$ mice compared to WT, suggesting that neutrophils were driving the exacerbated pulmonary infection.

Chapter 5 explored the mechanistic action of CD200R$^{-/-}$ neutrophils to better understand their reduced ability to deal with *F. tularensis* infection. It was hypothesised that lack of CD200R was causing a dysfunction in neutrophil effector functions crucial for pathogen killing and clearance, and that depletion of these dysfunctional neutrophils in CD200R$^{-/-}$ mice would abrogate the exacerbated pulmonary infection. This hypothesis was confirmed by showing that antibody-mediated neutrophil depletion in CD200R$^{-/-}$ mice led to a decrease in pulmonary *F. tularensis* burden, with burden returning to levels observed in WT mice. Furthermore, CD200R$^{-/-}$ neutrophils displayed a reduced ability to produce ROS that could explain a reduced ability to clear *F. tularensis* infection.

This thesis has defined an important role for CD200R in protection against pulmonary *F. tularensis* infection through the regulation of neutrophil recruitment

and ROS production (Figure 6.1). Lack of CD200R induces excessive neutrophilia in response to *F. tularensis* infection, but a reduced ability to produce ROS results in the dysfunctional CD200R$^{-/-}$ neutrophils acting as a replicative niche rather than aiding bacterial clearance in the lung. This subsequently drives an exacerbated pulmonary *F. tularensis* burden. Here additional questions raised by the findings presented in this thesis will be discussed, as well as highlighting the broader therapeutic implications of this research.

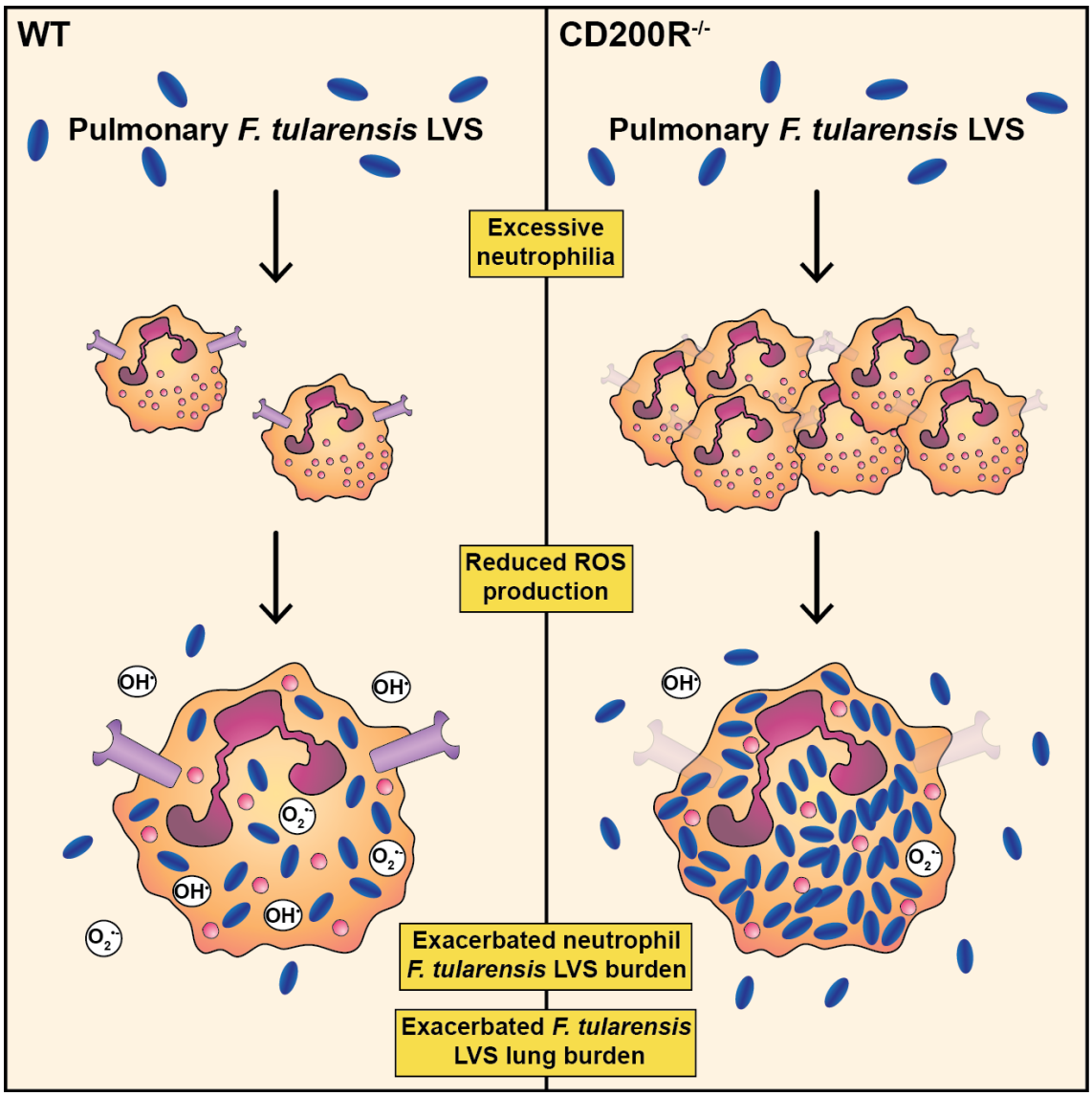

Figure 6.1 | Lack of CD200R in mice causes exacerbated pulmonary *F. tularensis* infection via neutrophil-dependent mechanisms. Pulmonary challenge with *F. tularensis* LVS causes an excessive neutrophilia in the lung of CD200R$^{-/-}$ mice compared to WT. Due to a reduced ability of CD200R$^{-/-}$ neutrophil to produce ROS, they provide a replicative niche for *F.* tularensis LVS, leading to an increased burden in CD200R$^{-/-}$ neutrophils. This ultimately leads to an increased overall *F. tularensis* LVS burden in the lung of CD200R$^{-/-}$ mice compared to WT.

6.2 CD200R as a negative immune regulator during *F. tularensis* infection

The initial hypothesis of this thesis was that due to the high expression of CD200R on alveolar macrophages, the initial niche of *F. tularensis* during early pulmonary infection, any differences in infectious outcome would be observed during the early stages of infection. However, this was not the case, raising the question of redundancy between regulatory pathways in airway alveolar macrophages. Although differential *F. tularensis* LVS burdens were observed during MH-S cell and BMDM infection assays upon manipulation of CD200R, this was not replicated in the more complex pulmonary environment found *in vivo*. This could be explained with the differences in the repertoire of receptor expression on MH-S cells and BMDM compared to alveolar macrophages (Brenner et al., 2016, Fernandes et al., 2016).

The wide variety of regulatory receptors and pathways present on alveolar macrophages which are important in maintaining airway immune homeostasis have been previously introduced (1.3.3 & Figure 1.3). It has been shown that STAT6, an important driver of Th-2 lung immunity and alternate activation of macrophages through IL-4 (Walford and Doherty, 2013), is significantly upregulated in draining lymph nodes of $CD200^{-/-}$ mice in response to inhaled antigen challenge (Taylor et al., 2005). Furthermore, CD200-Fc treatment induced alternative activation of rat macrophages but did not increase the expression of STAT6. Interestingly, STAT6 has been shown to be a downstream effector of CD200R and is important in prompting expression of FoxP3 and contributing to tissue repair in microglia (Yi et al., 2016). These data suggest differences in STAT6 regulation and signalling even within the CD200R pathway; therefore it is possible that there is significant cross-over between other regulatory pathways. For example, the mannose receptor and Mertk have been shown to be heavily involved in alternate activation of macrophages regulated by IL-4 (Linehan et al., 2003, Zizzo et al., 2012).

It is likely to be the case that in the absence of CD200R, other regulatory mechanisms are invoked to compensate during inflammation. Manipulation of these regulatory pathways specifically by *F. tularensis* in order to maintain a dampened immune environment during early infection could still be the case. It would be interesting to investigate the effect of inhibiting multiple pulmonary regulatory pathways during *F. tularensis* infection to better understand the role these regulatory pathways play. For example, it would be interesting to also inhibit SIRPα, which was also upregulated in MH-S cells during *F. tularensis* LVS infection,

although less so than for CD200R. Interestingly, SIRP-α can protect against cardiac hypertrophy through negative regulation of TLR4 signalling (Jiang et al., 2014). Similarly, a SIRP-α ligand, SP-A, has been shown to directly interact with TLR4 (Yamada et al., 2006, Janssen et al., 2008). Typically, TLR4 is key in mediating LPS-induced signal transduction during bacterial infections (Chow et al., 1999), yet the host response to *F. tularensis* is primarily TLR2, not TLR4-mediated (Katz et al., 2006). In addition to the unique structure of *F. tularensis* LPS eliciting a poor TLR4 response (Gunn and Ernst, 2007), perhaps the modulation of regulatory pathways such as SIRP-α could further dampen the TLR4-mediated inflammatory response during infection.

6.3 Secondary role for CD200R?

After dismissing the initial hypothesis of CD200R expression on alveolar macrophages playing a role during early *F. tularensis* LVS infection, it was subsequently shown that CD200R was protective against *F. tularensis* in the later stages of infection. Furthermore, this protection was conferred through neutrophil-dependent mechanisms. These findings, as well as the inconclusive data regarding the regulation of pro-inflammatory cytokine responses, may suggest a novel role for CD200R beyond its function as a negative immune regulator.

Significant research regarding the role of the CD200:CD200R signalling pathway has been conducted in $CD200^{-/-}$ mice (Hoek et al., 2000, Costello et al., 2011, Karnam et al., 2012). However, this may have led to the assumption that CD200 and CD200R solely function together. Interestingly, $CD200^{-/-}$ mice show increased susceptibility to influenza infection due to an exacerbated inflammatory response (Snelgrove et al., 2008); whereas $CD200R^{-/-}$ mice exhibit increased survival and viral clearance in response to influenza infection (Goulding et al., 2011). The authors explain these differences by highlighting the fact that CD200R has multiple variants that could bind to CD200. Therefore, knocking out only one inhibitory CD200R (CD200R1) variant would have different effects than knocking out the ligand CD200 that could bind multiple receptors. This could be the case; however it has been shown that CD200 does not bind to any other CD200R family variants other than CD200R1 (Wright et al., 2003, Hatherley et al., 2005). Therefore, another alternative could be that there is a novel function for CD200R yet to be fully elucidated.

Downstream targets of CD200R signalling Dok1 and Dok2 have been shown to play opposing roles when phosphorylated by CD200R. Dok1 can inhibit Dok2 activity,

which is the main effector of Ras signalling inhibition, in turn creating a negative feedback loop (Mihrshahi and Brown, 2010). Interestingly, Dok1/2 double knockout mice develop leukemia and have altered myelopoiesis independent of CD200R signalling (Rijkers et al., 2007). If the specific downstream signalling pathways of CD200R can function independently of receptor-ligand binding, perhaps there could be different functional roles for CD200R itself beyond its immunosuppressive activity.

6.4 Exacerbated recruitment of neutrophils

The critical role of neutrophils during pulmonary *F. tularensis* LVS infection in CD200R$^{-/-}$ mice became evident when excessive neutrophilia in the lung was observed from day 3-5 p.i. Neutrophil recruitment to the site of inflammation is an established process characteristic of many infections, including *F. tularensis* (Haraoka et al., 1999, van Faassen et al., 2007, Hall et al., 2008, Craig et al., 2009). A significantly increased level KC and IL-17A was observed in CD200R$^{-/-}$ mice at day 7 p.i., both of which can contribute to neutrophil recruitment (Frevert et al., 1995, Flannigan et al., 2017). These data could explain the later recruitment of neutrophils; however neutrophil infiltration began at day 3 p.i. before any cytokines were detected. Furthermore, the finding in Chapter 5 of increased IL-17A expression only in WT mice following neutrophil depletion raises questions about the role of cytokines during the excessive neutrophil recruitment in CD200R$^{-/-}$ mice.

Chemokines and chemokine receptors also play an important role in the migration of neutrophils out of the bone marrow and to the sites of infection (Kolaczkowska and Kubes, 2013). Colleagues have demonstrated by RNA sequencing that multiple cellular chemoattractants, including CXCL2, CCR2 and CCL9, are significantly upregulated in CD200R$^{-/-}$ neutrophils at steady state compared to WT (personal communication, M.E. Fife). CXCL2 can induce the recruitment of distinct pro-inflammatory neutrophils (Christoffersson et al., 2012). Similarly, the receptor for CXCL2, CXCR2, can positively regulate neutrophil trafficking from the bone marrow (Eash et al., 2010). If lack of CD200R induced the upregulation of CXCL2 in the bone marrow at steady state, neutrophils would be primed for increased migration to the site of infection, potentially explaining the excessive lung neutrophilia in CD200R$^{-/-}$ mice.

6.5 Neutrophil cross-talk with other cell types

The mechanisms behind the excessive neutrophilia in CD200R$^{-/-}$ mice in response to *F. tularensis* LVS are an interesting avenue to be investigated further. However, the role of CD200R on other cell types and their interaction with neutrophils during infection must also be considered. It has been shown that tissue resident macrophages produce the neutrophil chemoattractants KC and MIP-2 through TLR-mediated signalling (De Filippo et al., 2008). Although low levels of cytokine production was observed in early *F. tularensis* infection, further investigation of the early cytokine response of macrophages in WT and CD200R$^{-/-}$ mice may shed light on the interactions with neutrophils.

Furthermore, direct interactions between neutrophils and other cells types, such as epithelial cells, alveolar and interstitial macrophages and even T cells, in the infected lung environment of CD200R$^{-/-}$ mice may influence infectious outcome. Neutrophil death during infection is often cleared by macrophage phagocytosis (Silva, 2011). Perhaps the lack of CD200R on neutrophils or macrophages can disrupt the symbiotic relationship of these cell types during bacterial clearance. Furthermore, CD200 can be expressed on alveolar epithelial cells and has been primarily thought to bind to CD200R expressed on alveolar macrophages in the airway (Snelgrove et al., 2008, Jiang-Shieh et al., 2010). However, due to the loss of alveolar macrophages through the course of *F. tularensis* infection, it could be possible that neutrophil effector functions are further modulated around the airway through interactions with CD200-expressing cells.

Although this thesis has focused solely on the innate immune response, the subsequent adaptive immune response to *F. tularensis* in CD200R$^{-/-}$ mice should be investigated. As well as myeloid cells, CD200R is strongly expressed on CD4^{+} T cells (Rijkers et al., 2008). Interestingly, CD200$^{-/-}$ mice exhibit enhanced T cell-mediated pathology against influenza infection (Rygiel et al., 2009). With neutrophils being the main *F. tularensis*-infected cell type, the subsequent interactions with T cells in the context of CD200R signalling and their role in shaping the adaptive response would be interesting to investigate further.

6.6 CD200R and neutrophil effector functions

The final hypothesis of this thesis was that CD200R$^{-/-}$ neutrophils exhibited a dysfunction in crucial effector functions, limiting their ability to control *F. tularensis* burdens. It was subsequently shown that CD200R$^{-/-}$ neutrophils produced less ROS

than WT neutrophils, ultimately causing an exacerbated *F. tularensis* LVS burden in the lungs of CD200R$^{-/-}$ mice. Interestingly, it was also determined that the reduced ROS production in CD200R$^{-/-}$ neutrophils was not associated with reduced NET formation or expression of granule markers. As there is a close dependency between these three neutrophil effector functions, it was surprising to see that only ROS production was dysfunctional. Of course, a deeper investigation into NET formation at different time points, as well as measurement of granule content, may elucidate further abnormalities in CD200R$^{-/-}$ neutrophil effector functions.

It would be beneficial to monitor ROS production by neutrophils *in vivo* during *F. tularensis* LVS infection, allowing the confirmation of whether findings *in vitro* are supported in the complex environment of the infected lung. Similarly, differences in macrophage infection rates *in vitro* and *in vivo* were observed, which could well be explained through ROS production. Macrophages are also able to produce ROS during phagocytosis of invading pathogens (Aderem and Underhill, 1999); however, ROS also plays an important role in the differentiation of alternatively activated macrophages (Zhang et al., 2013). The anti-inflammatory phenotype of alternatively activated macrophages has also been shown to reduce neutrophil recruitment during wound repair (Campbell et al., 2014). If CD200R$^{-/-}$ macrophages also exhibited reduced ROS production, it could affect the rate of alternative activation *in vivo* and influence neutrophil recruitment during *F. tularensis* infection.

6.7 Targeting neutrophils and CD200R during respiratory *F. tularensis* infection

Chapter 4 investigated the therapeutic efficiency of CD200-Fc towards *F. tularensis* LVS, and discussed the potential treatments of CD200-Fc in combination with antibiotics. The mechanism of function behind multiple CD200-Fc treatments has been through targeting the pro-inflammatory response to infection (Snelgrove et al., 2008, Sarangi et al., 2009); however, data in this thesis have suggested that the inflammatory response may not be contributing to infectious outcome in the context of CD200R deficiency. Therefore, investigating the direct effect of CD200-Fc on the modulation of neutrophil effector functions could potentially be a more viable therapeutic option. If CD200R signalling via CD200 influences ROS production in neutrophils, increasing ROS production may prove beneficial in clearance of *F. tularensis* infection. Treatment of *M. tuberculosis* infection in BALB/c mice with Clofazimine, an immunosuppressant known to increase ROS production (Yano et al., 2011), efficiently reduced lung bacterial burden (Irwin et al., 2014).

It is known that *F. tularensis* is able to inhibit ROS production in neutrophils through disruption of NADPH oxidase assembly (McCaffrey et al., 2010). Thus, targeting ROS production through CD200R signalling may be an attractive therapeutic target not only against *F. tularensis* LVS, but other respiratory pathogens.

These findings could also have implications on other attempts to treat inflammation and inflammatory disorders with CD200-Fc modulation. As introduced previously (1.6.4), CD200-Fc has been shown to have beneficial effects in the treatment of influenza-induced inflammation (Snelgrove et al., 2008), severe arthritis (Simelyte et al., 2008) and allograft and xenograft survival (Gorczynski et al., 1999). Nevertheless, in the light of the findings in this thesis regarding the positive modulation of ROS production by CD200R, future studies modulating the CD200R must take into account potential pro-inflammatory actions of the signalling pathway.

Similarly, excessive neutrophil recruitment has been shown to contribute to the pathology in multiple diseases and infections such as *F. tularensis* (Malik et al., 2007), *M. tuberculosis* (Almeida et al., 2017), respiratory syncytial virus (RSV) (Stoppelenburg et al., 2013), chronic obstructive pulmonary disease (COPD) (Hoenderdos and Condliffe, 2013), asthma (McDougall and Helms, 2006) and cancer (Powell and Huttenlocher, 2016). Therefore, improving understanding of the role CD200R plays during neutrophil recruitment could have major therapeutic implications. Clinical trials involving CXCR2 antagonists to reduce the level of neutrophil recruitment have shown promising results in in COPD patients (Rennard et al., 2015), but not in treatment of chronic asthma (O'Byrne et al., 2016). These findings suggest there is still scope to explore different avenues of targeting neutrophil recruitment, of which CD200R may be an interesting alternative.

6.8 Future directions

This thesis has investigated the role of CD200R during pulmonary *F. tularensis* LVS infection; however it would be interesting to explore its role in response to challenge with the more virulent *F. tularensis* Schu S4. Some important differences between the response to pulmonary *F. tularensis* Schu S4 and LVS infection were introduced previously (1.2.7). In the context of the findings in this thesis, *F. tularensis* Schu S4 infection is associated with recruitment of large number of immature myeloid cells to the lung, which subsequently fail to mature and die. This necrotising inflammation ultimately leads to overt pulmonary pathology and host death. In contrast, *F. tularensis* LVS was associated with recruitment of mature neutrophils and monocytes associated with protection against lethal bacterial infection

(Periasamy et al., 2016). Similarly, a highly virulent *M. tuberculosis* strain induces enhanced neutrophil recruitment and necrosis compared to the less virulent laboratory strain (Almeida et al., 2017). These data suggest the robust host response and increased cell death against virulent strains are the cause of excessive pathology and death. It would be interesting to understand whether modulation of the CD200:CD200R pathway, in an increased pro-inflammatory environment, would help improve infectious outcome.

This thesis has demonstrated that CD200R plays a protective role during pulmonary *F. tularensis* LVS through neutrophil-dependent mechanisms, however the effect of using a global CD200R$^{-/-}$ mouse must also be taken into account. It has been shown that the CD200:CD200R pathway may play a role in the development of rat lung microvasculature and microglial development in the brain (Shrivastava et al., 2012, Tsai et al., 2015). Although the phenotypic changes of global CD200$^{-/-}$ and CD200R$^{-/-}$ mice are subtle, suggesting limited developmental implications (Hoek et al., 2000, Boudakov et al., 2007), the fundamental changes to the lung environment may only become apparent during inflammatory challenge. It would be beneficial to investigate the infectious outcome of pulmonary *F. tularensis* infection in inducible, cell-specific, CD200R deficiencies. This would not only remove the potential developmental bias of global knockouts, but also help elucidate the differences in CD200R-mediated cellular response between macrophages and neutrophils. Similarly, shielded chimeras of WT and CD200R$^{-/-}$ mice in which lung-protective ablation of bone marrow is achieved could provide insight into the differences influencing neutrophil influx during *F. tularensis* infection (Janssen et al., 2010). This may elucidate whether CD200R specifically affects neutrophil retention in the bone marrow or alternatively affects chemoattractant secretion by tissue resident macrophages.

6.9 Thesis conclusion

In concluding this thesis, the overarching aims initially outlined must be answered. Does CD200R play a role in the early immune suppression during *F. tularensis* infection? This thesis has demonstrated that CD200R does not play a prominent role during early pulmonary *F. tularensis* LVS infection, but offers significant protection during later stages of infection. CD200R$^{-/-}$ mice exhibited an exacerbated pulmonary *F. tularensis* LVS burden, characterised by excessive neutrophilia and an increase in *F. tularensis*-infected neutrophils. Which leads to the second aim: What are the mechanisms by which CD200R influences infectious outcome? The

data in this thesis has established that the pulmonary burden in CD200R$^{-/-}$ mice was dependent on neutrophils, with antibody-mediated neutrophil depletion abrogating the exacerbated burden. Furthermore, a potentially novel role for CD200R in the regulation of neutrophil effector functions has been highlighted. CD200R$^{-/-}$ neutrophils showed reduced ROS production compared to WT, ultimately contributing to an inability to deal with *F. tularensis* infection and an exacerbated pulmonary *F. tularensis* burden.

This thesis has highlighted areas of CD200R activity beyond its role as a negative immune regulator. These findings have opened the door for exciting opportunities to investigate the therapeutic potential of targeting neutrophils and CD200R signalling in the treatment of not only pneumonic *F. tularensis* infection, but also other pulmonary disorders.

7 References

ABPLANALP, A. L., MORRIS, I. R., PARIDA, B. K., TEALE, J. M. & BERTON, M. T. 2009. TLR-dependent control of Francisella tularensis infection and host inflammatory responses. *PLoS One,* 4**,** e7920.

ADEREM, A. & UNDERHILL, D. M. 1999. Mechanisms of phagocytosis in macrophages. *Annu Rev Immunol,* 17**,** 593-623.

AKKAYA, M., KWONG, L. S., AKKAYA, E., HATHERLEY, D. & BARCLAY, A. N. 2016. Rabbit CD200R binds host CD200 but not CD200-like proteins from poxviruses. *Virology,* 488**,** 1-8.

ALMEIDA, F. M., VENTURA, T. L., AMARAL, E. P., RIBEIRO, S. C., CALIXTO, S. D., MANHAES, M. R., REZENDE, A. L., SOUZAL, G. S., DE CARVALHO, I. S., SILVA, E. C., SILVA, J. A., CARVALHO, E. C., KRITSKI, A. L. & LASUNSKAIA, E. B. 2017. Hypervirulent Mycobacterium tuberculosis strain triggers necrotic lung pathology associated with enhanced recruitment of neutrophils in resistant C57BL/6 mice. *PLoS One,* 12**,** e0173715.

AMIN, K. 2012. The role of mast cells in allergic inflammation. *Respir Med,* 106**,** 9-14.

AMINI, A. A., SOLOVYOVA, A. S., SADEGHIAN, H., BLACKBOURN, D. J. & REZAEE, S. A. 2015. Structural properties of a viral orthologue of cellular CD200 protein: KSHV vOX2. *Virology,* 474**,** 94-104.

ANTHONY, L. D., BURKE, R. D. & NANO, F. E. 1991. Growth of Francisella spp. in rodent macrophages. *Infect Immun,* 59**,** 3291-6.

ANTHONY, L. S., GHADIRIAN, E., NESTEL, F. P. & KONGSHAVN, P. A. 1989. The requirement for gamma interferon in resistance of mice to experimental tularemia. *Microb Pathog,* 7**,** 421-8.

ASADUZZAMAN, M., LAVASANI, S., RAHMAN, M., ZHANG, S., BRAUN, O. O., JEPPSSON, B. & THORLACIUS, H. 2009. Platelets support pulmonary recruitment of neutrophils in abdominal sepsis. *Crit Care Med,* 37**,** 1389-96.

ATHMAN, J. J., SANDE, O. J., GROFT, S. G., REBA, S. M., NAGY, N., WEARSCH, P. A., RICHARDSON, E. T., ROJAS, R., BOOM, W. H., SHUKLA, S. & HARDING, C. V. 2017. Mycobacterium tuberculosis Membrane Vesicles Inhibit T Cell Activation. *J Immunol,* 198**,** 2028-2037.

BAGGIOLINI, M., DEWALD, B. & MOSER, B. 1994. Interleukin-8 and related chemotactic cytokines--CXC and CC chemokines. *Adv Immunol,* 55**,** 97-179.

BANDYOPADHYAY, S., LONG, M. E. & ALLEN, L. A. 2014. Differential expression of microRNAs in Francisella tularensis-infected human macrophages: miR-155-dependent downregulation of MyD88 inhibits the inflammatory response. *PLoS One,* 9**,** e109525.

BANG, B. R., CHUN, E., SHIM, E. J., LEE, H. S., LEE, S. Y., CHO, S. H., MIN, K. U., KIM, Y. Y. & PARK, H. W. 2011. Alveolar macrophages modulate allergic inflammation in a murine model of asthma. *Exp Mol Med,* 43**,** 275-80.

BAR-HAIM, E., GAT, O., MARKEL, G., COHEN, H., SHAFFERMAN, A. & VELAN, B. 2008. Interrelationship between Dendritic Cell Trafficking and Francisella tularensis Dissemination following Airway Infection. *PLoS Pathogens,* 4**,** e1000211.

BARCLAY, A. N. & WARD, H. A. 1982. Purification and chemical characterisation of membrane glycoproteins from rat thymocytes and brain, recognised by monoclonal antibody MRC OX 2. *Eur J Biochem,* 129**,** 447-58.
BAREL, M., MEIBOM, K. & CHARBIT, A. 2010. Nucleolin, a shuttle protein promoting infection of human monocytes by Francisella tularensis. *PLoS One,* 5**,** e14193.
BARKER, J. H., KAUFMAN, J. W., APICELLA, M. A. & WEISS, J. P. 2016. Evidence Suggesting That Francisella tularensis O-Antigen Capsule Contains a Lipid A-Like Molecule That Is Structurally Distinct from the More Abundant Free Lipid A. *PLoS One,* 11**,** e0157842.
BEN NASR, A., HAITHCOAT, J., MASTERSON, J. E., GUNN, J. S., EAVES-PYLES, T. & KLIMPEL, G. R. 2006. Critical role for serum opsonins and complement receptors CR3 (CD11b/CD18) and CR4 (CD11c/CD18) in phagocytosis of Francisella tularensis by human dendritic cells (DC): uptake of Francisella leads to activation of immature DC and intracellular survival of the bacteria. *J Leukoc Biol,* 80**,** 774-86.
BEN NASR, A. & KLIMPEL, G. R. 2008. Subversion of complement activation at the bacterial surface promotes serum resistance and opsonophagocytosis of Francisella tularensis. *J Leukoc Biol,* 84**,** 77-85.
BERDAL, B. P., MEHL, R., MEIDELL, N. K., LORENTZEN-STYR, A. M. & SCHEEL, O. 1996. Field investigations of tularemia in Norway. *FEMS Immunol Med Microbiol,* 13**,** 191-5.
BHATNAGAR, S., SHINAGAWA, K., CASTELLINO, F. J. & SCHOREY, J. S. 2007. Exosomes released from macrophages infected with intracellular pathogens stimulate a proinflammatory response in vitro and in vivo. *Blood,* 110**,** 3234-44.
BLOM, L. H., MARTEL, B. C., LARSEN, L. F., HANSEN, C. V., CHRISTENSEN, M. P., JUEL-BERG, N., LITMAN, T. & POULSEN, L. K. 2017. The immunoglobulin superfamily member CD200R identifies cells involved in type 2 immune responses. *Allergy*.
BOGDANOVICH, S., KIM, Y., MIZUTANI, T., YASUMA, R., TUDISCO, L., CICATIELLO, V., BASTOS-CARVALHO, A., KERUR, N., HIRANO, Y., BAFFI, J. Z., TARALLO, V., LI, S., YASUMA, T., ARPITHA, P., FOWLER, B. J., WRIGHT, C. B., APICELLA, I., GRECO, A., BRUNETTI, A., RUVO, M., SANDOMENICO, A., NOZAKI, M., IJIMA, R., KANEKO, H., OGURA, Y., TERASAKI, H., AMBATI, B. K., LEUSEN, J. H., LANGDON, W. Y., CLARK, M. R., ARMOUR, K. L., BRUHNS, P., VERBEEK, J. S., GELFAND, B. D., DE FALCO, S. & AMBATI, J. 2016. Human IgG1 antibodies suppress angiogenesis in a target-independent manner. *Signal Transduct Target Ther,* 1.
BOGOSLOWSKI, A., BUTCHER, E. C. & KUBES, P. 2018. Neutrophils recruited through high endothelial venules of the lymph nodes via PNAd intercept disseminating Staphylococcus aureus. *Proc Natl Acad Sci U S A,* 115**,** 2449-2454.
BOKHARI, S. M., KIM, K. J., PINSON, D. M., SLUSSER, J., YEH, H. W. & PARMELY, M. J. 2008. NK cells and gamma interferon coordinate the formation and function of hepatic granulomas in mice infected with the Francisella tularensis live vaccine strain. *Infect Immun,* 76**,** 1379-89.
BOSIO, C. M. 2011. The subversion of the immune system by francisella tularensis. *Front Microbiol,* 2**,** 9.

BOSIO, C. M., BIELEFELDT-OHMANN, H. & BELISLE, J. T. 2007. Active suppression of the pulmonary immune response by Francisella tularensis Schu4. *J Immunol,* 178**,** 4538-47.
BOSIO, C. M. & DOW, S. W. 2005. Francisella tularensis induces aberrant activation of pulmonary dendritic cells. *J Immunol,* 175**,** 6792-801.
BOUCHON, A., DIETRICH, J. & COLONNA, M. 2000. Cutting edge: inflammatory responses can be triggered by TREM-1, a novel receptor expressed on neutrophils and monocytes. *J Immunol,* 164**,** 4991-5.
BOUDAKOV, I., LIU, J., FAN, N., GULAY, P., WONG, K. & GORCZYNSKI, R. M. 2007. Mice lacking CD200R1 show absence of suppression of lipopolysaccharide-induced tumor necrosis factor-alpha and mixed leukocyte culture responses by CD200. *Transplantation,* 84**,** 251-7.
BOURNAZOS, S., WANG, T. T. & RAVETCH, J. V. 2016. The Role and Function of Fcγ Receptors on Myeloid Cells. *Microbiol Spectr,* 4.
BOYCE, J. M. 1975. Recent trends in the epidemiology of tularemia in the United States. *J Infect Dis,* 131**,** 197-9.
BRADBURNE, C. E., VERHOEVEN, A. B., MANYAM, G. C., CHAUDHRY, S. A., CHANG, E. L., THACH, D. C., BAILEY, C. L. & VAN HOEK, M. L. 2013. Temporal transcriptional response during infection of type II alveolar epithelial cells with Francisella tularensis live vaccine strain (LVS) supports a general host suppression and bacterial uptake by macropinocytosis. *J Biol Chem,* 288**,** 10780-91.
BRANZK, N., LUBOJEMSKA, A., HARDISON, S. E., WANG, Q., GUTIERREZ, M. G., BROWN, G. D. & PAPAYANNOPOULOS, V. 2014. Neutrophils sense microbe size and selectively release neutrophil extracellular traps in response to large pathogens. *Nat Immunol,* 15**,** 1017-25.
BRENNER, T. A., RICE, T. A., ANDERSON, E. D., PERCOPO, C. M. & ROSENBERG, H. F. 2016. Immortalized MH-S cells lack defining features of primary alveolar macrophages and do not support mouse pneumovirus replication. *Immunol Lett,* 172**,** 106-12.
BRINKMANN, V., REICHARD, U., GOOSMANN, C., FAULER, B., UHLEMANN, Y., WEISS, D. S., WEINRAUCH, Y. & ZYCHLINSKY, A. 2004. Neutrophil extracellular traps kill bacteria. *Science,* 303**,** 1532-5.
BROERE, F., APASOV, S. G., SITKOVSKY, M. V. & VAN EDEN, W. 2011. A2 T cell subsets and T cell-mediated immunity. *In:* NIJKAMP, F. P. & PARNHAM, M. J. (eds.) *Principles of Immunopharmacology: 3rd revised and extended edition.* Basel: Birkhäuser Basel.
BRUHN, K. W., DEKITANI, K., NIELSEN, T. B., PANTAPALANGKOOR, P. & SPELLBERG, B. 2016. Ly6G-mediated depletion of neutrophils is dependent on macrophages. *Results Immunol,* 6**,** 5-7.
BUCHER, K., SCHMITT, F., AUTENRIETH, S. E., DILLMANN, I., NURNBERG, B., SCHENKE-LAYLAND, K. & BEER-HAMMER, S. 2015. Fluorescent Ly6G antibodies determine macrophage phagocytosis of neutrophils and alter the retrieval of neutrophils in mice. *J Leukoc Biol,* 98**,** 365-72.
BURKE, D. S. 1977. Immunization against tularemia: analysis of the effectiveness of live Francisella tularensis vaccine in prevention of laboratory-acquired tularemia. *J Infect Dis,* 135**,** 55-60.
BURNS, A. R., SMITH, C. W. & WALKER, D. C. 2003. Unique structural features that influence neutrophil emigration into the lung. *Physiol Rev,* 83**,** 309-36.

BUTCHAR, J. P., CREMER, T. J., CLAY, C. D., GAVRILIN, M. A., WEWERS, M. D., MARSH, C. B., SCHLESINGER, L. S. & TRIDANDAPANI, S. 2008. Microarray analysis of human monocytes infected with Francisella tularensis identifies new targets of host response subversion. *PLoS One,* 3**,** e2924.

BUTCHAR, J. P., RAJARAM, M. V., GANESAN, L. P., PARSA, K. V., CLAY, C. D., SCHLESINGER, L. S. & TRIDANDAPANI, S. 2007. Francisella tularensis induces IL-23 production in human monocytes. *J Immunol,* 178**,** 4445-54.

CAMERON, C. M., BARRETT, J. W., MANN, M., LUCAS, A. & MCFADDEN, G. 2005. Myxoma virus M128L is expressed as a cell surface CD47-like virulence factor that contributes to the downregulation of macrophage activation in vivo. *Virology,* 337**,** 55-67.

CAMPBELL, L., EMMERSON, E., WILLIAMS, H., SAVILLE, C. R., KRUST, A., CHAMBON, P., MACE, K. A. & HARDMAN, M. J. 2014. Estrogen receptor-alpha promotes alternative macrophage activation during cutaneous repair. *J Invest Dermatol,* 134**,** 2447-2457.

CASE, E. D., CHONG, A., WEHRLY, T. D., HANSEN, B., CHILD, R., HWANG, S., VIRGIN, H. W. & CELLI, J. 2014. The Francisella O-antigen mediates survival in the macrophage cytosol via autophagy avoidance. *Cell Microbiol,* 16**,** 862-77.

CASERTA, S., NAUSCH, N., SAWTELL, A., DRUMMOND, R., BARR, T., MACDONALD, A. S., MUTAPI, F. & ZAMOYSKA, R. 2012. Chronic infection drives expression of the inhibitory receptor CD200R, and its ligand CD200, by mouse and human CD4 T cells. *PLoS One,* 7**,** e35466.

CASPAR, Y. & MAURIN, M. 2017. Francisella tularensis Susceptibility to Antibiotics: A Comprehensive Review of the Data Obtained In vitro and in Animal Models. *Front Cell Infect Microbiol,* 7**,** 122.

CHASE, J. C. & BOSIO, C. M. 2010. The presence of CD14 overcomes evasion of innate immune responses by virulent Francisella tularensis in human dendritic cells in vitro and pulmonary cells in vivo. *Infect Immun,* 78**,** 154-67.

CHASE, J. C., CELLI, J. & BOSIO, C. M. 2009. Direct and indirect impairment of human dendritic cell function by virulent Francisella tularensis Schu S4. *Infect Immun,* 77**,** 180-95.

CHECROUN, C., WEHRLY, T. D., FISCHER, E. R., HAYES, S. F. & CELLI, J. 2006. Autophagy-mediated reentry of Francisella tularensis into the endocytic compartment after cytoplasmic replication. *Proc Natl Acad Sci U S A,* 103**,** 14578-83.

CHEN, S. C., MEHRAD, B., DENG, J. C., VASSILEVA, G., MANFRA, D. J., COOK, D. N., WIEKOWSKI, M. T., ZLOTNIK, A., STANDIFORD, T. J. & LIRA, S. A. 2001. Impaired pulmonary host defense in mice lacking expression of the CXC chemokine lungkine. *J Immunol,* 166**,** 3362-8.

CHEN, W., KUOLEE, R., AUSTIN, J. W., SHEN, H., CHE, Y. & CONLAN, J. W. 2005a. Low dose aerosol infection of mice with virulent type A Francisella tularensis induces severe thymus atrophy and CD4+CD8+ thymocyte depletion. *Microb Pathog,* 39**,** 189-96.

CHEN, W., KUOLEE, R., SHEN, H., BUSA, M. & CONLAN, J. W. 2004a. Toll-like receptor 4 (TLR4) does not confer a resistance advantage on mice against low-dose aerosol infection with virulent type A Francisella tularensis. *Microb Pathog,* 37**,** 185-91.

CHEN, W., KUOLEE, R., SHEN, H., BUSA, M. & CONLAN, J. W. 2005b. Toll-like receptor 4 (TLR4) plays a relatively minor role in murine defense against primary intradermal infection with Francisella tularensis LVS. *Immunol Lett,* 97**,** 151-4.

CHEN, W., KUOLEE, R., SHEN, H. & CONLAN, J. W. 2004b. Susceptibility of immunodeficient mice to aerosol and systemic infection with virulent strains of Francisella tularensis. *Microb Pathog,* 36**,** 311-8.

CHEN, W., SHEN, H., WEBB, A., KUOLEE, R. & CONLAN, J. W. 2003. Tularemia in BALB/c and C57BL/6 mice vaccinated with Francisella tularensis LVS and challenged intradermally, or by aerosol with virulent isolates of the pathogen: protection varies depending on pathogen virulence, route of exposure, and host genetic background. *Vaccine,* 21**,** 3690-700.

CHEN, Z., CHEN, D. X., KAI, Y., KHATRI, I., LAMPTEY, B. & GORCZYNSKI, R. M. 2008. Identification of an expressed truncated form of CD200, CD200tr, which is a physiologic antagonist of CD200-induced suppression. *Transplantation,* 86**,** 1116-24.

CHERWINSKI, H. M., MURPHY, C. A., JOYCE, B. L., BIGLER, M. E., SONG, Y. S., ZURAWSKI, S. M., MOSHREFI, M. M., GORMAN, D. M., MILLER, K. L., ZHANG, S., SEDGWICK, J. D. & PHILLIPS, J. H. 2005. The CD200 receptor is a novel and potent regulator of murine and human mast cell function. *J Immunol,* 174**,** 1348-56.

CHIAVOLINI, D., ALROY, J., KING, C. A., JORTH, P., WEIR, S., MADICO, G., MURPHY, J. R. & WETZLER, L. M. 2008. Identification of immunologic and pathologic parameters of death versus survival in respiratory tularemia. *Infect Immun,* 76**,** 486-96.

CHONG, A. & CELLI, J. 2010. The francisella intracellular life cycle: toward molecular mechanisms of intracellular survival and proliferation. *Front Microbiol,* 1**,** 138.

CHONG, A., WEHRLY, T. D., NAIR, V., FISCHER, E. R., BARKER, J. R., KLOSE, K. E. & CELLI, J. 2008. The early phagosomal stage of Francisella tularensis determines optimal phagosomal escape and Francisella pathogenicity island protein expression. *Infect Immun,* 76**,** 5488-99.

CHOW, J. C., YOUNG, D. W., GOLENBOCK, D. T., CHRIST, W. J. & GUSOVSKY, F. 1999. Toll-like receptor-4 mediates lipopolysaccharide-induced signal transduction. *J Biol Chem,* 274**,** 10689-92.

CHRISTOFFERSSON, G., VAGESJO, E., VANDOOREN, J., LIDEN, M., MASSENA, S., REINERT, R. B., BRISSOVA, M., POWERS, A. C., OPDENAKKER, G. & PHILLIPSON, M. 2012. VEGF-A recruits a proangiogenic MMP-9-delivering neutrophil subset that induces angiogenesis in transplanted hypoxic tissue. *Blood,* 120**,** 4653-62.

CHRISTOPHER, G. W., CIESLAK, T. J., PAVLIN, J. A. & EITZEN, E. M., JR. 1997. Biological warfare. A historical perspective. *Jama,* 278**,** 412-7.

CLARK, M. J., GAGNON, J., WILLIAMS, A. F. & BARCLAY, A. N. 1985. MRC OX-2 antigen: a lymphoid/neuronal membrane glycoprotein with a structure like a single immunoglobulin light chain. *Embo j,* 4**,** 113-8.

CLEMENS, D. L. & HORWITZ, M. A. 2007. Uptake and intracellular fate of Francisella tularensis in human macrophages. *Ann N Y Acad Sci,* 1105**,** 160-86.

CLEMENS, D. L., LEE, B. Y. & HORWITZ, M. A. 2004. Virulent and avirulent strains of Francisella tularensis prevent acidification and maturation of their

phagosomes and escape into the cytoplasm in human macrophages. *Infect Immun,* 72**,** 3204-17.
CLEMENS, D. L., LEE, B. Y. & HORWITZ, M. A. 2005. Francisella tularensis enters macrophages via a novel process involving pseudopod loops. *Infect Immun,* 73**,** 5892-902.
CLEMENS, D. L., LEE, B. Y. & HORWITZ, M. A. 2009. Francisella tularensis phagosomal escape does not require acidification of the phagosome. *Infect Immun,* 77**,** 1757-73.
CLINTON, S. R., BINA, J. E., HATCH, T. P., WHITT, M. A. & MILLER, M. A. 2010. Binding and activation of host plasminogen on the surface of Francisella tularensis. *BMC Microbiol,* 10**,** 76.
COLE, L. E., SANTIAGO, A., BARRY, E., KANG, T. J., SHIREY, K. A., ROBERTS, Z. J., ELKINS, K. L., CROSS, A. S. & VOGEL, S. N. 2008. Macrophage proinflammatory response to Francisella tularensis live vaccine strain requires coordination of multiple signaling pathways. *J Immunol,* 180**,** 6885-91.
COLE, L. E., SHIREY, K. A., BARRY, E., SANTIAGO, A., RALLABHANDI, P., ELKINS, K. L., PUCHE, A. C., MICHALEK, S. M. & VOGEL, S. N. 2007. Toll-like receptor 2-mediated signaling requirements for Francisella tularensis live vaccine strain infection of murine macrophages. *Infect Immun,* 75**,** 4127-37.
COLLAZO, C. M., SHER, A., MEIEROVICS, A. I. & ELKINS, K. L. 2006. Myeloid differentiation factor-88 (MyD88) is essential for control of primary in vivo Francisella tularensis LVS infection, but not for control of intra-macrophage bacterial replication. *Microbes Infect,* 8**,** 779-90.
COLONNA, M. 2003. TREMs in the immune system and beyond. *Nat Rev Immunol,* 3**,** 445-53.
CONLAN, J. W., KUOLEE, R., SHEN, H. & WEBB, A. 2002. Different host defences are required to protect mice from primary systemic vs pulmonary infection with the facultative intracellular bacterial pathogen, Francisella tularensis LVS. *Microb Pathog,* 32**,** 127-34.
CONLAN, W. J. & OYSTON, P. C. 2007. Vaccines against Francisella tularensis. *Ann N Y Acad Sci,* 1105**,** 325-50.
CORTEZ, M., HUYNH, C., FERNANDES, M. C., KENNEDY, K. A., ADEREM, A. & ANDREWS, N. W. 2011. Leishmania promotes its own virulence by inducing expression of the host immune inhibitory ligand CD200. *Cell Host Microbe,* 9**,** 463-71.
COSTELLO, D. A., LYONS, A., DENIEFFE, S., BROWNE, T. C., COX, F. F. & LYNCH, M. A. 2011. Long term potentiation is impaired in membrane glycoprotein CD200-deficient mice: a role for Toll-like receptor activation. *J Biol Chem,* 286**,** 34722-32.
COWLEY, S. C. 2009. Editorial: Proinflammatory cytokines in pneumonic tularemia: too much too late? *J Leukoc Biol,* 86**,** 469-70.
COWLEY, S. C. & ELKINS, K. L. 2011. Immunity to Francisella. *Front Microbiol,* 2**,** 26.
COWLEY, S. C., HAMILTON, E., FRELINGER, J. A., SU, J., FORMAN, J. & ELKINS, K. L. 2005. CD4(−)CD8(−) T cells control intracellular bacterial infections both in vitro and in vivo. *J Exp Med,* 202**,** 309-19.
COWLEY, S. C., MEIEROVICS, A. I., FRELINGER, J. A., IWAKURA, Y. & ELKINS, K. L. 2010. Lung CD4-CD8- double-negative T cells are

prominent producers of IL-17A and IFN-gamma during primary respiratory murine infection with Francisella tularensis live vaccine strain. *J Immunol,* 184**,** 5791-801.
COX, F. F., CARNEY, D., MILLER, A. M. & LYNCH, M. A. 2012. CD200 fusion protein decreases microglial activation in the hippocampus of aged rats. *Brain Behav Immun,* 26**,** 789-96.
CRAIG, A., MAI, J., CAI, S. & JEYASEELAN, S. 2009. Neutrophil recruitment to the lungs during bacterial pneumonia. *Infect Immun,* 77**,** 568-75.
CREMER, T. J., BUTCHAR, J. P. & TRIDANDAPANI, S. 2011. Francisella Subverts Innate Immune Signaling: Focus On PI3K/Akt. *Frontiers in Microbiology,* 2**,** 13.
CROSS, A. R. & SEGAL, A. W. 2004. The NADPH oxidase of professional phagocytes--prototype of the NOX electron transport chain systems. *Biochim Biophys Acta,* 1657**,** 1-22.
CURRY, A., KHATRI, I., KOS, O., ZHU, F. & GORCZYNSKI, R. 2017. Importance of CD200 expression by tumor or host cells to regulation of immunotherapy in a mouse breast cancer model. *PLoS One,* 12**,** e0171586.
D'ALESSANDRO, D., NAPOLI, C., NUSCA, A., BELLA, A. & FUNARI, E. 2015. Human tularemia in Italy. Is it a re-emerging disease? *Epidemiol Infect,* 143**,** 2161-9.
D'ELIA, R., JENNER, D. C., LAWS, T. R., STOKES, M. G., JACKSON, M. C., ESSEX-LOPRESTI, A. E. & ATKINS, H. S. 2011a. Inhibition of Francisella tularensis LVS infection of macrophages results in a reduced inflammatory response: evaluation of a therapeutic strategy for intracellular bacteria. *FEMS Immunol Med Microbiol,* 62**,** 348-61.
D'ELIA, R., JENNER, D. C., LAWS, T. R., STOKES, M. G. M., JACKSON, M. C., ESSEX-LOPRESTI, A. E. & ATKINS, H. S. 2011b. Inhibition of Francisella tularensis LVS infection of macrophages results in a reduced inflammatory response: evaluation of a therapeutic strategy for intracellular bacteria. *FEMS Immunology & Medical Microbiology,* 62**,** 348-361.
D'ELIA, R. V., HARRISON, K., OYSTON, P. C., LUKASZEWSKI, R. A. & CLARK, G. C. 2013a. Targeting the "cytokine storm" for therapeutic benefit. *Clin Vaccine Immunol,* 20**,** 319-27.
D'ELIA, R. V., LAWS, T. R., CARTER, A., LUKASZEWSKI, R. & CLARK, G. C. 2013b. Targeting the "Rising DAMP" during a Francisella tularensis Infection. *Antimicrob Agents Chemother,* 57**,** 4222-4228.
D'ELIA, R. V., LAWS, T. R., NUNEZ, A., TAYLOR, C. & CLARK, G. C. 2015. Delayed presence of alternatively activated macrophages during a Francisella tularensis infection. *Microb Pathog,* 78**,** 37-42.
DE FILIPPO, K., HENDERSON, R. B., LASCHINGER, M. & HOGG, N. 2008. Neutrophil chemokines KC and macrophage-inflammatory protein-2 are newly synthesized by tissue macrophages using distinct TLR signaling pathways. *J Immunol,* 180**,** 4308-15.
DE FREITAS BALANCO, J. M., MOREIRA, M. E., BONOMO, A., BOZZA, P. T., AMARANTE-MENDES, G., PIRMEZ, C. & BARCINSKI, M. A. 2001. Apoptotic mimicry by an obligate intracellular parasite downregulates macrophage microbicidal activity. *Curr Biol,* 11**,** 1870-3.
DE HEER, H. J., HAMMAD, H., SOULLIE, T., HIJDRA, D., VOS, N., WILLART, M. A., HOOGSTEDEN, H. C. & LAMBRECHT, B. N. 2004. Essential role

of lung plasmacytoid dendritic cells in preventing asthmatic reactions to harmless inhaled antigen. *J Exp Med,* 200**,** 89-98.
DE PASCALIS, R., TAYLOR, B. C. & ELKINS, K. L. 2008. Diverse myeloid and lymphoid cell subpopulations produce gamma interferon during early innate immune responses to Francisella tularensis live vaccine strain. *Infect Immun,* 76**,** 4311-21.
DECKERT, M., SEDGWICK, J. D., FISCHER, E. & SCHLUTER, D. 2006. Regulation of microglial cell responses in murine Toxoplasma encephalitis by CD200/CD200 receptor interaction. *Acta Neuropathol,* 111**,** 548-58.
DECLEVA, E., MENEGAZZI, R., BUSETTO, S., PATRIARCA, P. & DRI, P. 2006. Common methodology is inadequate for studies on the microbicidal activity of neutrophils. *J Leukoc Biol,* 79**,** 87-94.
DEKKERS, G., BENTLAGE, A. E. H., STEGMANN, T. C., HOWIE, H. L., LISSENBERG-THUNNISSEN, S., ZIMRING, J., RISPENS, T. & VIDARSSON, G. 2017. Affinity of human IgG subclasses to mouse Fc gamma receptors. *MAbs,* 9**,** 767-773.
DENNIS, D. T., INGLESBY, T. V., HENDERSON, D. A., BARTLETT, J. G., ASCHER, M. S., EITZEN, E., FINE, A. D., FRIEDLANDER, A. M., HAUER, J., LAYTON, M., LILLIBRIDGE, S. R., MCDADE, J. E., OSTERHOLM, M. T., O'TOOLE, T., PARKER, G., PERL, T. M., RUSSELL, P. K. & TONAT, K. 2001. Tularemia as a biological weapon: medical and public health management. *Jama,* 285**,** 2763-73.
DEVI, S., WANG, Y., CHEW, W. K., LIMA, R., A-GONZÁLEZ, N., MATTAR, C. N. Z., CHONG, S. Z., SCHLITZER, A., BAKOCEVIC, N., CHEW, S., KEEBLE, J. L., GOH, C. C., LI, J. L. Y., EVRARD, M., MALLERET, B., LARBI, A., RENIA, L., HANIFFA, M., TAN, S. M., CHAN, J. K. Y., BALABANIAN, K., NAGASAWA, T., BACHELERIE, F., HIDALGO, A., GINHOUX, F., KUBES, P. & NG, L. G. 2013. Neutrophil mobilization via plerixafor-mediated CXCR4 inhibition arises from lung demargination and blockade of neutrophil homing to the bone marrow. *The Journal of Experimental Medicine,* 210**,** 2321.
DICK, A. D., BRODERICK, C., FORRESTER, J. V. & WRIGHT, G. J. 2001. Distribution of OX2 antigen and OX2 receptor within retina. *Invest Ophthalmol Vis Sci,* 42**,** 170-6.
DUCKETT, N. S., OLMOS, S., DURRANT, D. M. & METZGER, D. W. 2005. Intranasal interleukin-12 treatment for protection against respiratory infection with the Francisella tularensis live vaccine strain. *Infect Immun,* 73**,** 2306-11.
DUNCAN, J. L., LAVAIL, M. M., YASUMURA, D., MATTHES, M. T., YANG, H., TRAUTMANN, N., CHAPPELOW, A. V., FENG, W., EARP, H. S., MATSUSHIMA, G. K. & VOLLRATH, D. 2003. An RCS-like retinal dystrophy phenotype in mer knockout mice. *Invest Ophthalmol Vis Sci,* 44**,** 826-38.
DUPONT, E., VAN EECKHOUDT, S., THISSEN, X., AUSSELET, N., FRETIN, D., STEFANESCU, I., GLUPCZYNSKI, Y. & DELAERE, B. 2015. About three cases of ulceroglandular tularemia, is this the re-emergence of Francisella tularensis in Belgium? *Acta Clin Belg,* 70**,** 364-8.
EASH, K. J., GREENBAUM, A. M., GOPALAN, P. K. & LINK, D. C. 2010. CXCR2 and CXCR4 antagonistically regulate neutrophil trafficking from murine bone marrow. *J Clin Invest,* 120**,** 2423-31.

EIGELSBACH, H. T., BRAUN, W. & HERRING, R. D. 1951. Studies on the variation of Bacterium tularense. *J Bacteriol,* 61**,** 557-69.
EIGELSBACH, H. T. & DOWNS, C. M. 1961. Prophylactic effectiveness of live and killed tularemia vaccines. I. Production of vaccine and evaluation in the white mouse and guinea pig. *J Immunol,* 87**,** 415-25.
EIGELSBACH, H. T., HORNICK, R. B. & TULIS, J. J. 1967. Recent studies on live tularemia vaccine. *Med Ann Dist Columbia,* 36**,** 282-6.
EIGELSBACH, H. T., TULIS, J. J., MCGAVRAN, M. H. & WHITE, J. D. 1962. LIVE TULAREMIA VACCINE I. : Host-Parasite Relationship in Monkeys Vaccinated Intracutaneously or Aerogenically. *J Bacteriol,* 84**,** 1020-7.
EISERICH, J. P., HRISTOVA, M., CROSS, C. E., JONES, A. D., FREEMAN, B. A., HALLIWELL, B. & VAN DER VLIET, A. 1998. Formation of nitric oxide-derived inflammatory oxidants by myeloperoxidase in neutrophils. *Nature,* 391**,** 393-7.
ELKINS, K. L., BOSIO, C. M. & RHINEHART-JONES, T. R. 1999. Importance of B cells, but not specific antibodies, in primary and secondary protective immunity to the intracellular bacterium Francisella tularensis live vaccine strain. *Infect Immun,* 67**,** 6002-7.
ELKINS, K. L., COOPER, A., COLOMBINI, S. M., COWLEY, S. C. & KIEFFER, T. L. 2002. In vivo clearance of an intracellular bacterium, Francisella tularensis LVS, is dependent on the p40 subunit of interleukin-12 (IL-12) but not on IL-12 p70. *Infect Immun,* 70**,** 1936-48.
ELKINS, K. L., COWLEY, S. C. & BOSIO, C. M. 2003. Innate and adaptive immune responses to an intracellular bacterium, Francisella tularensis live vaccine strain. *Microbes Infect,* 5**,** 135-42.
ELKINS, K. L., RHINEHART-JONES, T. R., CULKIN, S. J., YEE, D. & WINEGAR, R. K. 1996. Minimal requirements for murine resistance to infection with Francisella tularensis LVS. *Infect Immun,* 64**,** 3288-93.
ENDERLIN, G., MORALES, L., JACOBS, R. F. & CROSS, J. T. 1994. Streptomycin and alternative agents for the treatment of tularemia: review of the literature. *Clin Infect Dis,* 19**,** 42-7.
EVANS, M. E., GREGORY, D. W., SCHAFFNER, W. & MCGEE, Z. A. 1985. Tularemia: a 30-year experience with 88 cases. *Medicine (Baltimore),* 64**,** 251-69.
FACHINGER, P., TINI, G. M., GROBHOLZ, R., GAMBAZZI, F., FANKHAUSER, H. & IRANI, S. 2015. Pulmonary tularaemia: all that looks like cancer is not necessarily cancer - case report of four consecutive cases. *BMC Pulm Med,* 15**,** 27.
FARLOW, J., WAGNER, D. M., DUKERICH, M., STANLEY, M., CHU, M., KUBOTA, K., PETERSEN, J. & KEIM, P. 2005. Francisella tularensis in the United States. *Emerg Infect Dis,* 11**,** 1835-41.
FELDMAN, K. A. 2003. Tularemia. *J Am Vet Med Assoc,* 222**,** 725-30.
FELDMAN, K. A., STILES-ENOS, D., JULIAN, K., MATYAS, B. T., TELFORD, S. R., CHU, M. C., PETERSEN, L. R. & HAYES, E. B. 2003. Tularemia on Martha's Vineyard: Seroprevalence and Occupational Risk. *Emerg Infect Dis,* 9**,** 350-4.
FERNANDES, T. D., CUNHA, L. D., RIBEIRO, J. M., MASSIS, L. M., LIMA-JUNIOR, D. S., NEWTON, H. J. & ZAMBONI, D. S. 2016. Murine Alveolar Macrophages Are Highly Susceptible to Replication of Coxiella burnetii Phase II In Vitro. *Infect Immun,* 84**,** 2439-48.

FINK, A., HASSAN, M. A., OKAN, N. A., SHEFFER, M., CAMEJO, A., SAEIJ, J. P. & KASPER, D. L. 2016. Early Interactions of Murine Macrophages with Francisella tularensis Map to Mouse Chromosome 19. *MBio,* 7**,** e02243.

FLANNIGAN, K. L., NGO, V. L., GEEM, D., HARUSATO, A., HIROTA, S. A., PARKOS, C. A., LUKACS, N. W., NUSRAT, A., GABORIAU-ROUTHIAU, V., CERF-BENSUSSAN, N., GEWIRTZ, A. T. & DENNING, T. L. 2017. IL-17A-mediated neutrophil recruitment limits expansion of segmented filamentous bacteria. *Mucosal Immunol,* 10**,** 673-684.

FORTIER, A. H., LEIBY, D. A., NARAYANAN, R. B., ASAFOADJEI, E., CRAWFORD, R. M., NACY, C. A. & MELTZER, M. S. 1995. Growth of Francisella tularensis LVS in macrophages: the acidic intracellular compartment provides essential iron required for growth. *Infect Immun,* 63**,** 1478-83.

FORTIER, A. H., SLAYTER, M. V., ZIEMBA, R., MELTZER, M. S. & NACY, C. A. 1991. Live vaccine strain of Francisella tularensis: infection and immunity in mice. *Infect Immun,* 59**,** 2922-8.

FOSTER-CUEVAS, M., WESTERHOLT, T., AHMED, M., BROWN, M. H., BARCLAY, A. N. & VOIGT, S. 2011. Cytomegalovirus e127 protein interacts with the inhibitory CD200 receptor. *J Virol,* 85**,** 6055-9.

FOSTER-CUEVAS, M., WRIGHT, G. J., PUKLAVEC, M. J., BROWN, M. H. & BARCLAY, A. N. 2004. Human herpesvirus 8 K14 protein mimics CD200 in down-regulating macrophage activation through CD200 receptor. *J Virol,* 78**,** 7667-76.

FRANCKE, A., HEROLD, J., WEINERT, S., STRASSER, R. H. & BRAUN-DULLAEUS, R. C. 2011. Generation of mature murine monocytes from heterogeneous bone marrow and description of their properties. *J Histochem Cytochem,* 59**,** 813-25.

FRASER, S. D., SADOFSKY, L. R., KAYE, P. M. & HART, S. P. 2016. Reduced expression of monocyte CD200R is associated with enhanced proinflammatory cytokine production in sarcoidosis. *Sci Rep,* 6**,** 38689.

FREVERT, C. W., HUANG, S., DANAEE, H., PAULAUSKIS, J. D. & KOBZIK, L. 1995. Functional characterization of the rat chemokine KC and its importance in neutrophil recruitment in a rat model of pulmonary inflammation. *J Immunol,* 154**,** 335-44.

GAO, X., DONG, Y., LIU, Z. & NIU, B. 2013. Silencing of triggering receptor expressed on myeloid cells-2 enhances the inflammatory responses of alveolar macrophages to lipopolysaccharide. *Mol Med Rep,* 7**,** 921-6.

GARDAI, S. J., XIAO, Y. Q., DICKINSON, M., NICK, J. A., VOELKER, D. R., GREENE, K. E. & HENSON, P. M. 2003. By binding SIRPalpha or calreticulin/CD91, lung collectins act as dual function surveillance molecules to suppress or enhance inflammation. *Cell,* 115**,** 13-23.

GAVRILIN, M. A. & WEWERS, M. D. 2011. Francisella Recognition by Inflammasomes: Differences between Mice and Men. *Front Microbiol,* 2**,** 11.

GAYNOR, C. D., MCCORMACK, F. X., VOELKER, D. R., MCGOWAN, S. E. & SCHLESINGER, L. S. 1995. Pulmonary surfactant protein A mediates enhanced phagocytosis of Mycobacterium tuberculosis by a direct interaction with human macrophages. *J Immunol,* 155**,** 5343-51.

GEIER, H. & CELLI, J. 2011. Phagocytic receptors dictate phagosomal escape and intracellular proliferation of Francisella tularensis. *Infect Immun,* 79**,** 2204-14.

GENTRY, M., TAORMINA, J., PYLES, R. B., YEAGER, L., KIRTLEY, M., POPOV, V. L., KLIMPEL, G. & EAVES-PYLES, T. 2007. Role of primary human alveolar epithelial cells in host defense against Francisella tularensis infection. *Infect Immun,* 75**,** 3969-78.

GILL, V. & CUNHA, B. A. 1997. Tularemia pneumonia. *Semin Respir Infect,* 12**,** 61-7.

GOLOVLIOV, I., BARANOV, V., KROCOVA, Z., KOVAROVA, H. & SJOSTEDT, A. 2003. An attenuated strain of the facultative intracellular bacterium Francisella tularensis can escape the phagosome of monocytic cells. *Infect Immun,* 71**,** 5940-50.

GOLOVLIOV, I., SANDSTROM, G., ERICSSON, M., SJOSTEDT, A. & TARNVIK, A. 1995. Cytokine expression in the liver during the early phase of murine tularemia. *Infect Immun,* 63**,** 534-8.

GORCZYNSKI, R., CHEN, Z., KAI, Y., LEE, L., WONG, S. & MARSDEN, P. A. 2004. CD200 is a ligand for all members of the CD200R family of immunoregulatory molecules. *J Immunol,* 172**,** 7744-9.

GORCZYNSKI, R. M., CATTRAL, M. S., CHEN, Z., HU, J., LEI, J., MIN, W. P., YU, G. & NI, J. 1999. An immunoadhesin incorporating the molecule OX-2 is a potent immunosuppressant that prolongs allo- and xenograft survival. *J Immunol,* 163**,** 1654-60.

GORCZYNSKI, R. M., CHEN, Z., HU, J., KAI, Y. & LEI, J. 2001a. Evidence of a role for CD200 in regulation of immune rejection of leukaemic tumour cells in C57BL/6 mice. *Clinical and Experimental Immunology,* 126**,** 220-229.

GORCZYNSKI, R. M., CHEN, Z., YU, K. & HU, J. 2001b. CD200 immunoadhesin suppresses collagen-induced arthritis in mice. *Clin Immunol,* 101**,** 328-34.

GORCZYNSKI, R. M., CLARK, D. A., ERIN, N. & KHATRI, I. 2011. Role of CD200 expression in regulation of metastasis of EMT6 tumor cells in mice. *Breast Cancer Res Treat,* 130**,** 49-60.

GORCZYNSKI, R. M., HU, J., CHEN, Z., KAI, Y. & LEI, J. 2002. A CD200FC immunoadhesin prolongs rat islet xenograft survival in mice. *Transplantation,* 73**,** 1948-53.

GORCZYNSKI, R. M., YU, K. & CLARK, D. 2000. Receptor engagement on cells expressing a ligand for the tolerance-inducing molecule OX2 induces an immunoregulatory population that inhibits alloreactivity in vitro and in vivo. *J Immunol,* 165**,** 4854-60.

GORDON, S. 2003. Alternative activation of macrophages. *Nat Rev Immunol,* 3**,** 23-35.

GORDON, S. & MARTINEZ, F. O. 2010. Alternative activation of macrophages: mechanism and functions. *Immunity,* 32**,** 593-604.

GOULDING, J., GODLEE, A., VEKARIA, S., HILTY, M., SNELGROVE, R. & HUSSELL, T. 2011. Lowering the threshold of lung innate immune cell activation alters susceptibility to secondary bacterial superinfection. *J Infect Dis,* 204**,** 1086-94.

GOVONI, G. & GROS, P. 1998. Macrophage NRAMP1 and its role in resistance to microbial infections. *Inflamm Res,* 47**,** 277-84.

GREEN, D. R., FERGUSON, T., ZITVOGEL, L. & KROEMER, G. 2009. Immunogenic and tolerogenic cell death. *Nat Rev Immunol,* 9**,** 353-63.

GRIFFIN, A. J., CRANE, D. D., WEHRLY, T. D., SCOTT, D. P. & BOSIO, C. M. 2013. Alternative activation of macrophages and induction of arginase are

not components of pathogenesis mediated by Francisella species. *PLoS One,* 8**,** e82096.
GUILLIAMS, M., DE KLEER, I., HENRI, S., POST, S., VANHOUTTE, L., DE PRIJCK, S., DESWARTE, K., MALISSEN, B., HAMMAD, H. & LAMBRECHT, B. N. 2013. Alveolar macrophages develop from fetal monocytes that differentiate into long-lived cells in the first week of life via GM-CSF. *J Exp Med,* 210**,** 1977-92.
GUNN, J. S. & ERNST, R. K. 2007. The structure and function of Francisella lipopolysaccharide. *Ann N Y Acad Sci,* 1105**,** 202-18.
GURCAN, S. 2014. Epidemiology of tularemia. *Balkan Med J,* 31**,** 3-10.
GURYCOVA, D. 1998. First isolation of Francisella tularensis subsp. tularensis in Europe. *Eur J Epidemiol,* 14**,** 797-802.
GYURANECZ, M., REICZIGEL, J., KRISZTALOVICS, K., MONSE, L., SZABONE, G. K., SZILAGYI, A., SZEPE, B., MAKRAI, L., MAGYAR, T., BHIDE, M. & ERDELYI, K. 2012. Factors influencing emergence of tularemia, Hungary, 1984-2010. *Emerg Infect Dis,* 18**,** 1379-81.
HAGER, M., COWLAND, J. B. & BORREGAARD, N. 2010. Neutrophil granules in health and disease. *J Intern Med,* 268**,** 25-34.
HALL, J. D., KURTZ, S. L., RIGEL, N. W., GUNN, B. M., TAFT-BENZ, S., MORRISON, J. P., FONG, A. M., PATEL, D. D., BRAUNSTEIN, M. & KAWULA, T. H. 2009. The impact of chemokine receptor CX3CR1 deficiency during respiratory infections with Mycobacterium tuberculosis or Francisella tularensis. *Clin Exp Immunol,* 156**,** 278-84.
HALL, J. D., WOOLARD, M. D., GUNN, B. M., CRAVEN, R. R., TAFT-BENZ, S., FRELINGER, J. A. & KAWULA, T. H. 2008. Infected-host-cell repertoire and cellular response in the lung following inhalation of Francisella tularensis Schu S4, LVS, or U112. *Infect Immun,* 76**,** 5843-52.
HARAOKA, M., HANG, L., FRENDEUS, B., GODALY, G., BURDICK, M., STRIETER, R. & SVANBORG, C. 1999. Neutrophil recruitment and resistance to urinary tract infection. *J Infect Dis,* 180**,** 1220-9.
HARRIS, S. 1992. Japanese biological warfare research on humans: a case study of microbiology and ethics. *Ann N Y Acad Sci,* 666**,** 21-52.
HATHERLEY, D., CHERWINSKI, H. M., MOSHREF, M. & BARCLAY, A. N. 2005. Recombinant CD200 protein does not bind activating proteins closely related to CD200 receptor. *J Immunol,* 175**,** 2469-74.
HAWRYLOWICZ, C. M. & O'GARRA, A. 2005. Potential role of interleukin-10-secreting regulatory T cells in allergy and asthma. *Nat Rev Immunol,* 5**,** 271-83.
HESTVIK, G., WARNS-PETIT, E., SMITH, L. A., FOX, N. J., UHLHORN, H., ARTOIS, M., HANNANT, D., HUTCHINGS, M. R., MATTSSON, R., YON, L. & GAVIER-WIDEN, D. 2015. The status of tularemia in Europe in a one-health context: a review. *Epidemiol Infect,* 143**,** 2137-60.
HOEK, R. M., RUULS, S. R., MURPHY, C. A., WRIGHT, G. J., GODDARD, R., ZURAWSKI, S. M., BLOM, B., HOMOLA, M. E., STREIT, W. J., BROWN, M. H., BARCLAY, A. N. & SEDGWICK, J. D. 2000. Down-regulation of the macrophage lineage through interaction with OX2 (CD200). *Science,* 290**,** 1768-71.
HOENDERDOS, K. & CONDLIFFE, A. 2013. The neutrophil in chronic obstructive pulmonary disease. *Am J Respir Cell Mol Biol,* 48**,** 531-9.

HOLMES, B., PAGE, A. R. & GOOD, R. A. 1967. Studies of the Metabolic Activity of Leukocytes from Patients with a Genetic Abnormality of Phagocytic Function. *J Clin Invest,* 46**,** 1422-32.
HOROWITZ, A., STEGMANN, K. A. & RILEY, E. M. 2011. Activation of natural killer cells during microbial infections. *Front Immunol,* 2**,** 88.
HORZEMPA, J., O'DEE, D. M., SHANKS, R. M. & NAU, G. J. 2010. Francisella tularensis DeltapyrF mutants show that replication in nonmacrophages is sufficient for pathogenesis in vivo. *Infect Immun,* 78**,** 2607-19.
HUBALEK, Z., SIXL, W. & HALOUZKA, J. 1998. Francisella tularensis in Dermacentor reticulatus ticks from the Czech Republic and Austria. *Wien Klin Wochenschr,* 110**,** 909-10.
HUSSELL, T. & BELL, T. J. 2014. Alveolar macrophages: plasticity in a tissue-specific context. *Nat Rev Immunol,* 14**,** 81-93.
HUTT, J. A., LOVCHIK, J. A., DEKONENKO, A., HAHN, A. C. & WU, T. H. 2017. The Natural History of Pneumonic Tularemia in Female Fischer 344 Rats after Inhalational Exposure to Aerosolized Francisella tularensis Subspecies tularensis Strain SCHU S4. *Am J Pathol,* 187**,** 252-267.
IBA, T., HASHIGUCHI, N., NAGAOKA, I., TABE, Y. & MURAI, M. 2013. Neutrophil cell death in response to infection and its relation to coagulation. *J Intensive Care,* 1.
IRWIN, S. M., GRUPPO, V., BROOKS, E., GILLILAND, J., SCHERMAN, M., REICHLEN, M. J., LEISTIKOW, R., KRAMNIK, I., NUERMBERGER, E. L., VOSKUIL, M. I. & LENAERTS, A. J. 2014. Limited activity of clofazimine as a single drug in a mouse model of tuberculosis exhibiting caseous necrotic granulomas. *Antimicrob Agents Chemother,* 58**,** 4026-34.
JACKSON, R. T. & LESTER, J. P. 1978. Case report. Tularemia presenting as unresponsive pneumonia: diagnosis and therapy with gentamicin. *J Tenn Med Assoc,* 71**,** 189-91.
JAHNSEN, F. L., STRICKLAND, D. H., THOMAS, J. A., TOBAGUS, I. T., NAPOLI, S., ZOSKY, G. R., TURNER, D. J., SLY, P. D., STUMBLES, P. A. & HOLT, P. G. 2006. Accelerated antigen sampling and transport by airway mucosal dendritic cells following inhalation of a bacterial stimulus. *J Immunol,* 177**,** 5861-7.
JANSSEN, W. J., MCPHILLIPS, K. A., DICKINSON, M. G., LINDERMAN, D. J., MORIMOTO, K., XIAO, Y. Q., OLDHAM, K. M., VANDIVIER, R. W., HENSON, P. M. & GARDAI, S. J. 2008. Surfactant proteins A and D suppress alveolar macrophage phagocytosis via interaction with SIRP alpha. *Am J Respir Crit Care Med,* 178**,** 158-67.
JANSSEN, W. J., MULDROW, A., KEARNS, M. T., BARTHEL, L. & HENSON, P. M. 2010. Development and characterization of a lung-protective method of bone marrow transplantation in the mouse. *J Immunol Methods,* 357**,** 1-9.
JENNER, D., DUCKER, C., CLARK, G., PRIOR, J. & ROWLAND, C. A. 2016. Using multispectral imaging flow cytometry to assess an in vitro intracellular Burkholderia thailandensis infection model. *Cytometry A,* 89**,** 328-37.
JIANG, D. S., ZHANG, X. F., GAO, L., ZONG, J., ZHOU, H., LIU, Y., ZHANG, Y., BIAN, Z. Y., ZHU, L. H., FAN, G. C., ZHANG, X. D. & LI, H. 2014. Signal Regulatory Protein-α Protects Against Cardiac Hypertrophy Via the Disruption of Toll-Like Receptor 4 Signaling. *Hypertension,* 63**,** 96-104.
JIANG, L., TIXEIRA, R., CARUSO, S., ATKIN-SMITH, G. K., BAXTER, A. A., PAONE, S., HULETT, M. D. & POON, I. K. 2016. Monitoring the

progression of cell death and the disassembly of dying cells by flow cytometry. *Nat Protoc,* 11**,** 655-63.
JIANG-SHIEH, Y. F., CHIEN, H. F., CHANG, C. Y., WEI, T. S., CHIU, M. M., CHEN, H. M. & WU, C. H. 2010. Distribution and expression of CD200 in the rat respiratory system under normal and endotoxin-induced pathological conditions. *J Anat,* 216**,** 407-16.
JOHNZON, C. F., RONNBERG, E. & PEJLER, G. 2016. The Role of Mast Cells in Bacterial Infection. *Am J Pathol,* 186**,** 4-14.
JOLY, E. & HUDRISIER, D. 2003. What is trogocytosis and what is its purpose? *Nat Immunol,* 4**,** 815.
JONES, B. D., FARON, M., RASMUSSEN, J. A. & FLETCHER, J. R. 2014. Uncovering the components of the Francisella tularensis virulence stealth strategy. *Front Cell Infect Microbiol,* 4**,** 32.
JONES, C. L., NAPIER, B. A., SAMPSON, T. R., LLEWELLYN, A. C., SCHROEDER, M. R. & WEISS, D. S. 2012. Subversion of host recognition and defense systems by Francisella spp. *Microbiol Mol Biol Rev,* 76**,** 383-404.
JUNCADELLA, I. J., KADL, A., SHARMA, A. K., SHIM, Y. M., HOCHREITER-HUFFORD, A., BORISH, L. & RAVICHANDRAN, K. S. 2013. Apoptotic cell clearance by bronchial epithelial cells critically influences airway inflammation. *Nature,* 493**,** 547-51.
KAHN, F., HURLEY, S. & SHANNON, O. 2013. Platelets promote bacterial dissemination in a mouse model of streptococcal sepsis. *Microbes Infect,* 15**,** 669-76.
KARNAM, G., RYGIEL, T. P., RAABEN, M., GRINWIS, G. C., COENJAERTS, F. E., RESSING, M. E., ROTTIER, P. J., DE HAAN, C. A. & MEYAARD, L. 2012. CD200 receptor controls sex-specific TLR7 responses to viral infection. *PLoS Pathog,* 8**,** e1002710.
KATZ, J., ZHANG, P., MARTIN, M., VOGEL, S. N. & MICHALEK, S. M. 2006. Toll-like receptor 2 is required for inflammatory responses to Francisella tularensis LVS. *Infect Immun,* 74**,** 2809-16.
KAYAL, S. & CHARBIT, A. 2006. Listeriolysin O: a key protein of Listeria monocytogenes with multiple functions. *FEMS Microbiol Rev,* 30**,** 514-29.
KEIM, P., JOHANSSON, A. & WAGNER, D. M. 2007. Molecular epidemiology, evolution, and ecology of Francisella. *Ann N Y Acad Sci,* 1105**,** 30-66.
KETAVARAPU, J. M., RODRIGUEZ, A. R., YU, J. J., CONG, Y., MURTHY, A. K., FORSTHUBER, T. G., GUENTZEL, M. N., KLOSE, K. E., BERTON, M. T. & ARULANANDAM, B. P. 2008. Mast cells inhibit intramacrophage Francisella tularensis replication via contact and secreted products including IL-4. *Proc Natl Acad Sci U S A,* 105**,** 9313-8.
KINKEAD, L. C. & ALLEN, L. A. 2016. Multifaceted effects of Francisella tularensis on human neutrophil function and lifespan. *Immunol Rev,* 273**,** 266-81.
KINKEAD, L. C., WHITMORE, L. C., MCCRACKEN, J. M., FLETCHER, J. R., KETELSEN, B. B., KAUFMAN, J. W., JONES, B. D., WEISS, D. S., BARKER, J. H. & ALLEN, L. H. 2017. Bacterial lipoproteins and other factors released by Francisella tularensis modulate human neutrophil lifespan: effects of a TLR1 SNP on apoptosis inhibition. *Cell Microbiol*.

KJELDSEN, L., SENGELOV, H., LOLLIKE, K., NIELSEN, M. H. & BORREGAARD, N. 1994. Isolation and characterization of gelatinase granules from human neutrophils. *Blood,* 83**,** 1640-9.
KLEBANOFF, S. J., KETTLE, A. J., ROSEN, H., WINTERBOURN, C. C. & NAUSEEF, W. M. 2013. Myeloperoxidase: a front-line defender against phagocytosed microorganisms. *J Leukoc Biol,* 93**,** 185-98.
KLIMPEL, G. R., EAVES-PYLES, T., MOEN, S. T., TAORMINA, J., PETERSON, J. W., CHOPRA, A. K., NIESEL, D. W., CARNESS, P., HAITHCOAT, J. L., KIRTLEY, M. & NASR, A. B. 2008. Levofloxacin rescues mice from lethal intra-nasal infections with virulent Francisella tularensis and induces immunity and production of protective antibody. *Vaccine,* 26**,** 6874-82.
KOLACZKOWSKA, E. & KUBES, P. 2013. Neutrophil recruitment and function in health and inflammation. *Nat Rev Immunol,* 13**,** 159-75.
KREISEL, D., NAVA, R. G., LI, W., ZINSELMEYER, B. H., WANG, B., LAI, J., PLESS, R., GELMAN, A. E., KRUPNICK, A. S. & MILLER, M. J. 2010. In vivo two-photon imaging reveals monocyte-dependent neutrophil extravasation during pulmonary inflammation. *Proc Natl Acad Sci U S A,* 107**,** 18073-8.
KROCOVA, Z., HARTLOVA, A., SOUCKOVA, D., ZIVNA, L., KROCA, M., RUDOLF, E., MACELA, A. & STULIK, J. 2008. Interaction of B cells with intracellular pathogen Francisella tularensis. *Microb Pathog,* 45**,** 79-85.
KUHN, R., LOHLER, J., RENNICK, D., RAJEWSKY, K. & MULLER, W. 1993. Interleukin-10-deficient mice develop chronic enterocolitis. *Cell,* 75**,** 263-74.
KURT-JONES, E. A., CHAN, M., ZHOU, S., WANG, J., REED, G., BRONSON, R., ARNOLD, M. M., KNIPE, D. M. & FINBERG, R. W. 2004. Herpes simplex virus 1 interaction with Toll-like receptor 2 contributes to lethal encephalitis. *Proc Natl Acad Sci U S A,* 101**,** 1315-20.
KURTZ, S. L., CHOU, A. Y., KUBELKOVA, K., CUA, D. J. & ELKINS, K. L. 2014. IL-23 p19 knockout mice exhibit minimal defects in responses to primary and secondary infection with Francisella tularensis LVS. *PLoS One,* 9**,** e109898.
KURTZ, S. L., FOREMAN, O., BOSIO, C. M., ANVER, M. R. & ELKINS, K. L. 2013. Interleukin-6 is essential for primary resistance to Francisella tularensis live vaccine strain infection. *Infect Immun,* 81**,** 585-97.
KWONG, L. S., AKKAYA, M., BARCLAY, A. N. & HATHERLEY, D. 2016. Herpesvirus orthologues of CD200 bind host CD200R but not related activating receptors. *J Gen Virol,* 97**,** 179-84.
LACY, P. 2006. Mechanisms of Degranulation in Neutrophils. *Allergy Asthma Clin Immunol,* 2**,** 98-108.
LAI, X. H., GOLOVLIOV, I. & SJOSTEDT, A. 2001. Francisella tularensis induces cytopathogenicity and apoptosis in murine macrophages via a mechanism that requires intracellular bacterial multiplication. *Infect Immun,* 69**,** 4691-4.
LAI, X. H. & SJOSTEDT, A. 2003. Delineation of the molecular mechanisms of Francisella tularensis-induced apoptosis in murine macrophages. *Infect Immun,* 71**,** 4642-6.
LAKSCHEVITZ, F. S., VISSER, M. B., SUN, C. & GLOGAUER, M. 2015. Neutrophil transcriptional profile changes during transit from bone marrow to sites of inflammation. *Cell Mol Immunol,* 12**,** 53-65.
LAMBRECHT, B. N. & HAMMAD, H. 2012. The airway epithelium in asthma. *Nat Med,* 18**,** 684-92.

LANDSMAN, L., BAR-ON, L., ZERNECKE, A., KIM, K. W., KRAUTHGAMER, R., SHAGDARSUREN, E., LIRA, S. A., WEISSMAN, I. L., WEBER, C. & JUNG, S. 2009. CX3CR1 is required for monocyte homeostasis and atherogenesis by promoting cell survival. *Blood,* 113**,** 963-72.

LARSSEN, K. W., BERGH, K., HEIER, B. T., VOLD, L. & AFSET, J. E. 2014. All-time high tularaemia incidence in Norway in 2011: report from the national surveillance. *Eur J Clin Microbiol Infect Dis,* 33**,** 1919-26.

LARSSON, P., OYSTON, P. C., CHAIN, P., CHU, M. C., DUFFIELD, M., FUXELIUS, H. H., GARCIA, E., HALLTORP, G., JOHANSSON, D., ISHERWOOD, K. E., KARP, P. D., LARSSON, E., LIU, Y., MICHELL, S., PRIOR, J., PRIOR, R., MALFATTI, S., SJOSTEDT, A., SVENSSON, K., THOMPSON, N., VERGEZ, L., WAGG, J. K., WREN, B. W., LINDLER, L. E., ANDERSSON, S. G., FORSMAN, M. & TITBALL, R. W. 2005. The complete genome sequence of Francisella tularensis, the causative agent of tularemia. *Nat Genet,* 37**,** 153-9.

LAWS, T. R., CLARK, G. & D'ELIA, R. V. 2013. Differential role for interleukin-6 during Francisella tularensis infection with virulent and vaccine strains. *Infect Immun,* 81**,** 3055-6.

LEMKE, G. & ROTHLIN, C. V. 2008. Immunobiology of the TAM receptors. *Nat Rev Immunol,* 8**,** 327-36.

LIM, S., CARAMORI, G., TOMITA, K., JAZRAWI, E., OATES, T., CHUNG, K. F., BARNES, P. J. & ADCOCK, I. M. 2004. Differential expression of IL-10 receptor by epithelial cells and alveolar macrophages. *Allergy,* 59**,** 505-14.

LIN, Y., RITCHEA, S., LOGAR, A., SLIGHT, S., MESSMER, M., RANGEL-MORENO, J., GUGLANI, L., ALCORN, J. F., STRAWBRIDGE, H., PARK, S. M., ONISHI, R., NYUGEN, N., WALTER, M. J., POCIASK, D., RANDALL, T. D., GAFFEN, S. L., IWAKURA, Y., KOLLS, J. K. & KHADER, S. A. 2009. Interleukin-17 is required for T helper 1 cell immunity and host resistance to the intracellular pathogen Francisella tularensis. *Immunity,* 31**,** 799-810.

LINEHAN, S. A., COULSON, P. S., WILSON, R. A., MOUNTFORD, A. P., BROMBACHER, F., MARTINEZ-POMARES, L. & GORDON, S. 2003. IL-4 receptor signaling is required for mannose receptor expression by macrophages recruited to granulomata but not resident cells in mice infected with Schistosoma mansoni. *Lab Invest,* 83**,** 1223-31.

LIVAK, K. J. & SCHMITTGEN, T. D. 2001. Analysis of relative gene expression data using real-time quantitative PCR and the 2(-Delta Delta C(T)) Method. *Methods,* 25**,** 402-8.

LLOYD, C. M. & MARSLAND, B. J. 2017. Lung Homeostasis: Influence of Age, Microbes, and the Immune System. *Immunity,* 46**,** 549-561.

LOPEZ, M. C., DUCKETT, N. S., BARON, S. D. & METZGER, D. W. 2004. Early activation of NK cells after lung infection with the intracellular bacterium, Francisella tularensis LVS. *Cell Immunol,* 232**,** 75-85.

LYONS, A., DOWNER, E. J., COSTELLO, D. A., MURPHY, N. & LYNCH, M. A. 2012. Dok2 mediates the CD200Fc attenuation of Abeta-induced changes in glia. *J Neuroinflammation,* 9**,** 107.

LYONS, A., DOWNER, E. J., CROTTY, S., NOLAN, Y. M., MILLS, K. H. & LYNCH, M. A. 2007. CD200 ligand receptor interaction modulates microglial activation in vivo and in vitro: a role for IL-4. *J Neurosci,* 27**,** 8309-13.

LYONS, A., MINOGUE, A. M., JONES, R. S., FITZPATRICK, O., NOONAN, J., CAMPBELL, V. A. & LYNCH, M. A. 2016. Analysis of the Impact of CD200 on Phagocytosis. *Mol Neurobiol*.
MADAR, M., BENCUROVA, E., MLYNARCIK, P., ALMEIDA, A. M., SOARES, R., BHIDE, K., PULZOVA, L., KOVAC, A., COELHO, A. V. & BHIDE, M. 2015. Exploitation of complement regulatory proteins by Borrelia and Francisella. *Mol Biosyst,* 11**,** 1684-95.
MAGGIO, S., TAKEDA, K., STARK, F., MEIEROVICS, A. I., YABE, I. & COWLEY, S. C. 2015. Control of Francisella tularensis Intracellular Growth by Pulmonary Epithelial Cells. *PLoS One,* 10**,** e0138565.
MALIK, M., BAKSHI, C. S., MCCABE, K., CATLETT, S. V., SHAH, A., SINGH, R., JACKSON, P. L., GAGGAR, A., METZGER, D. W., MELENDEZ, J. A., BLALOCK, J. E. & SELLATI, T. J. 2007. Matrix metalloproteinase 9 activity enhances host susceptibility to pulmonary infection with type A and B strains of Francisella tularensis. *J Immunol,* 178**,** 1013-20.
MALIK, M., BAKSHI, C. S., SAHAY, B., SHAH, A., LOTZ, S. A. & SELLATI, T. J. 2006. Toll-like receptor 2 is required for control of pulmonary infection with Francisella tularensis. *Infect Immun,* 74**,** 3657-62.
MAN, S. M., KARKI, R. & KANNEGANTI, T. D. 2016. AIM2 inflammasome in infection, cancer, and autoimmunity: Role in DNA sensing, inflammation, and innate immunity. *Eur J Immunol,* 46**,** 269-80.
MAN, S. M., KARKI, R., MALIREDDI, R. K., NEALE, G., VOGEL, P., YAMAMOTO, M., LAMKANFI, M. & KANNEGANTI, T. D. 2015. The transcription factor IRF1 and guanylate-binding proteins target activation of the AIM2 inflammasome by Francisella infection. *Nat Immunol,* 16**,** 467-75.
MARIATHASAN, S., WEISS, D. S., DIXIT, V. M. & MONACK, D. M. 2005. Innate immunity against Francisella tularensis is dependent on the ASC/caspase-1 axis. *J Exp Med,* 202**,** 1043-9.
MARKEL, G., BAR-HAIM, E., ZAHAVY, E., COHEN, H., COHEN, O., SHAFFERMAN, A. & VELAN, B. 2010. The involvement of IL-17A in the murine response to sub-lethal inhalational infection with Francisella tularensis. *PLoS One,* 5**,** e11176.
MARSH, J. C., BOGGS, D. R., CARTWRIGHT, G. E. & WINTROBE, M. M. 1967. Neutrophil kinetics in acute infection. *J Clin Invest,* 46**,** 1943-53.
MARTINON, F., CHEN, X., LEE, A. H. & GLIMCHER, L. H. 2010. TLR activation of the transcription factor XBP1 regulates innate immune responses in macrophages. *Nat Immunol,* 11**,** 411-8.
MASON, W. L., EIGELSBACH, H. T., LITTLE, S. F. & BATES, J. H. 1980. Treatment of tularemia, including pulmonary tularemia, with gentamicin. *Am Rev Respir Dis,* 121**,** 39-45.
MASUDA, S., SHIMIZU, S., MATSUO, J., NISHIBATA, Y., KUSUNOKI, Y., HATTANDA, F., SHIDA, H., NAKAZAWA, D., TOMARU, U., ATSUMI, T. & ISHIZU, A. 2017. Measurement of NET formation in vitro and in vivo by flow cytometry. *Cytometry A,* 91**,** 822-829.
MATSUNAGA, K., KLEIN, T. W., FRIEDMAN, H. & YAMAMOTO, Y. 2001. Alveolar macrophage cell line MH-S is valuable as an in vitro model for Legionella pneumophila infection. *Am J Respir Cell Mol Biol,* 24**,** 326-31.
MAUS, U. A., JANZEN, S., WALL, G., SRIVASTAVA, M., BLACKWELL, T. S., CHRISTMAN, J. W., SEEGER, W., WELTE, T. & LOHMEYER, J. 2006. Resident alveolar macrophages are replaced by recruited monocytes in

response to endotoxin-induced lung inflammation. *Am J Respir Cell Mol Biol,* 35**,** 227-35.
MBAWUIKE, I. N. & HERSCOWITZ, H. B. 1989. MH-S, a murine alveolar macrophage cell line: morphological, cytochemical, and functional characteristics. *J Leukoc Biol,* 46**,** 119-27.
MCCAFFREY, R. L. & ALLEN, L. A. 2006. Francisella tularensis LVS evades killing by human neutrophils via inhibition of the respiratory burst and phagosome escape. *J Leukoc Biol,* 80**,** 1224-30.
MCCAFFREY, R. L., SCHWARTZ, J. T., LINDEMANN, S. R., MORELAND, J. G., BUCHAN, B. W., JONES, B. D. & ALLEN, L. A. 2010. Multiple mechanisms of NADPH oxidase inhibition by type A and type B Francisella tularensis. *J Leukoc Biol,* 88**,** 791-805.
MCCARTHY, M. K., ZHU, L., PROCARIO, M. C. & WEINBERG, J. B. 2014. IL-17 Contributes to Neutrophil Recruitment but Not to Control of Viral Replication During Acute Mouse Adenovirus Type 1 Respiratory Infection. *Virology,* 0**,** 259-67.
MCCOY, G. W. & CHAPIN, C. W. 1912. Further Observations on a Plague-Like Disease of Rodents with a Preliminary Note on the Causative Agent, Bacterium tularense. *The Journal of Infectious Diseases,* 10**,** 61-72.
MCDOUGALL, C. M. & HELMS, P. J. 2006. Neutrophil airway inflammation in childhood asthma. *Thorax,* 61**,** 739-41.
MCKINSTRY, K. K., STRUTT, T. M., BUCK, A., CURTIS, J. D., DIBBLE, J. P., HUSTON, G., TIGHE, M., HAMADA, H., SELL, S., DUTTON, R. W. & SWAIN, S. L. 2009. IL-10 deficiency unleashes an influenza-specific Th17 response and enhances survival against high-dose challenge. *J Immunol,* 182**,** 7353-63.
MCLENDON, M. K., APICELLA, M. A. & ALLEN, L. A. 2006. Francisella tularensis: taxonomy, genetics, and Immunopathogenesis of a potential agent of biowarfare. *Annu Rev Microbiol,* 60**,** 167-85.
MEIBOM, K. L., BAREL, M. & CHARBIT, A. 2009. Loops and networks in control of Francisella tularensis virulence. *Future Microbiol,* 4**,** 713-29.
MELILLO, A. A., FOREMAN, O. & ELKINS, K. L. 2013. IL-12Rbeta2 is critical for survival of primary Francisella tularensis LVS infection. *J Leukoc Biol,* 93**,** 657-67.
MELO, M. D. & STOKES, R. W. 2000. Interaction of Mycobacterium tuberculosis with MH-S, an immortalized murine alveolar macrophage cell line: a comparison with primary murine macrophages. *Tuber Lung Dis,* 80**,** 35-46.
METZGER, D. W., SALMON, S. L. & KIRIMANJESWARA, G. 2013. Differing effects of interleukin-10 on cutaneous and pulmonary Francisella tularensis live vaccine strain infection. *Infect Immun,* 81**,** 2022-7.
MIHRSHAHI, R., BARCLAY, A. N. & BROWN, M. H. 2009. Essential roles for Dok2 and RasGAP in CD200 receptor-mediated regulation of human myeloid cells. *J Immunol,* 183**,** 4879-86.
MIHRSHAHI, R. & BROWN, M. H. 2010. Downstream of tyrosine kinase 1 and 2 play opposing roles in CD200 receptor signaling. *J Immunol,* 185**,** 7216-22.
MINAS, K. & LIVERSIDGE, J. 2006. Is The CD200/CD200 Receptor Interaction More Than Just a Myeloid Cell Inhibitory Signal? *Crit Rev Immunol,* 26**,** 213-30.

MISSTEAR, K., CHANAS, S. A., REZAEE, S. A., COLMAN, R., QUINN, L. L., LONG, H. M., GOODYEAR, O., LORD, J. M., HISLOP, A. D. & BLACKBOURN, D. J. 2012. Suppression of antigen-specific T cell responses by the Kaposi's sarcoma-associated herpesvirus viral OX2 protein and its cellular orthologue, CD200. *J Virol,* 86**,** 6246-57.

MIYAMOTO, M., PRAUSE, O., SJOSTRAND, M., LAAN, M., LOTVALL, J. & LINDEN, A. 2003. Endogenous IL-17 as a mediator of neutrophil recruitment caused by endotoxin exposure in mouse airways. *J Immunol,* 170**,** 4665-72.

MONTIEL, M., BONILLA, E., VALERO, N., MOSQUERA, J., ESPINA, L. M., QUIROZ, Y. & ÁLVAREZ-MON, M. 2015. Melatonin decreases brain apoptosis, oxidative stress, and CD200 expression and increased survival rate in mice infected by Venezuelan equine encephalitis virus. *Antivir Chem Chemother,* 24**,** 99-108.

MORNER, T. 1992. The ecology of tularaemia. *Rev Sci Tech,* 11**,** 1123-30.

MORRIS, D. G., HUANG, X., KAMINSKI, N., WANG, Y., SHAPIRO, S. D., DOLGANOV, G., GLICK, A. & SHEPPARD, D. 2003. Loss of integrin alpha(v)beta6-mediated TGF-beta activation causes Mmp12-dependent emphysema. *Nature,* 422**,** 169-73.

MUKHOPADHYAY, S., PLUDDEMANN, A., HOE, J. C., WILLIAMS, K. J., VARIN, A., MAKEPEACE, K., AKNIN, M. L., BOWDISH, D. M., SMALE, S. T., BARCLAY, A. N. & GORDON, S. 2010. Immune inhibitory ligand CD200 induction by TLRs and NLRs limits macrophage activation to protect the host from meningococcal septicemia. *Cell Host Microbe,* 8**,** 236-47.

MULLIGAN, M. J., STAPLETON, J. T., KEITEL, W. A., FREY, S. E., CHEN, W. H., ROUPHAEL, N., EDUPUGANTI, S., BECK, A., WINOKUR, P. L., EL SAHLY, H. M., PATEL, S. M., ATMAR, R. L., GRAHAM, I., ANDERSON, E., EL-KAMARY, S. S., PASETTI, M. F., SZTEIN, M. B., HILL, H. & GOLL, J. B. 2017. Tularemia vaccine: Safety, reactogenicity, "Take" skin reactions, and antibody responses following vaccination with a new lot of the Francisella tularensis live vaccine strain - A phase 2 randomized clinical Trial. *Vaccine*.

MUNGER, J. S., HUANG, X., KAWAKATSU, H., GRIFFITHS, M. J., DALTON, S. L., WU, J., PITTET, J. F., KAMINSKI, N., GARAT, C., MATTHAY, M. A., RIFKIN, D. B. & SHEPPARD, D. 1999. The integrin alpha v beta 6 binds and activates latent TGF beta 1: a mechanism for regulating pulmonary inflammation and fibrosis. *Cell,* 96**,** 319-28.

MURPHY, M. P. & LEVINE, H. 2010. Alzheimer's Disease and the β-Amyloid Peptide. *Journal of Alzheimer's disease : JAD,* 19**,** 311.

NA, Y. R., JUNG, D., GU, G. J. & SEOK, S. H. 2016. GM-CSF Grown Bone Marrow Derived Cells Are Composed of Phenotypically Different Dendritic Cells and Macrophages. *Mol Cells,* 39**,** 734-41.

NAEGELEN, I., BEAUME, N., PLANÇON, S., SCHENTEN, V., TSCHIRHART, E. J. & BRÉCHARD, S. 2015. Regulation of Neutrophil Degranulation and Cytokine Secretion: A Novel Model Approach Based on Linear Fitting. *J Immunol Res,* 2015.

NGUYEN, G. T., GREEN, E. R. & MECSAS, J. 2017. Neutrophils to the ROScue: Mechanisms of NADPH Oxidase Activation and Bacterial Resistance. *Front Cell Infect Microbiol,* 7**,** 373.
NICHOLLS, S. M., COPLAND, D. A., VITOVA, A., KUFFOVA, L., FORRESTER, J. V. & DICK, A. D. 2015. Local targeting of the CD200-CD200R axis does not promote corneal graft survival. *Exp Eye Res,* 130**,** 1-8.
NISHIKADO, H., MUKAI, K., KAWANO, Y., MINEGISHI, Y. & KARASUYAMA, H. 2011. NK cell-depleting anti-asialo GM1 antibody exhibits a lethal off-target effect on basophils in vivo. *J Immunol,* 186**,** 5766-71.
NOTHELFER, K., SANSONETTI, P. J. & PHALIPON, A. 2015. Pathogen manipulation of B cells: the best defence is a good offence. *Nat Rev Microbiol,* 13**,** 173-84.
O'BYRNE, P. M., METEV, H., PUU, M., RICHTER, K., KEEN, C., UDDIN, M., LARSSON, B., CULLBERG, M. & NAIR, P. 2016. Efficacy and safety of a CXCR2 antagonist, AZD5069, in patients with uncontrolled persistent asthma: a randomised, double-blind, placebo-controlled trial. *Lancet Respir Med,* 4**,** 797-806.
O'GORMAN, M. R. & CORROCHANO, V. 1995. Rapid whole-blood flow cytometry assay for diagnosis of chronic granulomatous disease. *Clin Diagn Lab Immunol,* 2**,** 227-32.
ODEGAARD, K., BOERSMA, B. & KEEGAN, J. 2017. Atypical Presentations of Tularemia. *S D Med,* 70**,** 207-209.
OHARA, Y., SATO, T., FUJITA, H., UENO, T. & HOMMA, M. 1991. Clinical manifestations of tularemia in Japan--analysis of 1,355 cases observed between 1924 and 1987. *Infection,* 19**,** 14-7.
ONG, E. Z., CHAN, K. R. & OOI, E. E. 2016. Viral Manipulation of Host Inhibitory Receptor Signaling for Immune Evasion. *PLoS Pathogens,* 12**,** e1005776.
OYSTON, P. C., SJOSTEDT, A. & TITBALL, R. W. 2004. Tularaemia: bioterrorism defence renews interest in Francisella tularensis. *Nat Rev Microbiol,* 2**,** 967-78.
PAPAYANNOPOULOS, V. 2018. Neutrophil extracellular traps in immunity and disease. *Nat Rev Immunol,* 18**,** 134-147.
PAPAYANNOPOULOS, V., METZLER, K. D., HAKKIM, A. & ZYCHLINSKY, A. 2010. Neutrophil elastase and myeloperoxidase regulate the formation of neutrophil extracellular traps. *J Cell Biol,* 191**,** 677-91.
PARK, M. K., AMICHAY, D., LOVE, P., WICK, E., LIAO, F., GRINBERG, A., RABIN, R. L., ZHANG, H. H., GEBEYEHU, S., WRIGHT, T. M., IWASAKI, A., WENG, Y., DEMARTINO, J. A., ELKINS, K. L. & FARBER, J. M. 2002. The CXC chemokine murine monokine induced by IFN-gamma (CXC chemokine ligand 9) is made by APCs, targets lymphocytes including activated B cells, and supports antibody responses to a bacterial pathogen in vivo. *J Immunol,* 169**,** 1433-43.
PASETTI, M. F., CUBEROS, L., HORN, T. L., SHEARER, J. D., MATTHEWS, S. J., HOUSE, R. V. & SZTEIN, M. B. 2008. An improved Francisella tularensis live vaccine strain (LVS) is well tolerated and highly immunogenic when administered to rabbits in escalating doses using various immunization routes. *Vaccine,* 26**,** 1773-85.

PEREZ, N. M. & RAMAKRISHNAN, G. 2014. The reduced genome of the Francisella tularensis live vaccine strain (LVS) encodes two iron acquisition systems essential for optimal growth and virulence. *PLoS One,* 9**,** e93558.
PERIASAMY, S., AVRAM, D., MCCABE, A., MACNAMARA, K. C., SELLATI, T. J. & HARTON, J. A. 2016. An Immature Myeloid/Myeloid-Suppressor Cell Response Associated with Necrotizing Inflammation Mediates Lethal Pulmonary Tularemia. *PLoS Pathog,* 12**,** e1005517.
PERIASAMY, S., SINGH, A., SAHAY, B., RAHMAN, T., FEUSTEL, P. J., PHAM, G. H., GOSSELIN, E. J. & SELLATI, T. J. 2011. Development of tolerogenic dendritic cells and regulatory T cells favors exponential bacterial growth and survival during early respiratory tularemia. *J Leukoc Biol,* 90**,** 493-507.
PHANSE, Y., RAMER-TAIT, A. E., FRIEND, S. L., CARRILLO-CONDE, B., LUETH, P., OSTER, C. J., PHILLIPS, G. J., NARASIMHAN, B., WANNEMUEHLER, M. J. & BELLAIRE, B. H. 2012. Analyzing cellular internalization of nanoparticles and bacteria by multi-spectral imaging flow cytometry. *J Vis Exp***,** e3884.
PHILLIPS, N. J., SCHILLING, B., MCLENDON, M. K., APICELLA, M. A. & GIBSON, B. W. 2004. Novel Modification of Lipid A of Francisella tularensis. *Infect Immun,* 72**,** 5340-8.
PIERINI, L. M. 2006. Uptake of serum-opsonized Francisella tularensis by macrophages can be mediated by class A scavenger receptors. *Cell Microbiol,* 8**,** 1361-70.
PIETRAS, E. M., MILLER, L. S., JOHNSON, C. T., O'CONNELL, R. M., DEMPSEY, P. W. & CHENG, G. 2011. A MyD88-dependent IFNgammaR-CCR2 signaling circuit is required for mobilization of monocytes and host defense against systemic bacterial challenge. *Cell Res,* 21**,** 1068-79.
PLACE, D. E., WILLIAMSON, D. R., YUZEFPOLSKIY, Y., KATKERE, B., SARKAR, S., KALIA, V. & KIRIMANJESWARA, G. S. 2017. Development of a novel Francisella tularensis Live Vaccine Strain expressing ovalbumin provides insight into antigen-specific CD8+ T cell responses. *PLoS One,* 12**,** e0190384.
PLZAKOVA, L., KROCOVA, Z., KUBELKOVA, K. & MACELA, A. 2015. Entry of Francisella tularensis into Murine B Cells: The Role of B Cell Receptors and Complement Receptors. *PLoS One,* 10**,** e0132571.
PLZAKOVA, L., KUBELKOVA, K., KROCOVA, Z., ZARYBNICKA, L., SINKOROVA, Z. & MACELA, A. 2014. B cell subsets are activated and produce cytokines during early phases of Francisella tularensis LVS infection. *Microb Pathog,* 75**,** 49-58.
PODNOS, A., CLARK, D. A., ERIN, N., YU, K. & GORCZYNSKI, R. M. 2012. Further evidence for a role of tumor CD200 expression in breast cancer metastasis: decreased metastasis in CD200R1KO mice or using CD200-silenced EMT6. *Breast Cancer Res Treat,* 136**,** 117-27.
POLSINELLI, T., MELTZER, M. S. & FORTIER, A. H. 1994. Nitric oxide-independent killing of Francisella tularensis by IFN-gamma-stimulated murine alveolar macrophages. *J Immunol,* 153**,** 1238-45.
POWELL, D. A. & FRELINGER, J. A. 2017. Efficacy of Resistance to Francisella Imparted by ITY/NRAMP/SLC11A1 Depends on Route of Infection. *Front Immunol,* 8.

POWELL, D. R. & HUTTENLOCHER, A. 2016. Neutrophils in the Tumor Microenvironment. *Trends Immunol,* 37**,** 41-52.
RAMADASS, M. & CATZ, S. D. 2016. Molecular mechanisms regulating secretory organelles and endosomes in neutrophils and their implications for inflammation. *Immunol Rev,* 273**,** 249-65.
RANDELL, S. H. & BOUCHER, R. C. 2006. Effective Mucus Clearance Is Essential for Respiratory Health. *Am J Respir Cell Mol Biol,* 35**,** 20-8.
RAVETCH, J. V. & LANIER, L. L. 2000. Immune inhibitory receptors. *Science,* 290**,** 84-9.
RENNARD, S. I., DALE, D. C., DONOHUE, J. F., KANNIESS, F., MAGNUSSEN, H., SUTHERLAND, E. R., WATZ, H., LU, S., STRYSZAK, P., ROSENBERG, E. & STAUDINGER, H. 2015. CXCR2 Antagonist MK-7123. A Phase 2 Proof-of-Concept Trial for Chronic Obstructive Pulmonary Disease. *Am J Respir Crit Care Med,* 191**,** 1001-11.
REZAEE, S. A., GRACIE, J. A., MCINNES, I. B. & BLACKBOURN, D. J. 2005. Inhibition of neutrophil function by the Kaposi's sarcoma-associated herpesvirus vOX2 protein. *Aids,* 19**,** 1907-10.
RICKLIN, D., HAJISHENGALLIS, G., YANG, K. & LAMBRIS, J. D. 2010. Complement: a key system for immune surveillance and homeostasis. *Nat Immunol,* 11**,** 785-97.
RIJKERS, E. S., DE RUITER, T., BARIDI, A., VENINGA, H., HOEK, R. M. & MEYAARD, L. 2008. The inhibitory CD200R is differentially expressed on human and mouse T and B lymphocytes. *Mol Immunol,* 45**,** 1126-35.
RIJKERS, E. S., DE RUITER, T., BUITENHUIS, M., VENINGA, H., HOEK, R. M. & MEYAARD, L. 2007. Ligation of CD200R by CD200 is not required for normal murine myelopoiesis. *Eur J Haematol,* 79**,** 410-6.
ROBERTS, L. M., LEDVINA, H. E., TULADHAR, S., RANA, D., STEELE, S. P., SEMPOWSKI, G. D. & FRELINGER, J. A. 2015. Depletion of alveolar macrophages in CD11c diphtheria toxin receptor mice produces an inflammatory response. *Immun Inflamm Dis,* 3**,** 71-81.
ROBERTS, L. M., TULADHAR, S., STEELE, S. P., RIEBE, K. J., CHEN, C. J., CUMMING, R. I., SEAY, S., FROTHINGHAM, R., SEMPOWSKI, G. D., KAWULA, T. H. & FRELINGER, J. A. 2014. Identification of early interactions between Francisella and the host. *Infect Immun,* 82**,** 2504-10.
RODRIGUEZ, A. R., YU, J. J., GUENTZEL, M. N., NAVARA, C. S., KLOSE, K. E., FORSTHUBER, T. G., CHAMBERS, J. P., BERTON, M. T. & ARULANANDAM, B. P. 2012. Mast cell TLR2 signaling is crucial for effective killing of Francisella tularensis. *J Immunol,* 188**,** 5604-11.
RODRIGUEZ, A. R., YU, J. J., NAVARA, C., CHAMBERS, J. P., GUENTZEL, M. N. & ARULANANDAM, B. P. 2016. Contribution of FcvarepsilonRI-associated vesicles to mast cell-macrophage communication following Francisella tularensis infection. *Innate Immun,* 22**,** 567-74.
ROHMER, L., BRITTNACHER, M., SVENSSON, K., BUCKLEY, D., HAUGEN, E., ZHOU, Y., CHANG, J., LEVY, R., HAYDEN, H., FORSMAN, M., OLSON, M., JOHANSSON, A., KAUL, R. & MILLER, S. I. 2006. Potential source of Francisella tularensis live vaccine strain attenuation determined by genome comparison. *Infect Immun,* 74**,** 6895-906.
ROSENBLUM, M. D., OLASZ, E. B., YANCEY, K. B., WOODLIFF, J. E., LAZAROVA, Z., GERBER, K. A. & TRUITT, R. L. 2004. Expression of

CD200 on epithelial cells of the murine hair follicle: a role in tissue-specific immune tolerance? *J Invest Dermatol,* 123**,** 880-7.
ROTHLIN, C. V., GHOSH, S., ZUNIGA, E. I., OLDSTONE, M. B. & LEMKE, G. 2007. TAM receptors are pleiotropic inhibitors of the innate immune response. *Cell,* 131**,** 1124-36.
RUSSELL, P., ELEY, S. M., FULOP, M. J., BELL, D. L. & TITBALL, R. W. 1998. The efficacy of ciprofloxacin and doxycycline against experimental tularaemia. *J Antimicrob Chemother,* 41**,** 461-5.
RYGIEL, T. P., RIJKERS, E. S., DE RUITER, T., STOLTE, E. H., VAN DER VALK, M., RIMMELZWAAN, G. F., BOON, L., VAN LOON, A. M., COENJAERTS, F. E., HOEK, R. M., TESSELAAR, K. & MEYAARD, L. 2009. Lack of CD200 enhances pathological T cell responses during influenza infection. *J Immunol,* 183**,** 1990-6.
SANTIC, M., MOLMERET, M., KLOSE, K. E. & ABU KWAIK, Y. 2006. Francisella tularensis travels a novel, twisted road within macrophages. *Trends Microbiol,* 14**,** 37-44.
SARANGI, P. P., WOO, S. R. & ROUSE, B. T. 2009. Control of viral immunoinflammatory lesions by manipulating CD200:CD200 receptor interaction. *Clin Immunol,* 131**,** 31-40.
SARMA, J. V. & WARD, P. A. 2011. The complement system. *Cell Tissue Res,* 343**,** 227-35.
SCHNEIDER, C. A., RASBAND, W. S. & ELICEIRI, K. W. 2012. NIH Image to ImageJ: 25 years of image analysis. *Nat Methods,* 9**,** 671-5.
SCHULERT, G. S. & ALLEN, L. A. 2006. Differential infection of mononuclear phagocytes by Francisella tularensis: role of the macrophage mannose receptor. *J Leukoc Biol,* 80**,** 563-71.
SCHWARTZ, J. T., BARKER, J. H., KAUFMAN, J., FAYRAM, D. C., MCCRACKEN, J. M. & ALLEN, L. A. 2012a. Francisella tularensis inhibits the intrinsic and extrinsic pathways to delay constitutive apoptosis and prolong human neutrophil lifespan. *J Immunol,* 188**,** 3351-63.
SCHWARTZ, J. T., BARKER, J. H., LONG, M. E., KAUFMAN, J., MCCRACKEN, J. & ALLEN, L. A. 2012b. Natural IgM mediates complement-dependent uptake of Francisella tularensis by human neutrophils via complement receptors 1 and 3 in nonimmune serum. *J Immunol,* 189**,** 3064-77.
SCOTT, R. S., MCMAHON, E. J., POP, S. M., REAP, E. A., CARICCHIO, R., COHEN, P. L., EARP, H. S. & MATSUSHIMA, G. K. 2001. Phagocytosis and clearance of apoptotic cells is mediated by MER. *Nature,* 411**,** 207-11.
SEGAL, A. W., DORLING, J. & COADE, S. 1980. Kinetics of fusion of the cytoplasmic granules with phagocytic vacuoles in human polymorphonuclear leukocytes. Biochemical and morphological studies. *J Cell Biol,* 85**,** 42-59.
SEGAL, B. H., LETO, T. L., GALLIN, J. I., MALECH, H. L. & HOLLAND, S. M. 2000. Genetic, biochemical, and clinical features of chronic granulomatous disease. *Medicine (Baltimore),* 79**,** 170-200.
SERBINA, N. V. & PAMER, E. G. 2006. Monocyte emigration from bone marrow during bacterial infection requires signals mediated by chemokine receptor CCR2. *Nat Immunol,* 7**,** 311-7.
SHAKERLEY, N. L., CHANDRASEKARAN, A., TREBAK, M., MILLER, B. A. & MELENDEZ, J. A. 2016. Francisella tularensis Catalase Restricts Immune Function by Impairing TRPM2 Channel Activity. *J Biol Chem,* 291**,** 3871-81.

SHARIF, O., GAWISH, R., WARSZAWSKA, J. M., MARTINS, R., LAKOVITS, K., HLADIK, A., DONINGER, B., BRUNNER, J., KOROSEC, A., SCHWARZENBACHER, R. E., BERG, T., KRALOVICS, R., COLINGE, J., MESTERI, I., GILFILLAN, S., SALMAGGI, A., VERSCHOOR, A., COLONNA, M. & KNAPP, S. 2014. The triggering receptor expressed on myeloid cells 2 inhibits complement component 1q effector mechanisms and exerts detrimental effects during pneumococcal pneumonia. *PLoS Pathog,* 10**,** e1004167.

SHARMA, J., MARES, C. A., LI, Q., MORRIS, E. G. & TEALE, J. M. 2011. Features of sepsis caused by pulmonary infection with Francisella tularensis Type A strain. *Microb Pathog,* 51**,** 39-47.

SHIBATA, T., HABIEL, D. M., COELHO, A. L., KUNKEL, S. L., LUKACS, N. W. & HOGABOAM, C. M. 2014. Axl receptor blockade ameliorates pulmonary pathology resulting from primary viral infection and viral exacerbation of asthma. *J Immunol,* 192**,** 3569-81.

SHIRATORI, I., YAMAGUCHI, M., SUZUKAWA, M., YAMAMOTO, K., LANIER, L. L., SAITO, T. & ARASE, H. 2005. Down-regulation of basophil function by human CD200 and human herpesvirus-8 CD200. *J Immunol,* 175**,** 4441-9.

SHIREY, K. A., COLE, L. E., KEEGAN, A. D. & VOGEL, S. N. 2008. Francisella tularensis live vaccine strain induces macrophage alternative activation as a survival mechanism. *J Immunol,* 181**,** 4159-67.

SHRIVASTAVA, K., GONZALEZ, P. & ACARIN, L. 2012. The immune inhibitory complex CD200/CD200R is developmentally regulated in the mouse brain. *J Comp Neurol,* 520**,** 2657-75.

SILVA, M. T. 2011. Macrophage phagocytosis of neutrophils at inflammatory/infectious foci: a cooperative mechanism in the control of infection and infectious inflammation. *J Leukoc Biol,* 89**,** 675-83.

SILVA, M. T. & CORREIA-NEVES, M. 2012. Neutrophils and Macrophages: the Main Partners of Phagocyte Cell Systems. *Front Immunol,* 3.

SIMELYTE, E., CRIADO, G., ESSEX, D., UGER, R. A., FELDMANN, M. & WILLIAMS, R. O. 2008. CD200-Fc, a novel antiarthritic biologic agent that targets proinflammatory cytokine expression in the joints of mice with collagen-induced arthritis. *Arthritis Rheum,* 58**,** 1038-43.

SINGH, B., SU, Y. C. & RIESBECK, K. 2010. Vitronectin in bacterial pathogenesis: a host protein used in complement escape and cellular invasion. *Mol Microbiol,* 78**,** 545-60.

SJÖSTEDT, A., CONLAN, J. W. & NORTH, R. J. 1994. Neutrophils are critical for host defense against primary infection with the facultative intracellular bacterium Francisella tularensis in mice and participate in defense against reinfection. *Infect Immun,* 62**,** 2779-83.

SJOSTEDT, A., NORTH, R. J. & CONLAN, J. W. 1996. The requirement of tumour necrosis factor-alpha and interferon-gamma for the expression of protective immunity to secondary murine tularaemia depends on the size of the challenge inoculum. *Microbiology,* 142 (Pt 6)**,** 1369-74.

SMITH, C. W. 2000. Possible steps involved in the transition to stationary adhesion of rolling neutrophils: a brief review. *Microcirculation,* 7**,** 385-94.

SNELGROVE, R. J., GODLEE, A. & HUSSELL, T. 2011. Airway immune homeostasis and implications for influenza-induced inflammation. *Trends Immunol,* 32**,** 328-34.

SNELGROVE, R. J., GOULDING, J., DIDIERLAURENT, A. M., LYONGA, D., VEKARIA, S., EDWARDS, L., GWYER, E., SEDGWICK, J. D., BARCLAY, A. N. & HUSSELL, T. 2008. A critical function for CD200 in lung immune homeostasis and the severity of influenza infection. *Nat Immunol,* 9**,** 1074-83.

SOBERMAN, R. J., MACKAY, C. R., VAINE, C. A., RYAN, G. B., CERNY, A. M., THOMPSON, M. R., NIKOLIC, B., PRIMO, V., CHRISTMAS, P., SHEIFFELE, P., ARONOV, L., KNIPE, D. M. & KURT-JONES, E. A. 2012. CD200R1 supports HSV-1 viral replication and licenses pro-inflammatory signaling functions of TLR2. *PLoS One,* 7**,** e47740.

STANDIFORD, T. J., KUNKEL, S. L., KASAHARA, K., MILIA, M. J., ROLFE, M. W. & STRIETER, R. M. 1991. Interleukin-8 gene expression from human alveolar macrophages: the role of adherence. *Am J Respir Cell Mol Biol,* 5**,** 579-85.

STEELE, S., BRUNTON, J., ZIEHR, B., TAFT-BENZ, S., MOORMAN, N. & KAWULA, T. 2013. Francisella tularensis harvests nutrients derived via ATG5-independent autophagy to support intracellular growth. *PLoS Pathog,* 9**,** e1003562.

STEELE, S., RADLINSKI, L., TAFT-BENZ, S., BRUNTON, J. & KAWULA, T. H. 2016. Trogocytosis-associated cell to cell spread of intracellular bacterial pathogens. *Elife,* 5.

STEINER, D. J., FURUYA, Y., JORDAN, M. B. & METZGER, D. W. 2017. A Protective Role for Macrophages in Respiratory Francisella tularensis Infection. *Infect Immun*.

STEINER, D. J., FURUYA, Y. & METZGER, D. W. 2014. Host-pathogen interactions and immune evasion strategies in Francisella tularensis pathogenicity. *Infect Drug Resist,* 7**,** 239-51.

STENMARK, S., SUNNEMARK, D., BUCHT, A. & SJOSTEDT, A. 1999. Rapid local expression of interleukin-12, tumor necrosis factor alpha, and gamma interferon after cutaneous Francisella tularensis infection in tularemia-immune mice. *Infect Immun,* 67**,** 1789-97.

STEWARD, J., PIERCY, T., LEVER, M. S., SIMPSON, A. J. & BROOKS, T. J. 2006. Treatment of murine pneumonic Francisella tularensis infection with gatifloxacin, moxifloxacin or ciprofloxacin. *Int J Antimicrob Agents,* 27**,** 439-43.

STEWART, S. J. 1996. Tularemia: association with hunting and farming. *FEMS Immunol Med Microbiol,* 13**,** 197-99.

STINSON, E., SMITH, L. P., COLE, K. S., BARRY, E. M. & REED, D. S. 2016. Respiratory and oral vaccination improves protection conferred by the live vaccine strain against pneumonic tularemia in the rabbit model. *Pathog Dis,* 74.

STOPPELENBURG, A. J., SALIMI, V., HENNUS, M., PLANTINGA, M., HUIS IN 'T VELD, R., WALK, J., MEERDING, J., COENJAERTS, F., BONT, L. & BOES, M. 2013. Local IL-17A potentiates early neutrophil recruitment to the respiratory tract during severe RSV infection. *PLoS One,* 8**,** e78461.

STORISTEANU, D. M. L., POCOCK, J. M., COWBURN, A. S., JUSS, J. K., NADESALINGAM, A., NIZET, V. & CHILVERS, E. R. 2017. Evasion of Neutrophil Extracellular Traps by Respiratory Pathogens. *Am J Respir Cell Mol Biol,* 56**,** 423-31.

STUMBLES, P. A., THOMAS, J. A., PIMM, C. L., LEE, P. T., VENAILLE, T. J., PROKSCH, S. & HOLT, P. G. 1998. Resting respiratory tract dendritic cells preferentially stimulate T helper cell type 2 (Th2) responses and require obligatory cytokine signals for induction of Th1 immunity. *J Exp Med,* 188**,** 2019-31.

SUTERA, V., LEVERT, M., BURMEISTER, W. P., SCHNEIDER, D. & MAURIN, M. 2014. Evolution toward high-level fluoroquinolone resistance in Francisella species. *J Antimicrob Chemother,* 69**,** 101-10.

TAMILSELVAM, B. & DAEFLER, S. 2008. Francisella targets cholesterol-rich host cell membrane domains for entry into macrophages. *J Immunol,* 180**,** 8262-71.

TAYLOR, N., MCCONACHIE, K., CALDER, C., DAWSON, R., DICK, A., SEDGWICK, J. D. & LIVERSIDGE, J. 2005. Enhanced tolerance to autoimmune uveitis in CD200-deficient mice correlates with a pronounced Th2 switch in response to antigen challenge. *J Immunol,* 174**,** 143-54.

THEPEN, T., VAN ROOIJEN, N. & KRAAL, G. 1989. Alveolar macrophage elimination in vivo is associated with an increase in pulmonary immune response in mice. *J Exp Med,* 170**,** 499-509.

TOMLINSON, G. S., BOOTH, H., PETIT, S. J., POTTON, E., TOWERS, G. J., MILLER, R. F., CHAIN, B. M. & NOURSADEGHI, M. 2012. Adherent Human Alveolar Macrophages Exhibit a Transient Pro-Inflammatory Profile That Confounds Responses to Innate Immune Stimulation. *PLOS ONE,* 7**,** e40348.

TRENT, M. S., STEAD, C. M., TRAN, A. X. & HANKINS, J. V. 2006. Diversity of endotoxin and its impact on pathogenesis. *J Endotoxin Res,* 12**,** 205-23.

TRINCHIERI, G. 2003. Interleukin-12 and the regulation of innate resistance and adaptive immunity. *Nat Rev Immunol,* 3**,** 133-46.

TSAI, M. H., CHU, C. C., WEI, T. S., CHIU, M. M., CHANG, C. Y., WEI, I. H., CHIEN, H. F., CHEN, H. M., WU, C. H. & JIANG-SHIEH, Y. F. 2015. CD200 in growing rat lungs: developmental expression and control by dexamethasone. *Cell Tissue Res,* 359**,** 729-42.

TSCHERNUTTER, M., JENKINS, S. A., WASEEM, N. H., SAIHAN, Z., HOLDER, G. E., BIRD, A. C., BHATTACHARYA, S. S., ALI, R. R. & WEBSTER, A. R. 2006. Clinical characterisation of a family with retinal dystrophy caused by mutation in the Mertk gene. *Br J Ophthalmol,* 90**,** 718-23.

TULIS, J. J., EIGELSBACH, H. T. & KERPSACK, R. W. 1970. Host-parasite relationship in monkeys administered live tularemia vaccine. *Am J Pathol,* 58**,** 329-36.

TWITO, T., CHEN, Z., KHATRI, I., WONG, K., SPANER, D. & GORCZYNSKI, R. 2013. Ectodomain shedding of CD200 from the B-CLL cell surface is regulated by ADAM28 expression. *Leuk Res,* 37**,** 816-21.

TYAGI, S. R., TAMURA, M., BURNHAM, D. N. & LAMBETH, J. D. 1988. Phorbol myristate acetate (PMA) augments chemoattractant-induced diglyceride generation in human neutrophils but inhibits phosphoinositide hydrolysis. Implications for the mechanism of PMA priming of the respiratory burst. *J Biol Chem,* 263**,** 13191-8.

ULLAND, T. K., BUCHAN, B. W., KETTERER, M. R., FERNANDES-ALNEMRI, T., MEYERHOLZ, D. K., APICELLA, M. A., ALNEMRI, E. S., JONES, B. D., NAUSEEF, W. M. & SUTTERWALA, F. S. 2010.

Cutting edge: mutation of Francisella tularensis mviN leads to increased macrophage absent in melanoma 2 inflammasome activation and a loss of virulence. *J Immunol,* 185**,** 2670-4.
UNKELESS, J. C. & EISEN, H. N. 1975. Binding of monomeric immunoglobulins to Fc receptors of mouse macrophages. *J Exp Med,* 142**,** 1520-33.
VAN FAASSEN, H., KUOLEE, R., HARRIS, G., ZHAO, X., CONLAN, J. W. & CHEN, W. 2007. Neutrophils Play an Important Role in Host Resistance to Respiratory Infection with Acinetobacter baumannii in Mice. *Infect Immun,* 75**,** 5597-608.
VAN KESSEL, K. P. M., BESTEBROER, J. & VAN STRIJP, J. A. G. 2014. Neutrophil-Mediated Phagocytosis of Staphylococcus aureus. *Front Immunol,* 5.
VAN ROOIJEN, N. & SANDERS, A. 1994. Liposome mediated depletion of macrophages: mechanism of action, preparation of liposomes and applications. *J Immunol Methods,* 174**,** 83-93.
WALFORD, H. H. & DOHERTY, T. A. 2013. STAT6 and lung inflammation. *Jakstat,* 2.
WALLET, P., BENAOUDIA, S., MOSNIER, A., LAGRANGE, B., MARTIN, A., LINDGREN, H., GOLOVLIOV, I., MICHAL, F., BASSO, P., DJEBALI, S., PROVOST, A., ALLATIF, O., MEUNIER, E., BROZ, P., YAMAMOTO, M., PY, B. F., FAUDRY, E., SJOSTEDT, A. & HENRY, T. 2017. IFN-gamma extends the immune functions of Guanylate Binding Proteins to inflammasome-independent antibacterial activities during Francisella novicida infection. *PLoS Pathog,* 13**,** e1006630.
WANG, C., YU, X., CAO, Q., WANG, Y., ZHENG, G., TAN, T. K., ZHAO, H., ZHAO, Y., WANG, Y. & HARRIS, D. C. 2013. Characterization of murine macrophages from bone marrow, spleen and peritoneum. *BMC Immunology,* 14**,** 6.
WANG, H., BLOOM, O., ZHANG, M., VISHNUBHAKAT, J. M., OMBRELLINO, M., CHE, J., FRAZIER, A., YANG, H., IVANOVA, S., BOROVIKOVA, L., MANOGUE, K. R., FAIST, E., ABRAHAM, E., ANDERSSON, J., ANDERSSON, U., MOLINA, P. E., ABUMRAD, N. N., SAMA, A. & TRACEY, K. J. 1999. HMG-1 as a late mediator of endotoxin lethality in mice. *Science,* 285**,** 248-51.
WANG, X., SJOLINDER, M., GAO, Y., WAN, Y. & SJOLINDER, H. 2016. Immune Homeostatic Macrophages Programmed by the Bacterial Surface Protein NhhA Potentiate Nasopharyngeal Carriage of Neisseria meningitidis. *MBio,* 7**,** e01670-15.
WANNER, A., SALATHE, M. & O'RIORDAN, T. G. 1996. Mucociliary clearance in the airways. *Am J Respir Crit Care Med,* 154**,** 1868-902.
WEBB, M. & BARCLAY, A. N. 1984. Localisation of the MRC OX-2 glycoprotein on the surfaces of neurones. *J Neurochem,* 43**,** 1061-7.
WEBER, I. B., TURABELIDZE, G., PATRICK, S., GRIFFITH, K. S., KUGELER, K. J. & MEAD, P. S. 2012. Clinical recognition and management of tularemia in Missouri: a retrospective records review of 121 cases. *Clin Infect Dis,* 55**,** 1283-90.
WICKSTRUM, J. R., HONG, K. J., BOKHARI, S., REED, N., MCWILLIAMS, N., HORVAT, R. T. & PARMELY, M. J. 2007. Coactivating signals for the hepatic lymphocyte gamma interferon response to Francisella tularensis. *Infect Immun,* 75**,** 1335-42.

WILLIAMS, J. C., CRAVEN, R. R., EARP, H. S., KAWULA, T. H. & MATSUSHIMA, G. K. 2009. TAM receptors are dispensable in the phagocytosis and killing of bacteria. *Cell Immunol,* 259**,** 128-34.
WISSINGER, E., GOULDING, J. & HUSSELL, T. 2009. Immune homeostasis in the respiratory tract and its impact on heterologous infection. *Semin Immunol,* 21**,** 147-55.
WOOLARD, M. D., HENSLEY, L. L., KAWULA, T. H. & FRELINGER, J. A. 2008. Respiratory Francisella tularensis live vaccine strain infection induces Th17 cells and prostaglandin E2, which inhibits generation of gamma interferon-positive T cells. *Infect Immun,* 76**,** 2651-9.
WOOLARD, M. D., WILSON, J. E., HENSLEY, L. L., JANIA, L. A., KAWULA, T. H., DRAKE, J. R. & FRELINGER, J. A. 2007. Francisella tularensis-infected macrophages release prostaglandin E2 that blocks T cell proliferation and promotes a Th2-like response. *J Immunol,* 178**,** 2065-74.
WRIGHT, G. J., CHERWINSKI, H., FOSTER-CUEVAS, M., BROOKE, G., PUKLAVEC, M. J., BIGLER, M., SONG, Y., JENMALM, M., GORMAN, D., MCCLANAHAN, T., LIU, M. R., BROWN, M. H., SEDGWICK, J. D., PHILLIPS, J. H. & BARCLAY, A. N. 2003. Characterization of the CD200 receptor family in mice and humans and their interactions with CD200. *J Immunol,* 171**,** 3034-46.
WRIGHT, G. J., JONES, M., PUKLAVEC, M. J., BROWN, M. H. & BARCLAY, A. N. 2001. The unusual distribution of the neuronal/lymphoid cell surface CD200 (OX2) glycoprotein is conserved in humans. *Immunology,* 102**,** 173-9.
WRIGHT, G. J., PUKLAVEC, M. J., WILLIS, A. C., HOEK, R. M., SEDGWICK, J. D., BROWN, M. H. & BARCLAY, A. N. 2000. Lymphoid/neuronal cell surface OX2 glycoprotein recognizes a novel receptor on macrophages implicated in the control of their function. *Immunity,* 13**,** 233-42.
XIONG, Z., AMPUDIA-MESIAS, E., SHAVER, R., HORBINSKI, C. M., MOERTEL, C. L. & OLIN, M. R. 2016. Tumor-derived vaccines containing CD200 inhibit immune activation: implications for immunotherapy. *Immunotherapy,* 8**,** 1059-71.
YAMADA, C., SANO, H., SHIMIZU, T., MITSUZAWA, H., NISHITANI, C., HIMI, T. & KUROKI, Y. 2006. Surfactant protein A directly interacts with TLR4 and MD-2 and regulates inflammatory cellular response. Importance of supratrimeric oligomerization. *J Biol Chem,* 281**,** 21771-80.
YANO, T., KASSOVSKA-BRATINOVA, S., TEH, J. S., WINKLER, J., SULLIVAN, K., ISAACS, A., SCHECHTER, N. M. & RUBIN, H. 2011. Reduction of clofazimine by mycobacterial type 2 NADH:quinone oxidoreductase: a pathway for the generation of bactericidal levels of reactive oxygen species. *J Biol Chem,* 286**,** 10276-87.
YI, M. H., ZHANG, E., KIM, J. J., BAEK, H., SHIN, N., KIM, S., KIM, S. R., KIM, H. R., LEE, S. J., PARK, J. B., KIM, Y., KWON, O. Y., LEE, Y. H., OH, S. H. & KIM, D. W. 2016. CD200R/Foxp3-mediated signalling regulates microglial activation. *Sci Rep,* 6**,** 34901.
YIN, Y., ZHAO, L., ZHANG, F. & ZHANG, X. 2016. Impact of CD200-Fc on dendritic cells in lupus-prone NZB/WF1 mice. *Sci Rep,* 6**,** 31874.
ZARBOCK, A., SINGBARTL, K. & LEY, K. 2006. Complete reversal of acid-induced acute lung injury by blocking of platelet-neutrophil aggregation. *J Clin Invest,* 116**,** 3211-9.

ZHANG, J., TACHADO, S. D., PATEL, N., ZHU, J., IMRICH, A., MANFRUELLI, P., CUSHION, M., KINANE, T. B. & KOZIEL, H. 2005. Negative regulatory role of mannose receptors on human alveolar macrophage proinflammatory cytokine release in vitro. *J Leukoc Biol,* 78**,** 665-74.

ZHANG, S., CHERWINSKI, H., SEDGWICK, J. D. & PHILLIPS, J. H. 2004. Molecular mechanisms of CD200 inhibition of mast cell activation. *J Immunol,* 173**,** 6786-93.

ZHANG, Y., CHOKSI, S., CHEN, K., POBEZINSKAYA, Y., LINNOILA, I. & LIU, Z. G. 2013. ROS play a critical role in the differentiation of alternatively activated macrophages and the occurrence of tumor-associated macrophages. *Cell Res,* 23**,** 898-914.

ZIZZO, G., HILLIARD, B. A., MONESTIER, M. & COHEN, P. L. 2012. Efficient clearance of early apoptotic cells by human macrophages requires "M2c" polarization and MerTK induction. *J Immunol,* 189**,** 3508-20.